

CHAPERONE ACTIVITY OF SPECTRIN: MOLECULAR ORIGIN OF SPECIFICITY

By

DIPAYAN BOSE

Enrolment No: LIFE05201404001

Saha Institute of Nuclear Physics

A thesis submitted to the

Board of Studies in Life Sciences

In partial fulfillment of requirements

for the Degree of

DOCTOR OF PHILOSOPHY

of

HOMI BHABHA NATIONAL INSTITUTE



August, 2019

Homi Bhabha National Institute

Recommendations of the Viva Voce Committee

As members of the Viva Voce Committee, we certify that we have read the dissertation prepared by **Dipayan Bose (Enrolment No: LIFE05201404001)** entitled "**Chaperone Activity of Spectrin: Molecular Origin of Specificity**" and recommend that it may be accepted as fulfilling the thesis requirement for the award of Degree of Doctor of Philosophy.

Chairman - **Prof. Subrata Banerjee**



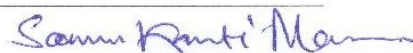
Guide / Convener - **Prof. Abhijit Chakrabarti**



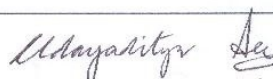
Examiner - **Prof. Rajendra P. Roy, NII, New Delhi**



Member 1 - **Prof. Soumen K. Manna**



Member 2 - **Prof. Udayaditya Sen**



Final approval and acceptance of this thesis is contingent upon the candidate's submission of the final copies of the thesis to HBNI.

I hereby certify that I/we have read this thesis prepared under my direction and recommend that it may be accepted as fulfilling the thesis requirement.

Date: 05-11-2019

Place: KOLKATA



Signature

Guide

Prof. Abhijit Chakrabarti
Head, C & MB Division
SAHA INSTITUTE OF NUCLEAR PHYSICS
Kolkata - 700 064

STATEMENT BY AUTHOR

This dissertation has been submitted in partial fulfillment of requirements for an advanced degree at Homi Bhabha National Institute (HBNI) and is deposited in the Library to be made available to borrowers under rules of the HBNI.

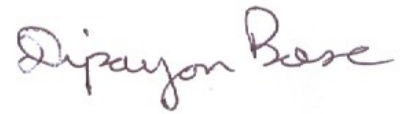
Brief quotations from this dissertation are allowable without special permission, provided that accurate acknowledgement of source is made. Requests for permission for extended quotation from or reproduction of this manuscript in whole or in part may be granted by the Competent Authority of HBNI when in his or her judgment the proposed use of the material is in the interests of scholarship. In all other instances, however, permission must be obtained from the author.

A handwritten signature in black ink that reads "Dipayan Bose". The signature is written in a cursive style with a large initial 'D' and 'B'.

Dipayan Bose

DECLARATION

I, hereby declare that the investigation presented in the thesis has been carried out by me. The work is original and has not been submitted earlier as a whole or in part for a degree / diploma at this or any other Institution / University.

A handwritten signature in black ink that reads "Dipayan Bose". The signature is written in a cursive style with a large initial 'D' and 'B'.

Dipayan Bose

List of Publications

In Thesis:

1. **Dipayan Bose**, Malay Patra & Abhijit Chakrabarti. Effect of pH on conformational stability, oligomerization and dynamics of erythroid and nonerythroid spectrin. (2017) *BBA Proteins & Proteomics*. 1865, 694 – 702.
2. **Dipayan Bose** & Abhijit Chakrabarti. Substrate specificity in the context of molecular chaperones. (2017). *IUBMB Life* 69, 647 – 659.
3. **Dipayan Bose** & Abhijit Chakrabarti. Localizing the chaperone activity of erythroid spectrin. (2019) *Cytoskeleton* 76(6), 383-397.
4. **Dipayan Bose**, Santanu Aggarwal, Sauvik Sarkar, Debashree Das, Chandravan Narayana & Abhijit Chakrabarti. Modulation of the peroxidase and catalase activity of heme proteins by erythroid spectrin. (manuscript communicated)
5. **Dipayan Bose** & Abhijit Chakrabarti. Chaperone potential of erythroid spectrin: effects of hemoglobin interaction, macromolecular crowders, phosphorylation and glycation. (2019) *BBA Proteins & Proteomics* 1867(11), 140267.
6. **Dipayan Bose** & Abhijit Chakrabarti. Spectrin Interactome under normal and HbE-disease conditions: possible role in red-ox regulation. (manuscript communicated)
7. **Dipayan Bose** & Abhijit Chakrabarti. Interaction of spectrin fragments with hemoglobin variants. (manuscript under preparation)

8. **Dipayan Bose** & Abhijit Chakrabarti. Probing the chaperone activity of erythroid spectrin (2019) Biophys J. 116(3), 191a.

Not included in Thesis:

1. Sauvik Sarkar, **Dipayan Bose**, Rajendra Giri, Mrinmay Mukhopadhyay & Abhijit Chakrabarti. Status of membrane asymmetry in erythrocytes: role of spectrin. (2018) Adv. Exp. Ed. Biol. 1112, 3 – 11.
2. Sauvik Sarkar, **Dipayan Bose**, Rajendra Giri, Mrinmay Mukhopadhyay & Abhijit Chakrabarti. Effects of GM1 on brain spectrin aminophospholipid interactions. (2019) Biochim Biophys Acta 1861, 298 – 305.
3. Kamini Mishra, Akriti Mishra, **Dipayan Bose**, Abhijit Chakrabarti & Puspendu K. Das. Adsorption of ADH on Gold Nanoparticle Surface: A Model Based Analysis versus Direct Measurement. (Manuscript communicated)
4. Sansa Dutta, **Dipayan Bose** & Abhijit Chakrabarti. Spectrin possesses a unique site for cytoskeletal drug binding. (under review)
5. **Dipayan Bose**, Sauvik Sarkar. & Abhijit Chakrabarti. Comparing the interaction of spectrin fragments with small unilamellar vesicles of aminophospholipids with different compositions. (Manuscript communicated).
6. **Dipayan Bose**, Sreetama Pal, Abhijit Chakrabarti & Amitabha Chattopadhyay. Organization and conformational dynamics of recombinant fragments of erythroid spectrin. (manuscript in preparation)



Dipayan Bose

Conferences attended

1. Annual Meeting of Indian Biophysical Society on *Molecules in Living Cells: Mechanistic Basis of Function*, Indian Institute of Science, Bengaluru, February 8-10, 2016. **Dipayan Bose**, Malay Patra & Abhijit Chakrabarti. Chaperone activity and ligand binding of erythroid spectrin at different pH.
2. 11th International Symposium on *Biochemical Roles of Eukaryotic Cell Surface Macromolecules* (11th ISCSM), IISER-Mohali, Chandigarh, February 24 – 28, 2017. **Dipayan Bose**, Udayaditya Sen and Abhijit Chakrabarti. Chaperone potential of spectrin and its recombinant fragments.
3. 9th Annual Meeting of Proteomics Society, India (PSI) & International Conference on *Proteomics in Health and Disease*, Institute of Life Science, Bhubaneswar, November 30 – December 2, 2017. **Dipayan Bose** and Abhijit Chakrabarti. Spectrin Interacting proteins in erythrocytes.
4. 63rd Annual Meeting of the Biophysical Society, BPS19, Baltimore, Maryland, USA, March 2-6, 2019. **Dipayan Bose** and Abhijit Chakrabarti. Probing the chaperone activity of erythroid spectrin.



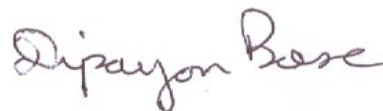
Dipayan Bose

DEDICATIONS

To my grandparents; in fond memory.

ACKNOWLEDGEMENTS

I would like to thank my guide, Prof. Abhijit Chakrabarti for his guidance and support over the years, and more importantly for allowing me the freedom to work independently. I would also like to acknowledge my lab members, Sauvik Sarkar and Sansa Dutta as well as my senior Dr. Debashree Das and my batch-mate Saran Chattopadhyaya. My thanks go to all the members of Crystallography & Molecular Biology Division, Chemical Sciences Division and Biophysics & Structural Genomics Division as well. It would be remiss of me to not thank my friends (you know who you are) and my family for their unwavering support.

A handwritten signature in black ink that reads "Dipayan Bose". The signature is written in a cursive style with a large initial 'D' and 'B'.

Dipayan Bose

CONTENTS

	Page. No.
Synopsis	xiii
List of Figures	xiv
List of Tables	xvii
Chapter 1: Introduction	1
1.1 The functions and properties of spectrin	4
1.2 The substrate specificity of molecular chaperones	4
1.2.1 Chaperone Specificity	6
1.2.1.1 General Chaperones	7
1.2.1.2 Specialized Chaperones	19
1.2.2 Discussions	25
1.3 Objectives	32
References	33
Chapter 2: The effect of pH on chaperone activity	53
2.1 Introduction	54
2.2 Materials and Methods	57
2.2.1 Isolation and purification of erythroid and non-erythroid spectrin	57
2.2.2 Characterizing conformational alterations of spectrin by tryptophan fluorescence	58
2.2.2.1 Intrinsic tryptophan fluorescence and anisotropy measurement	58
2.2.2.2 Steady state tryptophan fluorescence life time measurements	59
2.2.3 Circular Dichroism (CD) measurements	59
2.2.4 Tryptophan fluorescence quenching experiments	59

2.2.5 Determining the size of spectrin at different pH	60
2.2.5.1 Static light scattering measurements	60
2.2.5.2 Dynamic light scattering measurement	60
2.2.6 Determining pH induced conformational alteration of spectrin by fluorescent dye labeling	61
2.2.6.1 Pyrene Modification of erythroid and non-erythroid spectrin	61
2.2.6.2 Thioflavin –T (ThT) binding assay	61
2.2.6.3 ANS binding assay	62
2.2.7 Determining the stability of spectrin by urea induced unfolding at different pH	62
2.2.8 Effects of spectrin at different pH on prevention of protein aggregation	62
2.3 Result and Discussion	63
2.3.1 Conformational Alterations Probed by Intrinsic tryptophan Fluorescence	64
2.3.2 Changes in Secondary Structure Monitored by Far-UV CD	68
2.3.3 Evaluation of Trp Accessibility by Acrylamide Quenching	71
2.3.4 Detection of oligomeric spectrin by light scattering measurement	72
2.3.5 pH induced conformational alteration of spectrin monitored by pyrene and thioflavin T fluorescence	75
2.3.6 Detection of Exposed Hydrophobic Clusters by ANS Binding	78
2.3.7 Urea induced denaturation at different pH	79
2.3.8 pH dependent chaperone activity	82
Abbreviations	85
References	85
Chapter 3: The effect of post-translational modifications, phospholipid, hemoglobin binding and macromolecular crowders	92

3.1 Introduction	93
3.2 Materials and Methods	96
3.2.1 Isolation and purification of hemoglobin	96
3.2.2 Small unilamellar vesicle (SUV) preparation	97
3.2.3 Glycation of spectrin	98
3.2.4 Phosphorylation of spectrin	98
3.2.5 Protein aggregation assay	99
3.2.6 Enzyme refolding assay	100
3.2.7 AFM imaging	100
3.3 Results and Discussion	101
3.3.1 Effect of hemoglobin vs. non-specific crowder	101
3.3.2 Effect of phospholipid SUVs	104
3.2.3 AFM imaging	108
3.2.4 Spectrin glycation	110
3.2.5 Spectrin phosphorylation	112
3.2.6 Discussions	115
Abbreviations	119
References	119
Chapter 4: Localization and molecular origin of chaperone potential	127
4.1 Introduction	128
4.2 Materials and Methods	131
4.2.1 Isolation and purification of human Hemoglobin constituent α and β chains	131
4.2.2 Expression isolation and purification of recombinant spectrin domains	132
4.2.3 Characterization of spectrin fragments	134

4.2.4 Binding of fluorescent probes	135
4.2.5 Assay of protein aggregation	137
4.2.6 Folding of denatured enzymes	138
4.3 Results and Discussion	139
4.3.1 Expression and characterization of spectrin domains	139
4.3.2 Binding of fluorescent ligands	150
4.3.3 Assay of chaperone activity	158
4.3.4 Discussions	163
Abbreviations	168
References	169
4.4 Appendix Interaction of spectrin fragments with hemoglobin variants	179
Chapter 5: Interactors of spectrin and its biochemical significance	182
5.1 Introduction	183
4.2 Materials and Methods	186
5.2.1 Fluorescence binding study of spectrin with heme proteins	187
5.2.2 Peroxidase and catalase activity measurement of heme proteins	188
5.2.3 Effect of spectrin on enzyme activity of heme proteins	190
5.2.4 Assay of lipid peroxidation by TBA method	191
5.2.5 Raman spectra of heme proteins and hemin in presence and absence of spectrin	191
5.3 Results and Discussion	192
5.3.1 Determination of binding dissociation constants using fluorescein-conjugated spectrin	192
5.3.2 Determination of liner range of enzyme activity and MM constants	194
5.3.3 Effect of spectrin on enzyme activity	199

5.3.4 Assay of lipid peroxidation	204
5.3.5 Raman spectra of heme proteins and hemin	205
5.3.6 Discussions	207
Abbreviations	213
References	213
5.4 Appendix Interactome of spectrin under normal and HbE-disease conditions: possible role of spectrin in red-ox regulation	222
Chapter 6: conclusions	232
6.1 Conclusions	233
6.2 Future perspectives	240
7 Supporting Information	241

Synopsis

Spectrin, the major protein of the RBC membrane skeleton has canonically been thought to only serve a structural function. We have described a novel chaperone-like property of spectrin and have shown that it is able to prevent the aggregation of other proteins such as alcohol dehydrogenase, insulin and free globin chains. Moreover this chaperone activity is pH linked with spectrin displaying higher oligomeric states and consequently increased chaperone activity at lower pH, with maxima at pH 4.0. Hemoglobin and other heme proteins are implicated as clients of the chaperone activity of spectrin and we have demonstrated that as a consequence of spectrin-heme protein interaction, there is an increase in the enzymatic activity of these heme proteins. The peroxidase activities of hemoglobin, hemoglobin variants, free globin chains, cytochrome-c and hemin increase upon spectrin binding, as does the enzymatic activity of catalase. The K_m values of these heme proteins for H_2O_2 decreases in presence of spectrin while the V_{max} values are found to increase. Raman spectroscopy indicates spectrin binding induced conformational changes in the prosthetic heme groups of these proteins as the source of increased enzymatic activity. We have also found that the chaperone-like activity of spectrin competes with its phospholipid/hemoglobin binding ability and phospholipid/hemoglobin bound spectrin is a comparatively weaker chaperone. Non-enzymatic glycation has also been shown to decrease spectrin chaperone potential. We have tried to localize the molecular origin of chaperone-like activity in multi domain spectrin by cloning and investigating individual domains and our current understanding points to the presence of hydrophobic patches on the surface of these domains as the source of the chaperone activity of spectrin as notably seen in the self-association domain.

List of Figures:

Figures	Page No.
1.1: Chaperone function in a generalized cell.	28
1.2: Number of chaperone genes in humans.	30
2.1: SDS-PAGE of erythroid and non erythroid spectrin.	63
2.2: Fluorescence spectra of erythroid and non-erythroid spectrin.	64
2.3: Fluorescent parameters of erythroid and non-erythroid spectrin.	66
2.4: CD spectra of erythroid and non-erythroid spectrin.	69
2.5: Mean residual ellipticity.	70
2.4: CD spectra of erythroid and non-erythroid spectrin.	71
2.7: Dynamic and static light scattering of spectrin isoforms.	73
2.8: DLS profile of spectrin isoforms.	74
2.9: Pyrene fluorescence.	76
2.10: Th-T fluorescence.	77
2.11: ANS fluorescence.	79
2.12: Urea denaturation.	80
2.13: pH dependent chaperone activity.	83
3.1: Chaperone activity of spectrin in presence of BSA, PVP40 & HbA.	102
3.2: Chaperone activity of spectrin in presence of lipids.	105
3.3: AFM image of insulin aggregates in presence and absence of lipid ± spectrin.	109

3.4: Spectrin glycation.	110
3.5: Spectrin phosphorylation.	113
4.1: Plasmid map.	133
4.2: Spectrin domains.	139
4.3: SDS-PAGE of spectrin fragments.	140
4.4: Emission spectra of spectrin domains.	143
4.5: Elution profile of spectrin domains.	146
4.6: CD spectra of spectrin domains.	148
4.7: CD spectra under urea unfolded condition.	149
4.8: Prodan binding.	150
4.9: ANS binding to reconstituted self-association domain.	153
4.10: ANS binding to spectrin domains.	155
4.11: Scatchard plots of ANS binding.	156
4.12: Insulin aggregation in presence of BSA.	158
4.13: Chaperone activity of spectrin domains.	160
4.14: Reactivation of alkaline phosphatase.	162
4.15: K_d determination using FITC.	180
5.1: Spectrin binding to cytochrome-c.	193
5.2: Linear range and MM curve of hemoglobins.	195
5.3: Linear range of cytochrome-c, catalase, hemin; MM curve of cytochrome-c.	197
5.4: Effect of spectrin on enzyme activity of hemoglobins.	200
5.5: Effect of spectrin on enzyme activity of catalase, cytochrome-c & hemin.	201
5.6: Peroxide mediated deactivation.	203
5.7: Lipid peroxidation.	204

5.8: Raman spectra of hemoglobins and cytochrome-c.	206
5.9: Raman spectra of hemin.	207
5.10: SDS-PAGE of different fractions.	223
5.11: Representative elution profile.	224
5.12: Different classes of spectrin interactors.	226
6.1: pH dependent chaperone activity of spectrin.	235
6.2: Chaperone activity of spectrin in presence of interactors and modifications.	236
6.3: Chaperone activity of spectrin domains.	238
6.4: Spectrin induced enzyme activity modulation of hemoglobin (Hb).	239

List of Tables:

Tables

	Page No.
1.1: Summary of the substrate specificities of general chaperones.	7
1.2: Summary of the substrate specificities of specialized chaperones.	19
2.1: Urea denaturation parameters of spectrin isoforms.	81
4.1: Spectrin fragments, sequence and molecular weight.	141
4.2: Fluorescence parameters of spectrin domains.	144
4.3: Prodan binding parameters.	152
4.4: ANS binding parameters.	156
4.5: K_d values.	179
5.1: K_d values.	193
5.2: MM parameters.	198
5.3: Major spectrin interacting proteins.	227

Chapter 1:

Introduction

Spectrin is a hetero-dimeric protein composed of α and β subunits and is the major component of the membrane skeleton of all metazoan cells examined till date. It is a multi-domain protein composed mostly of tandem repeats of homologous motifs of α -helical 'spectrin repeat domain' units. It is most widely known and characterized in mammalian erythrocytes and neurons (1).

In erythrocytes, a network of spectrin oligomers cross linked with short actin filaments is bound to the membrane and makes up the membrane skeleton and provides stability to the cell membrane (2). Erythrocyte spectrin is coded by two genes, SPTA1 (UniProt [P02549](#)) for α I spectrin and SPTB (UniProt [P11277](#)) for β I spectrin. Spectrin is present on the intact cell membranes as a tetramer, which is formed by the "head-to-head" association of two hetero-dimers, comprising of a α subunit and a β subunit with molecular masses of 280 kDa and 246 kDa respectively (3). Both the subunits consist mostly of tandem repeats of spectrin repeat domains, each approximately 106 residues in length with about 30% identity and are aligned in an anti-parallel side to side orientation to give a flexible rod-shaped molecule (4,5). The spectrin repeat domains are folded into coiled coil of three anti parallel left handed helices which are connected through a helical linker. 90% of the intact spectrin molecule is made up of these 3-helix repeat (usually 20 in α - and 17 in β -chains)(6,7). The X-ray structure of a single repeat motif shows that the 3-helix bundles are stabilized through hydrophobic interaction between the interior hydrophobic surfaces and electrostatic interactions between the charged surfaces (8). The last helix of the first domain is seen to form a continuous helix with the first helix of second repeat domain. The cooperativity of these spectrin domains has been attributed to the presence of linking helical property. These structural features of spectrin are thought to be the origin of its ability to expand and contract with mechanical stress.

Non-erythroid spectrin or brain spectrin found in neurons is very similar in structure but has less defined function and the two spectrin species are quite different in terms of their structure and stability (9). Brain spectrin is coded by SPTAN1(UniProt [Q13813](#)) for α II spectrin which has many isoforms and SPTBN1 (UniProt [Q01082](#)), SPTBN2 (UniProt [O15020](#)), SPTBN4 (UniProt [Q9H254](#)) and SPTBN5 (UniProt [Q9NRC6](#)) for β II-V spectrin which have their respective isoforms. While erythroid spectrin is predominantly a dimer *in-vitro* non-erythroid spectrin exists as a tetramer and it is seen that non-erythroid spectrin forms tetramer about 15 times stronger than erythroid spectrin (10). Structural data shows that the tetramerization site or the self-associating domain of erythroid spectrin is different from that of non-erythroid spectrin (11,12). Also it is seen that non-erythroid spectrin is more rigid and thermally stable than erythroid spectrin and interacts more strongly with anionic lipid membranes.

Spectrin is capable of oligomerization by sequential addition of dimers, this process can be called 'indefinite'; that is, the association process appears to have no limit. It involves opening up of the lateral interactions between the helices of each individual 3-helix bundle and the formation of a new 3-helix bundle with two helices being contributed from one peptide chain and one from the other (13). Another mechanism of oligomer formation of spectrin exists where the spectrins are cross-linked by protein 4.1 and actin (14). Oligomers larger than the tetramer have been reported in electron microscopic, non-denaturing gel electrophoresis and sedimentation equilibrium studies (15,16).

Various spectroscopic and physical studies have shown that spectrin is a highly dynamic protein with multiple classes of internal segmental motions that give rise to its unique mobility and flexibility necessary for its function.

1.1 The functions and properties of spectrin

Spectrin is a multi-functional protein with a host of functions associated with it. Here are listed the functions and properties of spectrin which form the starting point of this thesis.

- Spectrin is the major functional component responsible for maintaining cell membrane elasticity and strength in erythrocyte (17-19).
- Spectrin interacts with membrane phospholipids directly (20-23).
- Spectrin can specifically bind to hydrophobic ligands (24-26).
- Spectrin can bind hemoglobin and other heme containing proteins (27-29).
- Spectrin can act as a chaperone (30,31).

Keeping in mind that spectrin has chaperone like properties, it is interesting to note that the 'spectrin-repeat' domains share structural and sequence similarity to AHSP (α hemoglobin stabilizing protein), a major RBC resident chaperone specific to only one substrate i.e. α -globin (32,33). As such a pertinent question to ask is if spectrin also possesses substrate specificity towards α -globin. Moreover a broader question becomes whether or not chaperones in general have specific substrates in the same sense as enzymes do. What does substrate specificity mean in the context of molecular chaperones?

The next segment of this thesis tries to answer that question.

1.2 The substrate specificity of molecular chaperones

The term "Molecular Chaperone" was coined by Ellis in 1987 (34,35) to describe the function of the Rubisco large subunit binding protein. In time this term came to denote all those proteins that assist other proteins to reach their native conformations and maintain it. Currently, molecular chaperones are defined as a set of conserved, unrelated protein families

that possess the ability to recognize and selectively bind non-native states of cellular proteins under physiological and stress conditions. Alternately they may be defined as proteins that assist the correct non-covalent assembly/folding of other proteins in-vivo but which themselves are not part of the final product during normal biological functions (36).

Chaperones prevent irreversible aggregation reactions and keep proteins on the productive folding pathway and also facilitate the folding of nascent polypeptides and their partially folded intermediates, as well as assist in their association into functional oligomers (37). On a broader scale chaperones also assist any changes in the degree of either folding or association of a protein when it is transported across a membrane, or is repaired or destroyed (38).

In view of the immense importance of chaperones, their mechanisms of action and structures have been thoroughly investigated and reviewed (39-43). However not much work has been done to address the question of chaperone substrate specificity.

Biological interactions are driven by specific recognition between interacting partners, the definitive example being enzyme-substrate recognition. As such it is important to question what specificity means in the context of molecular chaperones: do chaperones have specific substrates?

It is seen that every cell possesses multiple chaperone families each with several members. It would be logical to conclude that there must be differences in the substrates of these chaperones since if chaperones did not have substrate specificity and could recognize non-native conformations of proteins as a whole, having multiple kinds of chaperones in a cell would be an unnecessary energetic burden. It is seen that not all chaperones are equally essential to a cell, for example trigger factor in *E. coli* can be mutated without causing cell lethality (44), conversely *E. coli* cells with a mutation in the GroEL chaperone showed

temperature sensitive cell death (45), proving that some chaperones are indispensable. Thus while there is an overlap between the substrates of chaperones as in the case of trigger factor and DnaK (46), chaperones also seem to have substrates that are specific to them as in the case of GroEL. Moreover some chaperones are known to have only one specific client protein, showing that general recognition of non-native proteins is not sufficient in all cases and that substrate specificity justifies the added energetic cost of having extra chaperones (47).

A further complication to the issue of substrate specificity is that multiple mechanisms may be used even by a single chaperone to aid substrate folding. This effectively increases the substrate pool of a chaperone as it can select its mechanism of action in a substrate dictated manner and bind substrates that it could not have with just one mode of action (48). For example GroEL binds proteins it cannot accommodate into its central cavity by its apical lids (49).

Thus the importance of the importance of the question of substrate specificity of chaperones becomes abundantly clear.

There is not much data available on the substrate specificity of chaperones; most studies have been performed using model proteins.

1.2.1 Chaperone Specificity

Chaperones are typically grouped into families depending on sequence homology and phylogenetic analysis. For the sake of convenient comparison we have arbitrarily grouped chaperones into two broad classes, namely - 'general chaperones' i.e. those that have very broad substrate specificity and perform generalized functions and, 'specialized chaperones'

i.e. those that have only one/particular kind of substrate or those that perform some specific specialized function in the cell.

1.2.1.1 General Chaperones

They include the classical chaperone families, have broad substrate range and perform generalized functions; they are listed in **Table 1.1**.

Table 1.1: Summary of the substrate specificities of general chaperones.

Chaperone Family/ Type -	Representative Chaperone(s) -	Substrate(s) -	Recognition Motif -
Hsp70	Mammalian- HSC70/HSP73, HSP72, BiP/Grp78, mHSP70/Grp75. Yeast- Ssa1-4, Ssb1-2, Kar2. <i>E. coli</i> - DnaK (50).	Binds partially folded or unfolded proteins, usually not native proteins except in some cases like clathrin and ζ^{32} (51,52). Does not interact with short lived partially folded intermediates with lifetimes below a threshold value (40,53). Substrate specificity of HSP70 is greatly	For DnaK- Recognizes hydrophobic amino-acids like Ile, Phe, Leu and Val (57). Two classes of amino-acid binding sites present, one recognizes aliphatic and the other aromatic residues (58,59). Recognition motif consists of a 4-5 residue hydrophobic core enriched in Ile, Val, Phe and Tyr, flanked by basic amino-acids. Acidic residues

		<p>modulated by co-chaperone HSP40 binding and binding of other proteins such as Hip (54-56).</p>	<p>are excluded from the core and disfavoured in the flanking sequence. Such recognition sites occur statistically every 36 residues in proteins and remain buried in native conformations (60,61).</p> <p>For BiP- BiP binds peptide sequences in an extended conformation with alternate hydrophobic and aromatic residues and also interacts with the side chains of the amino acids in the binding sequence (62,63).</p>
HSP40	<p><i>E. coli</i>- DnaJ. Yeast- Mdj1, Ydj1 (64,65).</p>	<p>Binds denatured proteins like firefly luciferase and rhodanase and is also known to interact with some native proteins such as</p>	<p>For DnaJ- Shares majority of binding peptides with DnaK even though binding motif is different. Binding site consists of hydrophobic core</p>

	<i>Drosophila</i> - dHdj1.	σ^{32} -transcription factor (66). May be required for ubiquitin mediated degradation of abnormally folded proteins.	of 8 residues enriched in aromatic and relatively larger aliphatic residues and arginine (67). DnaJ can bind both D- and L- amino acids and interact with the side chains of amino acids allowing it to scan hydrophobic protein surfaces and bind to non-native proteins (40). For dHdj1- Recognises expanded polyglutamine repeats in toxic mutant proteins (68).
HSP60	Eukaryotes- TCP1/CCT/TRiC, Rubisco large subunit binding protein. E. coli-	GroEL can only accommodate proteins of 40-50kDa size by itself but incorporate up to 60kDa proteins when it is complexed with GroES (69).	For GroEL- Hydrophobic, β -sheet forming amino acids Ile, Phe, Val, Leu and Trp have been shown to have the strongest interaction. Also interacts with α -helix forming amino

	GroEL (50).	TRiC has been shown to bind multidomain proteins and beta-strand rich regions of proteins that are slow folding and are prone to aggregation (70). It binds to actin, tubulin and WD40 β -propeller proteins (71,72).	acids Glu, Ala, Gln, and His (73,74).
HSP90	Eukaryotic- HSP90, Grp94. <i>E. coli</i> - HtpG (75).	Binds late folding intermediates and intrinsically disordered proteins. Binds proteins that have greater difficulty reaching their native conformations. It is also seen that under stress conditions the substrate range of HSP90 expands over that in normal conditions in-vivo. In-	For HSP90- Two chaperone sites located at the N- and C-terminal are present. The C-terminal fragment binds partially folded proteins in an ATP-independent way. The N-terminal domain contains a peptide binding site that preferentially binds peptides longer than 10 amino acids and peptide release is ATP dependent (79). A 106-Å

		<p>vitro HSP90 shows a more general function.</p> <p>Binds cytoskeletal elements, signal transduction proteins, steroid hormone receptor and protein kinases and Tau protein (76,77).</p> <p>HSP90 interactions are modulated by co-chaperones, of which, GCUNC45 can even show α/β isoform specificity (78).</p>	<p>long substrate-binding interface is present on the Hsp90 surface which enables many low-affinity contacts. This allows recognition of scattered hydrophobic residues in late folding intermediates that remain after early burial of the Hsp70 sites (80).</p>
HSP100	<p>Eukaryotic-HSP104.</p> <p><i>E. coli</i>-ClpA, ClpX (81).</p>	<p>Eukaryotic HSP104 binds to and dissolves lower order aggregated proteins <i>in vivo</i> and <i>in vitro</i> (82). Prokaryotic ClpA and ClpX bind proteins targeted for</p>	<p>For ClpX- It preferentially binds to hydrophobic amino acids in the target protein (84).</p>

		<p>degradation; in conjunction with ClpP protease they mediate ATP dependent unfolding of target protein. ClpX also interacts with lambda-O protein (83).</p>	
sHSPs	Eukaryotic- α – crystallin (85).	<p>High affinity binding to partially folded intermediates (86,87). Specific towards proteins that aggregate in a nucleation dependent manner (88). Do not refold bound proteins but act as substrate pools for HSP70.</p>	Binding motif is not clearly defined for sHSPs.
SecB like prokaryotic chaperones	<i>E. coli</i> - SecB	Binds polypeptides that fold slowly, and maintains precursors of exported proteins in a partially unfolded state	For SecB- The binding motif is about 9 amino-acid residues long and is enriched in aromatic and basic residues and acidic

		fit to be transported by SecA (89).	residues are disfavored. Statistically SecB binding motifs occur every 20–30 residues (90). SecB does not recognize signal sequences.
Extra-cellular secreted chaperones	Mammalian-Clusterin & Haptoglobin.	Clusterin binds to and protects stress induced denatured proteins via ATP independent mechanism. It cannot refold them and acts as a substrate pool for HSP70 (91). It is specific for slow aggregating proteins (92). Haptoglobin binds and protects proteins denatured by heat or oxidative stress. It is most active at mildly alkaline pH (93).	Binding sequences are not known.
Peptidyl Prolyl	Eukaryotic-	PPIs act as chaperones independent of their	Binding sequences are not

<p>Isomerase (PPI)</p>	<p>Cyclophilin, RanBP2. <i>E. coli</i>- FkpA (94), Trigger Factor (TF). <i>Drosophila</i>- NinaA.</p>	<p>enzyme activity (95). Cyclophilin Cyp-40 acts as a chaperone in the steroid aporeceptor complex (96). RanBP2 is a chaperone for red/green opsin and NinaA is a more general opsin chaperone (97). FkpA has been proposed as a chaperone for envelope proteins in the bacterial periplasm. TF binds to and maintains the precursors of secretory proteins in a translocation competent form; substrate pool overlaps with DnaK (98).</p>	<p>well known in general. For TF- Binding motif is an eight residue stretch enriched in basic and aromatic amino acids with a net positive charge; interaction with ribosome is needed for productive interaction with polypeptides (99).</p>
<p>Protein Disulfide Isomerase (PDI)</p>	<p>Mammalian- PDI, ERp57. Yeast-</p>	<p>Can act as chaperones independent of enzyme activity (101,102). Has been shown to bind</p>	<p>While there is some data regarding the binding motif of PDI in regard to its enzyme activity, the binding</p>

	Eug1p (100).	GADPH, rhodonase, citrate synthase and lysozyme (100,103). PDI has also been shown to act as a redox dependent chaperone and unfold cholera toxin (104).	motif for its chaperone function remains unclear. It is also shown that individual members of the PDI family prefer different substrates but this too is in regard to their enzymatic activity. (105).
Translation linked chaperones	Eukaryotes- Nascent polypeptide associated complex (NAC). Signal Recognition Particle (SRP). Human- TRC40/Asna-1. Yeast- Get3. Plants- ArsA1/2.	Bind nascent polypeptides as they emerge from the ribosome. NAC is a general chaperone while SRP mostly binds signal sequences that are specific to ER delivery and not cytosolic or mitochondrial proteins (106). TRC40/Asna-1 recognizes the trans-membrane domain (TMD) of tail anchored proteins (TA) and	For SRP- Binding motif is hydrophobic in nature such as N-terminal signal sequences and trans-membrane domains of nascent polypeptides. For NAC- It can bind very short nascent chain and three subunits of NAC have different specificities for features on the nascent chain (106).

		<p>delivers them to the ER (107). Get3 also recognized TMDs of TAs in yeast (108). In plants Arsa1 is responsible for the insertion of TOC34 into the chloroplast membrane in a TMD dependent manner and Arsa1/2 are also shown to help in TA insertion into membranes in a more general way (109,110).</p>	
N/A	Eukaryotic-Calnexin, Calreticulin.	<p>Both recognize early processing intermediates of glycoproteins, specifically N-linked monoglucosylated proteins where the glycan is present within fifty residues of the N-terminal of the</p>	<p>For Calreticulin-Binding motif is five residues long, enriched in hydrophobic amino acids. Presence of hydrophilic amino-acids diminishes binding (114). Interaction with N-glycosylated polypeptides is mediated by the glycan</p>

		<p>polypeptide. Divalent metal ions play important role in substrate binding. Calreticulin plays a role in folding of class I MHC (111-113).</p>	<p>Glc₁Man₇₋₉GlcNAc₂ (115,116).</p>
<p>YidC/Alb3/ Oxa1 family of insertases</p>	<p>Prokaryotic- YidC. Eukaryotic- Alb3, Oxa1.</p>	<p>Function as membrane chaperones and help newly synthesised proteins fold into the membrane bi-layer (117). Oxa1 acts as a chaperone for Cox2 and Alb3.2 acts as a chaperone for PSII (118).</p>	<p>Not clearly defined.</p>
<p>N/A</p>	<p>Human- DJ-1.</p>	<p>High affinity for α-synuclein. Redox active protein active in oxidative cytoplasmic environment (119). It is also a copper chaperone acting on SOD1</p>	<p>Not clearly defined.</p>

		activation (120). Also implicated as a chaperone for MAP1b-LC (121).	
N/A	Mammalian- α_s -casein.	Protects wide variety of proteins against thermal, chemical or light induced aggregation in vitro (122).	Not clearly defined.
N/A	Mammalian- Tubulin.	Acts as a chaperone for a number of unrelated proteins like ADH, insulin and protects them against thermal and non-thermal aggregation in vitro (123).	Not clearly defined.
Bacterial periplasmic chaperones	E. coli- Spy, SurA, Skp and DegP.	Spy is a periplasmic chaperone that stabilizes a broad range of substrates under stress and is abundantly produced in spheroplasts (124,125). SurA, Skp	Not clearly defined.

		and DegP are involved in the membrane insertion of a major class of outer membrane proteins (OMPs) - the integral β -barrel proteins (126-128).	
--	--	---	--

1.2.1.2 Specialized Chaperones

Some chaperones though have a narrow substrate range sometimes even one substrate. They are listed in brief in **Table 1.2**.

Table 1.2: Summary of the substrate specificities of specialized chaperones.

Chaperone Family/ Type-	Representative chaperone(s)-	Substrate(s) -	Recognition Motif -
Prokaryotic secretion chaperones.	<i>E. coli</i> - PapD. <i>Shigella flexneri</i> - Spa15. <i>Yersinia</i> - Syc..	PapD – specific for pilus subunits (129,130). Spa15 - broad substrate specificity (131). Syc – specific for cognate Yop proteins (132).	Not clearly defined.

Histone chaperones	<p>Eukaryotes-</p> <p>Nucleoplasmin, N1/N2 proteins, CAF-1, Asf1, HIRA, NASP.</p>	<p>Specific for cognate histone, selectivity based on type of histone and post translational modification.</p> <p>Asf1, CAF-1, N1/N2 proteins- specific for histone H3/H4 (133,134).</p> <p>NASP- specific for histone H1 (135).</p> <p>Nucleoplasmin- specific for histone H2A and H2B (136).</p>	Not clearly defined.
Proteasomal assembly chaperones	<p>Mammalian-</p> <p>P28, S5b, p27, PAC1-4, UMP1.</p> <p>Yeast-</p> <p>Nas2, Hsm3, Nas6, Rpn14, Adc17.</p>	<p>PAC1-4 - bind to and promote the correct assembly of the alpha rings of the 20S subunit of the 26S proteasome.</p> <p>UMP1- binds to the beta subunit containing complex of the 20S proteasome (137-139).</p> <p>p28, S5b, p27- specific for</p>	Not clearly defined.

		<p>Rpt3, Rpt1 and Rpt5 proteins of the 19S proteasomal subunit (140).</p> <p>Nas2- specific for Rpt4, Rpt5 (141).</p> <p>Adc17- specific for Rpt6 (142).</p>	
N/A	Mammalian- HSP47	<p>Specific for collagen.</p> <p>Regulates procollagen chain folding and assembly by binding to pro-alpha1N propeptide until correct C-terminal associations have been made to yield the collagen triple helix (47,143)</p>	<p>The binding motif is Yaa-Gly-Pro-Arg-Gly where Yaa is either Thr or Pro to give high affinity binding.</p> <p>Moreover correct folding and 3D structure of procollagen is needed for</p>

			HSP47 binding (144).
N/A	Mammalian- Receptor-associated protein (RAP)	Specific for low-density lipoprotein receptor-related protein or LPR (145).	Not clearly defined.
Ubiquitinated protein chaperones	mammalian- VCP/p97. Yeast- CDC48.	VCP – specific for HDAC- ubiquitin complexes & multi-ubiquitin chains; targets the ubiquitinated substrates to the proteasome (146). CDC48 - binds to only ubiquitinated p90 and preferentially ubiquitinated substrates (147).	Not clearly defined.
N/A	Eukaryotic- UNC45.	Specific for Myosin. Also can interact with HSP90 and act as a co-chaperone (148).	Not clearly defined.

MHC chaperones	Mammalian- TAP, tapasin, HLA-DM.	TAP, tapasin – specific for class I MHC (149). For HLA-DM - Class II MHC (150).	Not clearly defined.
N/A	E. coli- HSC66/HSC20.	Fe/S template protein IscU in <i>E. coli</i> .	For HSC66- Prefers binding to peptides with centrally located Pro-Pro motifs. Interacts specifically with an invariant region comprising of residues 99–103 (LPPVK) of IscU (151).
Haemoglobin chaperones	Human- Alpha Haemoglobin Stabilizing Protein	AHSP- specific for α -globin chain of haemoglobin, binding seems to be	Not clearly defined.

	(AHSP), Spectrin.	dependent on the redox state of α -Hb (152) (153). Spectrin- proposed as an α -globin chaperone (29-31).	
N/A	Human- HYPK.	Specific for huntingtin (47,154). It is also able to prevent the aggregation of ADH (154).	Binds to N-terminal 17 amino acids of huntingtin (155).
N/A	<i>Pseudomonas</i> - Lim.	Specific for prelipase produced from lipA, converts prelipase to its active form (156).	Not clearly defined.
N/A	Prokaryotic- ExbB.	Specific for TonB (157)	Not clearly defined.
N/A	Eukaryotic- Tim9/10.	Specific for hydrophobic proteins of the mitochondrial inner	Not clearly defined.

		membrane (158).	
N/A	Eukaryotic- Tubulin cofactors A- E, Arl2.	Near native tubulin α , β subunits formed after interaction with TriC (47,159) .	Not clearly defined.
N/A	Human- Adenovirus 100K protein.	Major capsid protein hexon (47,160).	Not clearly defined.

1.2.2 Discussions

The picture that emerges is that the vast majority of chaperones do not have specific substrates in the sense that enzyme do. Substrate recognition is not mediated by complimentary surface recognition; in fact in some cases substrate binding happens in an extended conformation like in the case of BiP. Chaperones recognize conformations of their substrate that are non-native.

The majority of chaperones recognize these non-native conformations by recognizing hydrophobic patches exposed when proteins are structurally perturbed as for example in the case of HSP70, HSP60, HSP90 and HSP40. The exact identity of these patches is different from one chaperone to the other. For example DnaK recognizes motifs 4-5 amino acids in length composed of hydrophobic amino acids while Bip recognizes motifs with alternating hydrophobic and aromatic amino acids. Moreover the length of these recognition motifs

varies between chaperones; for example 4-5 residues for DnaK and 8 residues for DnaJ. These binding motifs thus have a different statistical chance of occurring within any given protein, for example the SecB binding motif occurs 20-30 times while the DnaK binding motif occurs 36 times in a given protein. Based on the exact nature of the binding motif and the statistical chance of occurrence of the motif the substrate pools for the different chaperones get delineated giving rise to specificity of substrate binding. The co-chaperones that interact with a given chaperone are major dictators of their specificity, HSP40 is well known for being a co-chaperone of HSP70 and modulating its substrate binding (55). Proteins that have to be kept in a non-native fold competent for translocation across membranes are also major chaperone clients and are specific to chaperones that recognize translocation signals such as SecB.

Some chaperones also recognize binding motifs that are charged, for example TF binds to motifs with a net positive charge and histone chaperones bind to histones which are positively charged. Presence of the correct charge on the binding motifs also should separate the substrate pools of chaperones.

In addition to binding motifs chaperones may also recognize post-translational modifications such as glycosylation and ubiquitination thereby creating a specific substrate pool as in the case of Calnexin and CDC48 respectively.

Another factor that leads to varying substrates of chaperones is their size and by extension the size of the substrate they can interact with; for example prokaryotic GroES has a cavity 40-50kDa in size by itself or 60kDa with GroEL and can only accommodate substrates up to that size. This is further corroborated by the fact that multimeric proteins like tubulin are usually major clients of HSP60.

Sub-cellular localization also has a major role to play in defining the substrate specificity of chaperones- for example HSP60 is not present in the ER, so cannot act as a chaperone for proteins targeted there or synthesized there. Similarly Tim9/10 is resident on the mitochondrial membrane and as a result their substrate pool is constrained by it.

Also the folding nature of proteins dictate the chaperones that they bind to; proteins that are fast folders interact with HSP70 as the HSP70 motifs are buried early in the hydrophobic protein core, conversely HSP90 usually binds to those proteins that are slow folders and need more chaperone assistance even after they have interacted with HSP70. Chaperones also show specificity towards the nature of aggregation they prevent, for example α -crystallin is specific for the proteins that aggregate in a nucleation dependent manner.

The emerging view of chaperone substrate selection is thus a network where chaperones select substrates based on recognition motifs, sub-cellular localization, post-translational modification and folding nature of the protein. A schematic view of chaperone action in a generalized cell is provided in **Figure 1.1**.

Figure 1.1: Chaperone function in a generalized cell.

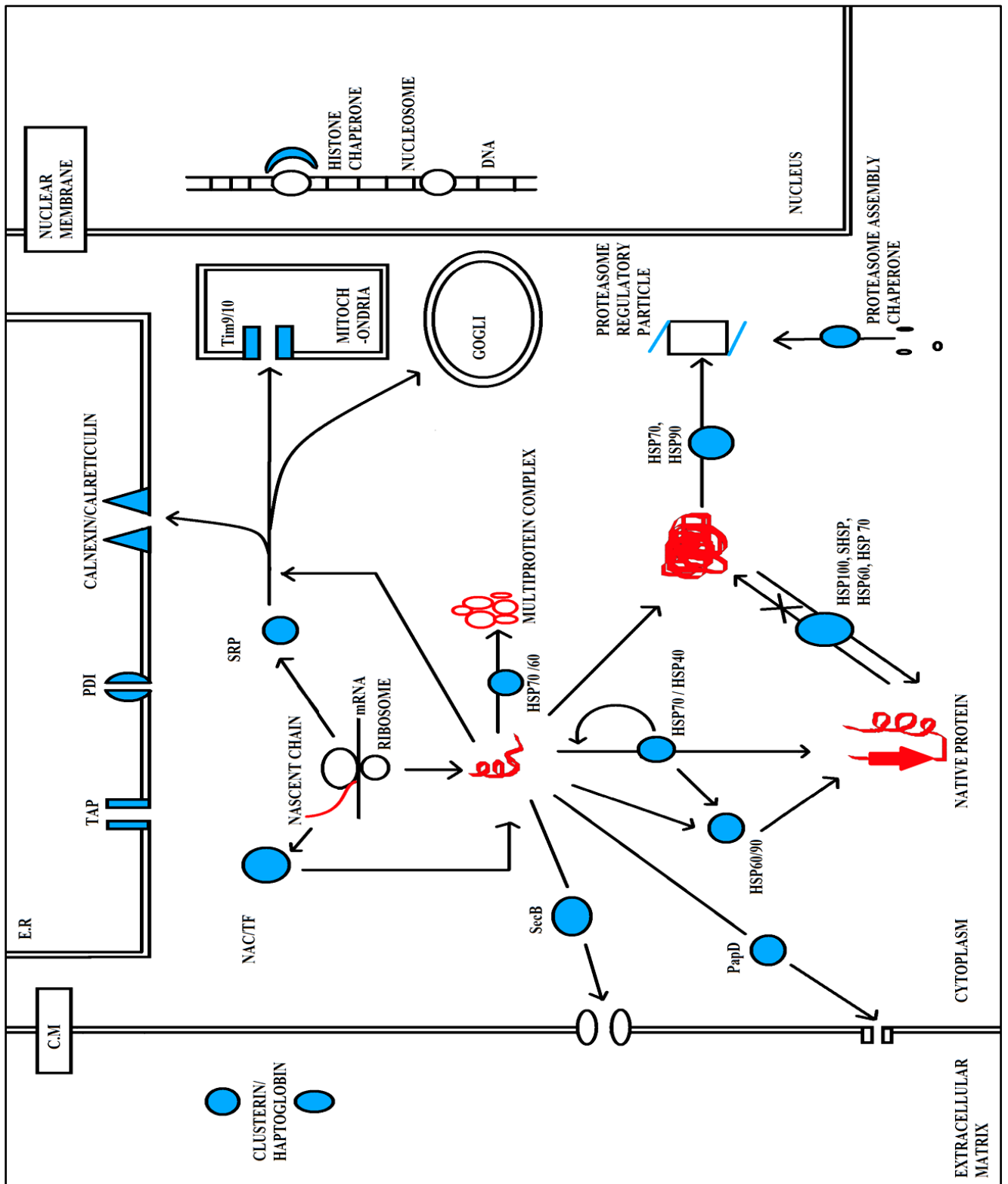


Figure 1: Diagrammatic representation of the chaperone function in a generalised cell. The different families of chaperones are shown in the major pathways they function in.

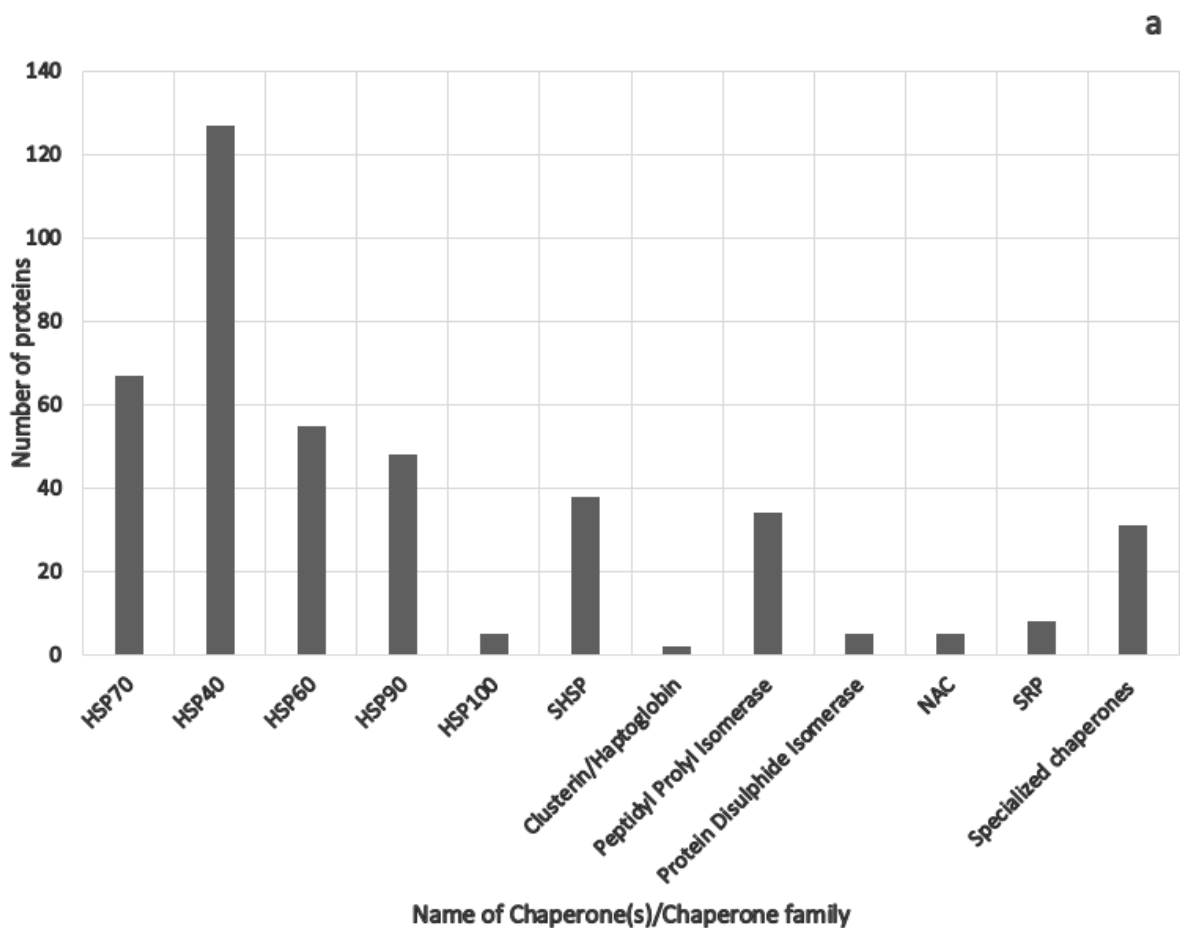
Immediately upon synthesis a nascent polypeptide encounters chaperones associated with translation such as NAC, TF or SRP all of which can partly fold proteins and maintain them in this state. In case of translocated proteins SRP can translocate them to the desired cellular compartment. These semi-folded proteins are then exported out of the cell in case they are secreted proteins by chaperones like SecB or PapD. In case of cytosolic proteins, the next chaperone that a protein encounters is HSP70. HSP70 along with co-chaperone HSP40 may by itself fold the protein and it may require one or more cycle of binding. In case of proteins that have more difficulty reaching their native states binding with HSP90, HSP60 may be required. Oligomeric proteins and multiprotein complexes often require HSP60, HSP70 for their assembly. Proteasomes are assembled by dedicated proteasomal chaperones and histones are handled by histone chaperones. In the ER chaperones such as TAP, PDI and calnexin are present which each have their own subset of client proteins. During stress proteins misfold and are rescued directly by HSP70 or from pools stored in sHSPs. Aggregated proteins may be rescued by HSP100 and HSP60, HSP90 prevent aggregation of proteins. In case a protein is damaged beyond repair, HSP70 and HSP90 target it for degradation.

On the other hand there are plenty of reports of specific chaperones with just one known client protein. In these cases recognition is based on complimentary surface recognition like in the case of enzymes. An example is AHSP bound to α -globin (161). Also HYPK and HSP47 are specialized chaperones as well. It is worth noting that HYPK can also act as a chaperone for ADH *in vitro* proving that all of the specialized chaperones may not indeed have just one substrate. Maybe only one substrate has been discovered so far or chaperone activity may itself be a generalized function and the specificity to only one substrate is just an effect of the *in vivo* context of its function. Moreover there are individual chaperones specific for one substrate only from chaperone families that are known to have a

broad substrate range, for example RanBP2 is specific for red/green opsin and it belongs to the PPI family of chaperones. This further illustrates the point that chaperone specificity is contextual.

In summary most chaperones are broad range and their substrate pool is modulated by their exact binding motif, interacting co-chaperone and sub-cellular localization. Some specialized chaperones do exist but they are a minority in number. A comparison of the chaperone genes in humans underlines this fact. It is diagrammatically represented in **Figure 1.2**.

Figure 1.2: Number of chaperone genes in humans.



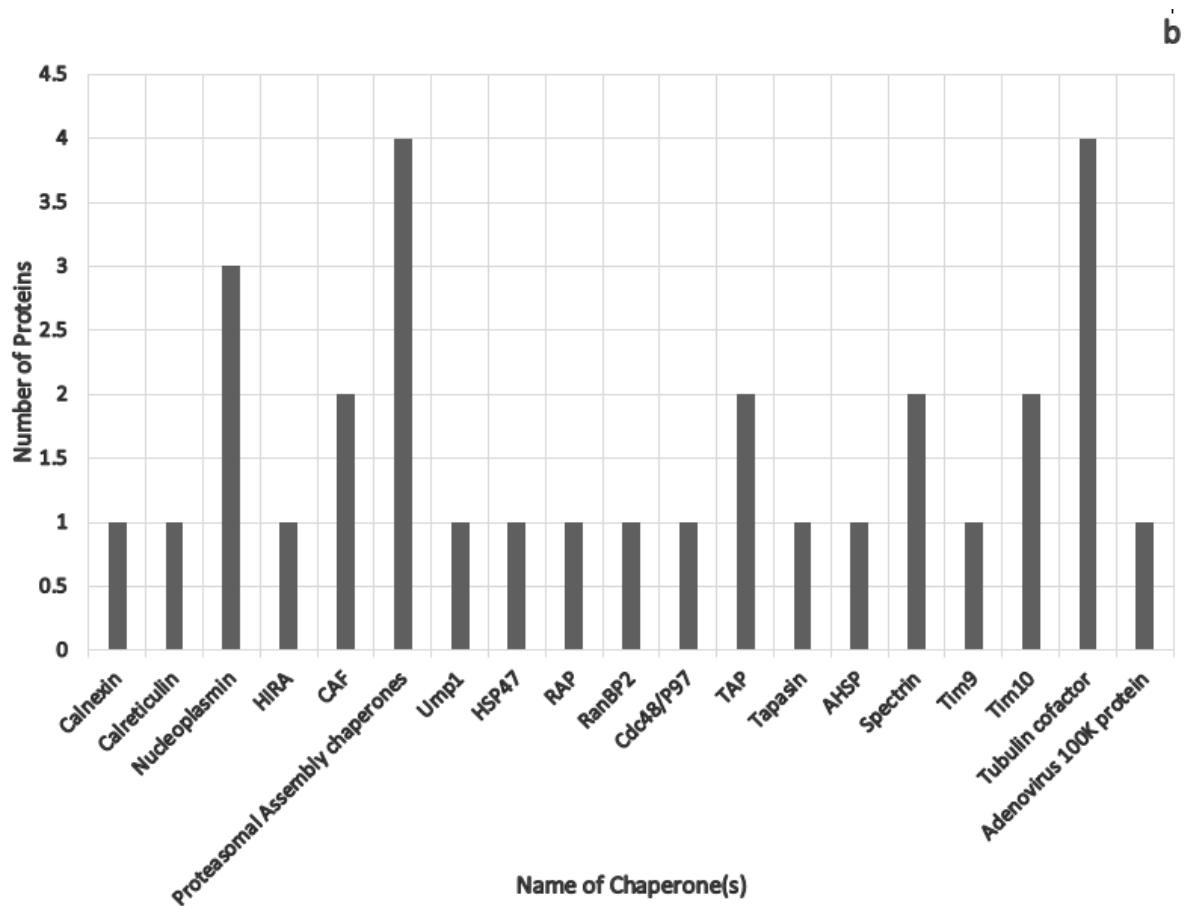


Figure 2: Diagrammatic representation of the number of chaperone genes in humans. Panel (a) shows the total number of general chaperones and specialized chaperones taken together [data sourced from HSPIR database (162)]. Panel (b) shows the breakup of specialized chaperones [data sourced from UniProt database].

1.3 Objectives

Starting with the knowledge of the interactions and properties of spectrin discussed above, the work of the present thesis was undertaken with the **objective** of addressing the following questions:

- Gain a deeper understanding of the chaperone activity of spectrin, how is it influenced by its environment? Specifically, we want to probe if pH has any modulatory role to play.
- Understand the chaperone activity of spectrin under conditions that resemble *in-vivo* states. Probe if specific phospholipid interactions or hemoglobin interactions have any effect on the chaperone activity of spectrin. Moreover we want to understand the role of post translational modifications such as glycation and phosphorylation on the chaperone activity of spectrin.
- Localize the chaperone activity of spectrin. Understand if it is located in any one of the domains in multidomain spectrin or it is more generally distributed. Probe the molecular origin of the chaperone potential.
- Probe the interactors of spectrin and understand if these interactions are driven by chaperone activity and if these interactions have any functional or biochemical significance.

References

1. Goodman, S. R., Krebs, K. E., Whitfield, C. F., Riederer, B. M., and Zagon, I. S. (1988) Spectrin and related molecules. *CRC critical reviews in biochemistry* **23**, 171-234
2. Chakrabarti, A., Kelkar, D. A., and Chattopadhyay, A. (2006) Spectrin organization and dynamics: new insights. *Bioscience Reports* **26**, 369-386
3. Yoshino, H., and Marchesi, V. T. (1984) Isolation of spectrin subunits and reassociation in vitro. Analysis by fluorescence polarization. *The Journal of biological chemistry* **259**, 4496-4500
4. Yan, Y., Winograd, E., Viel, A., Cronin, T., Harrison, S. C., and Branton, D. (1993) Crystal structure of the repetitive segments of spectrin. *Science* **262**, 2027-2030
5. Speicher, D. W., and Marchesi, V. T. (1984) Erythrocyte spectrin is comprised of many homologous triple helical segments. *Nature* **311**, 177-180
6. Pascual, J., Pfuhl, M., Rivas, G., Pastore, A., and Saraste, M. (1996) The spectrin repeat folds into a three-helix bundle in solution. *FEBS letters* **383**, 201-207
7. DeSilva, T. M., Harper, S. L., Kotula, L., Hensley, P., Curtis, P. J., Otvos, L., Jr., and Speicher, D. W. (1997) Physical properties of a single-motif erythrocyte spectrin peptide: a highly stable independently folding unit. *Biochemistry* **36**, 3991-3997
8. Sali, D., Bycroft, M., and Fersht, A. R. (1988) Stabilization of protein structure by interaction of alpha-helix dipole with a charged side chain. *Nature* **335**, 740-743
9. Bennett, V., Davis, J., and Fowler, W. E. (1982) Brain spectrin, a membrane-associated protein related in structure and function to erythrocyte spectrin. *Nature* **299**, 126-131

10. Li, Q., and Fung, L. W. (2009) Structural and dynamic study of the tetramerization region of non-erythroid alpha-spectrin: a frayed helix revealed by site-directed spin labeling electron paramagnetic resonance. *Biochemistry* **48**, 206-215
11. Park, S., Caffrey, M. S., Johnson, M. E., and Fung, L. W. (2003) Solution structural studies on human erythrocyte alpha-spectrin tetramerization site. *The Journal of biological chemistry* **278**, 21837-21844
12. Mehboob, S., Song, Y., Witek, M., Long, F., Santarsiero, B. D., Johnson, M. E., and Fung, L. W. (2010) Crystal structure of the nonerythroid alpha-spectrin tetramerization site reveals differences between erythroid and nonerythroid spectrin tetramer formation. *The Journal of biological chemistry* **285**, 14572-14584
13. Henniker, A., and Ralston, G. B. (1996) Assessment of the validity of the Adams and Fujita approximation for the higher oligomers of human spectrin. *Biophysical chemistry* **60**, 143-148
14. Beaven, G. H., Jean-Baptiste, L., Ungewickell, E., Baines, A. J., Shahbakhti, F., Pinder, J. C., Lux, S. E., and Gratzer, W. B. (1985) An examination of the soluble oligomeric complexes extracted from the red cell membrane and their relation to the membrane cytoskeleton. *European journal of cell biology* **36**, 299-306
15. Morrow, J. S., and Marchesi, V. T. (1981) Self-assembly of spectrin oligomers in vitro: a basis for a dynamic cytoskeleton. *The Journal of cell biology* **88**, 463-468
16. Liu, S. C., Windisch, P., Kim, S., and Palek, J. (1984) Oligomeric states of spectrin in normal erythrocyte membranes: biochemical and electron microscopic studies. *Cell* **37**, 587-594
17. Kirkpatrick, F. (1976) Spectrin: current understanding of its physical, biochemical, and functional properties. *Life sciences* **19**, 1-17

18. Bennett, V. (1985) The membrane skeleton of human erythrocytes and its implications for more complex cells. *Annual review of biochemistry* **54**, 273-304
19. Goodman, S. R., and Shiffer, K. (1983) The spectrin membrane skeleton of normal and abnormal human erythrocytes: a review. *The American journal of physiology* **244**, C121-141
20. Sarkar, S., Bose, D., Giri, R. P., Mukhopadhyay, M. K., and Chakrabarti, A. (2019) Effects of GM1 on brain spectrin-aminophospholipid interactions. *Biochimica et biophysica acta. Biomembranes* **1861**, 298-305
21. Mitra, M., Patra, M., and Chakrabarti, A. (2015) Fluorescence study of the effect of cholesterol on spectrin-aminophospholipid interactions. *European biophysics journal : EBJ* **44**, 635-645
22. An, X., Guo, X., Sum, H., Morrow, J., Gratzer, W., and Mohandas, N. (2004) Phosphatidylserine binding sites in erythroid spectrin: location and implications for membrane stability. *Biochemistry* **43**, 310-315
23. Sarkar, S., Bose, D., Giri, R. P., Mukhopadhyay, M. K., and Chakrabarti, A. (2018) Status of Membrane Asymmetry in Erythrocytes: Role of Spectrin. *Advances in experimental medicine and biology* **1112**, 3-11
24. Haque, M. E., Ray, S., and Chakrabarti, A. (2000) Polarity estimate of the hydrophobic binding sites in erythroid spectrin: a study by pyrene fluorescence. *Journal of fluorescence* **10**, 1-6
25. Patra, M., Mitra, M., Chakrabarti, A., and Mukhopadhyay, C. (2014) Binding of polarity-sensitive hydrophobic ligands to erythroid and nonerythroid spectrin: fluorescence and molecular modeling studies. *Journal of biomolecular structure & dynamics* **32**, 852-865

26. Chakrabarti, A. (1996) Fluorescence of spectrin-bound prodan. *Biochemical and biophysical research communications* **226**, 495-497
27. Datta, P., Chakrabarty, S. B., Chakrabarty, A., and Chakrabarti, A. (2003) Interaction of erythroid spectrin with hemoglobin variants: implications in beta-thalassemia. *Blood cells, molecules & diseases* **30**, 248-253
28. Datta, P., Basu, S., Chakravarty, S. B., Chakravarty, A., Banerjee, D., Chandra, S., and Chakrabarti, A. (2006) Enhanced oxidative cross-linking of hemoglobin E with spectrin and loss of erythrocyte membrane asymmetry in hemoglobin E β -thalassemia. *Blood Cells, Molecules, and Diseases* **37**, 77-81
29. Chakrabarti, A., Bhattacharya, S., Ray, S., and Bhattacharyya, M. (2001) Binding of a denatured heme protein and ATP to erythroid spectrin. *Biochemical and biophysical research communications* **282**, 1189-1193
30. Bhattacharyya, M., Ray, S., Bhattacharya, S., and Chakrabarti, A. (2004) Chaperone activity and prodan binding at the self-associating domain of erythroid spectrin. *The Journal of biological chemistry* **279**, 55080-55088
31. Basu, A., and Chakrabarti, A. (2015) Hemoglobin interacting proteins and implications of spectrin hemoglobin interaction. *Journal of proteomics* **128**, 469-475
32. Feng, L., Zhou, S., Gu, L., Gell, D. A., Mackay, J. P., Weiss, M. J., Gow, A. J., and Shi, Y. (2005) Structure of oxidized alpha-haemoglobin bound to AHSP reveals a protective mechanism for haem. *Nature* **435**, 697-701
33. Luzzatto, L., and Notaro, R. (2002) Haemoglobin's chaperone. *Nature* **417**, 703-705
34. Ellis, J. (1987) Proteins as molecular chaperones. *Nature* **328**, 378-379
35. Ellis, R. J. (1996) Discovery of molecular chaperones. *Cell stress & chaperones* **1**, 155-160

36. Ellis, R. J. (1993) The general concept of molecular chaperones. *Philosophical transactions of the Royal Society of London. Series B, Biological sciences* **339**, 257-261
37. Young, J. C., Agashe, V. R., Siegers, K., and Hartl, F. U. (2004) Pathways of chaperone-mediated protein folding in the cytosol. *Nature reviews. Molecular cell biology* **5**, 781-791
38. Young, J. C., Barral, J. M., and Ulrich Hartl, F. (2003) More than folding: localized functions of cytosolic chaperones. *Trends in biochemical sciences* **28**, 541-547
39. Mayer, M. P., and Bukau, B. (2005) Hsp70 chaperones: cellular functions and molecular mechanism. *Cellular and molecular life sciences : CMLS* **62**, 670-684
40. Fink, A. L. (1999) Chaperone-mediated protein folding. *Physiological reviews* **79**, 425-449
41. Ellis, R. J., and van der Vies, S. M. (1991) Molecular chaperones. *Annual review of biochemistry* **60**, 321-347
42. Ben-Zvi, A. P., and Goloubinoff, P. (2001) Review: mechanisms of disaggregation and refolding of stable protein aggregates by molecular chaperones. *Journal of structural biology* **135**, 84-93
43. Hartl, F. U., and Hayer-Hartl, M. (2002) Molecular chaperones in the cytosol: from nascent chain to folded protein. *Science* **295**, 1852-1858
44. Kramer, G., Rauch, T., Rist, W., Vorderwulbecke, S., Patzelt, H., Schulze-Specking, A., Ban, N., Deuerling, E., and Bukau, B. (2002) L23 protein functions as a chaperone docking site on the ribosome. *Nature* **419**, 171-174
45. Horwich, A. L., Low, K. B., Fenton, W. A., Hirshfield, I. N., and Furtak, K. (1993) Folding in vivo of bacterial cytoplasmic proteins: role of GroEL. *Cell* **74**, 909-917

46. Genevoux, P., Keppel, F., Schwager, F., Langendijk-Genevoux, P. S., Hartl, F. U., and Georgopoulos, C. (2004) In vivo analysis of the overlapping functions of DnaK and trigger factor. *EMBO reports* **5**, 195-200
47. Szolajska, E., and Chroboczek, J. (2011) Faithful chaperones. *Cellular and molecular life sciences : CMLS* **68**, 3307-3322
48. Koldewey, P., Horowitz, S., and Bardwell, J. C. A. (2017) Chaperone-client interactions: non-specificity engenders multi-functionality. *The Journal of biological chemistry*
49. Priya, S., Sharma, S. K., Sood, V., Mattoo, R. U., Finka, A., Azem, A., De Los Rios, P., and Goloubinoff, P. (2013) GroEL and CCT are catalytic unfoldases mediating out-of-cage polypeptide refolding without ATP. *Proceedings of the National Academy of Sciences of the United States of America* **110**, 7199-7204
50. Bukau, B., and Horwich, A. L. (1998) The Hsp70 and Hsp60 chaperone machines. *Cell* **92**, 351-366
51. Palleros, D. R., Welch, W. J., and Fink, A. L. (1991) Interaction of hsp70 with unfolded proteins: effects of temperature and nucleotides on the kinetics of binding. *Proceedings of the National Academy of Sciences of the United States of America* **88**, 5719-5723
52. Eisenberg, E., and Greene, L. E. (2007) Multiple roles of auxilin and hsc70 in clathrin-mediated endocytosis. *Traffic* **8**, 640-646
53. Mayer, M. P., Rudiger, S., and Bukau, B. (2000) Molecular basis for interactions of the DnaK chaperone with substrates. *Biological chemistry* **381**, 877-885
54. Hohfeld, J., Minami, Y., and Hartl, F. U. (1995) Hip, a novel cochaperone involved in the eukaryotic Hsc70/Hsp40 reaction cycle. *Cell* **83**, 589-598

55. Kampinga, H. H., and Craig, E. A. (2010) The HSP70 chaperone machinery: J proteins as drivers of functional specificity. *Nature reviews. Molecular cell biology* **11**, 579-592
56. Qiu, X. B., Shao, Y. M., Miao, S., and Wang, L. (2006) The diversity of the DnaJ/Hsp40 family, the crucial partners for Hsp70 chaperones. *Cellular and molecular life sciences : CMLS* **63**, 2560-2570
57. Rudiger, S., Germeroth, L., Schneider-Mergener, J., and Bukau, B. (1997) Substrate specificity of the DnaK chaperone determined by screening cellulose-bound peptide libraries. *The EMBO journal* **16**, 1501-1507
58. Rudiger, S., Mayer, M. P., Schneider-Mergener, J., and Bukau, B. (2000) Modulation of substrate specificity of the DnaK chaperone by alteration of a hydrophobic arch. *Journal of molecular biology* **304**, 245-251
59. Gragerov, A., Zeng, L., Zhao, X., Burkholder, W., and Gottesman, M. E. (1994) Specificity of DnaK-peptide binding. *Journal of molecular biology* **235**, 848-854
60. Gragerov, A., and Gottesman, M. E. (1994) Different peptide binding specificities of hsp70 family members. *Journal of molecular biology* **241**, 133-135
61. Richarme, G., and Kohiyama, M. (1993) Specificity of the Escherichia coli chaperone DnaK (70-kDa heat shock protein) for hydrophobic amino acids. *The Journal of biological chemistry* **268**, 24074-24077
62. Flynn, G. C., Pohl, J., Flocco, M. T., and Rothman, J. E. (1991) Peptide-binding specificity of the molecular chaperone BiP. *Nature* **353**, 726-730
63. Blond-Elguindi, S., Cwirla, S. E., Dower, W. J., Lipshutz, R. J., Sprang, S. R., Sambrook, J. F., and Gething, M. J. (1993) Affinity panning of a library of peptides displayed on bacteriophages reveals the binding specificity of BiP. *Cell* **75**, 717-728
64. Caplan, A. J. (2003) What is a co-chaperone? *Cell stress & chaperones* **8**, 105-107

65. Luders, J., Demand, J., Schonfelder, S., Frien, M., Zimmermann, R., and Hohfeld, J. (1998) Cofactor-induced modulation of the functional specificity of the molecular chaperone Hsc70. *Biological chemistry* **379**, 1217-1226
66. McCarty, J. S., Rudiger, S., Schonfeld, H. J., Schneider-Mergener, J., Nakahigashi, K., Yura, T., and Bukau, B. (1996) Regulatory region C of the E. coli heat shock transcription factor, sigma32, constitutes a DnaK binding site and is conserved among eubacteria. *Journal of molecular biology* **256**, 829-837
67. Rudiger, S., Schneider-Mergener, J., and Bukau, B. (2001) Its substrate specificity characterizes the DnaJ co-chaperone as a scanning factor for the DnaK chaperone. *The EMBO journal* **20**, 1042-1050
68. Chan, H. Y., Warrick, J. M., Gray-Board, G. L., Paulson, H. L., and Bonini, N. M. (2000) Mechanisms of chaperone suppression of polyglutamine disease: selectivity, synergy and modulation of protein solubility in Drosophila. *Human molecular genetics* **9**, 2811-2820
69. Tang, Y. C., Chang, H. C., Roeben, A., Wischnewski, D., Wischnewski, N., Kerner, M. J., Hartl, F. U., and Hayer-Hartl, M. (2006) Structural features of the GroEL-GroES nano-cage required for rapid folding of encapsulated protein. *Cell* **125**, 903-914
70. Yam, A. Y., Xia, Y., Lin, H. T., Burlingame, A., Gerstein, M., and Frydman, J. (2008) Defining the TRiC/CCT interactome links chaperonin function to stabilization of newly made proteins with complex topologies. *Nature structural & molecular biology* **15**, 1255-1262
71. Yaffe, M. B., Farr, G. W., Miklos, D., Horwich, A. L., Sternlicht, M. L., and Sternlicht, H. (1992) TCP1 complex is a molecular chaperone in tubulin biogenesis. *Nature* **358**, 245-248

72. Buchberger, A., Schroder, H., Hesterkamp, T., Schonfeld, H. J., and Bukau, B. (1996) Substrate shuttling between the DnaK and GroEL systems indicates a chaperone network promoting protein folding. *Journal of molecular biology* **261**, 328-333
73. Lin, Z., Schwartz, F. P., and Eisenstein, E. (1995) The hydrophobic nature of GroEL-substrate binding. *The Journal of biological chemistry* **270**, 1011-1014
74. Richarme, G., and Kohiyama, M. (1994) Amino acid specificity of the Escherichia coli chaperone GroEL (heat shock protein 60). *The Journal of biological chemistry* **269**, 7095-7098
75. Genest, O., Hoskins, J. R., Camberg, J. L., Doyle, S. M., and Wickner, S. (2011) Heat shock protein 90 from Escherichia coli collaborates with the DnaK chaperone system in client protein remodeling. *Proceedings of the National Academy of Sciences of the United States of America* **108**, 8206-8211
76. Scheibel, T., and Buchner, J. (1998) The Hsp90 complex--a super-chaperone machine as a novel drug target. *Biochemical pharmacology* **56**, 675-682
77. Karagoz, G. E., Duarte, A. M., Akoury, E., Ippel, H., Biernat, J., Moran Luengo, T., Radli, M., Didenko, T., Nordhues, B. A., Veprintsev, D. B., Dickey, C. A., Mandelkow, E., Zweckstetter, M., Boelens, R., Madl, T., and Rudiger, S. G. (2014) Hsp90-Tau complex reveals molecular basis for specificity in chaperone action. *Cell* **156**, 963-974
78. Chadli, A., Felts, S. J., and Toft, D. O. (2008) GCUNC45 is the first Hsp90 co-chaperone to show alpha/beta isoform specificity. *The Journal of biological chemistry* **283**, 9509-9512
79. Prodromou, C., Roe, S. M., O'Brien, R., Ladbury, J. E., Piper, P. W., and Pearl, L. H. (1997) Identification and structural characterization of the ATP/ADP-binding site in the Hsp90 molecular chaperone. *Cell* **90**, 65-75

80. Scheibel, T., Weikl, T., and Buchner, J. (1998) Two chaperone sites in Hsp90 differing in substrate specificity and ATP dependence. *Proceedings of the National Academy of Sciences of the United States of America* **95**, 1495-1499
81. Weber-Ban, E. U., Reid, B. G., Miranker, A. D., and Horwich, A. L. (1999) Global unfolding of a substrate protein by the Hsp100 chaperone ClpA. *Nature* **401**, 90-93
82. Neuwald, A. F., Aravind, L., Spouge, J. L., and Koonin, E. V. (1999) AAA+: A class of chaperone-like ATPases associated with the assembly, operation, and disassembly of protein complexes. *Genome research* **9**, 27-43
83. Wawrzynow, A., Wojtkowiak, D., Marszalek, J., Banecki, B., Jonsen, M., Graves, B., Georgopoulos, C., and Zylicz, M. (1995) The ClpX heat-shock protein of Escherichia coli, the ATP-dependent substrate specificity component of the ClpP-ClpX protease, is a novel molecular chaperone. *The EMBO journal* **14**, 1867-1877
84. Thibault, G., Yudin, J., Wong, P., Tsitrin, V., Sprangers, R., Zhao, R., and Houry, W. A. (2006) Specificity in substrate and cofactor recognition by the N-terminal domain of the chaperone ClpX. *Proceedings of the National Academy of Sciences of the United States of America* **103**, 17724-17729
85. Haslbeck, M. (2002) sHsps and their role in the chaperone network. *Cellular and Molecular Life Sciences* **59**, 1649-1657
86. Basha, E., Friedrich, K. L., and Vierling, E. (2006) The N-terminal arm of small heat shock proteins is important for both chaperone activity and substrate specificity. *The Journal of biological chemistry* **281**, 39943-39952
87. McHaourab, H. S., Godar, J. A., and Stewart, P. L. (2009) Structure and mechanism of protein stability sensors: chaperone activity of small heat shock proteins. *Biochemistry* **48**, 3828-3837

88. Devlin, G. L., Carver, J. A., and Bottomley, S. P. (2003) The selective inhibition of serpin aggregation by the molecular chaperone, alpha-crystallin, indicates a nucleation-dependent specificity. *The Journal of biological chemistry* **278**, 48644-48650
89. Randall, L. L., and Hardy, S. J. (1995) High selectivity with low specificity: how SecB has solved the paradox of chaperone binding. *Trends in biochemical sciences* **20**, 65-69
90. Knoblauch, N. T., Rudiger, S., Schonfeld, H. J., Driessen, A. J., Schneider-Mergener, J., and Bukau, B. (1999) Substrate specificity of the SecB chaperone. *The Journal of biological chemistry* **274**, 34219-34225
91. Poon, S., Easterbrook-Smith, S. B., Rybchyn, M. S., Carver, J. A., and Wilson, M. R. (2000) Clusterin is an ATP-independent chaperone with very broad substrate specificity that stabilizes stressed proteins in a folding-competent state. *Biochemistry* **39**, 15953-15960
92. Poon, S., Treweek, T. M., Wilson, M. R., Easterbrook-Smith, S. B., and Carver, J. A. (2002) Clusterin is an extracellular chaperone that specifically interacts with slowly aggregating proteins on their off-folding pathway. *FEBS letters* **513**, 259-266
93. Yerbury, J. J., Rybchyn, M. S., Easterbrook-Smith, S. B., Henriques, C., and Wilson, M. R. (2005) The acute phase protein haptoglobin is a mammalian extracellular chaperone with an action similar to clusterin. *Biochemistry* **44**, 10914-10925
94. Arie, J. P., Sassoon, N., and Betton, J. M. (2001) Chaperone function of FkpA, a heat shock prolyl isomerase, in the periplasm of Escherichia coli. *Molecular microbiology* **39**, 199-210

95. Freskgard, P. O., Bergenheim, N., Jonsson, B. H., Svensson, M., and Carlsson, U. (1992) Isomerase and chaperone activity of prolyl isomerase in the folding of carbonic anhydrase. *Science* **258**, 466-468
96. Freeman, B. C., Toft, D. O., and Morimoto, R. I. (1996) Molecular chaperone machines: chaperone activities of the cyclophilin Cyp-40 and the steroid aporeceptor-associated protein p23. *Science* **274**, 1718-1720
97. Ferreira, P. A., Nakayama, T. A., Pak, W. L., and Travis, G. H. (1996) Cyclophilin-related protein RanBP2 acts as chaperone for red/green opsin. *Nature* **383**, 637-640
98. Deuerling, E., Patzelt, H., Vorderwulbecke, S., Rauch, T., Kramer, G., Schaffitzel, E., Mogk, A., Schulze-Specking, A., Langen, H., and Bukau, B. (2003) Trigger Factor and DnaK possess overlapping substrate pools and binding specificities. *Molecular microbiology* **47**, 1317-1328
99. Patzelt, H., Rudiger, S., Brehmer, D., Kramer, G., Vorderwulbecke, S., Schaffitzel, E., Waitz, A., Hesterkamp, T., Dong, L., Schneider-Mergener, J., Bukau, B., and Deuerling, E. (2001) Binding specificity of Escherichia coli trigger factor. *Proceedings of the National Academy of Sciences of the United States of America* **98**, 14244-14249
100. Wilkinson, B., and Gilbert, H. F. (2004) Protein disulfide isomerase. *Biochimica et biophysica acta* **1699**, 35-44
101. Cai, H., Wang, C. C., and Tsou, C. L. (1994) Chaperone-like activity of protein disulfide isomerase in the refolding of a protein with no disulfide bonds. *The Journal of biological chemistry* **269**, 24550-24552
102. Wang, C. C., and Tsou, C. L. (1993) Protein disulfide isomerase is both an enzyme and a chaperone. *FASEB journal : official publication of the Federation of American Societies for Experimental Biology* **7**, 1515-1517

103. Puig, A., and Gilbert, H. F. (1994) Protein disulfide isomerase exhibits chaperone and anti-chaperone activity in the oxidative refolding of lysozyme. *The Journal of biological chemistry* **269**, 7764-7771
104. Tsai, B., Rodighiero, C., Lencer, W. I., and Rapoport, T. A. (2001) Protein disulfide isomerase acts as a redox-dependent chaperone to unfold cholera toxin. *Cell* **104**, 937-948
105. Jessop, C. E., Watkins, R. H., Simmons, J. J., Tasab, M., and Bulleid, N. J. (2009) Protein disulphide isomerase family members show distinct substrate specificity: P5 is targeted to BiP client proteins. *Journal of cell science* **122**, 4287-4295
106. del Alamo, M., Hogan, D. J., Pechmann, S., Albanese, V., Brown, P. O., and Frydman, J. (2011) Defining the specificity of cotranslationally acting chaperones by systematic analysis of mRNAs associated with ribosome-nascent chain complexes. *PLoS biology* **9**, e1001100
107. Stefanovic, S., and Hegde, R. S. (2007) Identification of a targeting factor for posttranslational membrane protein insertion into the ER. *Cell* **128**, 1147-1159
108. Mateja, A., Paduch, M., Chang, H. Y., Szydlowska, A., Kossiakoff, A. A., Hegde, R. S., and Keenan, R. J. (2015) Protein targeting. Structure of the Get3 targeting factor in complex with its membrane protein cargo. *Science* **347**, 1152-1155
109. Formighieri, C., Cazzaniga, S., Kuras, R., and Bassi, R. (2013) Biogenesis of photosynthetic complexes in the chloroplast of *Chlamydomonas reinhardtii* requires ARSA1, a homolog of prokaryotic arsenite transporter and eukaryotic TRC40 for guided entry of tail-anchored proteins. *The Plant journal : for cell and molecular biology* **73**, 850-861

110. Maestre-Reyna, M., Wu, S. M., Chang, Y. C., Chen, C. C., Maestre-Reyna, A., Wang, A. H., and Chang, H. Y. (2017) In search of tail-anchored protein machinery in plants: reevaluating the role of arsenite transporters. *Scientific reports* **7**, 46022
111. Moremen, K. W., and Molinari, M. (2006) N-linked glycan recognition and processing: the molecular basis of endoplasmic reticulum quality control. *Current opinion in structural biology* **16**, 592-599
112. Molinari, M., and Helenius, A. (2000) Chaperone selection during glycoprotein translocation into the endoplasmic reticulum. *Science* **288**, 331-333
113. Lindquist, J. A., Jensen, O. N., Mann, M., and Hammerling, G. J. (1998) ER-60, a chaperone with thiol-dependent reductase activity involved in MHC class I assembly. *The EMBO journal* **17**, 2186-2195
114. Sandhu, N., Duus, K., Jorgensen, C. S., Hansen, P. R., Bruun, S. W., Pedersen, L. O., Hojrup, P., and Houen, G. (2007) Peptide binding specificity of the chaperone calreticulin. *Biochimica et biophysica acta* **1774**, 701-713
115. Kapoor, M., Srinivas, H., Kandiah, E., Gemma, E., Ellgaard, L., Oscarson, S., Helenius, A., and Surolia, A. (2003) Interactions of substrate with calreticulin, an endoplasmic reticulum chaperone. *The Journal of biological chemistry* **278**, 6194-6200
116. Patil, A. R., Thomas, C. J., and Surolia, A. (2000) Kinetics and the mechanism of interaction of the endoplasmic reticulum chaperone, calreticulin, with monoglucosylated (Glc1Man9GlcNAc2) substrate. *The Journal of biological chemistry* **275**, 24348-24356
117. Kuhn, A., Stuart, R., Henry, R., and Dalbey, R. E. (2003) The Alb3/Oxa1/YidC protein family: membrane-localized chaperones facilitating membrane protein insertion? *Trends in cell biology* **13**, 510-516

118. Hennon, S. W., Soman, R., Zhu, L., and Dalbey, R. E. (2015) YidC/Alb3/Oxa1 Family of Insertases. *The Journal of biological chemistry* **290**, 14866-14874
119. Shendelman, S., Jonason, A., Martinat, C., Leete, T., and Abeliovich, A. (2004) DJ-1 is a redox-dependent molecular chaperone that inhibits alpha-synuclein aggregate formation. *PLoS biology* **2**, e362
120. Girotto, S., Cendron, L., Bisaglia, M., Tessari, I., Mammi, S., Zanotti, G., and Bubacco, L. (2014) DJ-1 is a copper chaperone acting on SOD1 activation. *The Journal of biological chemistry* **289**, 10887-10899
121. Wang, Z., Zhang, Y., Zhang, S., Guo, Q., Tan, Y., Wang, X., Xiong, R., Ding, J., and Chen, S. (2011) DJ-1 can inhibit microtubule associated protein 1 B formed aggregates. *Molecular neurodegeneration* **6**, 38
122. Bhattacharyya, J., and Das, K. P. (1999) Molecular chaperone-like properties of an unfolded protein, alpha(s)-casein. *The Journal of biological chemistry* **274**, 15505-15509
123. Guha, S., Manna, T. K., Das, K. P., and Bhattacharyya, B. (1998) Chaperone-like activity of tubulin. *The Journal of biological chemistry* **273**, 30077-30080
124. Hagenmaier, S., Stierhof, Y. D., and Henning, U. (1997) A new periplasmic protein of *Escherichia coli* which is synthesized in spheroplasts but not in intact cells. *Journal of bacteriology* **179**, 2073-2076
125. Quan, S., Koldewey, P., Tapley, T., Kirsch, N., Ruane, K. M., Pfizenmaier, J., Shi, R., Hofmann, S., Foit, L., Ren, G., Jakob, U., Xu, Z., Cygler, M., and Bardwell, J. C. (2011) Genetic selection designed to stabilize proteins uncovers a chaperone called Spy. *Nature structural & molecular biology* **18**, 262-269

126. Sklar, J. G., Wu, T., Kahne, D., and Silhavy, T. J. (2007) Defining the roles of the periplasmic chaperones SurA, Skp, and DegP in Escherichia coli. *Genes & development* **21**, 2473-2484
127. Schiffrin, B., Calabrese, A. N., Devine, P. W., Harris, S. A., Ashcroft, A. E., Brockwell, D. J., and Radford, S. E. (2016) Skp is a multivalent chaperone of outer-membrane proteins. *Nature structural & molecular biology* **23**, 786-793
128. Soltes, G. R., Schwalm, J., Ricci, D. P., and Silhavy, T. J. (2016) The Activity of Escherichia coli Chaperone SurA Is Regulated by Conformational Changes Involving a Parvulin Domain. *Journal of bacteriology* **198**, 921-929
129. Kuehn, M. J., Normark, S., and Hultgren, S. J. (1991) Immunoglobulin-like PapD chaperone caps and uncaps interactive surfaces of nascently translocated pilus subunits. *Proceedings of the National Academy of Sciences of the United States of America* **88**, 10586-10590
130. Kuehn, M. J., Ogg, D. J., Kihlberg, J., Slonim, L. N., Flemmer, K., Bergfors, T., and Hultgren, S. J. (1993) Structural basis of pilus subunit recognition by the PapD chaperone. *Science* **262**, 1234-1241
131. van Eerde, A., Hamiaux, C., Perez, J., Parsot, C., and Dijkstra, B. W. (2004) Structure of Spa15, a type III secretion chaperone from Shigella flexneri with broad specificity. *EMBO reports* **5**, 477-483
132. Wattiau, P., Bernier, B., Deslee, P., Michiels, T., and Cornelis, G. R. (1994) Individual chaperones required for Yop secretion by Yersinia. *Proceedings of the National Academy of Sciences of the United States of America* **91**, 10493-10497
133. Natsume, R., Eitoku, M., Akai, Y., Sano, N., Horikoshi, M., and Senda, T. (2007) Structure and function of the histone chaperone CIA/ASF1 complexed with histones H3 and H4. *Nature* **446**, 338-341

134. Tang, Y., Poustovoitov, M. V., Zhao, K., Garfinkel, M., Canutescu, A., Dunbrack, R., Adams, P. D., and Marmorstein, R. (2006) Structure of a human ASF1a-HIRA complex and insights into specificity of histone chaperone complex assembly. *Nature structural & molecular biology* **13**, 921-929
135. Wang, H., Walsh, S. T., and Parthun, M. R. (2008) Expanded binding specificity of the human histone chaperone NASP. *Nucleic acids research* **36**, 5763-5772
136. Ramos, I., Martin-Benito, J., Finn, R., Bretana, L., Aloria, K., Arizmendi, J. M., Ausio, J., Muga, A., Valpuesta, J. M., and Prado, A. (2010) Nucleoplasmin binds histone H2A-H2B dimers through its distal face. *The Journal of biological chemistry* **285**, 33771-33778
137. Matias, A. C., Ramos, P. C., and Dohmen, R. J. (2010) Chaperone-assisted assembly of the proteasome core particle. *Biochemical Society transactions* **38**, 29-33
138. Murata, S., Yashiroda, H., and Tanaka, K. (2009) Molecular mechanisms of proteasome assembly. *Nature reviews. Molecular cell biology* **10**, 104-115
139. Rosenzweig, R., and Glickman, M. H. (2008) Chaperone-driven proteasome assembly. *Biochemical Society transactions* **36**, 807-812
140. Kaneko, T., Hamazaki, J., Iemura, S., Sasaki, K., Furuyama, K., Natsume, T., Tanaka, K., and Murata, S. (2009) Assembly pathway of the Mammalian proteasome base subcomplex is mediated by multiple specific chaperones. *Cell* **137**, 914-925
141. Funakoshi, M., Tomko, R. J., Jr., Kobayashi, H., and Hochstrasser, M. (2009) Multiple assembly chaperones govern biogenesis of the proteasome regulatory particle base. *Cell* **137**, 887-899
142. Hanssum, A., Zhong, Z., Rousseau, A., Krzyzosiak, A., Sigurdardottir, A., and Bertolotti, A. (2014) An inducible chaperone adapts proteasome assembly to stress. *Molecular cell* **55**, 566-577

143. Nagata, K. (1998) Expression and function of heat shock protein 47: a collagen-specific molecular chaperone in the endoplasmic reticulum. *Matrix biology : journal of the International Society for Matrix Biology* **16**, 379-386
144. Koide, T., Nishikawa, Y., Asada, S., Yamazaki, C. M., Takahara, Y., Homma, D. L., Otaka, A., Ohtani, K., Wakamiya, N., Nagata, K., and Kitagawa, K. (2006) Specific recognition of the collagen triple helix by chaperone HSP47. II. The HSP47-binding structural motif in collagens and related proteins. *The Journal of biological chemistry* **281**, 11177-11185
145. Bu, G. (1998) Receptor-associated protein: a specialized chaperone and antagonist for members of the LDL receptor gene family. *Current opinion in lipidology* **9**, 149-155
146. Boyault, C., Gilquin, B., Zhang, Y., Rybin, V., Garman, E., Meyer-Klaucke, W., Matthias, P., Muller, C. W., and Khochbin, S. (2006) HDAC6-p97/VCP controlled polyubiquitin chain turnover. *The EMBO journal* **25**, 3357-3366
147. Rape, M., Hoppe, T., Gorr, I., Kalocay, M., Richly, H., and Jentsch, S. (2001) Mobilization of processed, membrane-tethered SPT23 transcription factor by CDC48(UFD1/NPL4), a ubiquitin-selective chaperone. *Cell* **107**, 667-677
148. Barral, J. M., Hutagalung, A. H., Brinker, A., Hartl, F. U., and Epstein, H. F. (2002) Role of the myosin assembly protein UNC-45 as a molecular chaperone for myosin. *Science* **295**, 669-671
149. Solheim, J. C., Carreno, B. M., and Hansen, T. H. (1997) Are transporter associated with antigen processing (TAP) and tapasin class I MHC chaperones? *Journal of immunology* **158**, 541-543
150. Kropshofer, H., Arndt, S. O., Moldenhauer, G., Hammerling, G. J., and Vogt, A. B. (1997) HLA-DM acts as a molecular chaperone and rescues empty HLA-DR molecules at lysosomal pH. *Immunity* **6**, 293-302

151. Hoff, K. G., Ta, D. T., Tapley, T. L., Silberg, J. J., and Vickery, L. E. (2002) Hsc66 substrate specificity is directed toward a discrete region of the iron-sulfur cluster template protein IscU. *The Journal of biological chemistry* **277**, 27353-27359
152. Kihm, A. J., Kong, Y., Hong, W., Russell, J. E., Rouda, S., Adachi, K., Simon, M. C., Blobel, G. A., and Weiss, M. J. (2002) An abundant erythroid protein that stabilizes free alpha-haemoglobin. *Nature* **417**, 758-763
153. Kiger, L., Vasseur, C., Domingues-Hamdi, E., Truan, G., Marden, M. C., and Baudin-Creuz, V. (2014) Dynamics of alpha-Hb chain binding to its chaperone AHSP depends on heme coordination and redox state. *Biochimica et biophysica acta* **1840**, 277-287
154. Raychaudhuri, S., Sinha, M., Mukhopadhyay, D., and Bhattacharyya, N. P. (2008) HYPK, a Huntingtin interacting protein, reduces aggregates and apoptosis induced by N-terminal Huntingtin with 40 glutamines in Neuro2a cells and exhibits chaperone-like activity. *Human molecular genetics* **17**, 240-255
155. Choudhury, K. R., and Bhattacharyya, N. P. (2015) Chaperone protein HYPK interacts with the first 17 amino acid region of Huntingtin and modulates mutant HTT-mediated aggregation and cytotoxicity. *Biochemical and biophysical research communications* **456**, 66-73
156. Hobson, A. H., Buckley, C. M., Aamand, J. L., Jorgensen, S. T., Diderichsen, B., and McConnell, D. J. (1993) Activation of a bacterial lipase by its chaperone. *Proceedings of the National Academy of Sciences of the United States of America* **90**, 5682-5686
157. Karlsson, M., Hannavy, K., and Higgins, C. F. (1993) ExbB acts as a chaperone-like protein to stabilize TonB in the cytoplasm. *Molecular microbiology* **8**, 389-396
158. Wiedemann, N., Frazier, A. E., and Pfanner, N. (2004) The protein import machinery of mitochondria. *The Journal of biological chemistry* **279**, 14473-14476

159. Nithianantham, S., Le, S., Seto, E., Jia, W., Leary, J., Corbett, K. D., Moore, J. K., and Al-Bassam, J. (2015) Tubulin cofactors and Arl2 are cage-like chaperones that regulate the soluble alphabeta-tubulin pool for microtubule dynamics. *eLife* **4**
160. Hong, S. S., Szolajska, E., Schoehn, G., Franqueville, L., Myhre, S., Lindholm, L., Ruigrok, R. W., Boulanger, P., and Chroboczek, J. (2005) The 100K-chaperone protein from adenovirus serotype 2 (Subgroup C) assists in trimerization and nuclear localization of hexons from subgroups C and B adenoviruses. *Journal of molecular biology* **352**, 125-138
161. Feng, L., Gell, D. A., Zhou, S., Gu, L., Kong, Y., Li, J., Hu, M., Yan, N., Lee, C., Rich, A. M., Armstrong, R. S., Lay, P. A., Gow, A. J., Weiss, M. J., Mackay, J. P., and Shi, Y. (2004) Molecular mechanism of AHSP-mediated stabilization of alpha-hemoglobin. *Cell* **119**, 629-640
162. R, R. K., N. S, N., S. P, A., Sinha, D., Veedin Rajan, V. B., Esthaki, V. K., and D'Silva, P. (2012) HSPiR: a manually annotated heat shock protein information resource. *Bioinformatics* **28**, 2853-2855

Chapter 2:

The effect of pH on chaperone activity

2.1 Introduction

It is known that under physiological conditions spectrin exists as a hetero-dimer composed of α and β subunits each of which is made up of tandem repeats of alpha helical 'spectrin-repeat' domains. The major forces that stabilize the 3-helix bundle of the repeat motifs in spectrin is hydrophobic interactions between the middle amphiphilic helix and the two polar helices and electrostatic interactions between the two hydrophilic helices. Spectrin dimerization is also dependent largely on the hydrophobic and electrostatic lateral interactions between the two subunits (1,2). Similarly tetramer formation is also dependent on these forces (3-5). The molecular basis for these interactions are not well elucidated, though the structure of the repeat motif has been solved, little is known of the structure and interactions between consecutive repeat motifs, or of the lateral interactions between the α and β chains, and the influence of these interactions on the morphology, function and self-association of spectrins.

It would seem that for both spectrin structure and function the oligomerization state and flexibility plays a major role (6). This in turn seems to be governed by the lateral interactions of the protein subunits and head to head associations of the dimers, both of which are heavily influenced by electrostatic and hydrophobic interactions.

It would be logical to think that since these forces are influenced strongly by the pH of the media which dictates the ionization state of the side chains in amino acids, the properties of the protein as a whole should also be pH dependent especially the oligomeric status (7).

At low pH stomatocytosis of the RBC was observed with possible involvement of the spectrin based membrane skeleton (8). According to Cudd *et al.*, acid media excercises a

biphasic effect on erythrocyte hemolysis, with a fast hemolysis between pH 3.6 and pH 4.7 and a slower one between pH 5 and pH 6 (9,10).

The cytoskeletal spectrin network precipitates at its isoelectrical pH 4.5, forming membrane particles (11) which are responsible for the shape changes in acidic media (12). Moreover spectrin has been found to interact with anionic lipid-containing model membranes in a pH-dependent manner (13,14).

Indeed it has been shown that the ionic strength and pH of the medium plays an important role in the structure and conformation of spectrin (15). Detergent extracted red blood cell membrane skeleton have been shown to expand or shrink with changing ionic strength (16,17).

Fujita and coworkers have shown the effects of alkaline pH on spectrin extraction from erythrocyte membrane skeletons (18). And Narla *et. al* have shown the effect of temperature on spectrin (19) Extraction of spectrin oligomers from the cytoskeletal network was reported at $\text{pH} > 9$. At $\text{pH} \geq 11.5$, most of the extracted spectrin had dissociated into spectrin dimers, as determined by non-denaturing gel electrophoresis performed at neutral pH (20).

Thus it is important to study structural stability of spectrin in a pH dependent manner and how its structural changes affect its functional property.

Extremes of pH do not always completely denature a protein but may lead to only partly folded states (21). Although the exact conformational state attained by a given protein at low pH is a complex interplay between a variety of stabilizing and destabilizing forces (22,23), it has been shown that certain proteins under conditions of low pH have a compact dimension, abundant secondary structure and largely disordered tertiary structure, which are

the characteristics of the molten globule state (24), which is considered to be a general intermediate in the folding pathway of proteins (25,26). It is also to be noted that acid denaturation of proteins usually results in a denatured state that is less unfolded than the completely unfolded form obtained in high concentrations of urea and GdHCl (27-29).

In acid denaturation, the major driving force for unfolding is intramolecular charge repulsion which may fail to overcome interactions that favour folding, such as hydrophobic forces, disulfide bonds, salt bridges and metal ion protein interactions (30,31).

Alternatively, if a titratable group is buried in an un-ionized form in the interior of the protein and can be titrated only upon unfolding, the unfolded state will be favored upon titration of the group by changing the pH (32). The pH dependence of protein stability needs to be explained on the basis of the coupling of the protonation reactions that occur on changing pH with the unfolding reaction, with the unfolded and folded states binding protons to different extents.

We have shown earlier that erythroid spectrin exhibits chaperone activity by preventing both thermal and non-thermal aggregation of proteins (33). We hypothesize that like many chaperones spectrin should also show modulation of chaperone potential with pH. Often it is seen that the structural perturbations caused by changes in the pH of the medium increase or decrease the chaperone like activity of a protein. There are many examples where chaperone activity is triggered by acidic or alkaline pH where the protein has lost some of its tertiary structure (34). Moreover oligomeric state plays a major role in the chaperone activity with a well-known class of chaperones, the sHSPs only showing appreciable chaperone potential in an oligomeric state (35). It is of importance to investigate the chaperone potential of spectrin under different pH and correlate it to the conformational changes brought about by pH dependent modulations.

2.2 Materials and Methods

Tris, glycine, citric acid, KCl, dithiothreitol (DTT), EDTA, imidazole, MgCl₂, NaCl, pyrene, thioflavin-T, urea, bovine serum albumin and acrylamide were obtained from Sigma-Aldrich chemical Co. St. Louis, Mo, USA. 8-anilino-1-naphthalene-sulphonic acid (ANS) was obtained from Molecular Probe. Ovine blood and brain tissue samples were obtained from local slaughterhouse, Salt Lake, Kolkata, from animals slaughtered for commercial purposes.

2.2.1 Isolation and purification of erythroid and non-erythroid spectrin

Dimeric erythroid spectrin was isolated from clean white RBC ghost membranes following protocol elaborated in earlier studies from our lab (33,36). Briefly, ovine blood was collected from animals slaughtered for commercial purposes, RBCs were pelleted by centrifugation, washed with PBS containing 5mM sodium phosphate, 155mM NaCl, 1mM EDTA, pH 8.0 and lysed in hypotonic lysis buffer containing 5mM sodium phosphate, 1mM EDTA and 20µg/ml PMSF. RBC membranes were collected by centrifugation and contaminating hemoglobin was removed by washing with lysis buffer to yield clean white ghosts. Spectrin was removed from ghost membranes by 30 min incubation at 37°C in low salt spectrin removal buffer containing 0.2mM sodium phosphate, 0.1mM EDTA, 0.2mM DTT, 20µg/ml PMSF, pH 8.0. Spectrin was further purified by 30% ammonium sulphate precipitation from crude extract and resultant preparation was run through Sepharose CL-4B column to give final pure product. Purity of preparation was checked by 8% SDS PAGE analysis and concentration of preparation was determined from known O.D. of 10.7 at 280 nm for 1% spectrin solution (37). Spectrin preparation was stored at - 20°C for a maximum of one month.

Neuronal Spectrin was purified from ovine brain following published procedure elaborated in earlier studies from our lab (37) (38-40). Purity of the preparations was checked by 8% SDS polyacrylamide gel electrophoresis under reducing conditions, and concentrations were determined by Bradford method (41) with bovine serum albumin as a standard. Erythrocyte spectrin preparation contained only α I and β I spectrins while the brain spectrin preparation was a mixture of α II and β II-V spectrins and their isoforms.

2.2.2 Characterizing conformational alterations of spectrin by tryptophan fluorescence

2.2.2.1 Intrinsic tryptophan fluorescence and anisotropy measurement

Erythroid and non-erythroid spectrin were diluted from their stock solution into buffers of different pH of the range of 2 to 9; typically 15 fold dilution was done and the protein concentration was kept at 0.1mg/ml for each sample. Spectrin was incubated for two hours to allow time for equilibration in case of each sample. Buffers used were glycine-HCl – pH 2, Sodium citrate- citric acid – pH 3 to 6, tris-HCl – pH 7 to 9. Buffer strength was 10mM with 20mM KCl in each case,

Intrinsic tryptophan fluorescence measurements were done by selectively exciting tryptophan residues at 295 nm using Cary Eclipse fluorescence spectrophotometer with thermostated cell holders at 25°C. The spectra were recorded from 310 nm to 400nm with 5 nm slit width for both excitation and emission.

Steady state fluorescence anisotropy (r) measurements were performed using the Polarization accessory of the same instrument. All experiments were done multiple times and an average of 5 independent measurements of anisotropy was recorded for each sample.

2.2.2.2 Steady state tryptophan fluorescence life time measurements

Tryptophan fluorescence life times of the both the spectrins were measured by time correlated single photon counting in Fluoromax-3 spectrophotometer using Nano LED as a light source. Protein in the pH range of 2 to 9 was taken in a concentration of 0.1mg/ml for each sample. The excitation and emission wavelength were maintained 295nm and 340nm respectively. To optimize signal to noise ratio 5000 counts were collected in the peak channel with a nominal band pass of 4nm (42). The observed fluorescence decay profiles were fitted by using a non linear least-squares fitting procedure.

2.2.3 Circular Dichroism (CD) measurements

Far UV CD measurements of erythroid, non-erythroid spectrin in a concentration of 0.1mg/ml under different pH from 2 to 9 were carried out in a BioLogic Science Instruments MOS 450 Spectrometer using a quartz cuvette of path length of 1 cm at 25°C. All the measurements were taken between 190 nm and 250 nm at a scan rate of 3nm/min. An average of five scans was done to generate a single spectra from which the appropriate blank was deducted to give the CD profile of the protein (43,44). The spectra were subjected to moderate degree of noise reduction analysis by smoothing making sure that the overall spectrum remains unaltered. The results were expressed as the molar ellipticity per mean residue [θ , deg cm² dmol⁻¹]. The pH induced denaturation curves at constant temperature were obtained by recording the CD signal at 222 nm for each independent sample.

2.2.4 Tryptophan fluorescence quenching experiments

Intrinsic tryptophan fluorescence quenching of the two forms of spectrin was monitored by measuring tryptophan fluorescence after adding successive small aliquots of acrylamide from a 1M stock solution to each sample (45). The two proteins were incubated in

buffers of pH 2 to 9 in a final concentration of 0.1mg/ml prior to the quenching experiments. The excitation wave length used was 295 nm and emission was monitored at 340 nm. The fluorescence intensities obtained were corrected for dilution of the protein and for absorbance of light by acrylamide. Quenching data were analyzed by fitting to the Stern-Volmer equation.

2.2.5 Determining the size of spectrin at different pH

2.2.5.1 Static light scattering measurements

Static (90°) light scattering of both the spectrins was done in a Cary Eclipse spectrofluorimeter using excitation and emission wavelength both 360nm and using slit width 5 nm for excitation and emission both. The samples had a final concentration of 0.1 mg/ ml in requisite buffers in a pH range of 2 to 9. All the measurements were performed after samples were passed through 0.22µm nylon filter membrane (Millipore, USA). Multiple sets of data were taken and averaged to give final reading of each sample.

2.2.5.2 Dynamic light scattering measurement

DLS measurements were done to study the effects of pH on overall size of both the spectrins. The measurements were performed on a DLS spectrometer of Nano Series from Malvern instruments, equipped with thermostat chamber and 633nm laser. The protein concentrations were again maintained at 0.1 mg/ml in requisite buffers in the range of pH 9 to 2. Before carrying out the DLS experiments all solutions were passed through 0.22µm membrane filter (Millipore).

2.2.6 Determining pH induced conformational alteration of spectrin by fluorescent dye labeling

2.2.6.1 Pyrene Modification of erythroid and non-erythroid spectrin

Erythroid and non-erythroid spectrin(s) in a concentration of 2 mg/ml were labeled with pyrene maleimide for 60 minutes at 25°C by adding 50-fold molar excess of pyrene maleimide (Molecular Probes) in dimethylformamide (DMF) in a buffer of 10 mM Tris-HCl, pH 8 containing 20 mM KCl. The reaction was quenched by adding excess of 2-mercaptoethanol. The labeled protein was then separated from free pyrene maleimide by gel filtration on a Sephadex G-25 column. Labeled proteins were diluted in buffers of different pH from 2 to 9 in a final concentration of 0.1 mg/ml of protein. Fluorescence emission spectra of pyrene-labeled protein in different pH were measured by using excitation at 345 nm and the emission spectra were recorded in the range of 350-550 nm. Band pass of 5 nm for the excitation and 5 nm for emission slits were used to measure the fluorescence of pyrene labeled protein.

2.2.6.2 Thioflavin –T (ThT) binding assay

Erythroid and non-erythroid spectrin were incubated at a concentration of 0.2 mg/ml for 2 hr in Na-acetate buffer pH 4 and aliquots of this sample were added to a solution of ThT in 50 mM Na-MES pH 6. Final concentration of protein and ThT after mixing was kept at 0.03 mg/ml and 25 μ M respectively. Steady state fluorescence measurements were carried out on Cary Eclipse spectrofluorimeter. The emission spectra of free ThT and in the presence of protein were recorded from 465 to 600 nm using excitation wavelength of 445 nm and excitation and emission slits of 2 nm each.

2.2.6.3 ANS binding assay

A stock solution of ANS was prepared in DMF and the concentration was determined using an extinction coefficient of 7800 at 372 nm. Erythroid and non-erythroid spectrin solutions in pH range of 2 to 9 and concentration 0.1mg/ml were incubated with a 100 fold molar excess of ANS for 30 minutes in the dark at room temperature. Fluorescence measurements were taken on Cary Eclipse spectrofluorimeter. Fluorescence emission spectra were recorded from 450 to 600nm using excitation at 380nm and emission and excitation slits 5 nm each.

2.2.7 Determining the stability of spectrin by urea induced unfolding at different pH

Chemical denaturation of erythroid and non-erythroid spectrin, at a given pH was performed with increasing concentration of urea. The protein solutions were allowed to equilibrate at a desired concentration of denaturant for 1 hr before taking fluorescence measurement at 25°C using excitation at 295 nm. The data was expressed in terms of changes of fluorescence emission maxima with respect to intensity with increasing concentration of denaturant. The analysis of unfolding was performed using the two state model and values of the fraction of unfolded protein was calculated in the same way (37).

2.2.8 Effects of spectrin at different pH on prevention of protein aggregation

The chaperone potential of erythroid and brain spectrin was assayed at different pH using bovine serum albumin (BSA) as target proteins. 6 mg/ml BSA was heated at 50°C to aggregate it in presence and absence of spectrin at 0.1mg/ml concentration at pH 4 and pH 8. Aggregation was followed by 90° light scattering at 450nm in Cary eclipse spectrophotometer.

Moreover, the ability of both the forms of spectrin to inhibit insulin aggregation at the pH range of 2 – 9 was checked by pre-incubating spectrin at different pH and then adding 0.1mg of it to a 0.3mg/ml final concentration solution of insulin at pH 7. Aggregation was induced by adding 25 μ l of DTT and monitored by measuring the apparent O.D at 360 nm.

2.3 Result and Discussion

The isolated spectrin isoforms were found to be pure with distinctive doublet bands being seen in SDS-PAGE in case of erythroid spectrin as shown in **Figure 2.1**.

Figure 2.1: SDS-PAGE of erythroid and non erythroid spectrin.

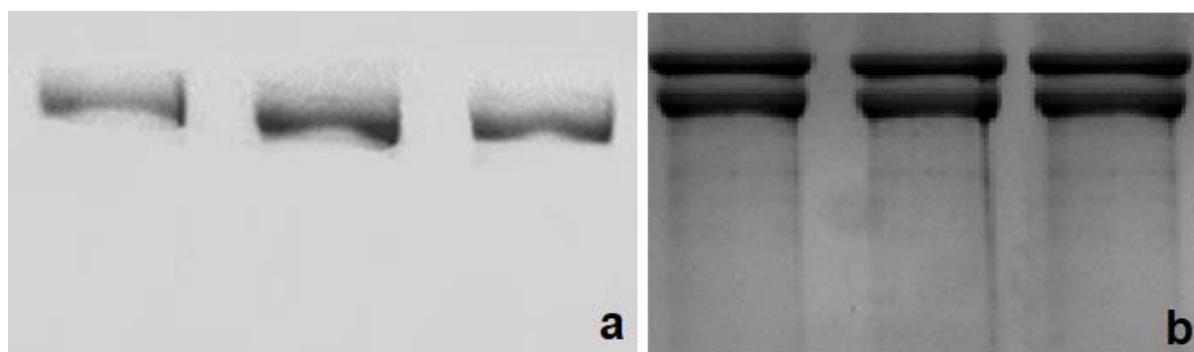


Figure 2.1: Panel 'a' shows SDS-PAGE of non-erythroid, brain spectrin and panel 'b' shows erythroid spectrin as seen on 8% gel after CBB staining.

It has been shown that both erythroid and brain spectrin have a two-state transition where only folded and unfolded states of the protein exist in rapid equilibrium without the intermediates accumulating sufficiently to be detectable (37). A considerable amount of efforts have been devoted to identify and study the partially folded structures of proteins. The partially folded intermediates can be made to accumulate in equilibrium by low concentrations of denaturants at low pH. It is crucial to identify and define the partially folded structures to understand the principles governing protein folding and stability.

Moreover it is known that many molecular chaperones exhibit a higher activity on structural perturbation or oligomerization (46-48). It is thus important to probe the structural changes of spectrin as a function of pH and correlate it to the chaperone potential of spectrin.

2.3.1 Conformational Alterations Probed by Intrinsic tryptophan Fluorescence

We have used intrinsic fluorescence of tryptophan to probe the conformational changes of spectrin as a function of pH. Tryptophan fluorescence gives us an idea of the conformational changes and microenvironment locally i.e. immediately surrounding the tryptophan residue (49). In spectrin this is very convenient as a probe of protein structure as typically the 106 amino acid long ‘spectrin repeat domain’ units in spectrin have tryptophans strongly conserved at 45th position in. So tryptophans act as probes for each of the repeating units (50-52). Representative curves for spectrin fluorescence spectra are given in **Figure 2.2**.

Figure 2.2: Fluorescence spectra of erythroid and non-erythroid spectrin.

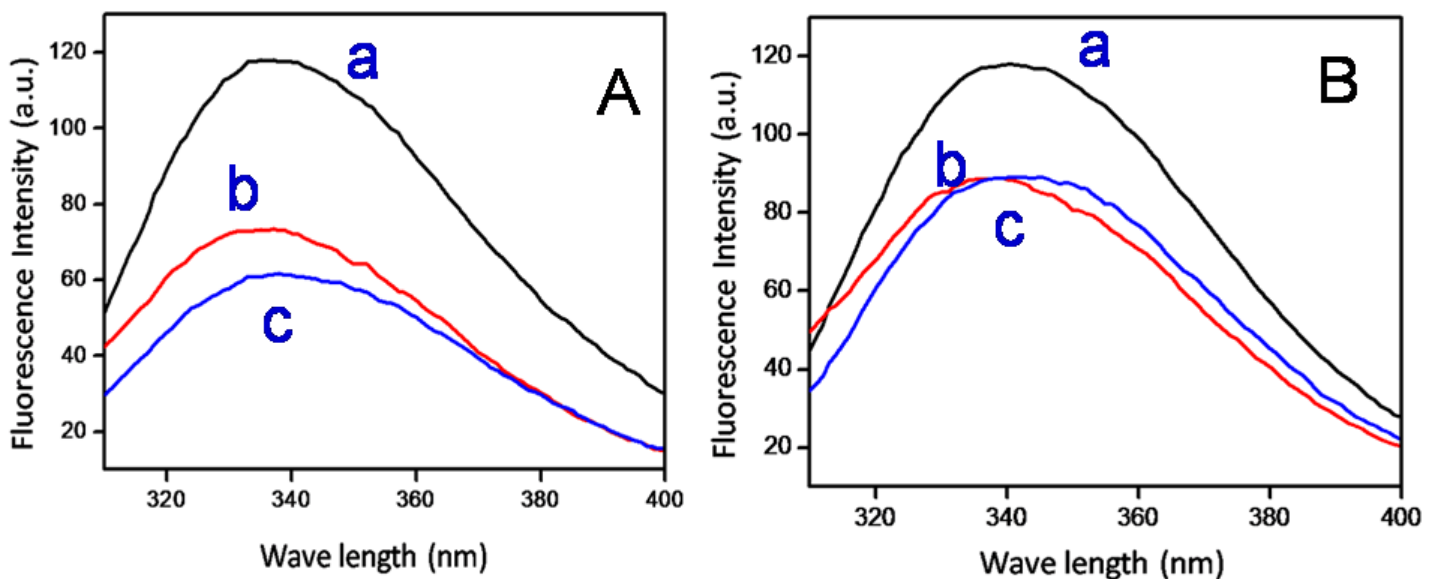


Figure 2.2: *Fluorescence emission spectra of (A) erythroid spectrin and (B) non-erythroid spectrin are shown in pH 8 (a) black, pH 4 (b) red and pH 2 (c) blue.*

As shown in **Figure 2.3**, panel a, which summarizes the pH dependent changes in fluorescence emission maxima (λ_{max}) of erythroid and non-erythroid spectrin respectively, the native state of both dimeric erythroid spectrin and tetrameric non-erythroid spectrin exhibited emission maxima at 338 nm which suggests buried tryptophan residues in the folded protein, an observation consistent with previous studies. At pH 4.0, fluorescent intensity (FI) was reduced by about 35% along with a blue shift of 5 nm indicating that tryptophan microenvironment became non-polar. Probably the structural change induced by low pH causes the burying of the Trp residues in a non-polar environment. Progressive lowering of pH leads to rise in λ_{max} with further decrease in FI (in case of erythroid spectrin, not brain spectrin) indicating that the microenvironment of the tryptophans is the most non-polar at pH 4. **Figure 2.3**, panel b shows the changes in FI of both erythroid and non-erythroid spectrin as a function of pH.

Figure 2.3: Fluorescent parameters of erythroid and non-erythroid spectrin.

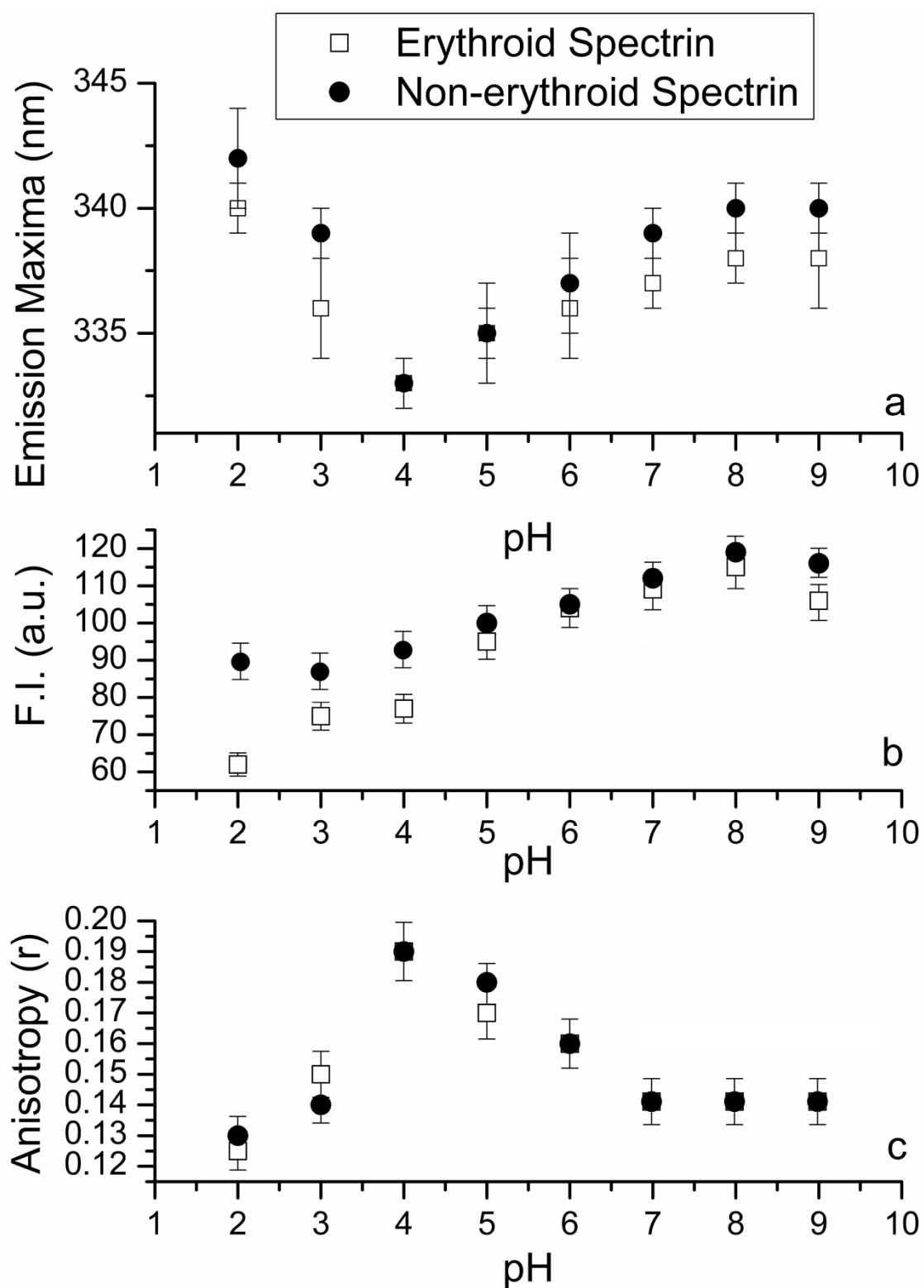


Figure 2.3: Panels a, b and c respectively shows the emission maxima, fluorescence intensity at emission maxima and anisotropy of erythroid and non-erythroid spectrin as a function of

pH. Data points show the mean values from 4 independent experiments with error bars denoting the standard error of mean.

Here we see that the tertiary structure of the proteins follow a biphasic transition. The first phase of transition is seen from pH 9 to pH 4 where a blue-shift of 5 nm (λ_{\max} at 333 nm) along with about 35% reduction in FI was observed. The second transition phase is from pH 4 to pH 2 which consists of a gradual decrease in FI in case of erythroid spectrin only along with a red-shift in λ_{\max} till pH 2. The observed changes in tryptophan fluorescence intensity can be due to a lot of mechanisms, namely excited-state electron transfer or proton transfer or energy transfer i.e. homo-FRET (53). The fluorescence intensity is quenched not only by the solvent molecules but also by intrinsic quenchers present in the protein. It is also well known that the characteristics of tryptophan fluorescence during pH induced conformational changes vary from protein to protein depending upon the location of tryptophan residues in the protein and the neighboring microenvironment. The λ_{\max} is red-shifted in more polar and blue-shifted in more non-polar microenvironment. It would seem that in the first phase of the transition, tryptophan residues initially get buried in non-polar environment with the appearance of a different conformational state at about pH 4 with a concomitant blue-shift in λ_{\max} and decrease in fluorescent intensity. The second phase consists of a further decrease in fluorescent intensity in case of erythroid spectrin only and a red-shifting of λ_{\max} indicating that the tryptophans are more solvent exposed and the protein has reached an acid denatured open conformation.

Fluorescence anisotropy provides information about the fluorophore's mobility, if the environment is crowded or the motion of the protein is constrained by aggregation or oligomerization the motion of the fluorophore is restricted and fluorescence anisotropy is expected to increase and vice versa. **Figure 2.3**, panel c show the intrinsic fluorescence

anisotropy values for erythroid and non-erythroid spectrin respectively under different pH conditions. Under native conditions of pH 8, the fluorescence anisotropy value was 0.14, at pH 4 and 2; this value was shifted to 0.19 and 0.13 respectively suggesting that the tryptophan motion is constrained at pH 4 and with further decrease of pH it reaches values less than that in native states. This indicates that at pH 4 some conformational change is happening that causes the protein structure to become rigid and with lowering of pH this rigidity is lost and the protein structure becomes more flexible supporting the hypothesis drawn from intrinsic fluorescence studies.

2.3.2 Changes in Secondary Structure Monitored by Far-UV CD

The CD spectra of a protein in the 190–250 nm region can be used to monitor the changes in secondary structure and give an idea of the percentage of α -helix and β -sheet content of a protein. In case of spectrin at native conditions of pH 8, the far UV CD spectra shows a minima at 208 and 222 nm, with the 222nm minima being more prominent indicating a major contribution of α -helix in the protein's secondary structure as shown in **Figure 2.4**. To explore the influence of pH on secondary structure of spectrin, we followed changes in mean residual ellipticity (MRE) at 222 nm. No large changes in the ellipticity values were observed in the pH range 9 to 6 for brain spectrin; in case of erythroid spectrin however a lowering of MRE was observed. This differential behavior may be due to the different dimeric/tetrameric nature of erythroid and brain spectrin; in case of erythroid spectrin the last segments of the α and β chains are unstructured and only fold into the typical spectrin repeat domain like triple helix when in a tetramer, while brain spectrin being a dimer has no such unstructured elements.

Figure 2.4: CD spectra of erythroid and non-erythroid spectrin.

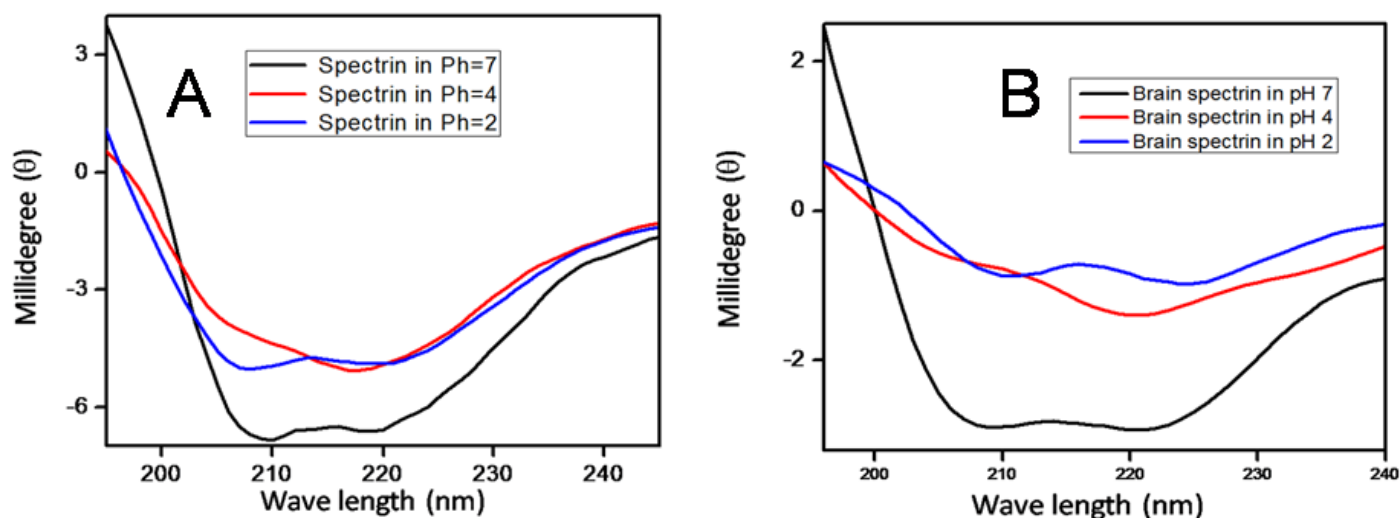


Figure 2.4: CD spectra of (A) erythroid spectrin and (B) non-erythroid spectrin showing at pH 7 (black), pH 4 (red) and at pH 2 (blue).

Interestingly at pH 4.0, the minima at 208 and 222 nm were reduced to a single negative peak around 217 nm indicating significant loss of secondary structure and acquisition of β -strand like conformation with only 40% of the native structure left intact as shown in **Figure 2.4**. However most of the spectral features of the native state were regained at pH 2 with helical content decreasing by about 50% suggesting the loss of significant amount of secondary structure, with residual retention of native structure at this acid denatured state.

Such conformational changes at pH 4 could be caused by helix-helix repulsion due to the protonation of ionizable side chains due to lowered pH. This α -helix to β -strand like conformational change could be an indication of oligomerization of protein which is also found in some other typical α -helical proteins. At pH 2 spectrin was found to regain some of

its native state like features and some helical content. This indicates that electrostatic interactions play a major role in the structural stability of such a multi-domain protein.

A comparison of the mean residue ellipticity at 222nm for erythroid and non-erythroid spectrin at different pH is shown in **Figure 2.5**.

Figure 2.5: Mean residual ellipticity.

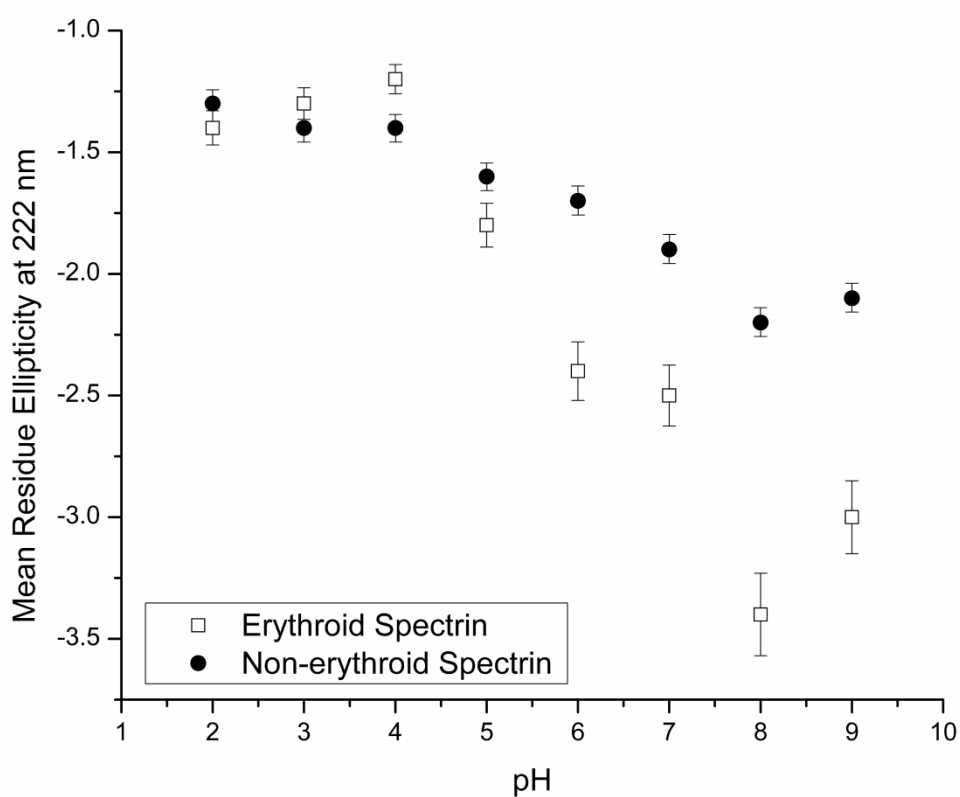


Figure 2.5: The mean residue ellipticity ($[\Theta]_{222} \times 10^4 \text{ deg-cm}^2\text{dmole}^{-1}$) for both the forms of spectrin is shown as a function of pH. Data points show the mean values from 4 independent experiments with error bars denoting the standard error of mean.

2.3.3 Evaluation of Trp Accessibility by Acrylamide Quenching

Fluorescence quenching by acrylamide was carried out to determine the extent of accessibility of tryptophan residues under different pH conditions. **Figure 2.6** shows the Stern-Volmer constant K_{SV} for erythroid and non-erythroid spectrin(s) at different pH. The bimolecular rate constant (k_q) was determined and it confirmed the dynamic nature of quenching.

Figure 2.6: K_{SV} values.

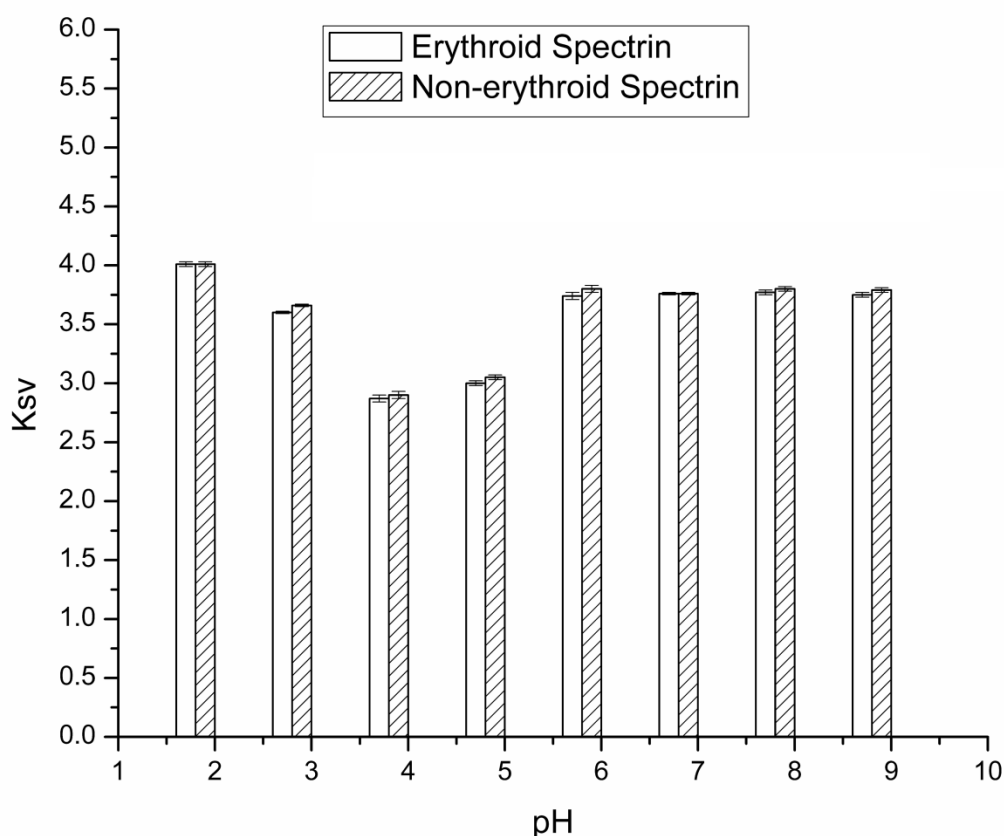


Figure 2.6: Bar diagram shows the Stern-Volmer quenching constant (K_{SV}) for both forms of spectrin at different pH. Data points show the mean values from 4 independent experiments with error bars denoting the standard error of mean.

The Stern-Volmer constant, K_{SV} was the lowest for both proteins at pH 4 of 2.9 M^{-1} for erythroid & 2.5 M^{-1} for non-erythroid spectrin, supporting the hypothesis of formation of spectrin oligomer at pH 4. pH induced conformational changes in the protein hindered solvent accessibility of the tryptophans and thus decreased K_{SV} values. With increasing tryptophan accessibility at pH 2 where protein is in an acid denatured state, K_{SV} increased to 3.75 M^{-1} and 4.2 M^{-1} for erythroid and non-erythroid spectrin respectively.

2.3.4 Detection of oligomeric spectrin by light scattering measurement

Changes in hydrodynamic radii (R_H) of both spectrins as a function of pH were evaluated by dynamic light scattering measurements as shown in **Figure 2.7**.

Figure 2.7: Dynamic and static light scattering of spectrin isoforms.

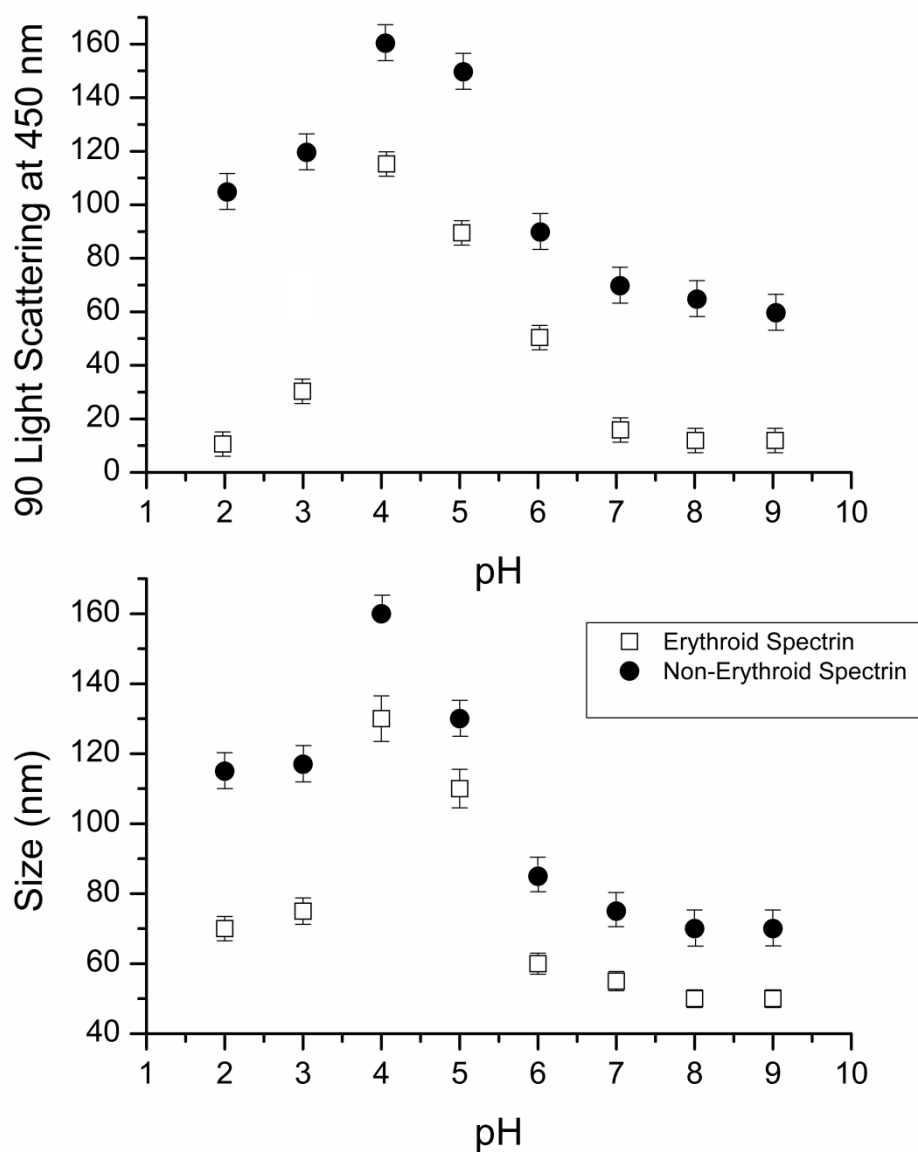


Figure 2.7: The change in 90° light scattering and hydrodynamic radius of both forms of spectrin is plotted as a function of pH. Data points show the mean values from 4 independent experiments with error bars denoting the standard error of mean.

The representative DLS profiles are given in **Figure 2. 8**. The R_H at pH 8 was found to be 50 and 70 nm for erythroid and brain spectrin respectively. A sharp increase in R_H at pH 4 was noted; R_H was found to be 160 nm for non-erythroid spectrin and 130 nm for erythroid spectrin. At pH 2 the R_H decreased again to 70 and 110 nm respectively. Static light scattering at 90° corroborates the DLS data and shows that at pH 4 the scattering intensity increased for both forms of spectrin. Both data shows the formation of spectrin species at pH 4 which is larger in size than that at native pH, indicating the formation of oligomers.

Figure 2.8: DLS profile of spectrin isoforms.

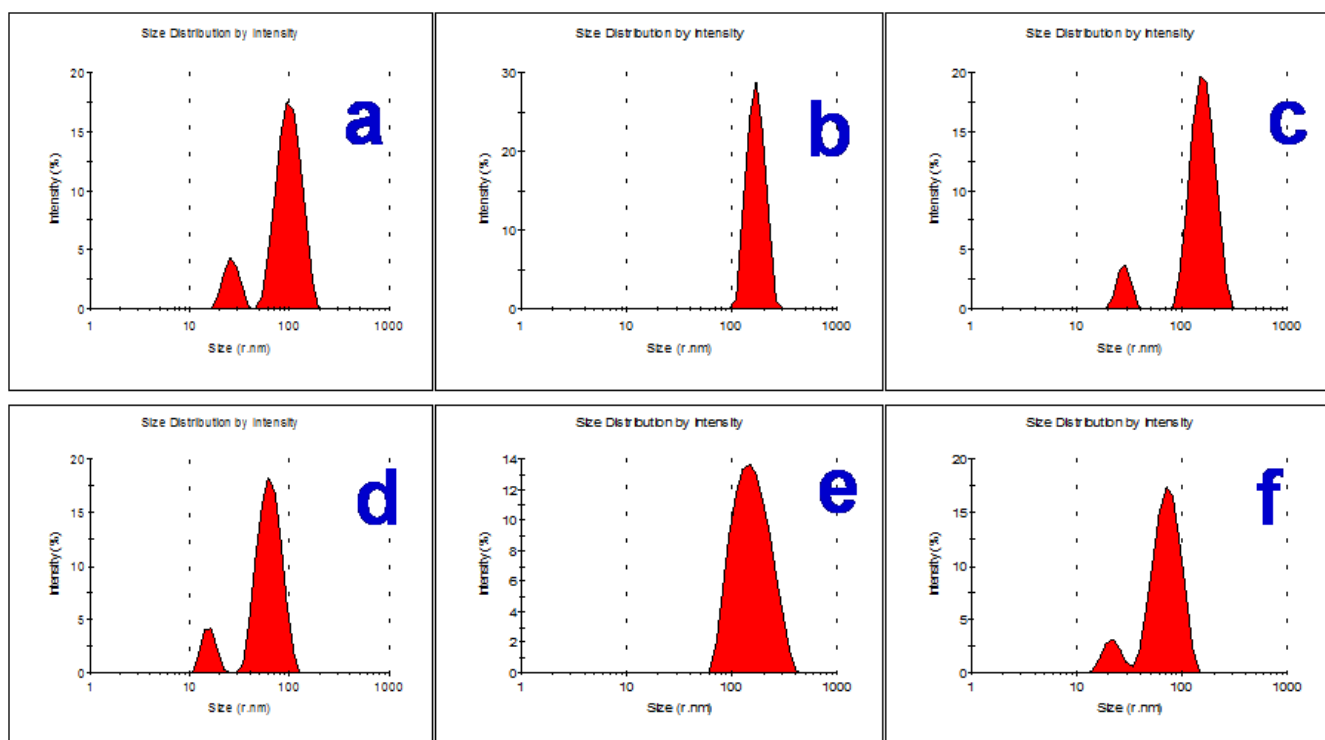


Figure 2.8: Representative histograms showing size distribution of spectrin species obtained by DLS measurements of non-erythroid spectrin in (a) pH 8; (b) pH 4 and (c) pH 2 and of erythroid spectrin in (d) pH 8; (e) pH 4 and (f) pH 2.

2.3.5 pH induced conformational alteration of spectrin monitored by pyrene and thioflavin T fluorescence

When a pyrene monomer is attached specifically to a single free sulfhydryl group, it typically exhibits fluorescence emission maxima at 375 and 395 nm when it is excited at 345 nm. However, in the presence of a second bound pyrene within 10 Å in proximity, it displays an additional broad and red-shifted fluorescence emission at 460nm, attributed to formation of an excited state dimer or 'excimer'. When two pyrene molecules giving rise to excimer fluorescence move away from each other, the excimer fluorescence emission intensity is decreased or entirely lost (54).

This unique spectral feature of pyrene is exploited to assess pH-induced conformational change of spectrin. Pyrene bound erythroid spectrin and non-erythroid spectrin in buffer of pH 8, **Figure 2.9**, reveals the presence of a mild excimer peak centered at 465 nm, in addition to the characteristic emission at 375, 385, and 395 nm. The excimer fluorescence decreased with decrease in pH from 8 to 6, on the other hand, at pH 4, the intensity increased. The increase in excimer emission intensity of both forms of pyrene conjugated spectrin was indicative of the fact that the pyrenes bound to spectrin were getting closer to each other at pH 4. We conclude that the increase in proximity of pyrene groups is probably due to the oligomeric association of spectrin.

Figure 2.9: Pyrene fluorescence.

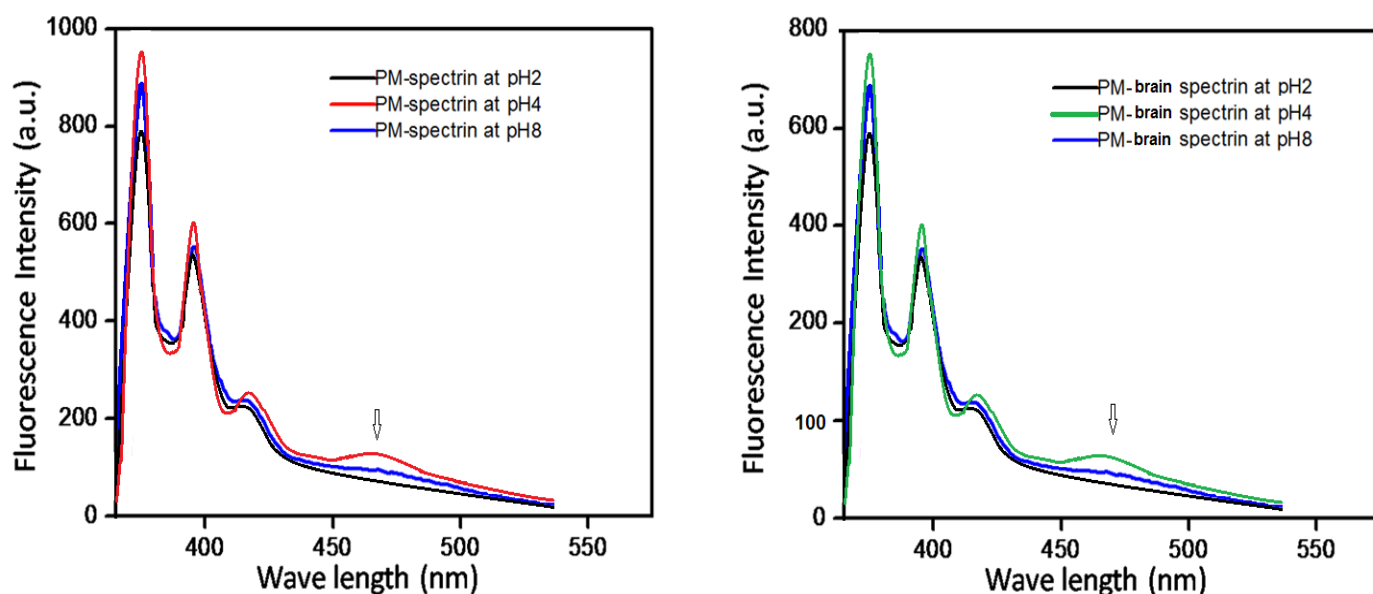


Figure 2.9: The pyrene bound fluorescence of erythroid and brain spectrin at pH 8, 4 and 2. Presence of excimer peak is denoted by the arrow mark.

Many α -helical proteins form soluble aggregates on structural perturbation which are characterized by a high content of β -sheet and amyloid superstructure and increase of hydrodynamic radius. Spectrins at pH 4 also show increase in hydrodynamic radius, so it becomes important to distinguish if this increase in size is due to oligomerization or aggregation. Amyloid fibrillar aggregates are usually detected by using dyes such as thioflavin-T or Congo-red, which change their spectroscopic properties by interaction with the aggregates. The fluorescence intensity at the λ_{\max} increases in presence of aggregates and vice versa. In order to detect whether spectrin at pH 4 undergoes aggregation or oligomerization thioflavin T binding assays were performed. **Figure 2.10** shows that with decreasing pH from 8 to 4 the Th-T fluorescence signal also decreased. This clearly indicates

that at pH 4 spectrin does not aggregate as it shows no enhancement of Th-T fluorescence. Rather it seems that the increase in size is due to oligomerization.

Figure 2.10: Th-T fluorescence.

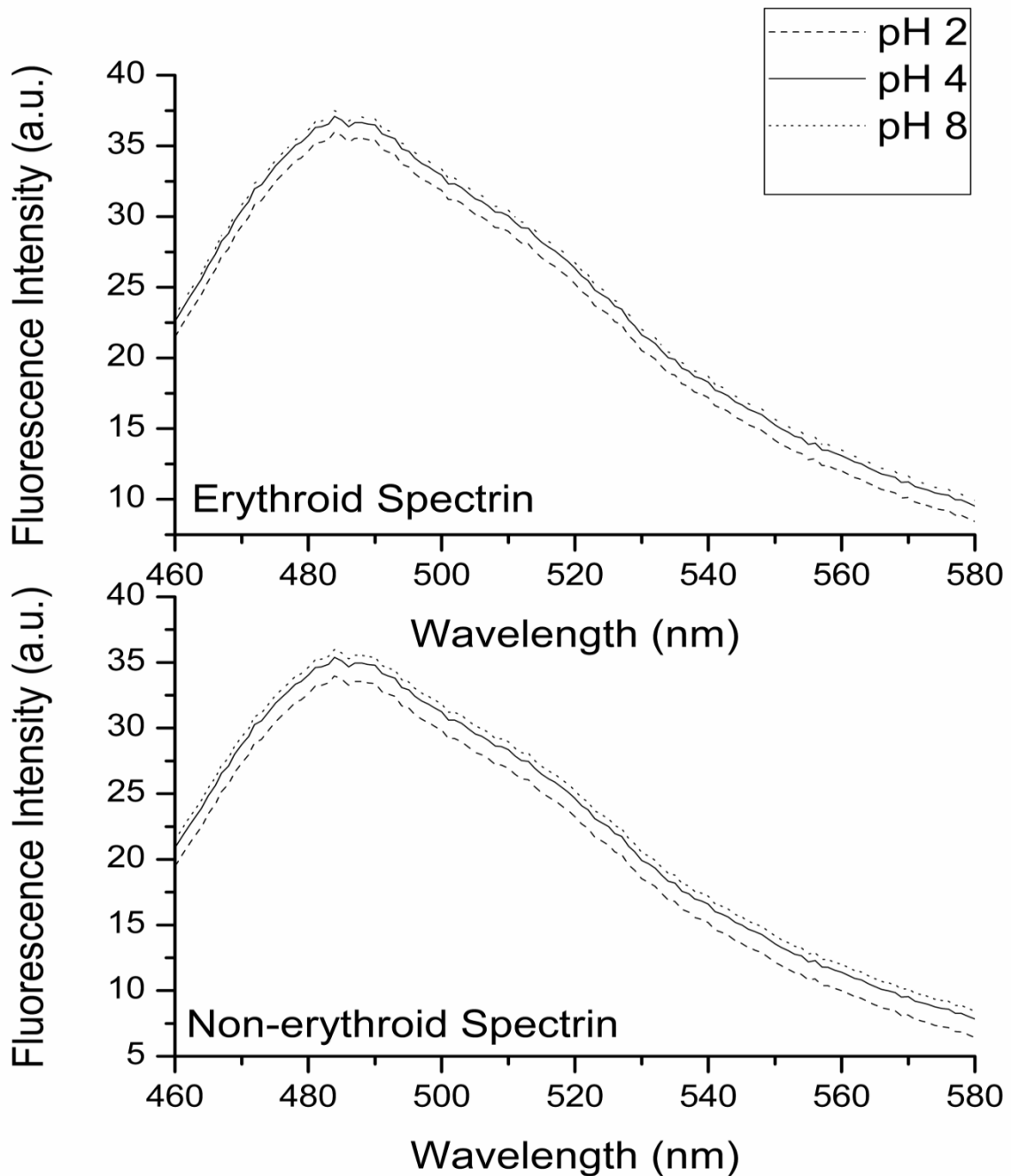


Figure 2.10: The Th-T fluorescence of both forms of spectrin is shown at pH 8, 4 and 2.

2.3.6 Detection of Exposed Hydrophobic Clusters by ANS Binding

ANS shows increased fluorescence intensity as well as a shift in λ_{max} from 471 to 468nm on binding with exposed hydrophobic patches in a protein. As such the folding intermediates of protein can be distinguished from their native state by a change in ANS fluorescence. As compared to the native state of a protein where the hydrophobic residues are well buried, the partially unfolded state of a protein molecule shows exposed hydrophobic surfaces which can interact with ANS molecules producing enhancement in fluorescence. At pH 4, ANS fluorescence was 8 times more than native state indicating enhanced exposure of hydrophobic patches. A plot of ANS fluorescence at 480 nm of both forms of spectrin as a function of pH is shown in **Figure 2.11**. No significant change in fluorescence was observed from pH 9 to pH 6. The increase in fluorescence showed a maximum at pH 4 indicating a conformational change that exposed maximum amount of hydrophobic patches to the solvent. This supports the hypothesis of oligomerization of spectrin at pH 4 as oligomers may be formed by the association of these exposed hydrophobic patches.

Figure 2.11: ANS fluorescence.

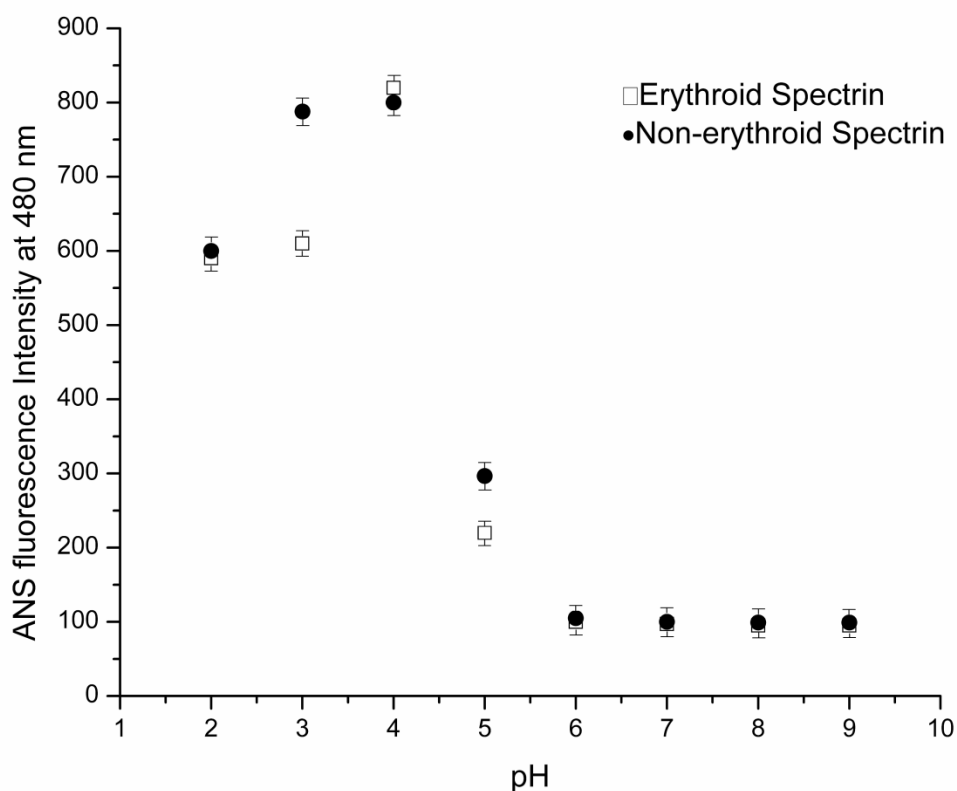


Figure 2.11: The fluorescence intensity at 480 nm for spectrin bound ANS fluorescence for both forms of spectrin is plotted as a function of pH. Data points show the mean values from 4 independent experiments with error bars denoting the standard error of mean.

2.3.7 Urea induced denaturation at different pH

In order to estimate the stability of the oligomeric spectrin formed at pH 4, urea induced denaturation was performed and monitored by fluorescence spectroscopy. The fluorescence emission maximum was plotted against increasing urea concentration, shown in **Figure 2.12** at three different pH 8, 4 and 2. The urea induced transition reveals a two step

transition with mid-point of transition (C_m) of both forms of spectrin summarized in **Table 2.1**.

Figure 2.12: Urea denaturation.

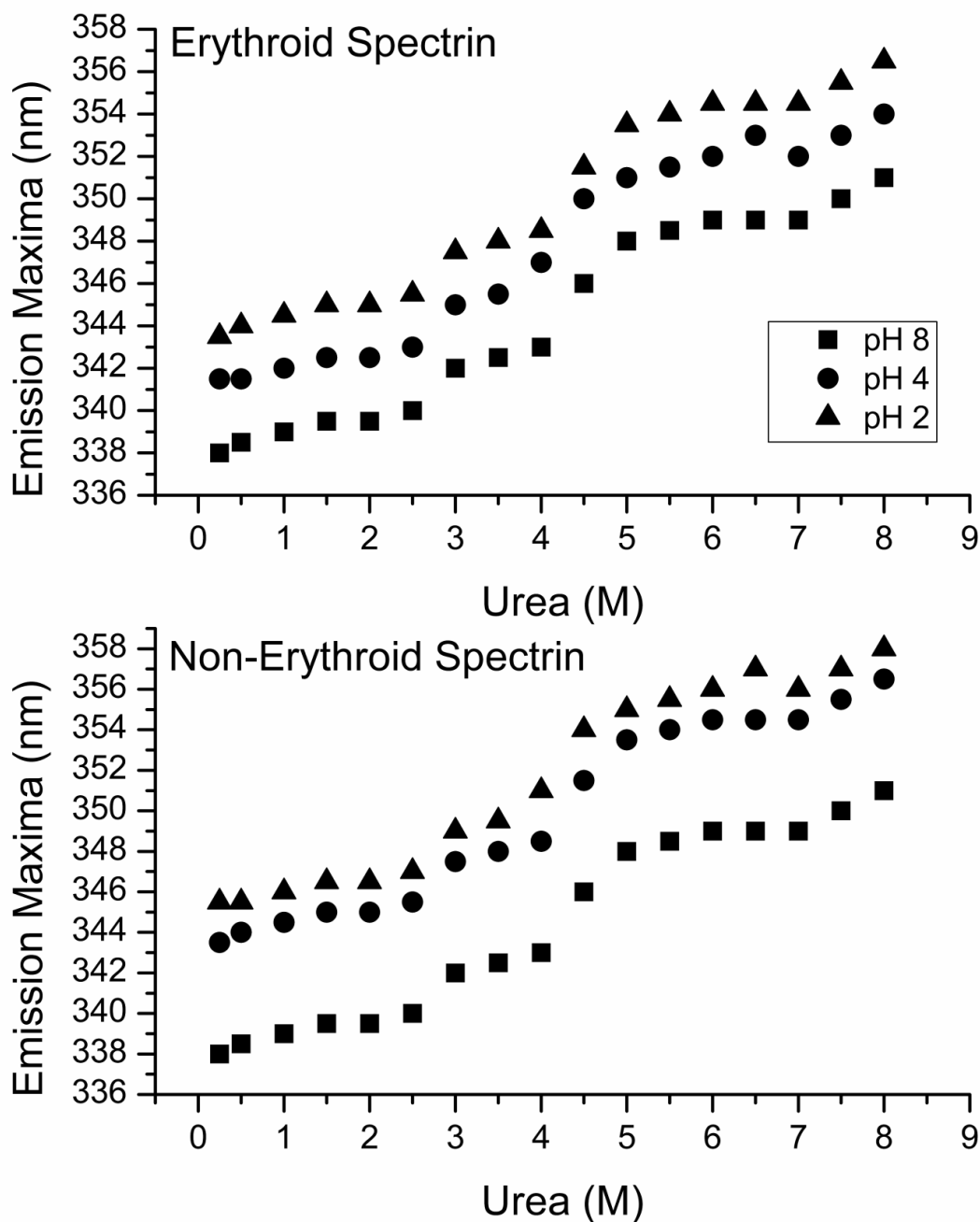


Figure 2.12: The emission maxima are plotted as a function of urea concentration at different pH for both forms of spectrin.

At pH 8 the λ_{\max} for 8 M urea denatured state for both kinds of spectrin was red shifted to 350 nm from that of the native state with concomitant increase in FI indicating that tryptophan residues are maximally exposed to the solvent. Decreasing the pH to 4 from 8 led to the red shifting of λ_{\max} of the 8 M urea denatured state with an accompanied drop in FI. As pH was lowered further to 2, the emission maxima became further red shifted for the 8 M urea denatured state with associated decrease in FI. These observations suggest that protein conformations under acidic conditions are different from that in native pH in a urea denatured state.

Table 2.1: Urea denaturation parameters of spectrin isoforms.

Protein	[Urea] _{1/2}
<ul style="list-style-type: none"> • Erythroid Spectrin in pH 7 • Erythroid Spectrin in pH 4 • Erythroid Spectrin in pH 2 	<ul style="list-style-type: none"> • 3.9±0.2 • 3.3±0.2 • 3.8±0.2
<ul style="list-style-type: none"> • Non-erythroid Spectrin in pH 7 • Non-erythroid Spectrin in pH 4 • Non-erythroid Spectrin in pH 2 	<ul style="list-style-type: none"> • 4.0±0.2 • 3.4±0.2 • 3.±0.2

Table 2.1: Urea induced unfolding: Parameters characterizing the urea induced unfolding of erythroid and non-erythroid spectrin at different pH, the concentrations of urea for half maximal unfolding are given.

2.3.8 pH dependent chaperone activity

It is seen that both forms of spectrin are better chaperones at pH 4 than they are at their native pH. At pH 4 we see that aggregation of BSA is prevented by about 60% while at pH 8 the prevention of aggregation is only 30% as shown in **Figure 2.13**. The maximum light scattered by BSA aggregated by itself is considered as the index of 100 % aggregation; comparing the maximum light scattered by BSA aggregated in the presence of spectrin at pH 4 and pH 2 with that of BSA aggregated by itself gives us the % to which spectrin is able to prevent BSA aggregation. Insulin aggregation with spectrins pre-incubated at different pH also shows the same trend (Fig S 5). In the case of insulin the actual aggregation had to be carried out at pH 7 because at lower pH DTT used to initiate aggregation does not work. Thus we pre-incubated spectrin to oligomerize it and then used the oligomerized spectrin in the aggregation reaction of insulin as a chaperone. This supports our hypothesis that at pH 4 the conformational changes in the protein have functional implications as seen by a higher chaperone potential. Several other chaperones are known which act better on structural perturbation, most well known of which are the sHSPs.

Figure 2.13: pH dependent chaperone activity.

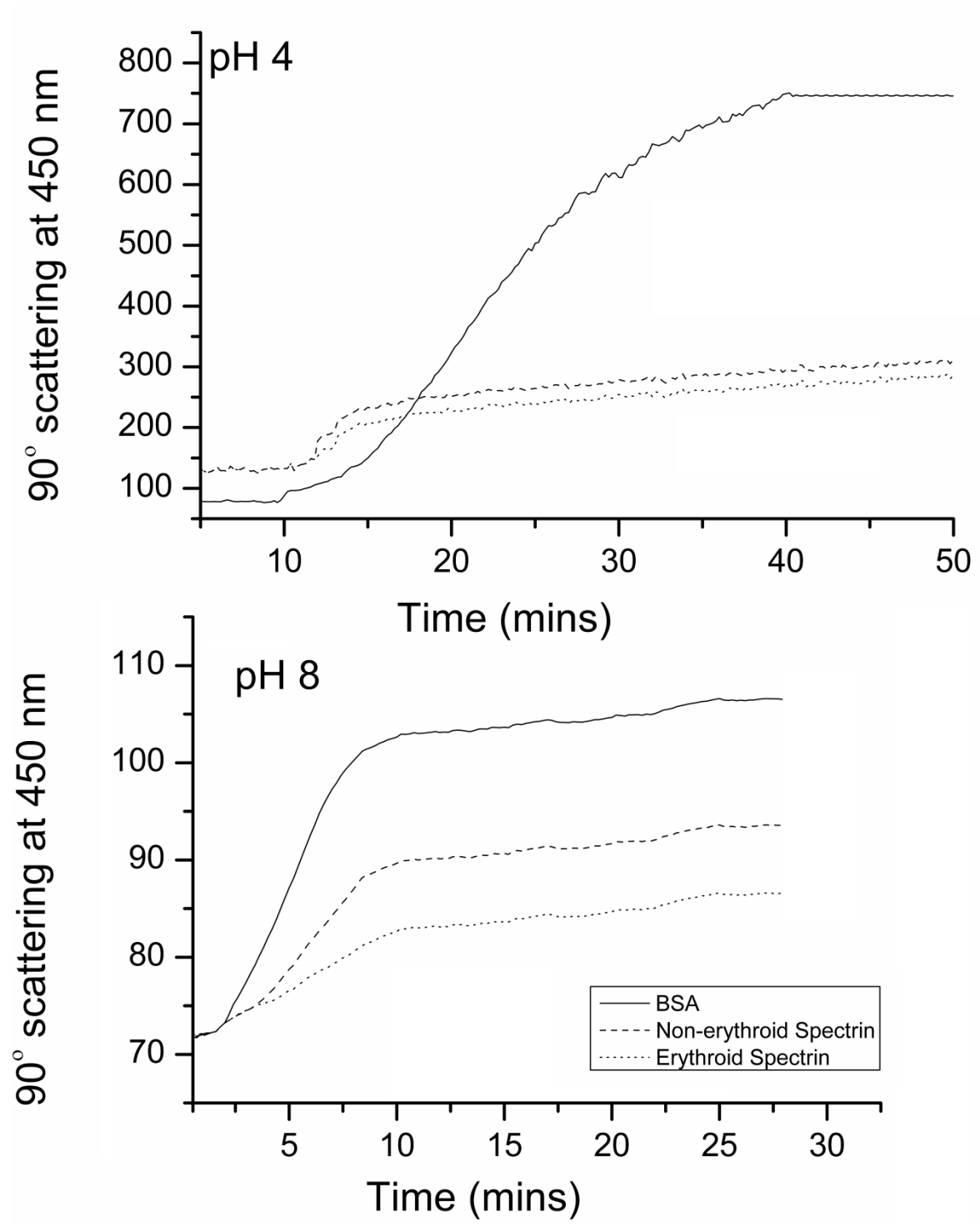


Figure 2.13: The thermal aggregation of BSA is followed at pH 8 and 4 in presence and absence of both forms of spectrin.

In summary we propose that both dimeric spectrin and tetrameric fodrin undergoes oligomerization at low pH of around 4 and these oligomers are better chaperones than the native dimeric or tetrameric proteins. Fluorescence data shows that at pH 4 spectrin lacks well defined tertiary structure with 5 nm hypsochromic shift of the emission maximum but on further decreasing pH below 4, spectrin undergoes denaturation. The mean residue ellipticity at 222nm showed a transition at pH 4 with appreciable loss of α -helical structure and probable formation β -sheet like structure. This is a further indication of oligomerization as is seen in some chaperones like α -crystallins. Maximum enhancement of ANS fluorescence intensity is observed again at pH 4, compared to its native state at pH 8 or acid denatured state at pH 2, indicating maximum exposure of hydrophobic clusters at pH 4, it is also reflected in the enhanced chaperone-like activity of spectrin. Acrylamide quenching measurements showed that at pH 4, the proteins assume a conformation where the tryptophans are less exposed to the solvent compared to the same in its native conformation at pH 8. This could be due to the fact that the tryptophan residues get buried inside the protein when it oligomerizes at pH 4. Dynamic light scattering data indicates at pH 4 the size of the hydrodynamic radius of the protein increases significantly compared to its native or unfolded state, which is also supported by 90° light scattering measurements. Urea induced unfolding data indicate that this state at pH 4 is chemically less stable compared to native state. The data is summarized in **Table 2.1**. The structural transition at pH 4 enhances the protective ability of erythroid and non-erythroid spectrin perhaps by increasing or reorganizing the hydrophobic surfaces. Poon and co workers have shown a similar pH-dependent chaperon interaction between BSA and clusterin (34). Our hypothesis is that at pH 4 the pH induced conformational changes in spectrin cause it to expose more hydrophobic patches to the solvent and oligomerize which makes it a better chaperone.

Abbreviations:

BSA, bovine serum albumin; CD, Circular Dichroism ; DLS, Dynamic Light Scattering; DMF, dimethylformamide; DTT, dithiothreitol; EDTA, ethylene diamine tetraacetic acid; EGTA, ethylene glycol tetraacetic acid; PAGE, Poly acrylamide gel electrophoresis; PMSF, phenyl methylsulfonyl fluoride; SDS, Sodium Dodecyl sulphate; Th-T, Thioflavin-T.

References

1. Begg, G. E., Morris, M. B., and Ralston, G. B. (1997) Comparison of the salt-dependent self-association of brain and erythroid spectrin. *Biochemistry* **36**, 6977-6985
2. Morris, S. A., Eber, S. W., and Gratzer, W. B. (1989) Structural basis for the high activation energy of spectrin self-association. *FEBS letters* **244**, 68-70
3. DeSilva, T. M., Peng, K. C., Speicher, K. D., and Speicher, D. W. (1992) Analysis of human red cell spectrin tetramer (head-to-head) assembly using complementary univalent peptides. *Biochemistry* **31**, 10872-10878
4. Shammass, S. L., Rogers, J. M., Hill, S. A., and Clarke, J. (2012) Slow, reversible, coupled folding and binding of the spectrin tetramerization domain. *Biophysical journal* **103**, 2203-2214
5. Batey, S., Scott, K. A., and Clarke, J. (2006) Complex folding kinetics of a multidomain protein. *Biophysical journal* **90**, 2120-2130
6. McGough, A. M., and Josephs, R. (1990) On the structure of erythrocyte spectrin in partially expanded membrane skeletons. *Proceedings of the National Academy of Sciences of the United States of America* **87**, 5208-5212
7. Ralston, G. B. (1991) Temperature and pH dependence of the self-association of human spectrin. *Biochemistry* **30**, 4179-4186

8. Gedde, M. M., Yang, E., and Huestis, W. H. (1999) Resolution of the paradox of red cell shape changes in low and high pH. *Biochimica et biophysica acta* **1417**, 246-253
9. Cudd, A., Arvinte, T., Schulz, B., and Nicolau, C. (1989) Dextran protection of erythrocytes from low-pH-induced hemolysis. *FEBS letters* **250**, 293-296
10. Ivanov, I. T. (1999) Low pH-induced hemolysis of erythrocytes is related to the entry of the acid into cytosole and oxidative stress on cellular membranes. *Biochimica et biophysica acta* **1415**, 349-360
11. Elgsaeter, A., Shotton, D. M., and Branton, D. (1976) Intramembrane particle aggregation in erythrocyte ghosts. II. The influence of spectrin aggregation. *Biochimica et biophysica acta* **426**, 101-122
12. Gros, M., Vrhovec, S., Brumen, M., Svetina, S., and Zeks, B. (1996) Low pH induced shape changes and vesiculation of human erythrocytes. *General physiology and biophysics* **15**, 145-163
13. Sikorski, A. F., Michalak, K., and Bobrowska, M. (1987) Interaction of spectrin with phospholipids. Quenching of spectrin intrinsic fluorescence by phospholipid suspensions. *Biochimica et biophysica acta* **904**, 55-60
14. Mombers, C., de Gier, J., Demel, R. A., and van Deenen, L. L. (1980) Spectrin-phospholipid interaction. A monolayer study. *Biochimica et biophysica acta* **603**, 52-62
15. Cole, N., and Ralston, G. B. (1992) The effects of ionic strength on the self-association of human spectrin. *Biochimica et biophysica acta* **1121**, 23-30
16. Lange, Y., Hadesman, R. A., and Steck, T. L. (1982) Role of the reticulum in the stability and shape of the isolated human erythrocyte membrane. *The Journal of cell biology* **92**, 714-721

17. Johnson, R. M., Taylor, G., and Meyer, D. B. (1980) Shape and volume changes in erythrocyte ghosts and spectrin-actin networks. *The Journal of cell biology* **86**, 371-376
18. Fujita, T., Ralston, G. B., and Morris, M. B. (1998) Purification of erythrocyte spectrin alpha- and beta-subunits at alkaline pH and structural and hydrodynamic properties of the isolated subunits. *Biochemistry* **37**, 272-280
19. An, X., Zhang, X., Salomao, M., Guo, X., Yang, Y., Wu, Y., Gratzer, W., Baines, A. J., and Mohandas, N. (2006) Thermal stabilities of brain spectrin and the constituent repeats of subunits. *Biochemistry* **45**, 13670-13676
20. Fujita, T., Ralston, G. B., and Morris, M. B. (1998) Biophysical properties of human erythrocyte spectrin at alkaline pH: implications for spectrin structure, function, and association. *Biochemistry* **37**, 264-271
21. Redfield, C., Smith, R. A., and Dobson, C. M. (1994) Structural characterization of a highly-ordered 'molten globule' at low pH. *Nature structural biology* **1**, 23-29
22. Fink, A. L., Calciano, L. J., Goto, Y., Kurotsu, T., and Palleros, D. R. (1994) Classification of acid denaturation of proteins: intermediates and unfolded states. *Biochemistry* **33**, 12504-12511
23. Goto, Y., Takahashi, N., and Fink, A. L. (1990) Mechanism of acid-induced folding of proteins. *Biochemistry* **29**, 3480-3488
24. Vassilenko, K. S., and Uversky, V. N. (2002) Native-like secondary structure of molten globules. *Biochimica et biophysica acta* **1594**, 168-177
25. Dill, K. A., and Shortle, D. (1991) Denatured states of proteins. *Annual review of biochemistry* **60**, 795-825
26. Baldwin, R. L. (1975) Intermediates in protein folding reactions and the mechanism of protein folding. *Annual review of biochemistry* **44**, 453-475

27. Shortle, D., and Ackerman, M. S. (2001) Persistence of native-like topology in a denatured protein in 8 M urea. *Science* **293**, 487-489
28. Ray, S., Bhattacharyya, M., and Chakrabarti, A. (2005) Conformational study of spectrin in presence of submolar concentrations of denaturants. *Journal of fluorescence* **15**, 61-70
29. Dubey, V. K., and Jagannadham, M. V. (2003) Differences in the unfolding of procerain induced by pH, guanidine hydrochloride, urea, and temperature. *Biochemistry* **42**, 12287-12297
30. Tanford, C. (1968) Protein denaturation. *Advances in protein chemistry* **23**, 121-282
31. Tanford, C. (1970) Protein denaturation. C. Theoretical models for the mechanism of denaturation. *Advances in protein chemistry* **24**, 1-95
32. Anderson, D. E., Becktel, W. J., and Dahlquist, F. W. (1990) pH-induced denaturation of proteins: a single salt bridge contributes 3-5 kcal/mol to the free energy of folding of T4 lysozyme. *Biochemistry* **29**, 2403-2408
33. Bhattacharyya, M., Ray, S., Bhattacharya, S., and Chakrabarti, A. (2004) Chaperone activity and prodan binding at the self-associating domain of erythroid spectrin. *The Journal of biological chemistry* **279**, 55080-55088
34. Poon, S., Rybchyn, M. S., Easterbrook-Smith, S. B., Carver, J. A., Pankhurst, G. J., and Wilson, M. R. (2002) Mildly acidic pH activates the extracellular molecular chaperone clusterin. *The Journal of biological chemistry* **277**, 39532-39540
35. Stengel, F., Baldwin, A. J., Painter, A. J., Jaya, N., Basha, E., Kay, L. E., Vierling, E., Robinson, C. V., and Benesch, J. L. (2010) Quaternary dynamics and plasticity underlie small heat shock protein chaperone function. *Proceedings of the National Academy of Sciences* **107**, 2007-2012

36. Bose, D., Patra, M., and Chakrabarti, A. (2017) Effect of pH on stability, conformation, and chaperone activity of erythroid & non-erythroid spectrin. *Biochimica et biophysica acta. Proteins and proteomics* **1865**, 694-702
37. Patra, M., Mukhopadhyay, C., and Chakrabarti, A. (2015) Probing conformational stability and dynamics of erythroid and nonerythroid spectrin: effects of urea and guanidine hydrochloride. *PloS one* **10**, e0116991
38. Gratzer, W. (1982) [44] Preparation of spectrin. *Methods in enzymology* **85**, 475-480
39. Davis, J., and Bennett, V. (1983) Brain spectrin. Isolation of subunits and formation of hybrids with erythrocyte spectrin subunits. *Journal of Biological Chemistry* **258**, 7757-7766
40. Das, D., Patra, M., and Chakrabarti, A. (2015) Binding of hemin, hematoporphyrin, and protoporphyrin with erythroid spectrin: fluorescence and molecular docking studies. *European Biophysics Journal* **44**, 171-182
41. Bradford, M. M. (1976) A rapid and sensitive method for the quantitation of microgram quantities of protein utilizing the principle of protein-dye binding. *Analytical biochemistry* **72**, 248-254
42. Silva, N. D., Jr., and Prendergast, F. G. (1996) Tryptophan dynamics of the FK506 binding protein: time-resolved fluorescence and simulations. *Biophysical journal* **70**, 1122-1137
43. Johnson Jr, W. C. (1988) Secondary structure of proteins through circular dichroism spectroscopy. *Annual review of biophysics and biophysical chemistry* **17**, 145-166
44. Ray, S., and Chakrabarti, A. (2003) Erythroid spectrin in micellar detergents. *Cell motility and the cytoskeleton* **54**, 16-28
45. Eftink, M. R., and Ghiron, C. A. (1981) Fluorescence quenching studies with proteins. *Analytical biochemistry* **114**, 199-227

46. Raman, B., Ramakrishna, T., and Rao, C. M. (1995) Temperature dependent chaperone-like activity of alpha-crystallin. *FEBS letters* **365**, 133-136
47. Giese, K. C., and Vierling, E. (2002) Changes in oligomerization are essential for the chaperone activity of a small heat shock protein in vivo and in vitro. *The Journal of biological chemistry* **277**, 46310-46318
48. Hong, W., Jiao, W., Hu, J., Zhang, J., Liu, C., Fu, X., Shen, D., Xia, B., and Chang, Z. (2005) Periplasmic protein HdeA exhibits chaperone-like activity exclusively within stomach pH range by transforming into disordered conformation. *The Journal of biological chemistry* **280**, 27029-27034
49. Chattopadhyay, A., Rawat, S. S., Kelkar, D. A., Ray, S., and Chakrabarti, A. (2003) Organization and dynamics of tryptophan residues in erythroid spectrin: novel structural features of denatured spectrin revealed by the wavelength-selective fluorescence approach. *Protein science : a publication of the Protein Society* **12**, 2389-2403
50. Mitra, M., Chaudhuri, A., Patra, M., Mukhopadhyay, C., Chakrabarti, A., and Chattopadhyay, A. (2015) Organization and dynamics of tryptophan residues in brain spectrin: novel insight into conformational flexibility. *Journal of fluorescence* **25**, 707-717
51. Kahana, E., Pinder, J. C., Smith, K. S., and Gratzer, W. B. (1992) Fluorescence quenching of spectrin and other red cell membrane cytoskeletal proteins. Relation to hydrophobic binding sites. *The Biochemical journal* **282 (Pt 1)**, 75-80
52. Borgia, M. B., Borgia, A., Best, R. B., Steward, A., Nettels, D., Wunderlich, B., Schuler, B., and Clarke, J. (2011) Single-molecule fluorescence reveals sequence-specific misfolding in multidomain proteins. *Nature* **474**, 662-665

53. Nanda, V., and Brand, L. (2000) Aromatic interactions in homeodomains contribute to the low quantum yield of a conserved, buried tryptophan. *Proteins* **40**, 112-125
54. Hammarstrom, P., Kalman, B., Jonsson, B. H., and Carlsson, U. (1997) Pyrene excimer fluorescence as a proximity probe for investigation of residual structure in the unfolded state of human carbonic anhydrase II. *FEBS letters* **420**, 63-68

Chapter 3:

The effect of post-

translational modifications,

phospholipid, hemoglobin

binding and macromolecular

crowders

3.1 Introduction

Spectrin, is a multifunctional protein. Thus far the chaperone like activity of spectrin has only been shown in single component systems (1) and no studies have been performed to monitor the relationship of spectrin chaperone activity with its phospholipid or hemoglobin binding ability. Multifunctional chaperones are commonly found where their chaperone function is dependent on or modulated by their other functionalities such as in the case of PDI, where its chaperone activity is dependent on its disulfide isomerase enzyme activity (2-4). Similarly B23 is a multifunctional chaperone, that has protein interactive roles which depends on its chaperone activity (5). There are also reports of chaperones interacting directly with membrane lipids (6-8).

Available literature suggests that protein aggregation inside a cell is influenced by presence of biological membranes such as in the case of amyloid- β protein and α -synuclein (9). In case of spectrin it becomes important to probe how its chaperone property is influenced by the presence of biological membranes since it is a membrane associated protein and is also known to directly bind lipids (10,11). Further many reports exist that implicate spectrin in a variety of RBC diseases such as hereditary elliptocytosis and spherocytosis (12,13); specifically, spectrin detachment from cell membrane is known to be the major reason for the occurrence of these diseases.

In the present study we have used small unilamellar vesicles of different phospholipids to study the effect of phospholipid concentrations and compositions of membranes on the chaperone activity of spectrin, as measured by aggregation based assays using insulin and ADH. In addition, we have used enzyme refolding assays and AFM imaging to substantiate our findings.

While chaperones in general have a very broad range of substrates (14) some chaperones are known to have one or a limited few clients, like HSP47 (15) and AHSP (16) (17) which are specific for collagen and α -globin respectively. It has previously been shown that spectrin binds to hemoglobin and can act as a α - and β -globin chaperone (18,19). In this regard it is interesting to note that spectrin repeat domains, the 106 amino acid long modular units of which spectrin is composed, also shares the same general fold and has sequence similarity to AHSP (20), a known erythrocyte cytosol resident α -globin chaperone. Further it is known that spectrin can interact with hemoglobin variants (21). Spectrin hemoglobin interactions may also have implications in hemoglobin diseases like E β -thalassemias (21). It is thus important to probe the chaperone activity of spectrin in presence of hemoglobin. Similarly as above we have used protein aggregation and enzyme refolding assays to quantify spectrin chaperone activity in presence of hemoglobin.

Protein folding/misfolding and aggregation inside the crowded environment of a cell is a fundamentally more complex process than that in *in-vitro* systems where only one species of protein is probed in a crowder free environment. Macromolecular crowders are present in a high concentration inside a cell and exert an effect on protein aggregation predominantly via excluded volume effect and also by modulating solution viscosity and by non-specific protein interactions (22-24), and it has been shown that they can influence the aggregation pathway followed by an aggregating protein (25). This is of particular importance in cases where protein aggregation causes disease like Alzheimer's disease and human IAPP fibril induced cytotoxicity (26,27).

The exact nature of the crowder determines its interaction with the aggregating protein and thus the effect it has on protein aggregation. For example CI2 interacts more with lysozyme as a crowding agent and is more destabilized in its presence than it is with BSA as

a crowder (28); however there are reports that indicate that crowders irrespective of their exact nature, for example both proteins and polymers, act in the same way (29). Presence of macromolecular crowders can modulate weak protein-protein interactions and crowder-protein attractive interactions are destabilizing for protein-protein interactions (30,31). On the other hand it has been shown that crowders can also enhance chaperone-client interactions thereby reducing the aggregation of misfolded proteins (32).

Here we have investigated the chaperone activity of spectrin under conditions that more closely resemble those found *in-vivo* by probing the chaperone activity of spectrin in presence of protein crowder BSA and polymer crowder PVP40. As above the chaperone activity was measured by protein aggregation and enzyme refolding assays.

Post translational modifications are seen to affect the functions of molecular chaperones, such as in HSP90 (33) and α -crystallins (34). Glycation in general is thought to increase with protein age and generally decreases the chaperone function of a given molecular chaperone (35). Spectrin being RBC resident has a lifespan of about 120 days which makes it a long-lived protein and gives it time to interact with the glucose being carried in blood and accumulate glycation modifications. It has been reported that while spectrin can be easily glycated *in-vitro*; the RBC has mechanisms to prevent spectrin glycation (36) which depends on membrane association of spectrin and thus may be absent in disease states that cause membrane detachment of spectrin. Here we have glycated spectrin *in-vitro* and checked its chaperone function as described above.

Spectrin is also known to be a phospho-protein and it is known that the phosphorylation occurs at the C-terminus of the β -subunit (37,38). It is also known that spectrin can have a maximum of 6 phosphorylations, 5 being on serine residues and 1 being on threonine (37). Under normal conditions the majority of spectrin isolated from blood has

1-4 phosphorylations (37). It is known that spectrin phosphorylation influences its interactions with the cell membrane leading to changes in membrane mechanical properties (39). Also phosphorylation affects spectrin interaction with other proteins such as actin (40). There are chaperones whose activities are known to be modulated by phosphorylation such as Cdc37, endoplasmic reticulum protein 99 (erp99) and B23. As such it becomes important to probe the effect phosphorylation has on spectrin chaperone function. Here we have hyper- and hypo-phosphorylated spectrin and probed its chaperone activity as above.

3.2 Materials and Methods

Tris base, potassium chloride, sodium chloride, sodium hydrogen phosphate, sodium di-hydrogen phosphate, D-glucose, EDTA, phenylmethyl sulfonyl fluoride, DTT, Insulin from bovine pancreas, α -glucosidase from *Bacillus subtilis* and 4-nitrophenyl- α -D-glucopyranoside were obtained from Sigma Chemical Corporation. Glycoprotein detection kit was purchased from Sigma. DMPC, DMPE, DMPS, DOPC, DOPE, cholesterol and polycarbonate membranes filters of 30, and 100nm pore sizes were from Avanti Polar Lipids. Calf intestinal alkaline phosphatase, polyclonal primary antibodies against phosphoserine (goat) and phosphothreonine (rabbit), and monoclonal anti-rabbit and anti-goat secondary antibodies conjugated to HRP was acquired from Abcam. ECL western blotting substrate kit was purchased from Abcam. Water for the purpose of buffer preparation was purified through a MilliQ system and MilliQ water was used throughout all the experiments.

3.2.1 Isolation and purification of hemoglobin

Human hemoglobin variant HbA was isolated from blood samples collected from blood samples obtained from Ramkrishna Mission Seva Pratishthan Hospital, Kolkata, India, with informed written consent of the patients following the guidelines of the Institutional

Ethical Committee. Samples were characterized using Bio-Rad Variant HPLC system and variant hemoglobin content was determined (41).

RBCs were collected by centrifugation, washed with PBS and lysed with three volumes of 1mM Tris-HCl pH 8.0 at 4°C and lysate was purified by gel filtration on Sephadex G-100 column (45x1cm) using 5mM Tris-HCl 50mM KCl pH 8.0 buffer. Purity was checked by 12% SDS PAGE analysis and concentration was checked using molar extinction coefficient of 125000 at 415 nm. Presence of oxy form of hemoglobin was confirmed using absorbance at 415 nm and 541 nm (42). Hemoglobin preparation was stored at - 70° C for a maximum of one week.

3.2.2 Small unilamellar vesicle (SUV) preparation

Small unilamellar vesicles of defined lipid compositions were prepared by sonication according to previously published protocol (10,43). Briefly, appropriate amounts of phospholipids were weighed and dissolved in chloroform: methanol 2:1 (v/v) and the solvent was evaporated under dry nitrogen to produce thin films which were thoroughly desiccated under vacuum. The dry films were hydrated with 100 mM phosphate buffer in case of aggregation experiments and 50 mM phosphate buffer in case of enzyme refolding experiments. The lipid dispersions were then sonicated in a Sartorius Labsonic M sonicator in bursts of 1 min (full cycle, 50% amplitude), followed by rest in ice for 30 seconds, until the solution became visibly clear. After 1 hour annealing time the vesicles were centrifuged at $12,000 \times g$ for 10 minutes to remove aggregated phospholipids and titanium particles. Sizes of the SUVs were determined by DLS performed in a Malvern Zetasizer instrument. All liposomes were also made in 10 mM Tris, 20 mM KCl pH 8.0 and the total phospholipid concentrations were estimated as described earlier (2). We've used pure DOPE as poly-

disperse suspensions or dispersions since they do not form stable bi-layer at ambient temperatures (44).

3.2.3 Glycation of spectrin

Spectrin taken in 350 mM Na-phosphate buffer, pH 7.4 containing 350 mM glucose was incubated at 37 °C in presence of sodium azide to prevent contamination (36). Aliquots of the mixture was withdrawn every 24 hours and extensively dialysed against 10 mM Tris-HCl, 20 mM KCl, pH 8.0 to stop further reaction. The dialysed samples were subjected to SDS-PAGE and stained with glycoprotein detection kit according to manufacturer's instructions and the extent of glycation was estimated by densitometry of the developed bands via ImageJ software (45).

3.2.4 Phosphorylation of spectrin

White RBC ghosts were incubated in 100 mM Tris-acetate, pH 6.0, 1 mM ATP, 10 mM MgCl₂ at 37 °C overnight to induce hyperphosphorylation of spectrin (46,47). After the incubation period, spectrin was isolated as described above. Spectrin was hypophosphorylated by treating with calf intestinal phosphatase according to manufacturer's protocol. Calf intestine phosphatase was acquired from Sigma (product code 10567752001). The hypo- and hyper-phosphorylated spectrin samples were subjected to SDS-PAGE and Western blotted with anti-phosphoserine and anti-phosphothreonine antibodies also following manufacturer's recommendations. The antibodies used were: anti-phosphothreonine antibody (rabbit, polyclonal, Abcam, ab9337), anti-phosphoserine antibody (mouse, monoclonal, Abcam, ab6639), goat anti-mouse IgG H&L (HRP linked, Abcam, ab205719) and goat anti-rabbit IgG H&L (HRP linked, Abcam, ab205718). Extent of hyper or hypo-phosphorylation

was analysed by densitometry of bands developed by ECL method run according to manufacturer protocol.

3.2.5 Protein aggregation assay

Required amount of insulin was weighed and dissolved in a minimum volume of 20 mM NaOH and then diluted in 100 mM sodium phosphate buffer, pH 7.0 to make a stock of 3mg/ml from which appropriate amounts were taken to have a working concentration of 0.3mg/ml for each aggregation experiment. In all cases aggregation was induced by the addition of 20 μ l of 1M DTT and monitored by recording the apparent absorbance (scattering) at 360nm with respect to time in a Cary-Varian spectrometer (1,48).

To determine the effect of phospholipid composition of membranes on chaperone activity aggregation was monitored in the presence of 0.5mM (total lipid) of liposomes of different compositions (same size of 30 nm diameter, made by sonication) with and without added spectrin. Aggregation was also monitored in presence of increasing amounts of phospholipid (100% DMPC), 0.25, 0.5 and 1mM respectively with and without spectrin to probe effect of lipid concentration on chaperone activity.

To determine the effect of specific protein-protein interaction on chaperone activity insulin aggregation was monitored in the presence of increasing concentrations of HbA in the range of 0.15, 0.3 and 0.6mg/ml in the presence and absence of 0.15 mg/ml spectrin. Experiments were done at 25°C.

Similar experiments were carried out using 0.15, 0.3 and 0.6mg/ml of BSA and PVP40, both in the presence and absence of 0.15mg/ml of dimeric spectrin to determine the effect of nonspecific protein and non-protein macromolecular crowding.

To quantitate the effect of glycation, insulin aggregation was monitored in the presence of native and increasingly glycated spectrin in the same way as above. Effect of phosphorylation was measured using hyper-, hypo-phosphorylated and native spectrin in the same manner.

3.2.6 Enzyme refolding assay

Bacterial α -glucosidase was denatured at a concentration of 400 μ g/ml in 8M urea for 1.5 h in a buffer containing 50 mM sodium phosphate, pH 7.6. Refolding was initiated on 100-fold dilution in the same buffer and enzyme was allowed to refold for 20 minutes. The extent of reactivation of denatured α -glucosidase after refolding was determined assuming the activity of the equivalent amount of the native enzyme as 100% with 0.3mM 4-nitrophenyl- α -D-glucopyranoside as substrate. The enzyme activity of α -glucosidase was assayed by monitoring the continuous increase of absorbance at 400 nm with time to get the v_0 of the enzyme (49). Experiments were done at 25°C.

Refolding was carried out in the presence of specific protein interactor, HbA and non specific protein and non-protein crowder BSA and PVP40. Similarly refolding was monitored in the presence of phospholipid vesicles with and without spectrin to determine their effect on chaperone activity as in the above case. Glycated and differentially phosphorylated spectrin was also used to probe the effect of glycation and phosphorylation on chaperone activity in case of protein folding.

3.2.7 AFM imaging

Insulin was aggregated in the presence and absence of 0.5 mM (total lipid) of 100% DMPC vesicles of defined size (100nm), made by extrusion through membrane filter (Avanti). Spectrin was added to this aggregating mixture both in presence and absence of

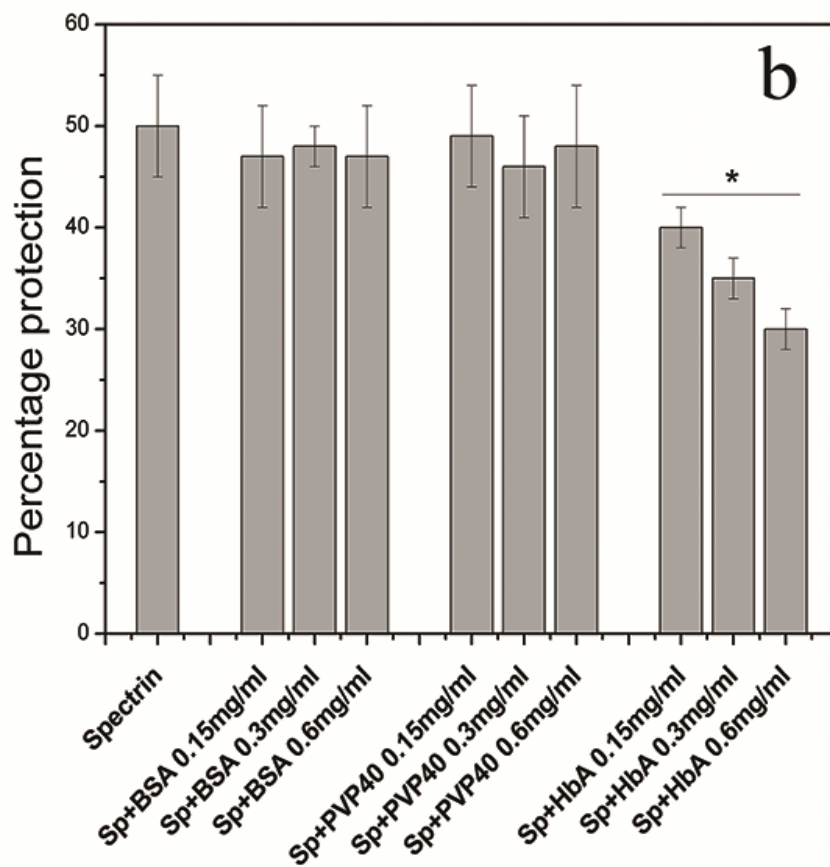
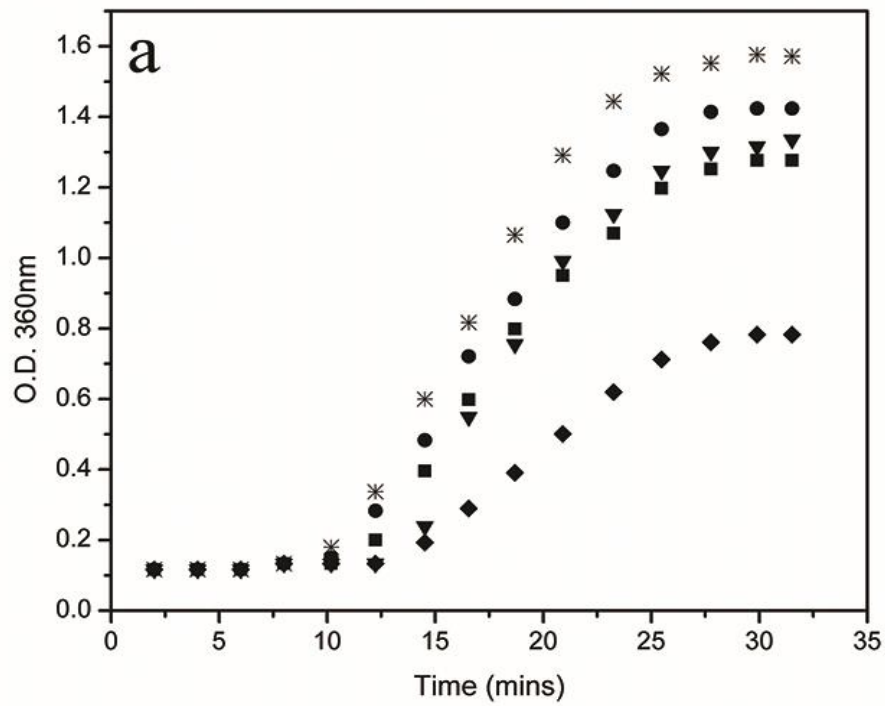
lipid. In all four cases, insulin aggregates were deposited onto clean silicon wafers and thoroughly dried in a vacuum desiccator. The surface morphology of the deposited aggregates was studied by AFM measurement using NanoScope IV MMAFM, Veeco in the tapping mode. The reproducibility of the observed features has been checked by collecting images at three different positions on the sample(50).

3.3 Results and Discussion

3.3.1 Effect of hemoglobin versus non-specific crowders

It was found that insulin aggregating only in the presence of hemoglobin showed slightly increased aggregation as measured by apparent absorbance at 360 nm, while the presence of BSA and PVP40 decreased the aggregation of insulin moderately. It was noted that in presence of BSA and PVP40 the chaperone activity of spectrin was found to remain almost unaffected, but for hemoglobin a significant decrease in chaperone activity was seen. Representative aggregation curve of insulin aggregating in presence and absence of spectrin is given in **Figure 3.1** panel 'a'. Panel 'b' shows the chaperone potential of spectrin expressed as percentage protection of insulin aggregation in presence and absence of HbA and crowders.

Figure 3.1: Chaperone activity of spectrin in presence of BSA, PVP40 & HbA.



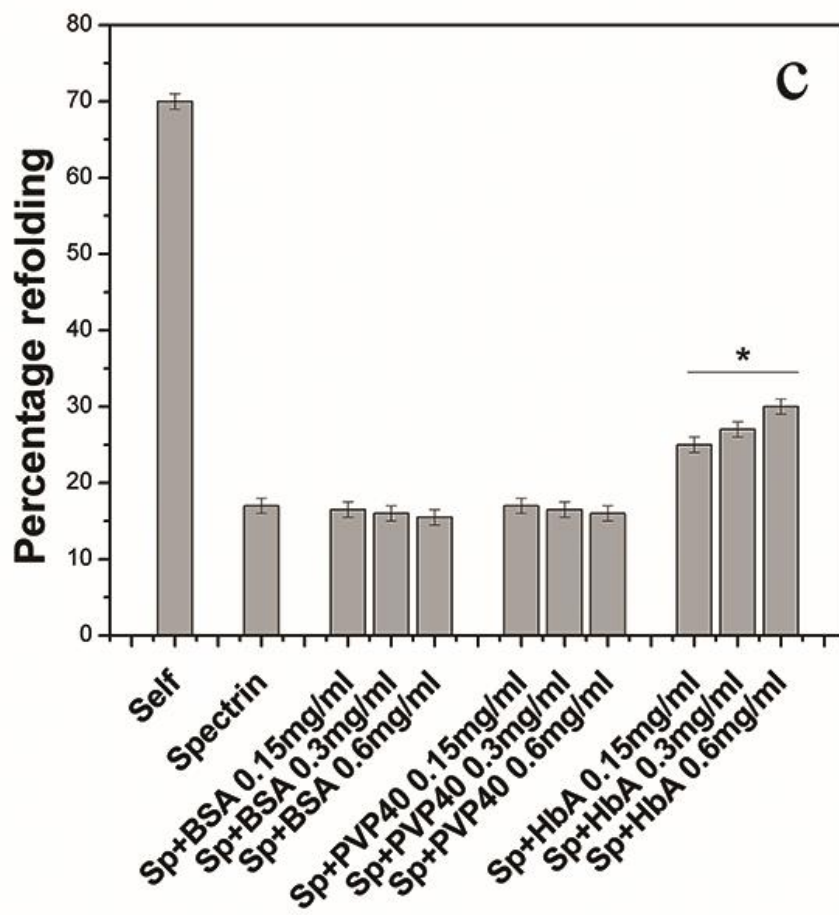


Figure 3.1: Panel 'a' shows the representative aggregation curves of 0.3 mg/ml insulin aggregating in 100 mM phosphate buffer, pH 7.0, induced by 20 mM DTT, and followed by measuring apparent absorbance at 360 nm. Symbol keys are as follows; (●) denotes aggregation curve for insulin; (*) denotes aggregation of insulin in presence of 0.15 mg/ml HbA, (▼) denotes that for insulin aggregation in presence of 0.15mg/ml BSA, (■) denotes insulin aggregation in presence of 0.15 mg/ml PVP40 and, (◆) denotes insulin aggregation in presence of 0.15 mg/ml spectrin. Panel 'b' shows the chaperone potential of spectrin under different conditions, as represented by normalized percentage of aggregation prevention. Insulin concentrations and buffer were kept the same, concentration of spectrin was 0.15mg/ml and the concentration of HbA, PVP40 and BSA were varied. It is seen that decrease in chaperone potential caused by the presence of hemoglobin is statistically significant with a p value of < 0.05 as compared to the modulation caused by PVP40 and

BSA, which are not statistically significant. Panel 'c' shows the refolding yield of α -glucosidase by itself and in presence of spectrin with or without modulators. Refolding yield is expressed as percentage, with the activity of same amount of native enzyme considered as 100%. Decrease in chaperone activity caused by the presence of hemoglobin is statistically significant with a p value of < 0.05 . All data expressed as the mean of at least three independent experiments with standard deviations expressed as error bars. Statistically most significant deviators are marked by () on top of bar plots.*

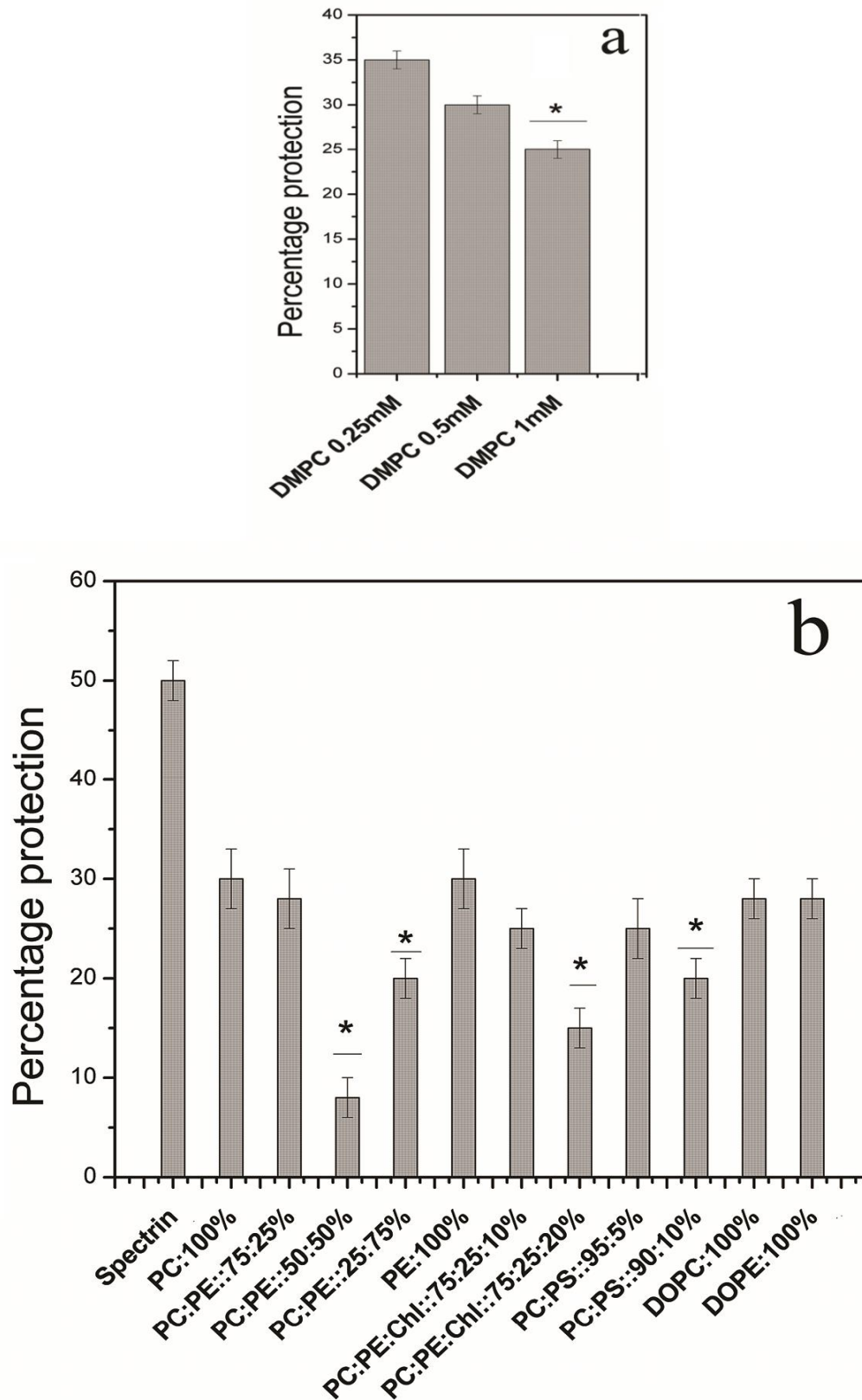
Macromolecular crowders and HbA by themselves however did not show appreciable effect on the refolding of α -glucosidase, refolding was almost the same in presence or absence of crowders and HbA. Presence of spectrin significantly lowered refolding yields. Effect of spectrin on refolding yield in presence of HbA was found to change, with refolding yields being increased in presence of HbA. Refolding yields were calculated as percentages with the activity of equivalent amount of native enzyme being taken as 100%. Data is summarized in **Figure 3.1** panel 'c'.

3.3.2 Effect of phospholipid SUVs

SUVs prepared by sonication were characterized by DLS and were found to have a mean size of ~ 30 nm. SUVs were prepared for AFM imaging by extrusion through 100nm pore size filter and DLS measurements showed mean sizes almost equivalent to 100nm.

In general SUVs by themselves caused slightly increased aggregation of insulin irrespective of their exact lipid composition. It was seen that presence of SUVs decreased spectrin chaperone activity in a dose dependent manner. Phospholipid compositions were also seen to greatly affect the extent of decrease in chaperone activity.

Figure 3.2: Chaperone activity of spectrin in presence of lipids.



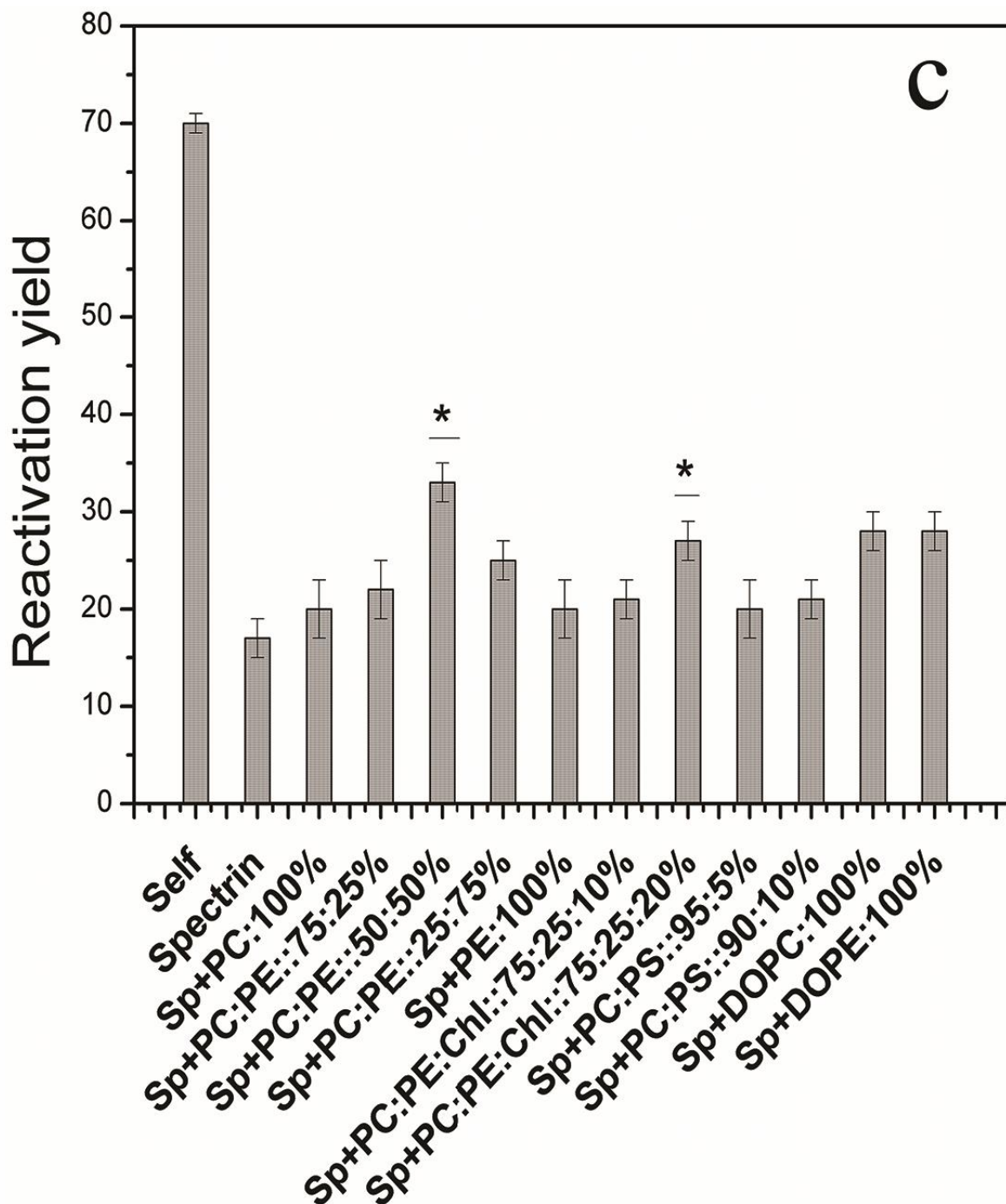


Figure 3.2: Panel 'a' shows the chaperone activity of spectrin expressed as percentage protection values, in presence of increasing amounts (total lipid) of fixed composition, 100% DMPC SUVs (30 nm diameter). Decrease in chaperone potential caused by 1 mM lipid is most statistically significant with p value of < 0.05 . In all cases 0.3 mg/ml insulin was aggregated in presence of 0.15 mg/ml spectrin in 100 mM phosphate buffer, pH 7.0, induced

by 20 mM DTT. Panel 'b' shows chaperone potential modulation similarly as panel 'a'. In this case 0.5 mM total lipids, 30 nm diameter SUVs of different lipid compositions are used as modulators. PC:PE::50:50 % shows most decrease in chaperone potential. Panel 'c' shows the refolding yield of α -glucosidase by itself and in presence of spectrin with or without the same SUV modulators as panel 'b'. Refolding yield is expressed as percentage, with the activity of same amount of native enzyme considered as 100%. Decrease in chaperone potential caused by PC:PE::50:50 % SUVs is most statistically significant with p value of < 0.05 . All data expressed as the mean of at least three independent experiments with standard deviations expressed as error bars. Statistically most significant deviators are marked by (*) on top of bar plots.

Data is summarized in **Figure 3.2**. Panel 'a' shows the effect of phospholipid SUV dose and panel 'b' shows the effect of phospholipid composition of SUVs on the chaperone activity of spectrin.

Like HbA and macromolecular crowders SUVs were found to not have significant modulation on enzyme refolding by themselves, but spectrin in presence of these SUVs showed a generally increased reactivation yield.. Data is summarized in **Figure 3.2** panel 'c'.

3.2.3 AFM imaging

AFM imaging gives the surface topology of protein aggregates of insulin aggregating alone or in presence and absence of insulin and SUVs. It can be seen that in the cases where SUVs are present they are clearly visualized and their sizes are in the expected range. Further the general nature of protein aggregation can clearly be seen to be different in all four cases.

Figure 3.3 shows representative AFM image.

In case of insulin aggregating alone it is seen that the nature of the aggregates is fibrillar in nature, with a web-like appearance in the AFM image. In presence of spectrin, the insulin aggregates are much more finely dispersed, assuming a smooth film like appearance in the AFM image. Addition of SUVs to insulin aggregation causes the insulin aggregates to clump together, with a patchy appearance in AFM imaging. When spectrin is present in aggregating mixtures of insulin and SUVs the nature of aggregates is more dispersed. Aggregates still appear in clumps in AFM imaging, but clumping is reduced from that in absence of spectrin. However smooth film like appearance is not seen like in the absence of SUVs.

Figure 3.3: AFM image of insulin aggregates in presence and absence of lipid \pm spectrin.

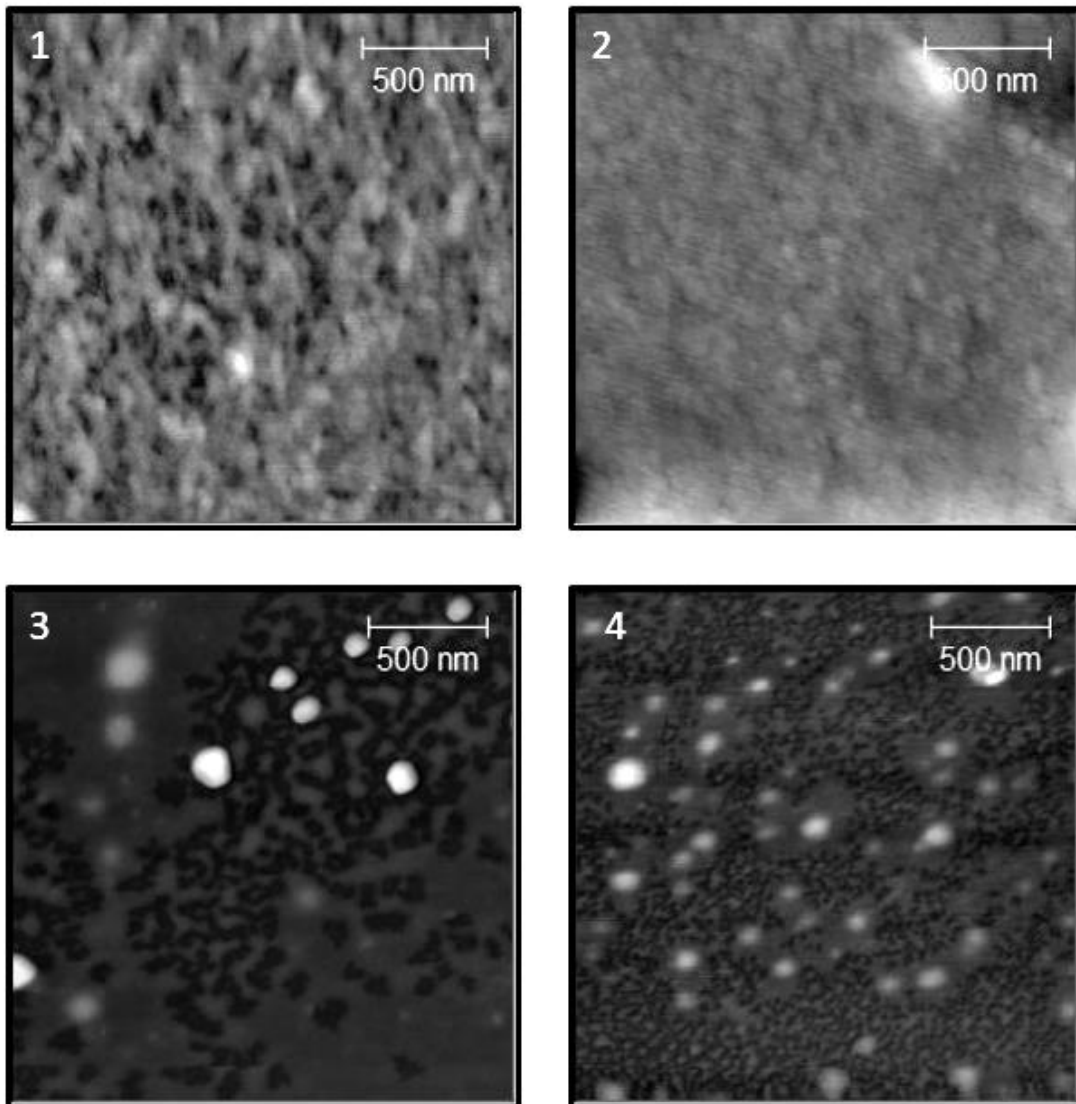


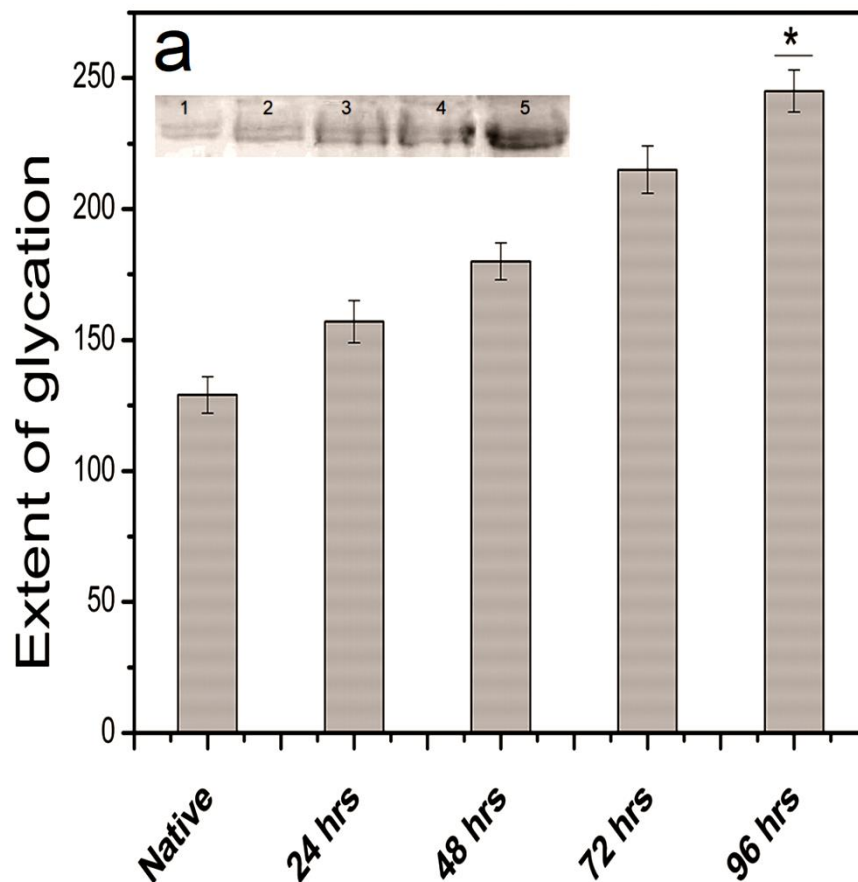
Figure 3.3: AFM image of insulin aggregation in presence and absence of spectrin, with or without modulators is shown. Panel '1' shows the profile of insulin aggregating alone. Panel '2' shows the profile for insulin aggregation in presence of spectrin. Panel '3' shows the aggregation of insulin in presence of SUVs. Panel '4' shows insulin aggregation in presence of SUV and spectrin. In all cases 0.3 mg/ml insulin was aggregated in 100 mM phosphate

buffer, pH 7.0, induced by 20 mM DTT. 0.15 mg/ml spectrin was used and 0.5 mM of 100% DMPC vesicles of 100 nm diameter was used. Bars represent 500 nm lengths.

3.2.4 Spectrin glycation

Glycoprotein detection on SDS gels gave characteristic pinkish bands, which were confirmed by similar detection of kit included positive control HRP. Spectrin was found to have a minimum level of naturally occurring glycation in the native state. Treatment with glucose led to the rapid increase in glycation levels as determined by densitometry. **Figure 3.4** panel 'a' shows bar diagrams for densitometry with glycoprotein gel in the inset. Panel 'b' and 'c' shows the results of the aggregation and refolding experiments.

Figure 3.4: Spectrin glycation.



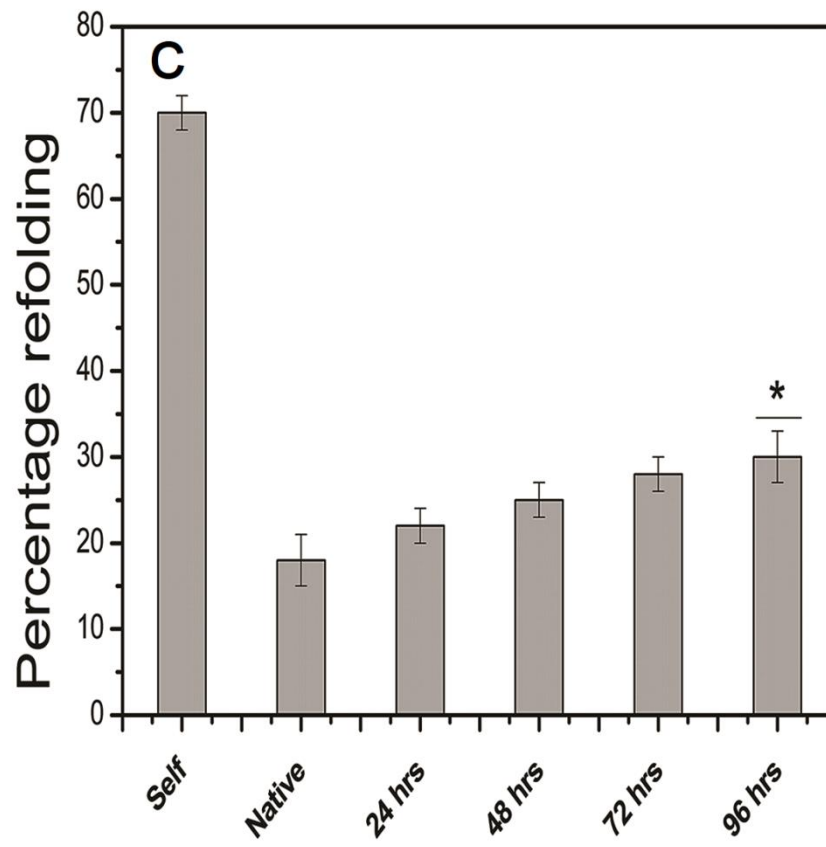
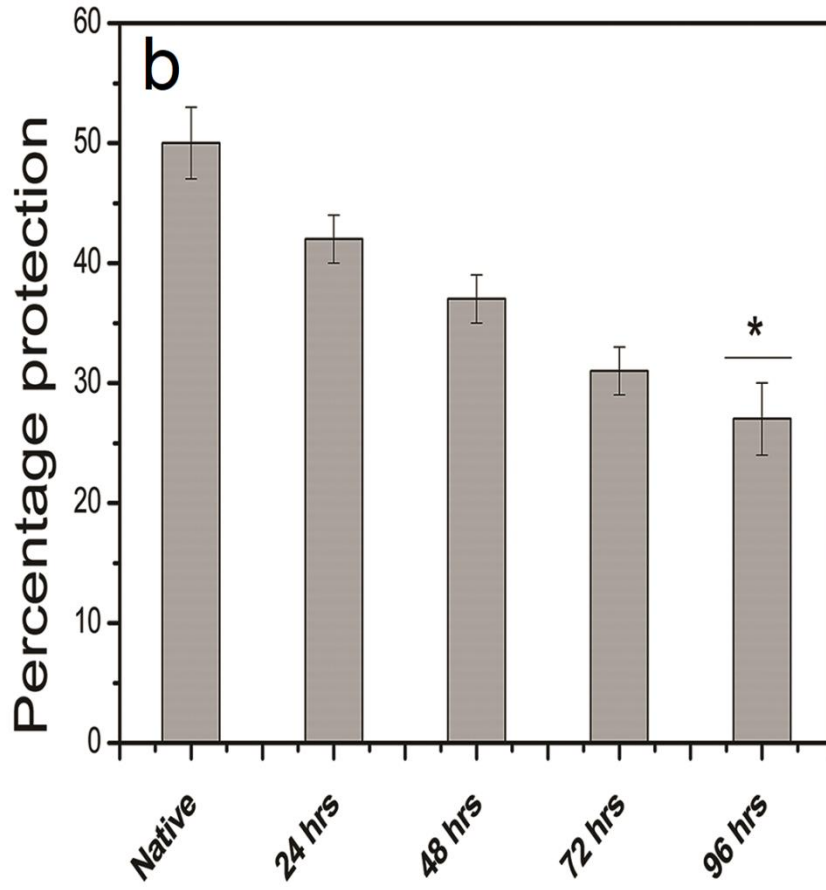
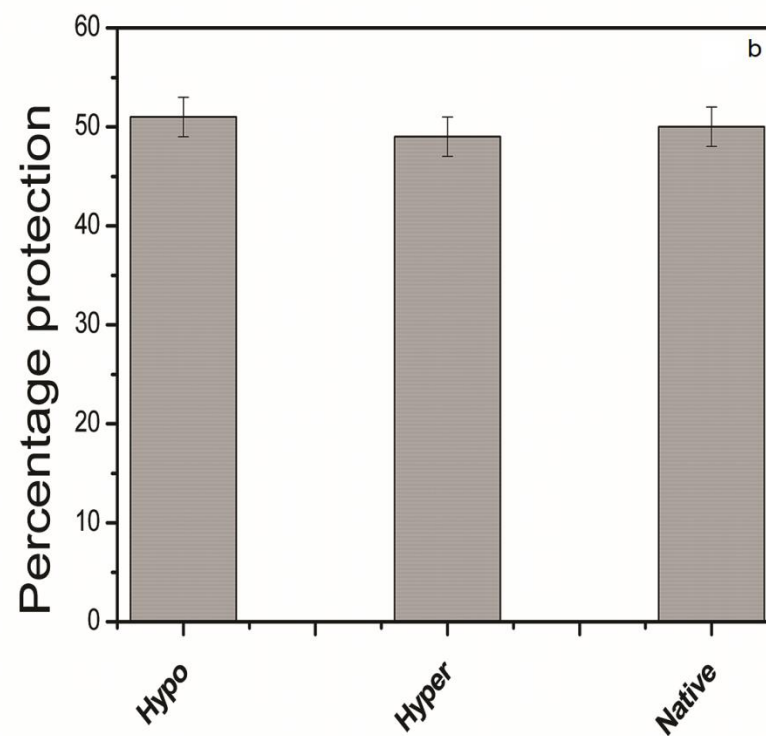
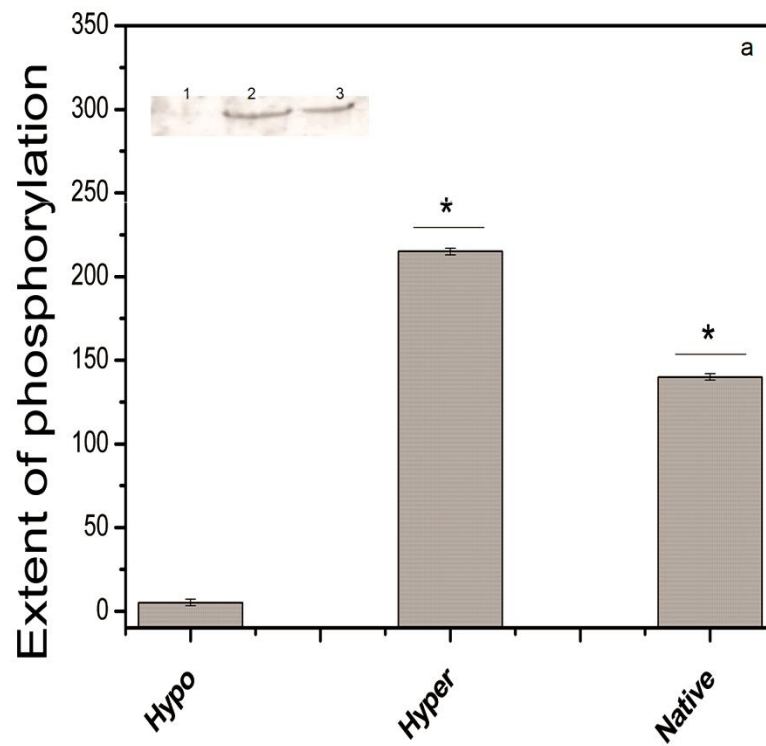


Figure 3.4: Panel 'a' shows the extent of glycation of spectrin in arbitrary units, as probed by in gel glycoprotein detection kit and measured by densitometric analysis. Inset shows the gel for the same. Lane '1' is native spectrin; lane '2' is spectrin glycosylated in 0.35 mM glucose solution at 37 °C for 24 hours, lane '3' for 48 hours, lane '4' for 72 hours and lane '5' for 96 hours. Panel 'b' shows the percentage protection from aggregation of 0.3 mg/ml insulin in 100 mM phosphate buffer, pH 7.0, induced by 20 mM DTT in the presence of 0.15 mg of the differently glycosylated spectrins. Spectrin glycosylated for 93 hours had the most statistically significant decrease in chaperone activity with a p value of < 0.05. Panel 'c' shows the refolding yields of α -glucosidase by itself and in presence of differently glycosylated spectrin. Spectrin glycosylated for 96 hours has the most statistically significant decrease in chaperone potential. All data expressed as the mean of at least three independent experiments with standard deviations expressed as error bars. Statistically most significant deviators are marked by (*) on top of bar plots.

3.2.5 Spectrin phosphorylation

Hyper-, hypo-phosphorylated and native spectrin was detected by western blotting. It was found that while serine phosphorylation could be reproducibly detected, threonine phosphorylation gave weak and non reproducible signal. So further probing was done using serine phosphorylation. **Figure 3.5** panel 'a' shows western blots probed with anti-phosphoserine antibodies in inset and the densitometries of the same. Panel 'b' and 'c' shows results of the aggregation and refolding experiments.

Figure 3.5: Spectrin phosphorylation.



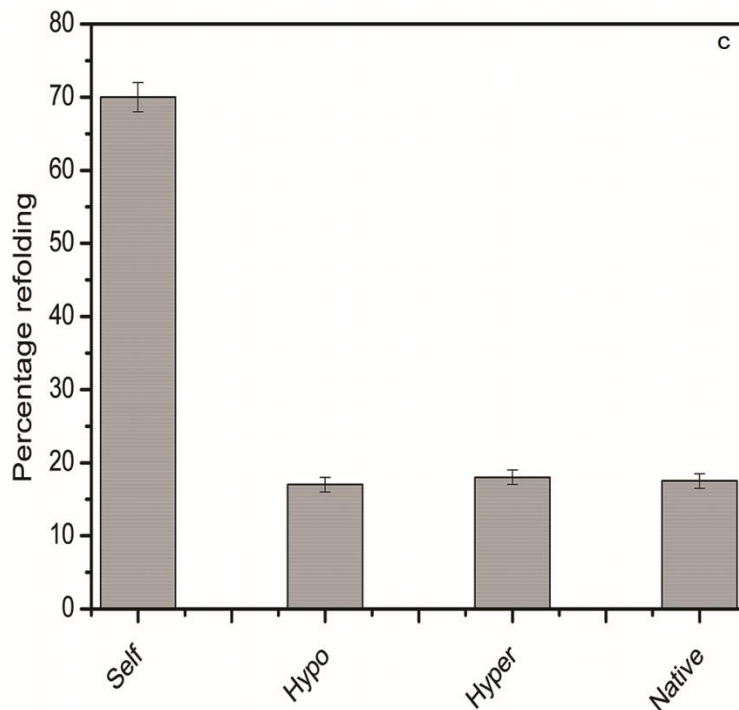


Figure 3.5: Panel 'a' shows the extent of phosphorylation of spectrin in arbitrary units, as probed by western blotting using anti-phosphoserine antibodies and measured by densitometric analysis. Inset shows the gel for the same. Lane '1' is spectrin hypo-phosphorylated using calf intestinal phosphatase; lane '2' is spectrin hyper-phosphorylated by ATP incubation on native membrane, lane '3' is native spectrin. Panel 'b' shows the percentage protection from aggregation of 0.3 mg/ml insulin in 100 mM phosphate buffer, pH 7.0, induced by 20 mM DTT in the presence of 0.15 mg of the differently phosphorylated spectrins. Panel 'c' shows the refolding yields of α -glucosidase by itself and in presence of differently phosphorylated spectrin. In all cases no statistically significant differences were found. All data expressed as the mean of at least three independent experiments with standard deviations expressed as error bars.

3.2.6 Discussions

From our data it can be seen that macromolecular crowders BSA and PVP40 have no significant effect on the chaperone activity of spectrin. While there are some reports of chaperone-client interactions being enhanced by the presence of crowders it has also to be kept in mind that the exact system under consideration is crucial, where the identity of the crowder, chaperone and aggregator all play a role(32). Specific interacting protein, HbA however was seen to decrease chaperone activity. This decrease cannot be explained by assuming that HbA itself aggregates under our experimental conditions as we have expressed chaperone potential as percentage protection normalized with respect to the optical density at 360nm of insulin aggregating in presence of HbA, thereby eliminating any contribution from HbA. The more probable explanation is that HbA competes with denatured insulin for spectrin binding and prevents chaperone-client interactions thereby increasing aggregation; as suggested by the observed HbA dose dependent decrease in chaperone function. HbA has a high stoichiometry for spectrin binding, 100:1-Hb:Sp, and thus probably out competes insulin for binding sites on spectrin. Recently our group has developed the ‘bead on a string’ model for spectrin-Hb interaction and from that we can see that hemoglobin can effectively mask spectrin and thereby prevent its interaction with other proteins(18,42). The present observation lends support to our hypothesis that the major client of spectrin chaperone function is hemoglobin and that this has implications in disease states like β -thalassemia (19,42).

These observations are supported by enzyme refolding data which shows the same general trends as aggregation. In all cases in the presence of spectrin the refolding yields are less than that of the enzyme refolding by itself; this is in line with the fact that some chaperones bind and sequester unfolded proteins acting as a substrate pool for other

chaperones to refold them (14,51). Here too we see that in presence of HbA the reactivation yield goes up indicating that HbA can compete and replace denatured protein for spectrin binding.

Spectrin is also a known lipid interactor and similarly by extension of the competition hypothesis we can explain the decrease in its chaperone activity in presence of phospholipid vesicles. As in the case of HbA there also exists dose dependence for phospholipids as well. More interestingly decrease of chaperone activity is found to be linked to the lipid composition of the membranes. It is seen that decrease in chaperone potential correlates to the presence of a larger amount of aminophospholipids, for example the greatest decrease is noted in the case of SUVs with compositions of DMPC:DMPE::50:50 %. This observation can be explained by the fact that in such conditions, a large part of the worm-like spectrin molecule physically interacts with the membranes, (10)⁵⁰ laminating the membrane bi-layer (43,52). Thereby the surface of spectrin is blocked and a pronounced effect is seen when spectrin and PC/PE vesicles are taken together, with only ~8% protection from aggregation being observed.

The interaction of spectrin with PE containing lipid mono- and bi-layers has also been previously described, and the interacting site for PE is known to lie on the ankyrin binding domain for spectrin (53) (54). As such it is expected that since PE interacts only with a small area of spectrin, the changes to chaperone activity would not be the most pronounced.

Marked decrease of chaperone activity is also seen in case of phospholipid membranes with cholesterol and phosphatidylserine (PS). This too can be rationalized by the fact that spectrin has stronger affinity and larger surface coverage for these membranes (43,55).

Similar to the case of macromolecular crowders enzyme refolding in presence of SUVs show the same overall trends as aggregation. General decrease of chaperone potential of spectrin in presence of phospholipid bi-layers can have important implications in disease states like hereditary elliptocytosis and spherocytosis (56,57) where spectrin is detached from the cell membrane (58-60); in such cases an increase in chaperone activity could be seen which help modulate cellular stress under such diseased conditions.

AFM imaging shows that insulin aggregates has a fibrillar character which is much reduced to a finer dispersion in presence of spectrin; this matches well with our observation of decreased optical density in presence of spectrin and is a visual evidence for its chaperone activity. Insulin aggregation in presence of phospholipid membranes shows same fibrillar type of aggregates looking more clumped and clustered together than in the absence of membranes. Addition of spectrin causes aggregates to become more finely dispersed but dispersion of aggregates is not as much as in the absence of SUVs which is in line with our observation of decreased chaperone activity in presence of membrane SUVs.

Glycation is known to decrease chaperone function in general (35), our results also show the same trend for spectrin. In case of spectrin it is known that the domains that get glycosylated are those that bind PS (36); our data shows that SUVs with PS in their compositions similarly decrease chaperone potential on spectrin binding. Preliminary CD experiments (data not shown) show us that in both cases the secondary structure of spectrin remains invariant. Therefore both of these processes act in a way that is not dependent on protein conformational alteration. Thus we can hypothesize that both glycation and PS binding act in similar ways, probably by binding to and occluding surfaces on spectrin thereby inhibiting interactions with its chaperone clients and thus decreasing chaperone activity.

While phosphorylation is known to affect the interactions of spectrin (40), it is seen that it does not affect chaperone activity. If we consider the possibility that spectrin binds to its chaperone clients via its extended rod like surface we can explain why the limited phosphorylation at the C-terminal of its β subunit does not affect the chaperone potential much.

We have tried to probe the chaperone function of spectrin in depth; the present work reveals important modulations of chaperone activity by other functionalities of spectrin. We demonstrate chaperone activity of spectrin under conditions closer to those found inside RBCs and we see that there exists a competition between chaperone activity and phospholipid / hemoglobin binding of spectrin. This provides further proof for the hypothesis that hemoglobin is a major client for spectrin chaperone function (19) and it can out compete other denatured proteins for spectrin binding. It is seen that composition of phospholipid membranes containing aminophospholipids primarily confined in the inner leaflet of the erythrocyte membranes e.g. PE and PS influence spectrin binding to phospholipid bilayers thereby regulating chaperone activity; increased membrane lamination leads to decreased activity. Under *in-vivo* conditions these interactions can modulate chaperone activity of spectrin and have implications especially in disease states such as hereditary elliptocytosis and spherocytosis where spectrin is detached from the cell membrane. It is seen that glycation decreases chaperone activity while phosphorylation does not affect it. From our previous work on spectrin and hemoglobin interaction, we have proposed a ‘bead on a string’ model where hemoglobin is adsorbed onto the surface of spectrin (4). Our current work indicates that chaperone function decreases via processes that occlude the surface of spectrin in a similar way. Hemoglobin binding decreases chaperone potential; lamination of spectrin onto the tailor-made membrane surface decreases the potential as does glycation. Moreover we see that the extent to which the surface of spectrin is blocked corresponds with the extent of

decrease in chaperone potential. This points us to the possibility that the chaperone clients of spectrin also bind like hemoglobin, i.e. via surface adsorption and we propose a model where chaperone clients adsorb onto spectrin's surface and processes that bind to and occlude these surfaces decrease chaperone activity.

Abbreviations

DMPC: 1, 2-Dimyristoyl-sn-glycero-3-phosphorylcholine; DMPE: 1, 2- Dimyristoyl-sn-glycero-3-phosphoethanolamine; DMPS: 1, 2-Dimyristoyl-sn-glycero-3-phospho- L –serine; DOPE: 1, 2-Dioleoyl-sn-glycero-3-phosphocholine; DOPC: 1, 2-Dioleoyl-sn-glycero-3-phosphoethanolamine; RBC: Red Blood Cell; Chl: Cholesterol; AFM: atomic force microscopy; PDI: protein disulfide isomerase; Hemoglobin A: HbA

References

1. Bhattacharyya, M., Ray, S., Bhattacharya, S., and Chakrabarti, A. (2004) Chaperone activity and prodan binding at the self-associating domain of erythroid spectrin. *The Journal of biological chemistry* **279**, 55080-55088
2. Noiva, R. (1999) Protein disulfide isomerase: the multifunctional redox chaperone of the endoplasmic reticulum. *Seminars in cell & developmental biology* **10**, 481-493
3. Puig, A., Lyles, M. M., Noiva, R., and Gilbert, H. F. (1994) The role of the thiol/disulfide centers and peptide binding site in the chaperone and anti-chaperone activities of protein disulfide isomerase. *The Journal of biological chemistry* **269**, 19128-19135
4. Puig, A., and Gilbert, H. F. (1994) Protein disulfide isomerase exhibits chaperone and anti-chaperone activity in the oxidative refolding of lysozyme. *The Journal of biological chemistry* **269**, 7764-7771

5. Lindstrom, M. S. (2011) NPM1/B23: A Multifunctional Chaperone in Ribosome Biogenesis and Chromatin Remodeling. *Biochemistry research international* **2011**, 195209
6. Torok, Z., Goloubinoff, P., Horvath, I., Tsvetkova, N. M., Glatz, A., Balogh, G., Varvasovszki, V., Los, D. A., Vierling, E., Crowe, J. H., and Vigh, L. (2001) Synechocystis HSP17 is an amphitropic protein that stabilizes heat-stressed membranes and binds denatured proteins for subsequent chaperone-mediated refolding. *Proceedings of the National Academy of Sciences of the United States of America* **98**, 3098-3103
7. Tsvetkova, N. M., Horvath, I., Torok, Z., Wolkers, W. F., Balogi, Z., Shigapova, N., Crowe, L. M., Tablin, F., Vierling, E., Crowe, J. H., and Vigh, L. (2002) Small heat-shock proteins regulate membrane lipid polymorphism. *Proceedings of the National Academy of Sciences of the United States of America* **99**, 13504-13509
8. Arispe, N., Doh, M., and De Maio, A. (2002) Lipid interaction differentiates the constitutive and stress-induced heat shock proteins Hsc70 and Hsp70. *Cell stress & chaperones* **7**, 330-338
9. Aisenbrey, C., Borowik, T., Bystrom, R., Bokvist, M., Lindstrom, F., Misiak, H., Sani, M. A., and Grobner, G. (2008) How is protein aggregation in amyloidogenic diseases modulated by biological membranes? *European biophysics journal : EBJ* **37**, 247-255
10. Ray, S., and Chakrabarti, A. (2004) Membrane interaction of erythroid spectrin: surface-density-dependent high-affinity binding to phosphatidylethanolamine. *Molecular membrane biology* **21**, 93-100

11. Sarkar, S., Bose, D., Giri, R. P., Mukhopadhyay, M. K., and Chakrabarti, A. (2018) Status of Membrane Asymmetry in Erythrocytes: Role of Spectrin. *Advances in experimental medicine and biology* **1112**, 3-11
12. Harper, S. L., Sriswasdi, S., Tang, H. Y., Gaetani, M., Gallagher, P. G., and Speicher, D. W. (2013) The common hereditary elliptocytosis-associated alpha-spectrin L260P mutation perturbs erythrocyte membranes by stabilizing spectrin in the closed dimer conformation. *Blood* **122**, 3045-3053
13. Blanc, L., Salomao, M., Guo, X., An, X., Gratzer, W., and Mohandas, N. (2010) Control of erythrocyte membrane-skeletal cohesion by the spectrin-membrane linkage. *Biochemistry* **49**, 4516-4523
14. Bose, D., and Chakrabarti, A. (2017) Substrate specificity in the context of molecular chaperones. *IUBMB life* **69**, 647-659
15. Nagata, K. (1996) Hsp47: a collagen-specific molecular chaperone. *Trends in biochemical sciences* **21**, 22-26
16. Yu, X., Kong, Y., Dore, L. C., Abdulmalik, O., Katein, A. M., Zhou, S., Choi, J. K., Gell, D., Mackay, J. P., Gow, A. J., and Weiss, M. J. (2007) An erythroid chaperone that facilitates folding of alpha-globin subunits for hemoglobin synthesis. *The Journal of clinical investigation* **117**, 1856-1865
17. Bank, A. (2007) AHSP: a novel hemoglobin helper. *The Journal of clinical investigation* **117**, 1746-1749
18. Mishra, K., Chakrabarti, A., and Das, P. K. (2017) Protein-Protein Interaction Probed by Label-free Second Harmonic Light Scattering: Hemoglobin Adsorption on Spectrin Surface as a Case Study. *The journal of physical chemistry. B* **121**, 7797-7802

19. Basu, A., and Chakrabarti, A. (2015) Hemoglobin interacting proteins and implications of spectrin hemoglobin interaction. *Journal of proteomics* **128**, 469-475
20. Feng, L., Zhou, S., Gu, L., Gell, D. A., Mackay, J. P., Weiss, M. J., Gow, A. J., and Shi, Y. (2005) Structure of oxidized alpha-haemoglobin bound to AHSP reveals a protective mechanism for haem. *Nature* **435**, 697-701
21. Datta, P., Basu, S., Chakravarty, S. B., Chakravarty, A., Banerjee, D., Chandra, S., and Chakrabarti, A. (2006) Enhanced oxidative cross-linking of hemoglobin E with spectrin and loss of erythrocyte membrane asymmetry in hemoglobin E beta-thalassemia. *Blood cells, molecules & diseases* **37**, 77-81
22. Breydo, L., Reddy, K. D., Piai, A., Felli, I. C., Pierattelli, R., and Uversky, V. N. (2014) The crowd you're in with: effects of different types of crowding agents on protein aggregation. *Biochimica et biophysica acta* **1844**, 346-357
23. Kuznetsova, I. M., Turoverov, K. K., and Uversky, V. N. (2014) What macromolecular crowding can do to a protein. *International journal of molecular sciences* **15**, 23090-23140
24. Wang, Y., Sarkar, M., Smith, A. E., Krois, A. S., and Pielak, G. J. (2012) Macromolecular crowding and protein stability. *Journal of the American Chemical Society* **134**, 16614-16618
25. Munishkina, L. A., Ahmad, A., Fink, A. L., and Uversky, V. N. (2008) Guiding protein aggregation with macromolecular crowding. *Biochemistry* **47**, 8993-9006
26. Latshaw, D. C., 2nd, and Hall, C. K. (2015) Effects of hydrophobic macromolecular crowders on amyloid beta (16-22) aggregation. *Biophysical journal* **109**, 124-134
27. Seeliger, J., Werkmuller, A., and Winter, R. (2013) Macromolecular crowding as a suppressor of human IAPP fibril formation and cytotoxicity. *PloS one* **8**, e69652

28. Feig, M., and Sugita, Y. (2012) Variable interactions between protein crowders and biomolecular solutes are important in understanding cellular crowding. *The journal of physical chemistry. B* **116**, 599-605
29. Zhou, H. X. (2013) Polymer crowders and protein crowders act similarly on protein folding stability. *FEBS letters* **587**, 394-397
30. Rosen, J., Kim, Y. C., and Mittal, J. (2011) Modest protein-crowder attractive interactions can counteract enhancement of protein association by intermolecular excluded volume interactions. *The journal of physical chemistry. B* **115**, 2683-2689
31. Sarkar, M., Lu, J., and Pielak, G. J. (2014) Protein crowder charge and protein stability. *Biochemistry* **53**, 1601-1606
32. Kinjo, A. R., and Takada, S. (2003) Competition between protein folding and aggregation with molecular chaperones in crowded solutions: insight from mesoscopic simulations. *Biophysical journal* **85**, 3521-3531
33. Mollapour, M., and Neckers, L. (2012) Post-translational modifications of Hsp90 and their contributions to chaperone regulation. *Biochimica et biophysica acta* **1823**, 648-655
34. Cherian, M., and Abraham, E. C. (1995) Decreased molecular chaperone property of alpha-crystallins due to posttranslational modifications. *Biochemical and biophysical research communications* **208**, 675-679
35. Kumar, P. A., Kumar, M. S., and Reddy, G. B. (2007) Effect of glycation on alpha-crystallin structure and chaperone-like function. *The Biochemical journal* **408**, 251-258
36. Manno, S., Mohandas, N., and Takakuwa, Y. (2010) ATP-dependent mechanism protects spectrin against glycation in human erythrocytes. *The Journal of biological chemistry* **285**, 33923-33929

37. Tang, H. Y., and Speicher, D. W. (2004) In vivo phosphorylation of human erythrocyte spectrin occurs in a sequential manner. *Biochemistry* **43**, 4251-4262
38. Harris, H. W., Jr., and Lux, S. E. (1980) Structural characterization of the phosphorylation sites of human erythrocyte spectrin. *The Journal of biological chemistry* **255**, 11512-11520
39. Manno, S., Takakuwa, Y., Nagao, K., and Mohandas, N. (1995) Modulation of erythrocyte membrane mechanical function by beta-spectrin phosphorylation and dephosphorylation. *The Journal of biological chemistry* **270**, 5659-5665
40. Pinder, J. C., Bray, D., and Gratzer, W. B. (1977) Control of interaction of spectrin and actin by phosphorylation. *Nature* **270**, 752-754
41. Chakrabarti, A., Bhattacharya, D., Deb, S., and Chakraborty, M. (2013) Differential thermal stability and oxidative vulnerability of the hemoglobin variants, HbA2 and HbE. *PloS one* **8**, e81820
42. Datta, P., Chakrabarty, S. B., Chakrabarty, A., and Chakrabarti, A. (2003) Interaction of erythroid spectrin with hemoglobin variants: implications in beta-thalassemia. *Blood cells, molecules & diseases* **30**, 248-253
43. Mitra, M., Patra, M., and Chakrabarti, A. (2015) Fluorescence study of the effect of cholesterol on spectrin-aminophospholipid interactions. *European biophysics journal : EBJ* **44**, 635-645
44. Toombes, G. E., Finnefrock, A. C., Tate, M. W., and Gruner, S. M. (2002) Determination of L α -HII phase transition temperature for 1, 2-dioleoyl-sn-glycero-3-phosphatidylethanolamine. *Biophysical journal* **82**, 2504-2510
45. Schneider, C. A., Rasband, W. S., and Eliceiri, K. W. (2012) NIH Image to ImageJ: 25 years of image analysis. *Nature methods* **9**, 671-675

46. Boivin, P. (1988) Role of the phosphorylation of red blood cell membrane proteins. *The Biochemical journal* **256**, 689-695
47. Hosey, M. M., and Tao, M. (1976) An analysis of the autophosphorylation of rabbit and human erythrocyte membranes. *Biochemistry* **15**, 1561-1568
48. Guha, S., Manna, T. K., Das, K. P., and Bhattacharyya, B. (1998) Chaperone-like activity of tubulin. *The Journal of biological chemistry* **273**, 30077-30080
49. Guagliardi, A., Cerchia, L., and Rossi, M. (1995) Prevention of in vitro protein thermal aggregation by the *Sulfolobus solfataricus* chaperonin. Evidence for nonequivalent binding surfaces on the chaperonin molecule. *The Journal of biological chemistry* **270**, 28126-28132
50. Giri, R. P., Chakrabarti, A., and Mukhopadhyay, M. K. (2017) Cholesterol-Induced Structural Changes in Saturated Phospholipid Model Membranes Revealed through X-ray Scattering Technique. *The journal of physical chemistry. B* **121**, 4081-4090
51. Raman, B., Ramakrishna, T., and Rao, C. M. (1997) Effect of the chaperone-like alpha-crystallin on the refolding of lysozyme and ribonuclease A. *FEBS letters* **416**, 369-372
52. Giri, R. P., Mukhopadhyay, M. K., Mitra, M., Chakrabarti, A., Sanyal, M. K., Ghosh, S. K., Bera, S., Lurio, L. B., Ma, Y., and Sinha, S. K. (2017) Differential adsorption of a membrane skeletal protein, spectrin, in phospholipid membranes. *EPL (Europhysics Letters)* **118**, 58002
53. Sikorski, A. F., Michalak, K., and Bobrowska, M. (1987) Interaction of spectrin with phospholipids. Quenching of spectrin intrinsic fluorescence by phospholipid suspensions. *Biochimica et Biophysica Acta (BBA)-Biomembranes* **904**, 55-60
54. Wolny, M., Grzybek, M., Bok, E., Chorzalska, A., Lenoir, M., Czogalla, A., Adamczyk, K., Kolondra, A., Diakowski, W., and Overduin, M. (2011) Key amino

- acid residues of ankyrin-sensitive phosphatidylethanolamine/phosphatidylcholine-lipid binding site of β I-spectrin. *PloS one* **6**, e21538
55. An, X., Guo, X., Sum, H., Morrow, J., Gratzner, W., and Mohandas, N. (2004) Phosphatidylserine binding sites in erythroid spectrin: location and implications for membrane stability. *Biochemistry* **43**, 310-315
 56. Zhang, R., Zhang, C., Zhao, Q., and Li, D. (2013) Spectrin: structure, function and disease. *Science China. Life sciences* **56**, 1076-1085
 57. Tse, W. T., and Lux, S. E. (1999) Red blood cell membrane disorders. *British journal of haematology* **104**, 2-13
 58. Mohandas, N., and Chasis, J. A. (1993) Red blood cell deformability, membrane material properties and shape: regulation by transmembrane, skeletal and cytosolic proteins and lipids. *Seminars in hematology* **30**, 171-192
 59. Goodman, S. R., and Shiffer, K. (1983) The spectrin membrane skeleton of normal and abnormal human erythrocytes: a review. *The American journal of physiology* **244**, C121-141
 60. Mohandas, N., and Evans, E. (1994) Mechanical properties of the red cell membrane in relation to molecular structure and genetic defects. *Annual review of biophysics and biomolecular structure* **23**, 787-818

Chapter 4:

Localization and molecular origin of chaperone potential

4.1 Introduction

The spectrin repeat domains have been implicated as the source of the remarkable elasticity, flexibility and structural strength of spectrin (1-3). They have also been shown to be the location of the protein binding and ligand binding property of spectrin (4,5). These domains have a high degree of homology (6), especially the presence of conserved tryptophans (7), within themselves; however they also have sufficiently different sequences to show distinct properties (8). There are 20 such repeat domains in α -spectrin and 16 domains in β -spectrin and the rest of the polypeptide sequences are made up of non-homologous motifs (9,10).

Previous literature on spectrin mostly points out the role of spectrin as a structural and mechanical component of the membrane skeleton (11,12). Newer studies point out the non-canonical roles of spectrin, for example as a platform for signal transducing complexes and as a protein-protein interaction module (13,14). The first report of the chaperone like property of erythroid spectrin was made by our group where we had also hypothesised that this property resides in the self-association domain of the hetero-dimer (15-18).

Keeping in mind the modular, repeating nature of the spectrin repeat domains of which the majority of erythroid spectrin is constituted it becomes important to determine if the chaperone property of spectrin is localized in one of these repeat domains or is a shared general property of these repeat motifs or is a function of the non-homologous motifs.

Spectrin presents an interesting case where like many cytoskeletal proteins, it was believed that the spectrin repeat domains serve only to flexibly link and spatially separate actin-binding function (19,20); however it has now been shown that the repeat domains too have their own functionality. Moreover the interactions of these repeat domains cannot be

generalized even though they share sequence and structural identity (5,8,21). Thus, keeping our question in mind, it becomes difficult to predict the functionality of a given repeat. Moreover spectrin has known functionality in some of its repeat domains such as actin binding and ankyrin binding (22,23), and there is homology with known chaperone calmodulin in its EF domain (24). This further complicates the question of localizing spectrin's chaperone activity. In our current work we have tried to test our old hypothesis and determine if the chaperone like potential of spectrin is localized in one of its many domains or is a property displayed by the entire polypeptide.

It is known that all chaperones have some features in common which aid in substrate recognition; most often these are charged and/or hydrophobic patches which are solvent exposed (25). Keeping in mind the known presence of hydrophobic patches on spectrin as well as our hypothesis linking hydrophobic patches to chaperone activity (16,26), the most likely loci on spectrin to harbour chaperone activity should also have hydrophobic patches. In our present study we have selected nine domains of spectrin, five from α and four from β spectrin to investigate their chaperone activity as versus the native protein. We have selected domains based on their likelihood of harbouring hydrophobic patches/chaperone like activity and the domains we have chosen to investigate are the α -tetramerization domain, α -dimerization domain, EF domain, SH3 domain, β -tetramerization domain, β -dimerization domain, actin binding domain, ankyrin binding domain, and a random non-specific spectrin repeat domain from α -spectrin.

The self association domain or Tetramerization domain of spectrin is the dimerized form of the N-terminal 1-158 amino acids of α (α -tetramerization domain) and C-terminal 1895-2137 amino acids of β -spectrin (β -tetramerization domain) (27). We have previously hypothesized that the chaperone function and Prodan binding site of spectrin is localized here

(16). Available literature indicates that this self association domain is where the hetero-dimers of spectrin link up to form tetramers (28) and mutations in this region lead to haemolytic diseases (29). Moreover available data shows this region to have hydrophobic residues present on the peptide surface (30,31). This presence of surface exposed hydrophobic patches has led us to include these two domains.

Similarly, we have selected the α -dimerization domain (2002-2233 amino acids of α -spectrin) and β -dimerization (271-500 amino acids of β -spectrin) domain of spectrin, which are the regions in the polypeptides that form the nucleation site of high affinity hetero-dimer formation and also have surface hydrophobic patches (32-35).

The C-terminal of α -spectrin is calmodulin like and is called the EF domain (2257-2429 amino acids) and has calcium dependent and independent EF hands; since calmodulin itself is a chaperone this domain too is a candidate for possessing chaperone like function (24,36).

SH3 domain (973-1055 amino acids of α -spectrin) is a protein interaction module present in α -spectrin and due to its broad range of protein interaction ability is also considered (37,38).

The ankyrin binding domain (1657-1876 amino acids of β -spectrin) (22,39) and actin binding domain (1-316 amino acids of β -spectrin) (23,40,41) of the of β -spectrin polypeptide are also protein binding domains and are thus included.

All of the said domains have some defined function and probable chaperone potential; we have also selected a random spectrin repeat domain of α -spectrin between amino acids 1470-1576 to act as a control (9).

We have expressed and purified these chosen domains from cloned sequences and characterized them using intrinsic tryptophan fluorescence, urea denaturation, CD-spectroscopy, time-resolved spectroscopy and ligand binding. We have estimated their chaperone potential by monitoring the extent of protection of protein aggregation thermally and non-thermally and by enzyme refolding assays.

4.2 Materials and Methods

pET151/D-TOPO plasmids containing the sequences of interest were acquired from Invitrogen; fluorescent probes Prodan (6-propionyl-2[dimethylamino]-naphthalene) and ANS (1-anilinonaphthalene-8-sulfonic acid) were also from Invitrogen; PMB, PMSF, EDTA, DTT, sodium hydrogen phosphate, NaOH, Tris, Sephadex G-100, Sepharose CL-4B, DEAE cellulose and CM cellulose were purchased from Sigma. Insulin from bovine pancreas, alcohol dehydrogenase from *S. cerevisiae*, alkaline phosphatase from *E. coli*, α -glucosidase from *S. cerevisiae*, 4-nitrophenyl- α -D-glucopyranoside and para-ithophenylphosphate were purchased from Sigma. Prism Ultra pre-stained protein ladder (3.5 – 254 kDa) was purchased from Abcam. All water used for experiments was purified via a Millipore system.

4.2.1 Isolation and purification of human Hemoglobin constituent α and β chains

Human hemoglobin variant HbA was isolated from blood samples collected from healthy volunteers with proper informed consent. α and β globin subunits were isolated from HbA using previously published protocol (42-44). Briefly, 100mg PMB per 1g of hemoglobin was dissolved in minimum volume of 0.1M KOH and 1M acetic acid was added till very light precipitate persisted. PMB solution was added to 50mg/ml solution of

hemoglobin in 10mM Tris-HCl 200mM NaCl, pH 8.0, and final pH was adjusted to 6.0 by addition of 1M acetic acid and mixture was incubated at 4° C for 12 hours.

PMB bound globin subunits were separated using two column selective ion exchange chromatography. α -PMB was isolated by equilibrating globin-PMB mixture with 10mM phosphate buffer pH 8.0 and passing through DEAE-cellulose column equilibrated with the same buffer. Similarly β -PMB was isolated by equilibrating globin-PMB mixture and passing through CM-cellulose column equilibrated with the same buffer. The PMB was removed from isolated globin chains by addition of 50 mM β -mercaptoethanol in 0.1M phosphate buffer pH 7.5. Globin chains were then purified by gel filtration on BioGel P2 column. The purity was checked by 12% SDS page analysis and concentration was measured by Bradford method using BSA as standard. Globin chains were stored at 4° C for not more than 48 hours.

4.2.2 Expression isolation and purification of recombinant spectrin domains

Utilizing the work of Forget *et. al.* (9,10) the polypeptide sequence of the chosen domains was determined from the cDNA and polypeptide sequence of human erythroid spectrin (EMBL Data Bank accession numbers J05244 & J05500). In case of the EF domain which did not have any tryptophans in its sequence a tyrosine was replaced with a tryptophan in the 2578th position in α -spectrin. pET151/D-TOPO plasmids with the sequences of interest inserted under control of Lac operon and T7 viral promoter with N-terminal hexa-histidine tag and Ampicillin selection marker was purchased from Invitrogen. Sequences were optimized for expression in *E. coli*. The representative plasmid map is given in **Figure 4.1**. Plasmids were sequentially electroporated into XL1-Blue and BL21(DE3) cells for cloning and protein expression respectively.

Figure 4.1: Plasmid map.

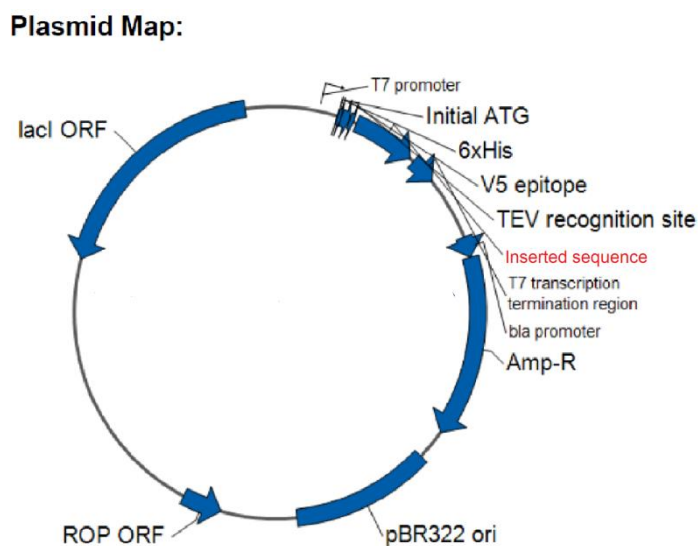


Figure 4.1: The representative plasmid map of the constructs purchased from Invitrogen is shown labelling the location of the different functional sequences.

It was noted from pilot experiments that the recombinant domains had appreciable solubility issues and were mostly incorporated into inclusion bodies. As such expression, extraction, purification and refolding methods were standardised for urea denatured extraction of the domains. Cells were grown in L.B. media with 100 µg/ml Ampicillin at 37 °C and protein expression was induced in a log phase culture, O.D._{280nm} 0.6, with 0.5 mM IPTG at 25 ° for four hours.

Cells were collected by centrifugation at 4000 x g and washed to remove excess media. Cells were lysed by sonication in a buffer containing 8 M urea, 10 mM Tris-HCl, 100 mM NaCl, pH 8.0 and lysate was clarified by centrifugation at 12000 x g to remove cell debris. Lysate was incubated with half its volume of Ni-NTA resin equilibrated with the same buffer for two hours at 25 ° C. The resin was then washed successively with buffer and 20 mM imidazole in the same buffer to elute non-specific binders. Finally the proteins were eluted in 200 mM imidazole in the same buffer.

The resulting unfolded proteins were then sequentially dialyzed against 7 M, 6 M, 5 M, 4 M, 3 M, 2 M, 1 M and 0.5 M urea in the same buffer before being dialyzed in pure buffer without urea to yield folded protein. The resulting solution was centrifuged at 7000 x g for 5 minutes to remove any misfolded proteins and the supernatant was passed through 0.22 μ m syringe filter to yield final pure folded proteins. The purity of the samples was checked by 15 % SDS-PAGE analysis and their concentration was measured using the Bradford method with BSA as standard. The proteins were stored at 4 °C for not more than 48 hours.

The self-association domain was reconstituted by incubating 20 μ M concentrations of α and β -tetramerization domains together in 150 mM NaCl, 10 mM Tris-HCl pH 8.0 overnight on ice. Resulting reconstituted self-association domain was purified by passing it through a 45 x 1 cm Sephadex G-100 column equilibrated with 10 mM Tris-HCl, 100 mM NaCl, pH 8.0 buffer.

4.2.3 Characterization of spectrin fragments

The fragments of spectrin were characterized using fluorescence and CD spectrometry both in native and urea denatured conditions. Steady state experiments were carried out in a Cary Varian and Fluoromax-3 spectrofluorometer using 10 mm path length quartz cuvettes at 25 °C using thermostated cuvette holders. 10 μ M of each fragment and the reconstituted self-association domain were taken and their emission was measured from 310 to 450 nm using 295 nm excitation with 5nm band pass slits for both excitation and emission channels. The fluorescence anisotropy of the tryptophans in the proteins was measured using the same instrument with band pass slits of 5 nm each for excitation and emission and excitation at 295nm and emission at 340nm. Fluorescence lifetimes of these proteins were measured using a Horiba Fluoromax 3 with TCSPC attachment. Tryptophans were excited at 295 nm using a

nano-LED and their emission was recorded at 340 nm. Decay curves were fitted using DAS6 software. CD spectroscopy was done using a 1 mm path length quartz sandwich type cuvette in a Applied Photophysics Chirascan instrument. An average of ten accumulations was taken for each sample using 0.5 nm steps in the interval of 190 to 250 nm. Machine data was converted to mean residual ellipticity for analysis and comparison. To check the oligomeric status of the expressed domains, they were run on G-100 columns and their elution profile checked.

4.2.4 Binding of fluorescent probes

Prodan and ANS were used as fluorescent probes and binding experiments were performed using a Cary Varian spectrofluorometer using 10 mm path length quartz cuvettes at 25 °C using thermostated cuvette holders. Stock concentrations of Prodan in dimethylformamide were determined using an extinction coefficient of 18000 at 360 nm. Binding experiments were carried out in 10 mM Tris-HCl, 100 mM NaCl, pH 8.0 buffer, using 0.2 – 0.5 µM Prodan solutions to which increasing concentrations of proteins were added and emission was monitored in the range of 375 to 600 nm using an excitation of 360 nm and with 5 nm slits for both excitation and emission channels. The emission intensity at 430 nm (I_{430}) and 520 nm (I_{520}) was monitored for bound and free Prodan respectively (45).

Stock concentration of ANS in dimethylformamide was determined using an extinction coefficient of 7800 at 372 nm. Reverse titrations were done using 15 µM of protein in each case to which increasing concentrations of ANS were added. Fluorescence intensity was measured at 470 nm for bound ANS with excitation at 372 nm and band pass of 5 nm for both excitation and emission channels (16).

The extent of binding of ANS/Prodan was analyzed by a non-linear model independent method using the following equations to give the apparent dissociation constant in each case (K_d).

$$K_d = \{ [C_0 - (\Delta F / \Delta F_{\max}) \cdot C_0] \cdot [C_L - \Delta F / \Delta F_{\max}] \} / \{ (\Delta F / \Delta F_{\max}) \cdot C_0 \} \dots (1)$$

$$C_0 \cdot (\Delta F / \Delta F_{\max})^2 - [(C_0 + C_L + K_d) \cdot (\Delta F / \Delta F_{\max})] + C_L = 0 \dots (2)$$

In equations (1) and (2), ΔF is the change in fluorescence emission intensity at 470 nm (for ANS) or the ratio of I_{520}/I_{430} (for Prodan) for each point on the titration curve and ΔF_{\max} denotes the same when a given probe is completely bound to a given protein, C_L is the concentration of the ligand protein being added at any given point in the titration curve, and C_0 is the initial concentration of Prodan (opposite in case of ANS since reverse titration is done).

The y-axis intercept of the plot of $1/\Delta F$ vs. $1/C_L$ gives the numerical value of $1/\Delta F_{\max}$. In turn the calculated ΔF_{\max} values can be put into equation 1 and the K_d values for each point on the titration curve can be generated, from which the mean K_d value is determined. The intersection of the tangents drawn on the initial and final linear region of the binding isotherm plot of $\Delta F/\Delta F_{\max}$ against C_L extrapolated to the ordinate gives the stoichiometry of Prodan binding to protein.

All experimental points for binding isotherm were fitted by least-square analysis using the Microcal Origin software package (Version 8.0) from Microcal Software Inc., Northampton, MA. The, K_d values are represented as mean \pm standard error of the mean (S.D.) of at least 4 independent experiments (16).

The Scatchard equation was also used to estimate the intrinsic binding constants (K_o) and the binding stoichiometry (n) according to the following equation.

$$r/C_f = K_o \cdot (n - r) \dots (3)$$

Where $r = C_b/C_p$, where C_b is the concentration of protein bound Prodan and C_p is the input concentration of protein. The concentration of bound Prodan was determined by normalizing the input concentration of Prodan with $\Delta F/\Delta F_{\max}$ and in the case of ANS it was determined as a function of the ΔF_{\max} of 5 μM of ANS titrated against increasing concentrations of spectrin. The Scatchard plot was obtained by plotting r/C_f against r where C_f is defined as $(C_o - C_b)$ and C_o is the total concentration of Prodan. The best linear fit of the experimental data gave the values for K_o and n . Likewise ANS binding was similarly analysed.

In case of both Prodan and ANS the polarization and anisotropies were measured as a parameter for monitoring binding with steady state lifetimes being additionally monitored in case of Prodan.

4.2.5 Assay of protein aggregation

Insulin, ADH, α and β globin were used as model substrates to check the chaperone potential of the spectrin domains.

A minimum volume of 20 mM NaOH was used to dissolve insulin which was then diluted to 0.3 mg/ml in 100 mM Na-phosphate buffer pH 7.0. Aggregation was induced by the addition of 25 μl of 1 M DTT to 1 ml of insulin solution and the aggregation was followed measuring the apparent increase in absorbance due to scattering at 360 nm as a function of time. Aggregation was carried out in the presence and absence of the spectrin domains and spectrin (16,18).

Similar aggregation experiments were carried out using 0.4 mg/ml of ADH in presence and absence of the spectrin domains and spectrin. Aggregation was induced by

heating at 50 °C and followed by measuring the 90° light scattering at 450 nm. In all cases buffer used was 50 mM Na-phosphate, pH 8.0.

Aggregation assays were carried out using α and β globin chains isolated from human hemoglobin using previously published protocol. Briefly, both kinds of globin chains were diluted with 50 mM Na-phosphate buffer pH 7.4, 150 mM NaCl, 1 mM EDTA to a final concentration of 13.5 μ M and pre-incubated at 4 °C with spectrin or the spectrin domains for one hour. The samples were warmed to 37 °C and 10 μ l of a 0.5 mM solution of potassium ferricyanide was added to induce aggregation. Aggregation was carried on in the presence and absence of spectrin or spectrin domains. Aggregation was monitored by measuring the apparent increase in absorbance due to scattering at 700 nm with time (17,46).

BSA in similar concentration as spectrin and expressed domains was used as negative control for all the aggregation experiments.

4.2.6 Folding of denatured enzymes

Alkaline phosphatase in a final concentration of 5 mg/ml was denatured in 6 M guanidine-HCl in 10 mM Tris-HCl pH 8.0 buffer at 25 °C for an hour and then diluted 1000 fold in 10 mM Tris-HCl pH 8.0 in presence and absence of spectrin and spectrin domains, to initiate refolding. Para-nitrophenylphosphate was added to a final concentration of 10 μ M and incubated for 20 minutes. 100 mM final concentration of K_2HPO_4 was added to quench the reaction and absorbance was measured at 400 nm to monitor reactivation yield taking the activity of the native enzyme as 100% (16).

α -glucosidase in final concentration of 4 mg/ml was denatured in 8 M urea in 50mM Na-phosphate pH 7.6 for two hours. Refolding was initiated by 1000 fold dilution in the same buffer in presence and absence of spectrin and spectrin domains. 0.3 mM final concentration

of para-nitrophenyl- α -D-glucopyranoside was used as enzyme substrate and the velocity of enzymatic reaction was followed by monitoring the increase in absorbance at 400 nm with time. Activity of native enzyme was taken as 100% (16).

4.3 Results and Discussion

4.3.1 Expression and characterization of spectrin domains

The spectrin domains were expressed, extracted and purified in urea denatured condition, and then refolded to give native domains. It was found from pilot experiments that presence of histidine tags did not alter the chaperone potential or fluorescence characteristics of the domains; so for ease of purification the tags were left un-cleaved for this study. The domains of spectrin that were selected for the present study are pictorially depicted in **Figure 4.2**, for easy visualization of their relative locations in spectrin.

Figure 4.2: Spectrin domains.

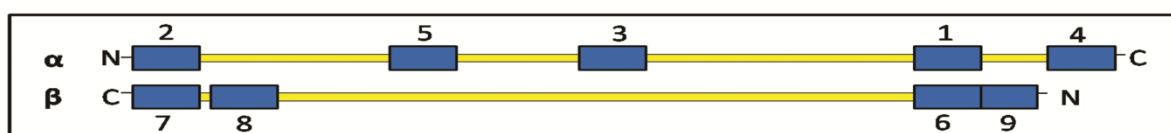


Figure 4.2: Panel 'a' shows a pictorial representation of the spectrin domains chosen for this study and their location in dimeric spectrin. The anti-parallel spectrin dimer is shown in yellow and the domains are highlighted in blue. The domains are numbered 1 through 9 and in numerical sequence they are: α -dimerization domain, α -tetramerization domain, spectrin repeat domain, EF domain, SH3 domain, β -dimerization domain, β -tetramerization, ankyrin binding domain and actin binding domain respectively.

The spectrin domains were expressed and purified as described and was run on 15% SDS-PAGE to check purity; **Figure 4.3** panels 'a' and 'b' show gels for crude and purified extracts respectively.

Figure 4.3: SDS-PAGE of spectrin fragments.

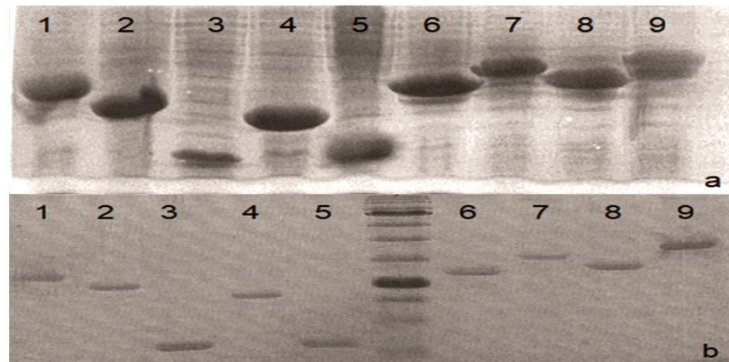


Figure 4.3: Panel 'a' shows the SDS-PAGE for the crude extracts of the domains and subpanel- 'b' shows the same for Ni-NTA resin purified samples. The lanes are numbered from 1 through 9 and numbering is the same as in the pictorial representation. The ladder used was Prism Ultra pre-stained protein ladder and the two most prominent bands show 24 kDa and 70 kDa.

Table 4.1 contains the polypeptide sequence for each domain and their calculated molecular weight.

Table 4.1: Spectrin fragments, sequence and molecular weight.

Domain name	Domain location	Calculated weight	Sequence
α -Tetramerization	α -spectrin, 1-158 residues	19 kDa	MEQFPKETVVESSGPKVLETAEIQERR QEVLTRYQSFKERVAERGQKLEDSYHLQ VFKRDADDLGKWIMEKVNILTDKSYEDP TNIQGKYQKHQSLEAEVQTKSRLMSELE KTREERFTMGHSAHEETKAHIEELRHLW DLLLELTLEKGDQLLRAL
SH3	α -spectrin, 973-1055 residues	9.5 kDa	VEGVAGEQRVMALYDFQARSPREVTMK KGDVLTLLSSINKDWWKVEAADHQQGIV PAVYVRRLAHDEFMPLPQRRREEPGNIT Q
Spectrin repeat	α -spectrin, 1470-1576 residues	12 kDa	EIATRLQRVLDLDRWKALKAQLIDERTKLG DYANLKQFYRDLEEELEEWISEMLPTACD ESYKDATNIQRKYLKHQTFAHEVDGRSE QVHGVINLGNSLIERSCDGNEEA
α -Dimerization	α -spectrin, 2002-2233 residues	27 kDa	KAIEERYAALLKRWEQLLEASAVHRQKL LEKQLPLQKAEDLFVEFAHKASALNNW CEKMEENLSEPVHCVSLNEIRQLQKDHE DFLASLARAQADFKCLELDDQQIKALGV PSSPYTWLTVVLELERTWKHLSDIIEEREQ ELQKEEARQVKNFEMCQEFEQNASTFLQ WILETRAYFLDGSLLKETGTLESQLEAN KRKQKEIQAMKRQLTKIVDLGDNLEDAL ILDIKYS
EF	α -spectrin, 2257-2429 residues	19 kDa	QIQAKDIKGVSEETLKEFSTIWKHFDENL TGRLTHKEFRSCLRGLNYLPMVEEDEH EPKFEKFLDAVDPGRKGYVSLDYTAFL IDKESENIKSSDEIENAFQALAEKSYIT KEDMKQALTPEQVSFCATHMQQYMDPR VEAISLAMTTLASPIPTLATNKQLLVDRR KS
Actin Binding	β - Spectrin, 1-136 residues	36 kDa	MTSATEFENVGNQPPYSRINARWDAPDD ELDNDNSSARLFERSRIKALADEREVVQ KKTFTKWVNSHLARVSCRITDLYKDLRD GRMLIKLLEVLSGEMLPKPTKGMRIHC LENVDKALQFLKEQRVHLENMGSHDIV DGNHRLVGLIWTIILRFQIQDIVVQTQE GRETRSAKDALLWCQMKTAGYPHVNV TNFTSSWKDGLAFNALIHKHRPDLIDFD KCLKDSNARHNLEHAFNVAERQLGIIPLL DPEDVFTENPDEKSIITYVVAFYHYFSK MKVLAVEGKRVGKVIDHAIETEKMIEKY SGLASDLLT

β -Dimerization	β - Spectrin, 271-500 residues	27 kDa	VAFYHYFSKMKVLA VEGKR V GKVIDHA IETEKMI EKYSGLASDLLTWIEQTITVLN SRKFANSLTGVQQQLQAFSTYRTVEKPP KFQEKGNLEVLLFTIQSR Met RANNQKVY TPHDGKLVSDINRAWESLEEAGYRRELA LRNELIRQEKLEQLARRFDRKAAMRETW LNENQRLVAQDNFGYDLAAVEAAKKKH EAIETDTAA YEERVRALEDLAQELEKEN YHDQKRIT
Ankyrin Binding	β - Spectrin, 1657-1876 residues	25 kDa	EGEQIIRLQGQVDKHYAGLKDVAEERKR KLENMYHLFQLKRETDLEQWISEKELV ASSPEMGQDFDHVTLRDKFRDFARETG AIGQERVDNVNAFIERLIDAGHSEAATIA EWDGGLNEMWADLLELIDTRMQLLAAS YDLHRYFYTGAEILGLIDEKHRELPEDV GLDASTAESFHRVHTAFERDVHLLGVQV QQFQDVATRLQTAYAGEKAEAIQN
β - Tetramerization	β - Spectrin, 1895-2137 residues	28 kDa	RRTQLVDTADKFRFFSMARDLLSWMESI IRQIETQERPRDVSSVELLMKYHQGINAE IETRSKNFSACLELGESLLQRQHQASEEI REKLQQVMSRRKEMNEKWEARWERLR MLLEV CQFSRDASVAEAWLIAQEPYLAS GDFGHTVDSVEKLIK RHEAFEKSTASWA ERFAALEKPTTLELKERQIAERPAEETGP QEEGETAGEAPVSHHAATERTSPVSLW SRLSSSWESLQPEPSHPY

Table 4.1: The polypeptide sequence, amino acid positions on the spectrin subunits and calculated molecular weight of the domains are given. In EF domain the tyrosine that was replaced by tryptophan is highlighted.

Figure 4.4: Emission spectra of spectrin domains.

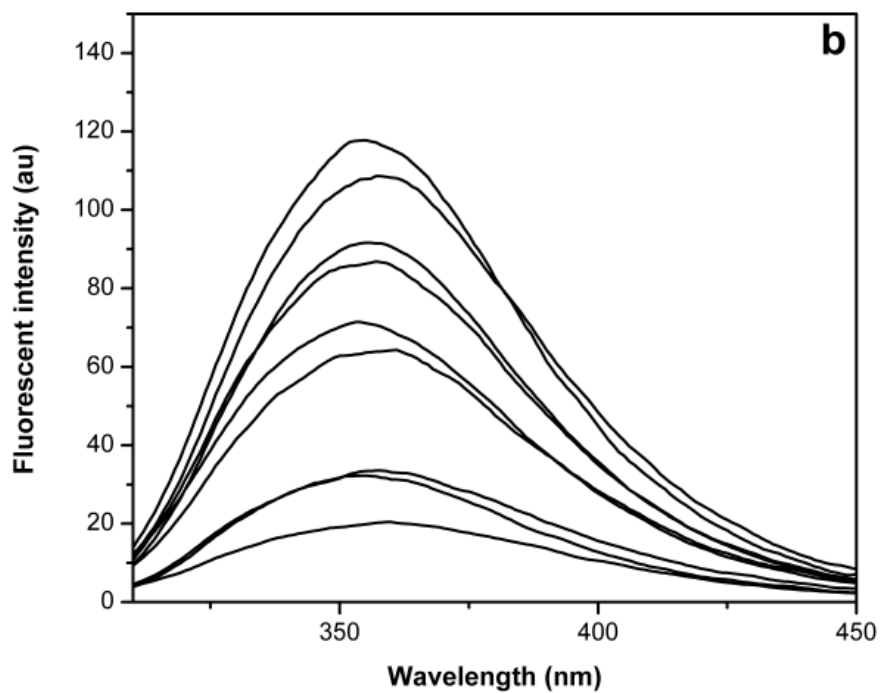
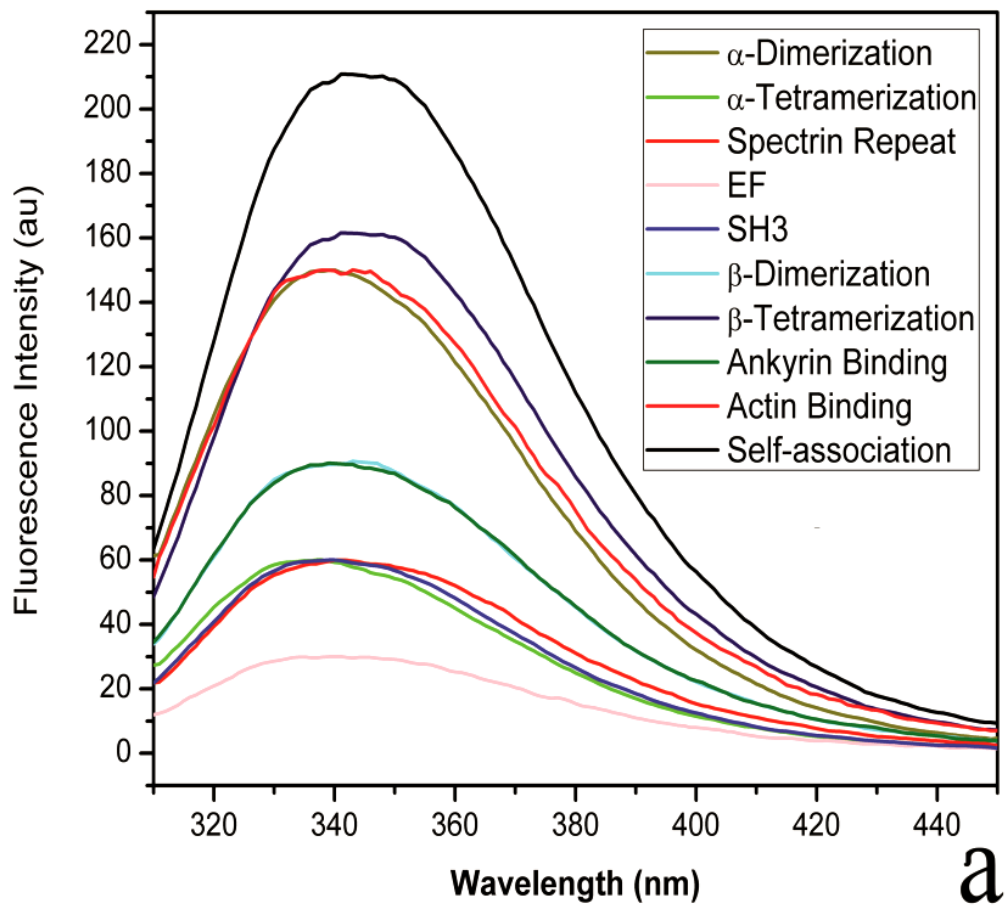


Figure 4.4: Panel 'a' shows the emission spectra of all the native spectrin domains, spectrin and self-association domain. Panel 'b' shows the emission spectra of the spectrin domains in 8 M urea denatured condition are shown. The emission maxima appear red shifted. In order from top to bottom the spectra are of the β -tetramerization, actin binding, α -dimerization, ankyrin binding, β -dimerization, spectrin repeat, SH3, α -tetramerization and EF domain respectively.

The parameters of fluorescence lifetime, anisotropy and polarization are tabulated in **Table 4.2**. It is seen that for almost all the fragments the parameters are close to spectrin.

Table 4.2: Fluorescence parameters of spectrin domains.

Domain/ protein	λ_{\max} (ex. 295nm)	Anisotropy (r)	Polarization (p)	Mean Lifetime (n.s.)	Mean Residual Ellipticity [θ] (10^3 deg. cm ² . dmol ⁻¹)
α - Tetramerization	336 \pm 1.2 (347 \pm 1.3)	0.083 \pm 0.002 (0.054 \pm 0.001)	0.121 \pm 0.003 (0.067 \pm 0.004)	3.87 \pm 0.2 (3 \pm 0.1)	-110.6 \pm 2.2
SH3	339 \pm 1.1 (347 \pm 1.1)	0.072 \pm 0.001 (0.044 \pm 0.002)	0.121 \pm 0.002 (0.06 \pm 0.003)	3.5 \pm 0.3 (2.9 \pm 0.1)	-17.5 \pm 5.3
Spectrin repeat	342 \pm 1.4 (347 \pm 1.5)	0.073 \pm 0.001 (0.034 \pm 0.002)	0.124 \pm 0.003 (0.045 \pm 0.003)	3.44 \pm 0.2 (2.7 \pm 0.3)	-134.1 \pm 3.1
α - Dimerization	337 \pm 1.1 (346 \pm 1.1)	0.087 \pm 0.002 (0.041 \pm 0.001)	0.101 \pm 0.003 (0.05 \pm 0.002)	3.7 \pm 0.1 (3.1 \pm 0.1)	-118.6 \pm 1.1
EF	340 \pm 1.2 (348 \pm 1.3)	0.063 \pm 0.001 (0.042 \pm 0.001)	0.09 \pm 0.003 (0.056 \pm 0.003)	3.6 \pm 0.2 (2.9 \pm 0.2)	-59.3 \pm 4.3
Actin Binding	337 \pm 1.1 (343 \pm 1.1)	0.083 \pm 0.002 (0.045 \pm 0.001)	0.117 \pm 0.002 (0.063 \pm 0.002)	4.0 \pm 0.3 (3.28 \pm 0.3)	-105 \pm 2.2
β - Dimerization	337 \pm 1.2 (344 \pm 1.3)	0.082 \pm 0.002 (0.05 \pm 0.001)	0.12 \pm 0.003 (0.065 \pm 0.001)	4.1 \pm 0.1 (3.5 \pm 0.1)	-97.5 \pm 4.6

Ankyrin Binding	336 ± 1.1 (348 ± 1.2)	0.092 ± 0.001 (0.041 ± 0.001)	0.148 ± 0.002 (0.073 ± 0.002)	3.8 ± 0.2 (3.49 ± 0.3)	-93.5 ± 3.2
β-Tetramerization	338 ± 1.1 (346 ± 1.1)	0.086 ± 0.002 (0.044 ± 0.001)	0.113 ± 0.002 (0.051 ± 0.003)	3.9 ± 0.2 (3.3 ± 0.3)	-49.5 ± 4.4
Spectrin	338 ± 1.1 (345 ± 1.1)	0.12 ± 0.001 (0.04 ± 0.001)	0.18 ± 0.002 (0.04 ± 0.002)	3.8 ± 0.1 (2.9 ± 0.1)	-84.8 ± 3.3
Self-association domain	337 ± 1.2 (346 ± 1.3)	0.1 ± 0.002 (0.06 ± 0.001)	0.147 ± 0.003 (0.076 ± 0.002)	3.9 ± 0.2 (2.8 ± 0.3)	-67.5 ± 4.1

Table 4.2: The emission maxima for 295 nm excitation; anisotropy, polarization and mean lifetime values for 295 nm excitation, 340 nm emission, of the tryptophans of the native spectrin domains and spectrin are tabulated. Values in parenthesis indicate the same for 8 M urea denatured condition. The α -helical content is represented as the mean residual ellipticity at 222 nm. Error values are calculated as the standard deviation of four independent experiments.

The self-association domain was reconstituted from α and β -tetramerization domains and was run on a Sephadex G-100 column for purification. It was seen that over a 12 hour period the majority of constituent fragments had dimerized to form the self-association domain. The elution profile for the same is given in **Figure 4.5**.

Figure 4.5: Elution profile of spectrin domains.

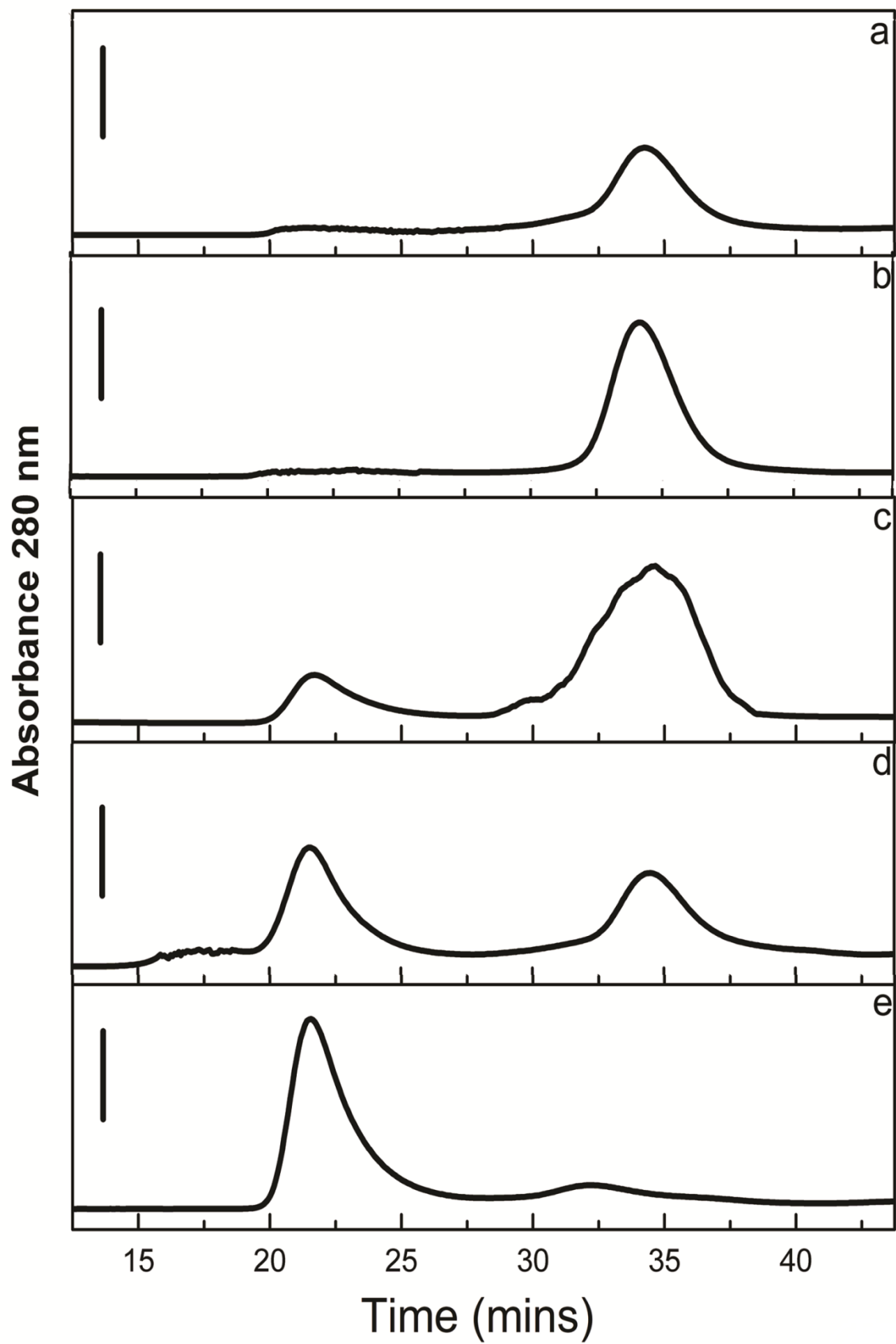


Figure 4.5: Figure shows the reconstitution of the self-association domain from the α - and β -tetramerization domains as followed by size exclusion chromatography on Sephadex G-100 column. Panels 'a' and 'b' show the elution profile for purified α - (~19 kDa) and β -tetramerization (~28 kDa) domains respectively. Panel 'c' shows the same for when the two domains are mixed and incubated for two hours, it is seen that a small self-association domain (~47kDa) peak starts to form. Panel 'd' shows increased self-association domain production at 4 hours and subpanel 'e' shows that the majority of the constituent domains have dimerized to form self-association domain at 8 hours.

CD spectroscopy reveals that the native domains all have an α -helical fold analogous to spectrin, except the SH3 domain which shows a more β -sheet like nature with the presence of a unique secondary minima which matches with previous literature (47). The CD spectra of spectrin superposed with that of the self-association domain is shown in **Figure 4.6** along with the rest of the fragments. The MRE values at 222 nm are tabulated in **Table 4.2**. Upon urea denaturation it was seen that the domains lost most of their secondary structure unlike spectrin which still retained some of its secondary structure. Representative CD spectra of the urea denatured domains are shown in **Figure 4.7**. Gel filtration chromatography reveals that the expressed domains are monomeric and show single elution peaks.

Figure 4.6: CD spectra of spectrin domains.

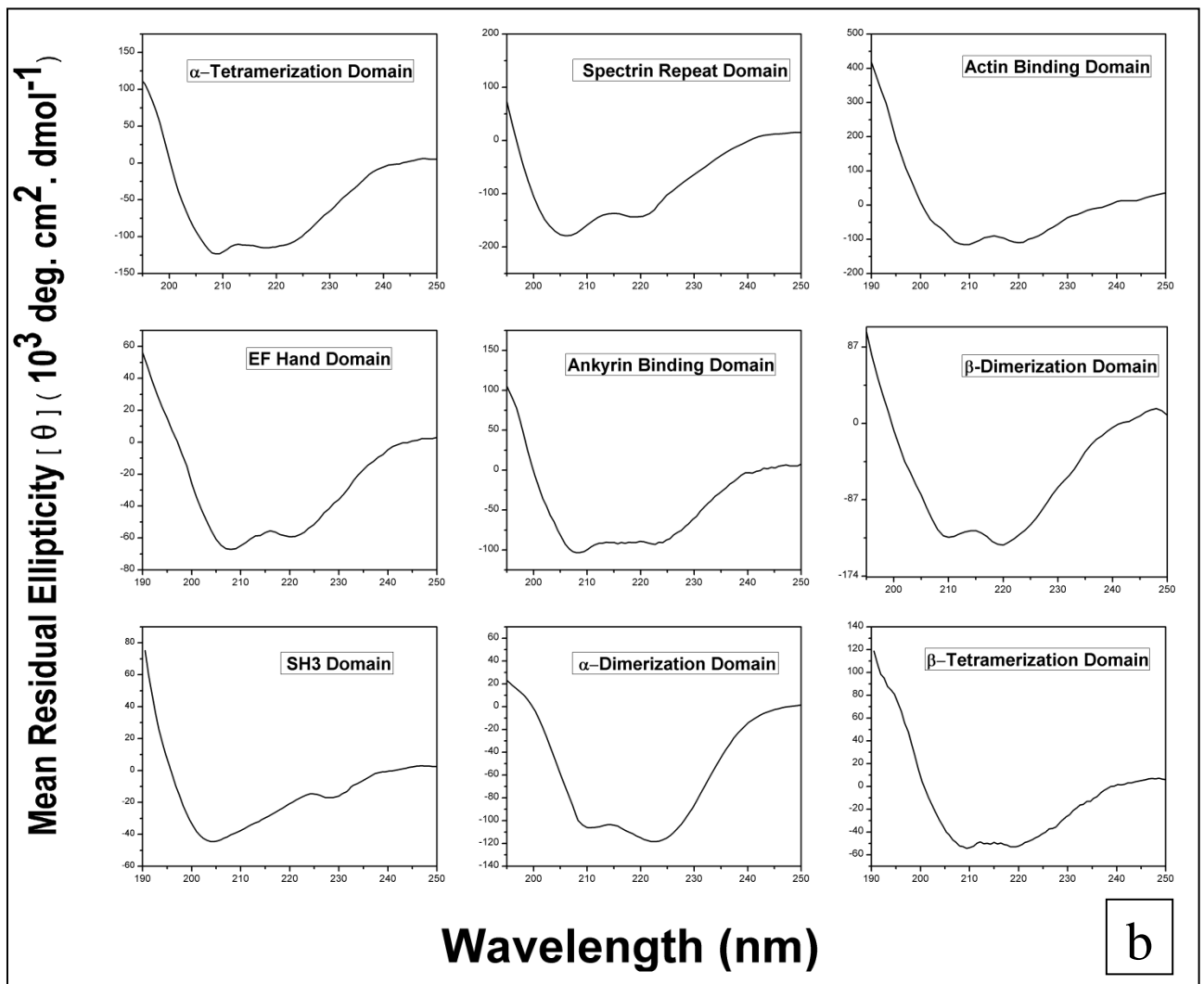
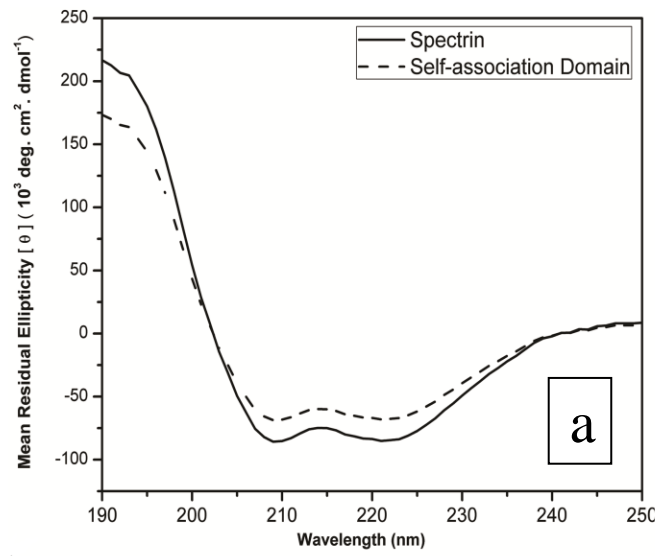


Figure 4.6: Panel 'a' shows the representative CD spectra of native spectrin and reconstituted self-association domain. Panel 'b' shows the CD spectra of the spectrin domains in the range of 190 to 250 nm; spectra reveal a predominantly α -helical nature except SH3 domain which is globular.

Figure 4.7: CD spectra under urea unfolded condition.

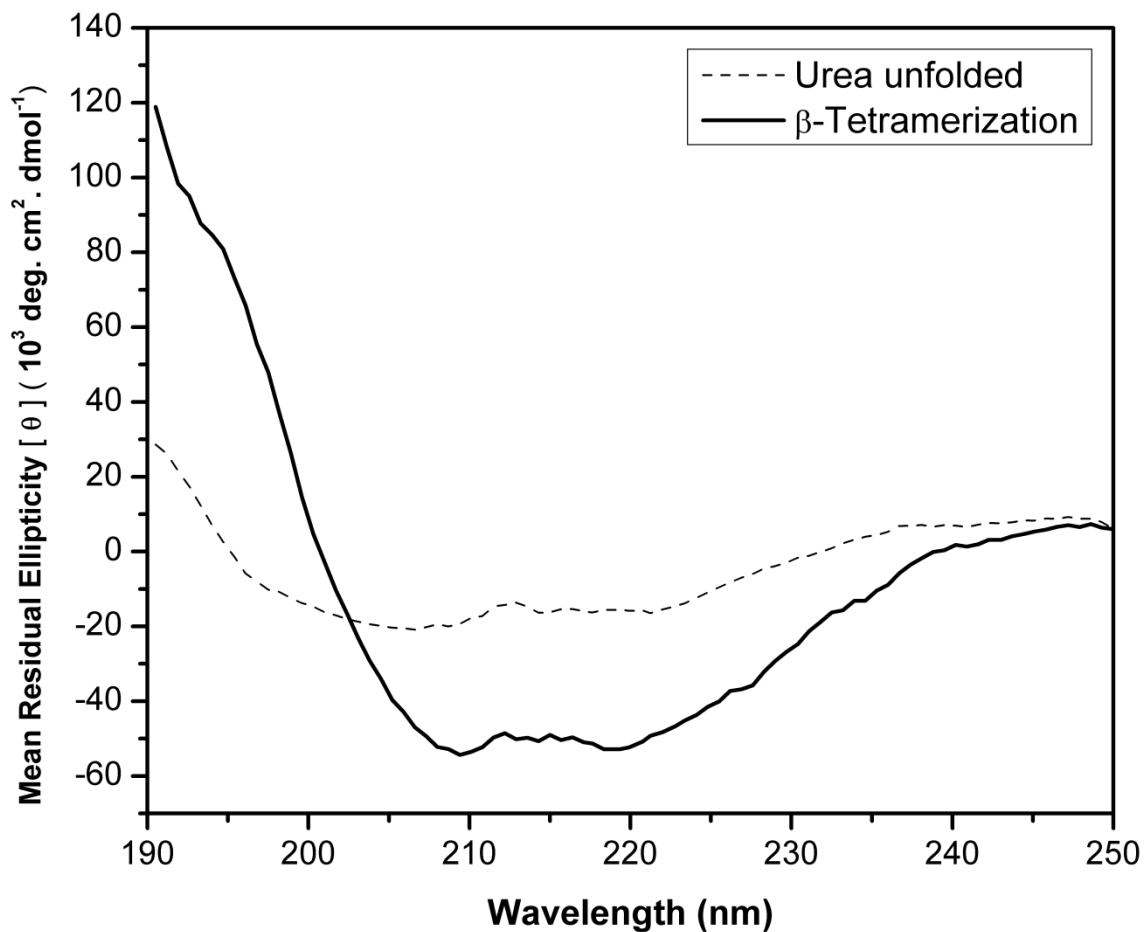
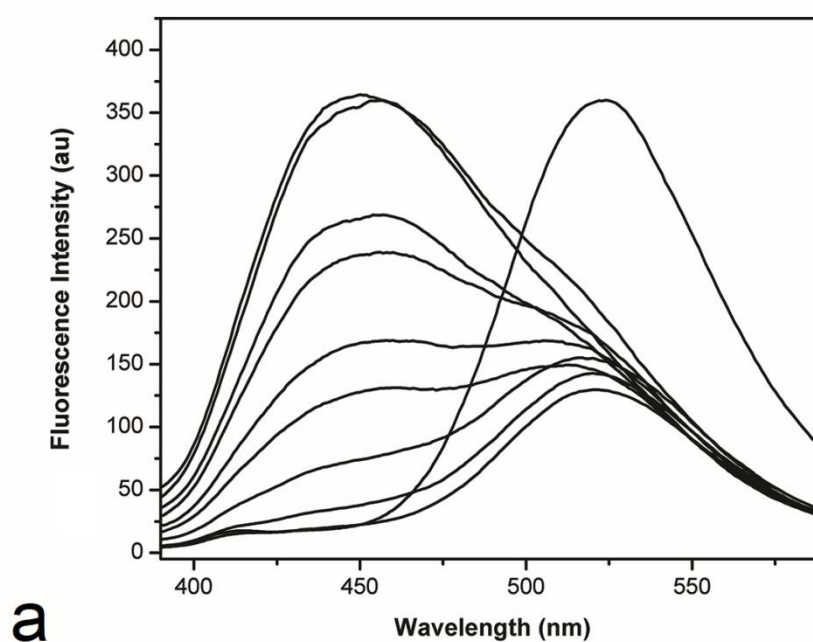


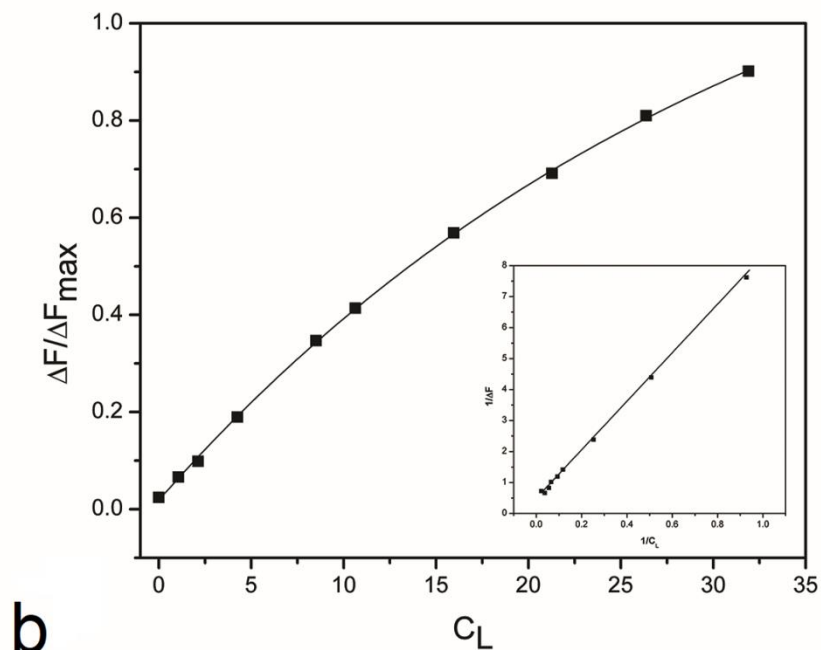
Figure 7: Representative CD spectra of β -tetramerization domain in 8 M urea denatured condition versus native condition are shown. Urea denatured condition leads to loss of secondary structure as evidenced by CD spectra from 190-250 nm.

4.3.2 Binding of fluorescent ligands

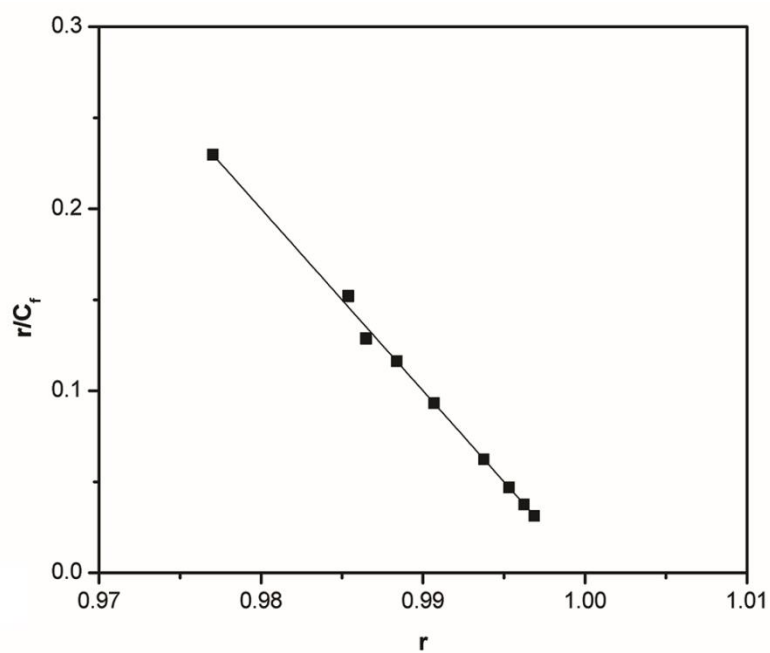
The emission maxima of Prodan in aqueous solution was found to be blue shifted from 520 nm to 430 nm upon spectrin and self-association domain binding with a concurrent large increase in emission intensity. It was found that other than the reconstituted self-association domain other spectrin domains did not appreciably bind with Prodan to a level that could be experimentally followed within the concentration range of the soluble spectrin fragments. Prodan binding was analysed using both the model independent and Scatchard methods. The dissociation constants and stoichiometries derived from these two methods are tabulated in **Table 4.3**. It was also noted that upon binding the fluorescence lifetime, polarization and anisotropy of Prodan increased appreciably; data is given in **Table 4.3**. The representative fluorescence spectra and binding isotherms of Prodan binding to self-association domain are shown in **Figure 4.8**.

Figure 4.8: Prodan binding.





b



c

Figure 4.8: Panel 'a' shows the fluorescence spectra of 5 μM Prodan titrated with increasing concentration of the self association domain. The excitation was at 360 nm, unbound emission was at 520 nm and bound emission at 430 nm. Sequential decrease in unbound and increase of bound emission peak was seen on titrating with spectrin. Panel 'b'

shows the binding isotherms calculated by the model independent method and panel 'c' shows the same for that calculated by the Scatchard method.

Table 4.3: Prodan binding parameters.

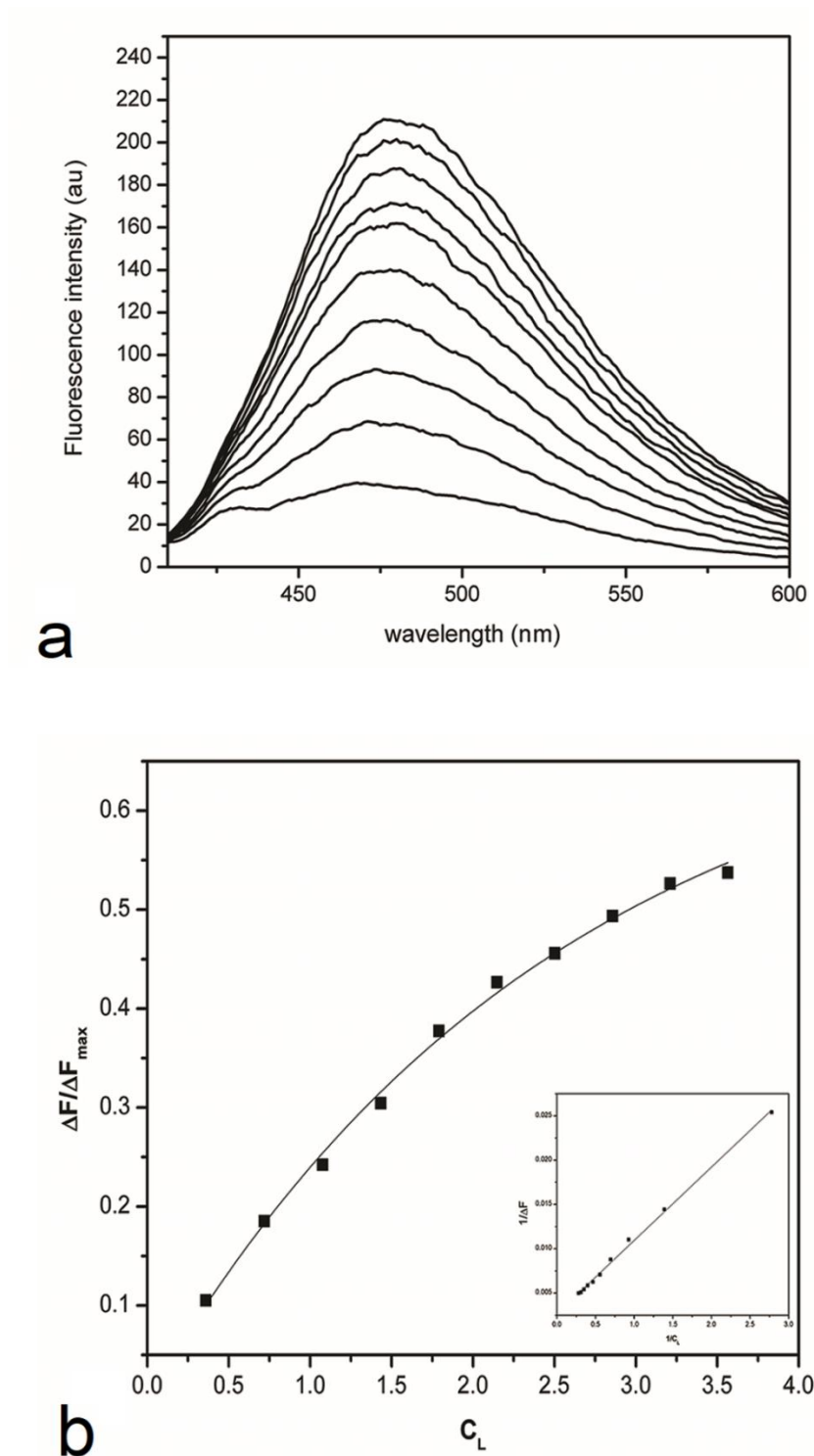
Domain/ Protein	K_d/K_o value (μM)	Stoichiometry (n)	Anisotropy (r)	Polarization (p)	Fluorescence Lifetime (ns)
Spectrin	0.44 ± 0.1 (0.38 ± 0.13)	1.1 ± 0.1 (1 ± 0.1)	0.18 ± 0.001 (0.02 ± 0.001)	0.28 ± 0.001 (0.03 ± 0.001)	5.4 ± 0.3 (1.5 ± 0.2)
Self- association Domain	14.3 ± 0.3 (12.5 ± 0.4)	1 ± 0.2 (1.1 ± 0.1)	0.16 ± 0.002	0.27 ± 0.002	5.2 ± 0.4

Table 4.3: The K_d values and stoichiometry of spectrin and self-association domain binding to Prodan are shown as derived from the model independent method. K_o values and stoichiometry are shown in parenthesis as derived from the Scatchard plot. The anisotropy, polarization and mean lifetimes of Prodan bound to spectrin and self-association domain are tabulated for 360 nm excitation and 430 nm emission. Values in parenthesis represent the same for Prodan in aqueous buffer. Error values are calculated as the standard deviation of four independent experiments.

Similarly in case of ANS it was seen that the fluorescence emission maxima was found to be blue shifted from 520 nm to 470 nm upon protein binding and the emission intensity was found to increase many fold over that of free ANS in aqueous buffer which has negligible fluorescence. The binding parameters of ANS to the spectrin fragments were evaluated by two methods as before and the stoichiometries and binding constants are tabulated in **Table 4**. The increase in fluorescence upon self-association domain binding, and

the analysis are graphically represented in **Figure 4.9, 4.10 and 4.11** along with the binding isotherms. The increase in polarization and anisotropy of ANS fluorescence upon protein binding are tabulated in **Table 4.4**.

Figure 4.9: ANS binding to reconstituted self-association domain.



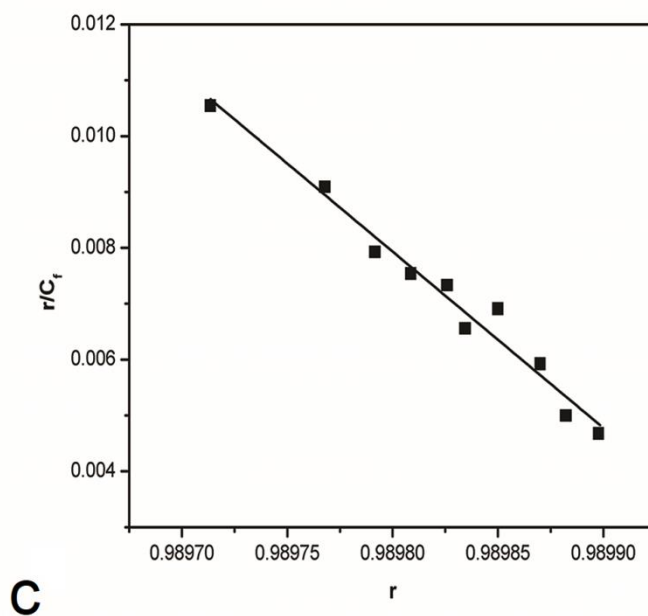


Figure 4.9: Panel 'a' shows the fluorescence spectra of self-association domain titrated with increasing concentration of the ANS. The excitation was at 372 nm, and bound emission at 470 nm. Sequential increase of bound emission peak was seen on titration, with unbound ANS having negligible fluorescence. Panel 'b' shows the binding isotherms calculated by the model independent method and panel 'c' shows the same for that calculated by the Scatchard method.

Figure 4.10: ANS binding to spectrin domains.

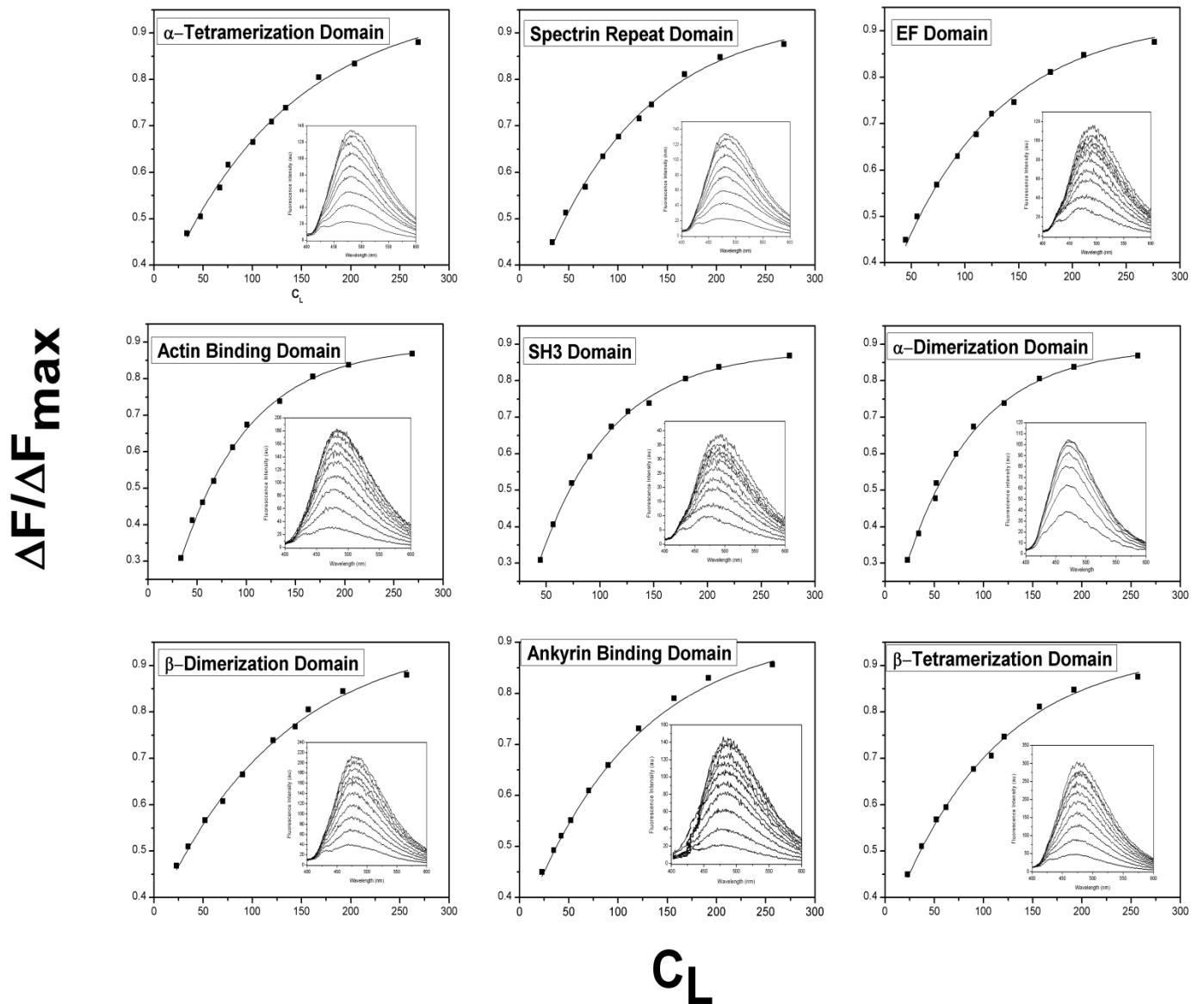


Figure 4.10: The binding isotherms generated by the model independent method for spectrin domain-ANS binding are shown; inset shows fluorescence spectra of the same.

Figure 4.11: Scatchard plots of ANS binding.

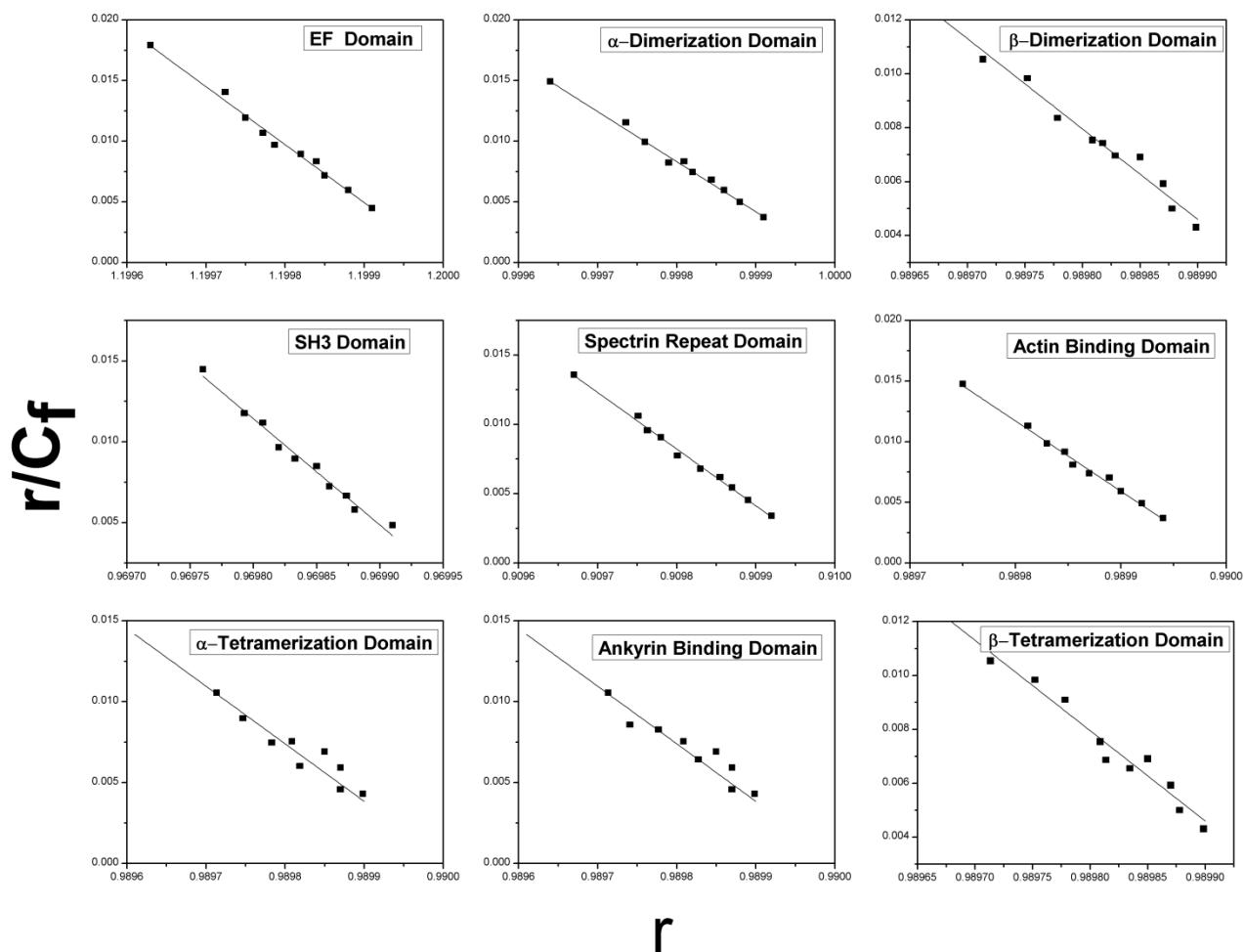


Figure 4.11: The Scatchard plots of ANS binding to spectrin domains are shown.

Table 4.4: ANS binding parameters.

Domain/ Protein	K_d/K_o value (μM)	Stoichiometry (n)	Anisotropy (r)	Polarization (p)
α -Tetramerization	45.37 ± 3.1 (35.59 ± 2.7)	1 ± 0.3 (1 ± 0.1)	0.183 ± 0.001	0.251 ± 0.003
SH3	64 ± 2.7 (57.92 ± 2.9)	1 ± 0.2 (1 ± 0.1)	0.171 ± 0.002	0.232 ± 0.001

Spectrin repeat	47.74 ± 2.9 (39.2 ± 3.1)	1 ± 0.2 (1 ± 0.1)	0.172 ± 0.002	0.243 ± 0.001
α-Dimerization	51.48 ± 3.2 (41.27 ± 2.9)	1 ± 0.3 (1 ± 0.2)	0.183 ± 0.001	0.238 ± 0.001
EF	58.55 ± 2.5 (47.76 ± 2.3)	1 ± 0.2 (1.21 ± 0.3)	0.176 ± 0.002	0.241 ± 0.002
Actin Binding	64.3 ± 3.9 (51.1 ± 3.3)	1 ± 0.1 (1 ± 0.2)	0.184 ± 0.002	0.251 ± 0.001
β-Dimerization	37.2 ± 3.1 (33.48 ± 2.7)	1 ± 0.3 (1 ± 0.2)	0.181 ± 0.001	0.244 ± 0.002
Ankyrin Binding	40 ± 2.8 (36.1 ± 2.2)	1 ± 0.2 (1 ± 0.1)	0.176 ± 0.002	0.249 ± 0.001
β-Tetramerization	48.2 ± 3.3 (33.5 ± 2.1)	1 ± 0.2 1 ± (0.1)	0.181 ± 0.002	0.246 ± 0.001
Spectrin	30.1 ± 2 (18.9 ± 1.7)	5 ± 0.2 (4 ± 0.1)	0.181 ± 0.001 (0.01 ± 0.002)	0.28 ± 0.001 (0.02 ± 0.002)
Self-association domain	38.9 ± 2.3 (29.7 ± 2.1)	1 ± 0.2 (1 ± 0.1)	0.181 ± 0.001	0.261 ± 0.002

Table 4.4: The K_d values and stoichiometry of spectrin, self-association domain and spectrin domain binding to ANS are shown as derived from the model independent method. K_0 values and stoichiometry are shown in parenthesis as derived from the Scatchard plot. The anisotropy, polarization and mean lifetimes of ANS bound to spectrin, self-association domain and spectrin domains are tabulated for 372 nm excitation and 470 nm emission. Values in parenthesis represent the same for ANS in aqueous buffer. Error values are calculated as the standard deviation of four independent experiments.

4.3.3 Assay of chaperone activity

In case of protein aggregation the maximum O.D. measured of the test proteins aggregating alone was taken as 100% and the reduction thereof by spectrin and its cloned fragments was expressed as the percentage of protection from aggregation. It was found that negative control BSA had negligible effect on the aggregation of insulin, ADH, globin chains or the refolding of enzymes; the representative curves for the same are given in **Figure 4.12**.

Figure 4.12: Insulin aggregation in presence of BSA.

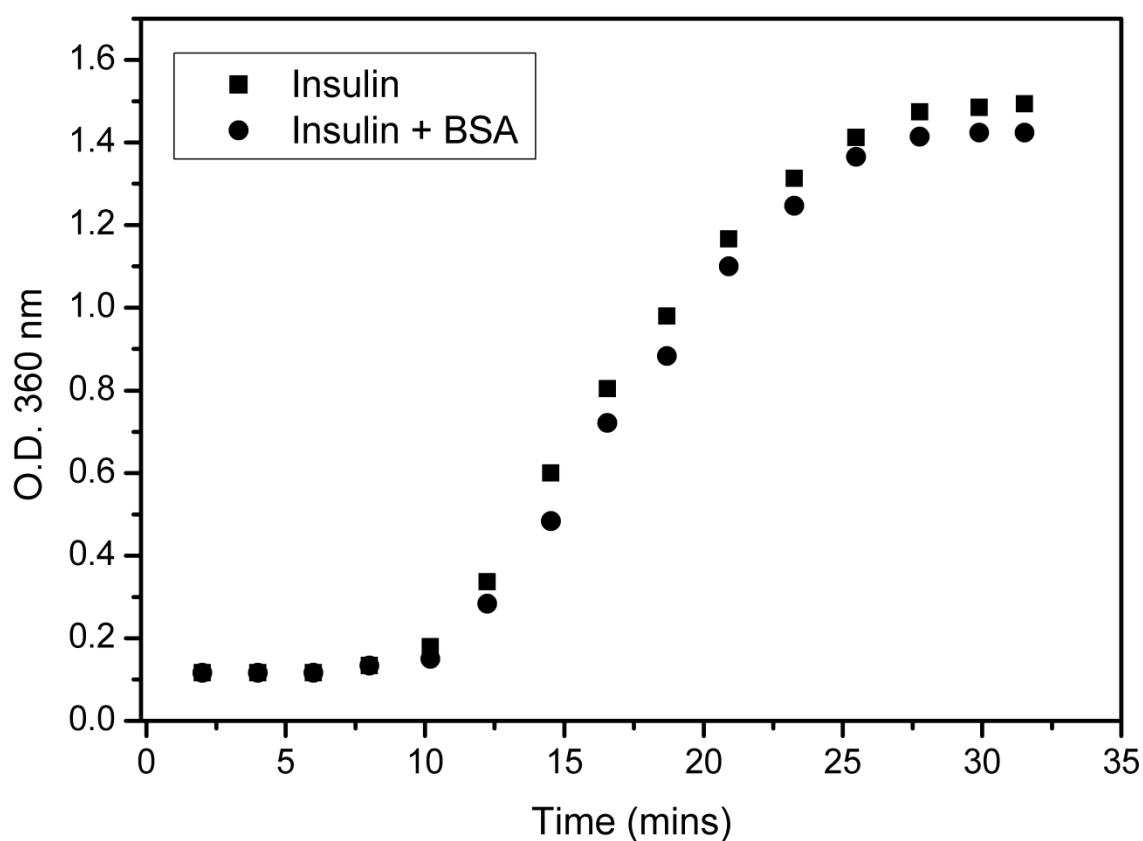


Figure 4.12: The aggregation curve of 0.3mg/ml insulin in the presence and absence of 0.15 mg/ml BSA in 100 mM Na-phosphate buffer, pH 8.0 is shown. Aggregation was carried out at 25 °C and was induced by 20 mM DTT addition.

It was seen that spectrin and spectrin fragments as well as the reconstituted self-association domain could all inhibit protein aggregation both in an aggregating protein to chaperone ratio of 1:0.5 and 1:1. It was seen that this inhibition of aggregation was dose dependent where more protection occurred for the 1:1 ratio than for the 1:0.5 ratio. Moreover it was seen that in case of insulin and globin chain aggregation the fragments behaved in a general way showing a similar extent of protection for all cases with the extent of protection being only slightly less than that of intact spectrin. In case of the thermal aggregation of ADH it was seen that the fragments showed a decreased overall protection than in the other two cases. For the aggregation of insulin native spectrin showed a protection of ~45 % in 1:0.5 weight ratio and about ~60 % for the 1:1 weight ratios. The fragments all showed a protection of ~ 35-40% and 50-55% for these two ratios respectively. In case of ADH aggregation, native spectrin showed ~ 40 % protection in the 1:0.5 and ~ 50% protection in the 1:1 weight ratio respectively with the fragments showing ~ 30 % and ~ 40 % protection in these two weight ratios respectively. For the globin chains it was seen that both native spectrin and the fragments were able to better protect α -globin from aggregation rather than β -globin. Representative aggregation curves of insulin aggregating in presence and absence of spectrin and its subunits is shown in **Figure 4.13**. **Figure 4.13** also shows the extent of protection from aggregation of the test proteins insulin, ADH, α and β -globin by spectrin and its fragments.

Figure 4.13: Chaperone activity of spectrin domains.

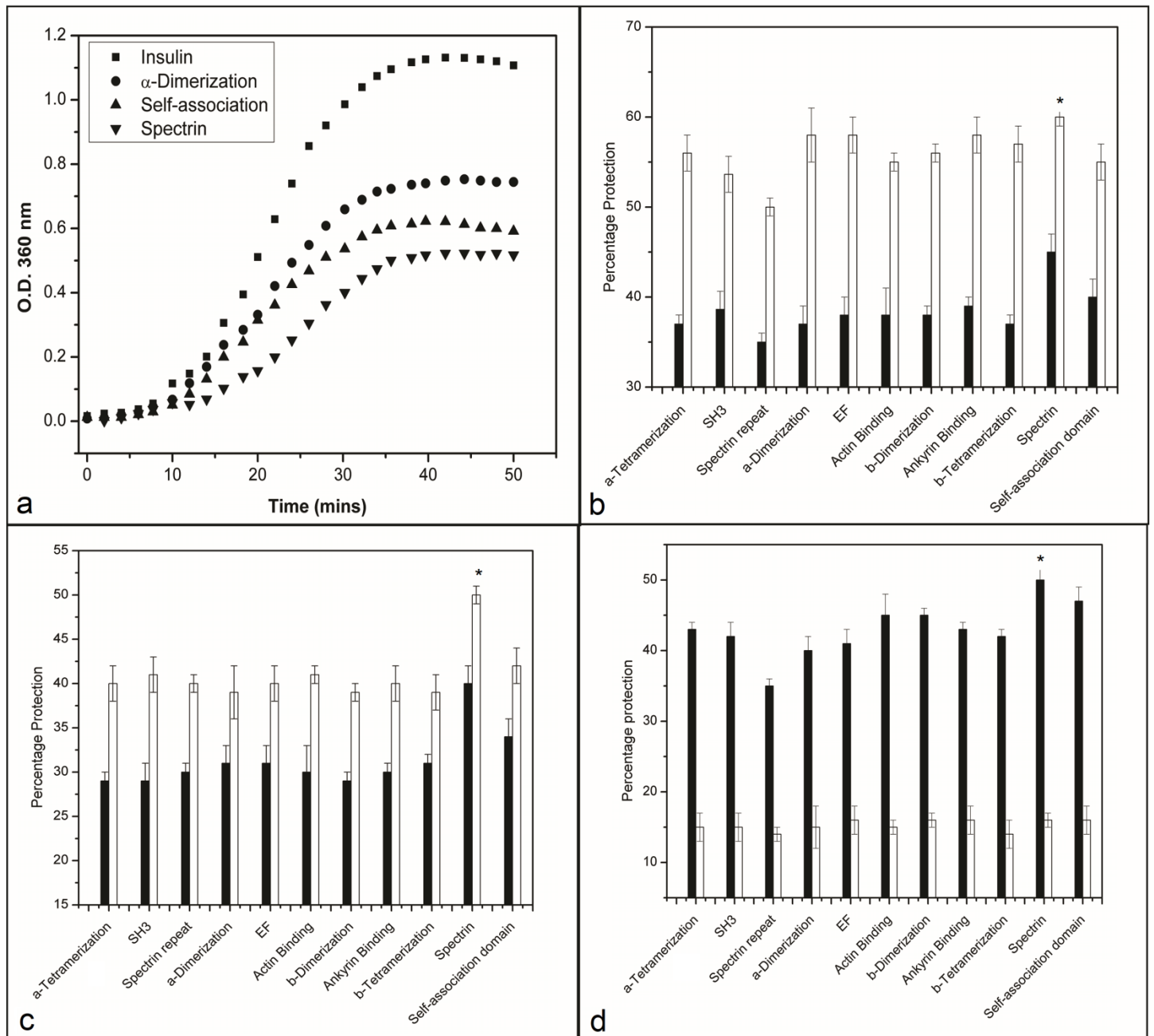


Figure 4.13: Panel 'a' shows representative aggregation curves of insulin aggregating alone or in presence of spectrin, reconstituted self-association domain or α -dimerization domain in a insulin: chaperone ratio of 1:0.5. In all cases 0.3mg/ml insulin and 0.15 mg/ml of chaperone was taken in 100 mM Na-phosphate buffer, pH 7.0, and aggregation was induced by addition of 20 mM of DTT, at a constant temperature of 25 °C. Aggregation was followed

by monitoring the apparent increase in absorbance at 360 nm. Panel 'b' shows the extent of protection as percentage from aggregation of insulin by spectrin, spectrin domains and self-association domain where the aggregation of insulin alone is considered as 100%. Filled in bars represent protection for 1:0.5 weight ratio and empty bars represent the same for 1:1 weight ratio. Panel 'c' shows the extent of protection as percentage from aggregation of ADH by spectrin, spectrin domains and self-association domain where the aggregation of ADH alone is considered as 100%. In all cases 0.4 mg/ml ADH was taken with 0.2mg/ml of different chaperone proteins in 50 mM Na-phosphate buffer, pH 8.0 and aggregation was induced by heating and maintaining temperature at 50 °C. Aggregation was followed by measuring the 90° scattering at 450 nm. Filled in bars represent protection for 1:0.5 weight ratio and empty bars represent the same for 1:1 weight ratio. Panel 'd' shows the percentage protection against aggregation of α - and β -globin by spectrin, self-association domain and spectrin domains. Aggregation was carried out as described in text. The filled in bars represent protection in case of α -globin and the empty bars represent that of β -globin. Aggregation was followed by measuring apparent increase in absorbance at 700 nm and the extent of aggregation of either of the two globins aggregating alone was taken to be 100%. Error bars are calculated as the standard deviation of four independent experiments. In all cases statistical analysis using Student's t-test reveals that there is no significant deviation between the chaperone activities of the expressed domains with the self-association domain being moderately different with p value <0.5.

It was seen that native spectrin and its recombinant fragments had an effect on the reactivation yield of the enzymes α -glucosidase and alkaline phosphatase. In case of alkaline phosphatase it was seen that presence of spectrin or its fragments caused an increase in the reactivation yield whereas in case of α -glucosidase there was a decrease. In case of alkaline phosphatase it was seen that native spectrin could increase the yield to ~35% from a self

refolding yield of ~ 20%. The fragments could increase the yield comparably to spectrin at around 30%. In case of α -glucosidase self refolding yields of ~25% was found to decrease in presence of spectrin to ~ 10% with the around same yield being seen in presence of the fragments. The reactivation yields are graphically represented in **Figure 4.14**.

Figure 4.14: Reactivation of alkaline phosphatase.

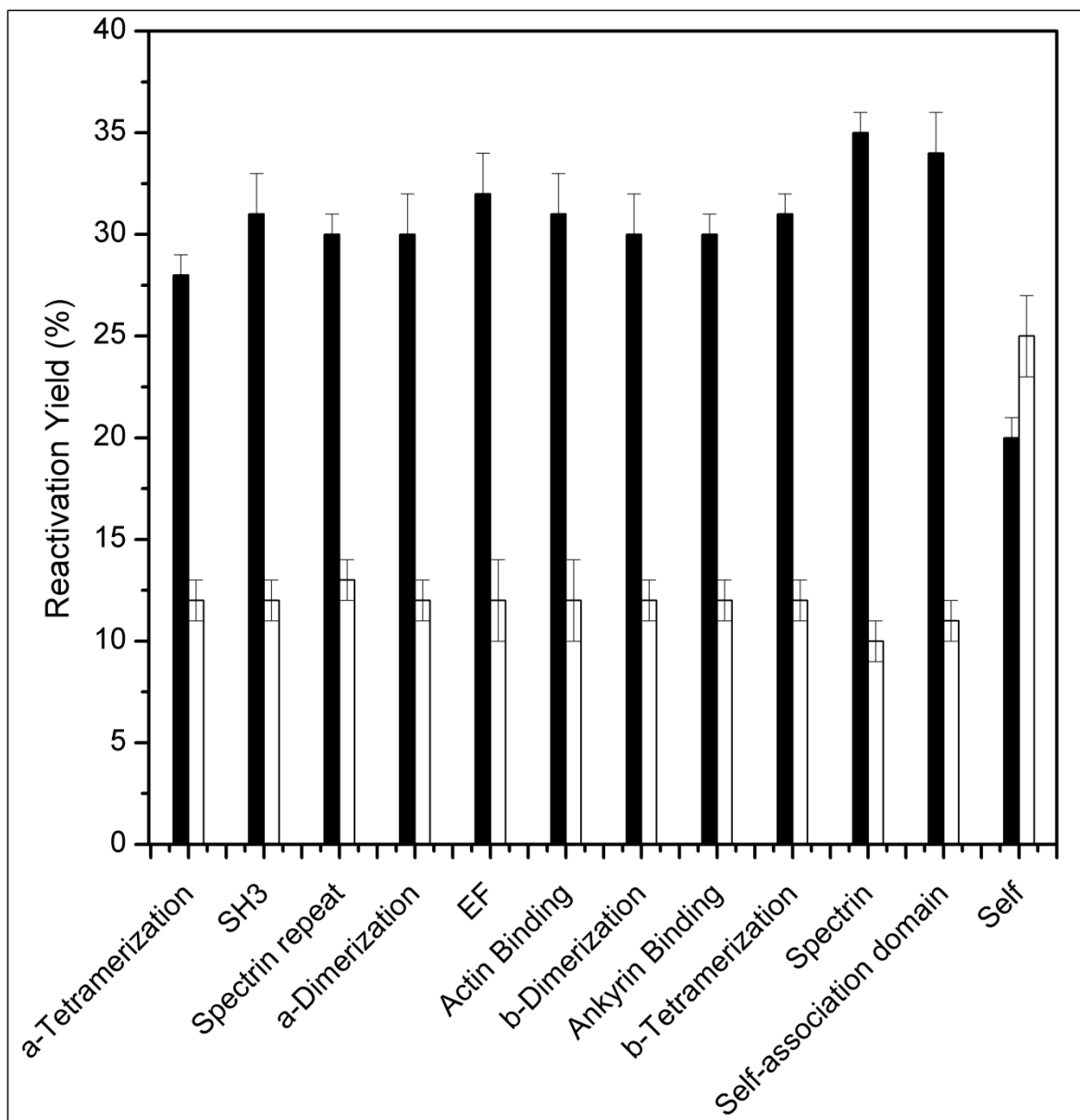


Figure 4.14: The percentage reactivation yields of alkaline phosphatase and α -glucosidase are shown. The filled in bars represent alkaline phosphatase while the empty bars represent

α -glucosidase. The enzymes were denatured in 8 M urea and 6 M guanidium-HCl respectively and refolding was induced by 1000 fold dilution in presence and absence of different chaperone proteins. The activity of equivalent amount of native enzyme was taken as 100%. Presence of spectrin, self-association domain and spectrin fragments was found to reduce reactivation yields for α -glucosidase, with the opposite being seen for alkaline phosphatase. Error bars are calculated as the standard deviation of four independent experiments. . In all cases statistical analysis using Student's t-test reveals that there is no significant deviation between the chaperone activities of the expressed domains with only the self-association domain being significantly different with p value <0.05 .

4.3.4 Discussions

Intrinsic tryptophan fluorescence is a very useful tool to probe the conformation and stability of spectrin. The tryptophans are conserved in their positions in the spectrin repeat domains and contribute to the overall stability and structure of the protein as evidenced by the fact that mutating them causes a decrease in stability of the spectrin repeat domains (7,48,49). Of our chosen spectrin domains all but the SH3, EF, Actin binding and the β -tetramerization domain are made up of the spectrin repeat motifs, and of the domains that do not share a consensus sequence with the spectrin repeat motif, only the SH3 domain has a non-alpha helical fold (50). So tryptophan fluorescence gives us a useful tool to probe the structure of the cloned spectrin domains. Experimental data shows that for all the domains a moderately high amount of constraint is present on the tryptophans, which is reflected by their anisotropy and polarization values which approach those of native spectrin (51,52). Notably, the SH3 domain and EF domain are exceptions to that general trend which can be explained by the fact that SH3 domain has a globular fold which does not put as much torsional constraint on the tryptophans and in case of the EF domain the single tryptophan being probed was

inserted artificially to aid in estimating protein folding. The anisotropy data is corroborated by emission maxima measurements which show the same trend and it is seen that the tryptophan emissions corroborate well with situations where the tryptophans are buried in a hydrophobic protein core (53). Moreover upon urea denaturation the anisotropy decreases and emission maxima are red shifted for the refolded domains as it is for native spectrin (54). Taken together the anisotropy, polarization and emission maxima data strongly indicate that the cloned, expressed and denatured domains were successfully refolded and the refolded proteins were structurally similar to native spectrin. This is supported by measurements of the mean tryptophan lifetimes which show that the refolded domains all have lifetimes comparable to that of native spectrin which decreases upon urea unfolding analogous to spectrin. CD spectroscopy confirmed the folding of the proteins; it was seen that the refolded domains shared the same α -helical fold of spectrin except SH3 domain which showed a CD spectra that matched with previous reports of the native domain (47). Urea denaturation was found to abolish the clean α -helical nature of the CD spectra of these domains further indicating that the domains were successfully renatured.

Interestingly it is seen that CD spectra reveals subtle differences in the folding and conformation of these spectrin domains which are consistent with previous literature on these domains. CD spectroscopy reveals that the lowest MRE values at 222 nm are those of the EF domain, SH3 domain and β -tetramerization domain, which can be explained by the fact that β -dimerization domain has a non-structured tail (55) which decreases its α -helical nature; similarly SH3 domain has a globular fold (47) and EF domain while α -helical is made up sequences non-homologous to the spectrin repeat domain (24).

Hydrophobic probe Prodan was found to bind only the reconstituted self-association domain of spectrin with binding affinity comparable to native spectrin. The rest of the

fragments either do not bind Prodan or bind weakly with appreciably lower binding affinity. This validates our earlier hypothesis that the Prodan binding site in spectrin is located in the self-association domain; moreover the stoichiometry is also found to be same as that seen in our previous studies (16,45). It is important to note that our previous study has shown that Prodan binds to both dimeric and tetrameric spectrin; in dimeric spectrin the self-association domain has not dimerized across two spectrin hetero-dimers to give the dimerized self-association domain. However available data indicates that the labile tail of the β -tetramerization domain forms a loop which mimics the same (56). In our present study neither the α -tetramerization domain nor the β -tetramerization domain could by themselves bind Prodan to a level that could be experimentally followed; only when they had dimerized to yield the reconstituted self-association domain could they bind Prodan. This can be explained by the fact that in both the spectrin dimer and tetramer the β -tetramerization domain's labile tail is in a complex which forms a completed spectrin repeat domain, either by forming a loop or by complexing with a partial repeat domain in α -tetramerization domain (56-58) and it can be hypothesized that only when this complexed domain exists can Prodan bind. In the present work it is seen that the affinity of Prodan binding to the self-association domain is lower than that of binding to spectrin; this can be explained by the fact that while the α and β -tetramerization domains are capable of reconstituting the self-association domain, the structure of the same is not exactly the same as in the native condition, this is due to the fact that spectrin domains by themselves have less stability and structure than the whole protein (59).

The hydrophobic probe ANS was seen to bind to all the fragments of spectrin and spectrin itself. Generally native proteins do not bind ANS and ANS binding indicates some denaturation of a protein (60-62); however in cases where a protein has surface exposed hydrophobic patches the native protein can also bind ANS (63), making it a good probe for

measuring protein surface hydrophobicity (64). We see that while all the domains bind ANS the affinity for the same is less than that in spectrin; moreover spectrin is shown to bind 5 ANS residues while the domains along with the self-association domain each bind 1 ANS for a total of 10. It is possible that intact spectrin has some hotspots of surface hydrophobicity which can bind ANS with much greater affinity thereby masking the binding of ANS to the other less-hydrophobic sites and the actual binding sites for ANS on spectrin is greater than 5. Present data shows us that all the fragments of spectrin have hydrophobic patches on their surface that can bind ANS and the hydrophobicity is of a comparable amount as evidenced by comparable dissociation constants for ANS binding.

The chaperone activity of spectrin fragments was assayed by following their ability to prevent protein aggregation and aid enzyme refolding. It was seen that in case of prevention of protein aggregation, intact spectrin was the best at protecting the aggregating proteins followed by the reconstituted self-association domain, all the other fragments had about the same activity which was slightly less than that of spectrin. It can be hypothesized that the spectrin fragments irrespective of their mutual structural differences act in a generalized manner when it comes to interacting with their chaperone substrates. It is plausible to think of the chaperone potential of spectrin fragments to be driven by the presence of surface exposed hydrophobic patches, as is the case with many chaperones (65,66), for example the chaperones such as sHSPs and GroEL also act with the help of exposed hydrophobic patches (67,68). It is known that chaperones act by recognizing the exposed hydrophobic clusters in structurally perturbed, misfolded, partially folded or stressed proteins with the help of hydrophobic patches of their own (25). As we have confirmed the presence of hydrophobic patches on all the spectrin domains and have determined that they all have about the same hydrophobicity it is reasonable to think that they are the determining factor in chaperone activity. However at this stage our data only points to a strong correlation between surface

hydrophobicity and chaperone activity; we cannot definitively state that hydrophobicity is the driving factor in chaperone activity but can only strongly infer it. Moreover the relatively unstable nature of the individual domains in comparison to intact spectrin (69,70) can be seen in the case of ADH aggregation where the difference in protection between spectrin and the cloned domains are most prominent probably due to the reduced stability of the domains in thermal stress.

Modular multi-domain proteins carrying tandemly repeated motifs such as the ankyrin motif, usually have different interactive and binding properties in different repeat domains which are not functionally interchangeable (71,72) as is seen to be the case in case of proteins carrying “spectrin-repeat” domains (8,21). However in our present study we see that all the domains show a similar extent of chaperone activity indicating that it may be a general feature of “spectrin-repeat” motif. This observation can also be logically extended to hypothesize that proteins carrying the “spectrin-repeat” domain or related to spectrin such as α -actinin may also have chaperone activity (20).

It is also interesting to note that spectrin and spectrin domains display a great specificity towards α -globin in favour of β -globin as a chaperone substrate as is evidenced by a large protection from aggregation of the former versus a modest one of the latter (17). Our previous studies have shown that spectrin displays a selective affinity towards α -globin as a substrate as versus β -globin. Basic sequence alignment and crystal structure comparison reveals that the spectrin repeat domains share a similar fold and moderate homology to the α -globin chaperone AHSP (73). We have hypothesised that α -globin may act as a major client for the chaperone activity of spectrin based on both its selective binding and high affinity (17,74). This selective chaperone activity may have significance in hemoglobin disease states, notably in β -thalassemias where it is seen that free α -globin causes cellular toxicity

and disease manifestations (75). Importantly in such conditions AHSP has a protective role which may also be fulfilled by spectrin due to its affinity for α -globin (76).

Enzyme refolding studies illuminate the fact that the mechanism of chaperone action is not the same for all client proteins; in case of alkaline phosphatase the addition of spectrin and spectrin domains give a larger reactivation yield versus self refolding while in case of α -glucosidase we see the opposite to be true. Chaperones are known to act by either helping a protein refold as in case of HSP70 (77) or they bind to an unfolded protein stopping aggregation until another chaperone can refold the protein as in case of α -crystallins (78). It would seem that depending on the nature of the client, spectrin is able to follow either one of these two routes.

From our present study it can be concluded that the molecular site of Prodan binding in native dimeric erythroid spectrin is located in the self-association domain and that the chaperone activity of spectrin is derived from the presence of many surface exposed hydrophobic patches which give its constituent domains comparable chaperone activity with the self association domain being moderately better in terms of preventing protein aggregation.

Abbreviations

DTT, di-thiothreitol; RBC, red blood cell; DEAE, diethylaminoethyl; CM, carboxymethyl; HbA, hemoglobin A; Prodan, 6-propionyl-2[dimethylamino]-naphthalene; ANS, 1-anilinonaphthalene-8-sulfonic acid; PMB, para-hydroxymercuribenzoic acid; ADH, alcohol dehydrogenase.

References

1. Grum, V. L., Li, D., MacDonald, R. I., and Mondragon, A. (1999) Structures of two repeats of spectrin suggest models of flexibility. *Cell* **98**, 523-535
2. Mirijanian, D. T., Chu, J. W., Ayton, G. S., and Voth, G. A. (2007) Atomistic and coarse-grained analysis of double spectrin repeat units: the molecular origins of flexibility. *Journal of molecular biology* **365**, 523-534
3. An, X., Guo, X., Zhang, X., Baines, A. J., Debnath, G., Moyo, D., Salomao, M., Bhasin, N., Johnson, C., Discher, D., Gratzer, W. B., and Mohandas, N. (2006) Conformational stabilities of the structural repeats of erythroid spectrin and their functional implications. *The Journal of biological chemistry* **281**, 10527-10532
4. Stabach, P. R., Simonovic, I., Ranieri, M. A., Aboodi, M. S., Steitz, T. A., Simonovic, M., and Morrow, J. S. (2009) The structure of the ankyrin-binding site of beta-spectrin reveals how tandem spectrin-repeats generate unique ligand-binding properties. *Blood* **113**, 5377-5384
5. Andrade, M. A., Perez-Iratxeta, C., and Ponting, C. P. (2001) Protein repeats: structures, functions, and evolution. *Journal of structural biology* **134**, 117-131
6. Speicher, D. W., and Marchesi, V. T. (1984) Erythrocyte spectrin is comprised of many homologous triple helical segments. *Nature* **311**, 177-180
7. MacDonald, R. I., Musacchio, A., Holmgren, R. A., and Saraste, M. (1994) Invariant tryptophan at a shielded site promotes folding of the conformational unit of spectrin. *Proceedings of the National Academy of Sciences of the United States of America* **91**, 1299-1303
8. Djinovic-Carugo, K., Gautel, M., Ylanne, J., and Young, P. (2002) The spectrin repeat: a structural platform for cytoskeletal protein assemblies. *FEBS letters* **513**, 119-123

9. Sahr, K. E., Laurila, P., Kotula, L., Scarpa, A. L., Coupal, E., Leto, T. L., Linnenbach, A. J., Winkelmann, J. C., Speicher, D. W., Marchesi, V. T., and et al. (1990) The complete cDNA and polypeptide sequences of human erythroid alpha-spectrin. *The Journal of biological chemistry* **265**, 4434-4443
10. Winkelmann, J. C., Chang, J. G., Tse, W. T., Scarpa, A. L., Marchesi, V. T., and Forget, B. G. (1990) Full-length sequence of the cDNA for human erythroid beta-spectrin. *The Journal of biological chemistry* **265**, 11827-11832
11. Bennett, V., and Gilligan, D. M. (1993) The spectrin-based membrane skeleton and micron-scale organization of the plasma membrane. *Annual review of cell biology* **9**, 27-66
12. Bennett, V., and Lambert, S. (1991) The spectrin skeleton: from red cells to brain. *The Journal of clinical investigation* **87**, 1483-1489
13. Machnicka, B., Grochowalska, R., Boguslawska, D. M., Sikorski, A. F., and Lecomte, M. C. (2012) Spectrin-based skeleton as an actor in cell signaling. *Cellular and molecular life sciences : CMLS* **69**, 191-201
14. Deng, H., Wang, W., Yu, J., Zheng, Y., Qing, Y., and Pan, D. (2015) Spectrin regulates Hippo signaling by modulating cortical actomyosin activity. *eLife* **4**, e06567
15. Chakrabarti, A., Bhattacharya, S., Ray, S., and Bhattacharyya, M. (2001) Binding of a denatured heme protein and ATP to erythroid spectrin. *Biochemical and biophysical research communications* **282**, 1189-1193
16. Bhattacharyya, M., Ray, S., Bhattacharya, S., and Chakrabarti, A. (2004) Chaperone activity and prodan binding at the self-associating domain of erythroid spectrin. *The Journal of biological chemistry* **279**, 55080-55088
17. Basu, A., and Chakrabarti, A. (2015) Hemoglobin interacting proteins and implications of spectrin hemoglobin interaction. *Journal of proteomics* **128**, 469-475

18. Bose, D., Patra, M., and Chakrabarti, A. (2017) Effect of pH on stability, conformation, and chaperone activity of erythroid & non-erythroid spectrin. *Biochimica et biophysica acta. Proteins and proteomics* **1865**, 694-702
19. Matsudaira, P. (1991) Modular organization of actin crosslinking proteins. *Trends in biochemical sciences* **16**, 87-92
20. Pascual, J., Castresana, J., and Saraste, M. (1997) Evolution of the spectrin repeat. *BioEssays : news and reviews in molecular, cellular and developmental biology* **19**, 811-817
21. Harper, S. Q., Crawford, R. W., DelloRusso, C., and Chamberlain, J. S. (2002) Spectrin-like repeats from dystrophin and alpha-actinin-2 are not functionally interchangeable. *Human molecular genetics* **11**, 1807-1815
22. Kennedy, S. P., Warren, S. L., Forget, B. G., and Morrow, J. S. (1991) Ankyrin binds to the 15th repetitive unit of erythroid and nonerythroid beta-spectrin. *The Journal of cell biology* **115**, 267-277
23. Bennett, V. (1989) The spectrin-actin junction of erythrocyte membrane skeletons. *Biochimica et biophysica acta* **988**, 107-121
24. Trave, G., Pastore, A., Hyvonen, M., and Saraste, M. (1995) The C-terminal domain of alpha-spectrin is structurally related to calmodulin. *European journal of biochemistry* **227**, 35-42
25. Bose, D., and Chakrabarti, A. (2017) Substrate specificity in the context of molecular chaperones. *IUBMB life* **69**, 647-659
26. Sarkar, S., Bose, D., Giri, R. P., Mukhopadhyay, M. K., and Chakrabarti, A. (2019) Effects of GM1 on brain spectrin-aminophospholipid interactions. *Biochimica et biophysica acta. Biomembranes* **1861**, 298-305

27. Ipsaro, J. J., Harper, S. L., Messick, T. E., Marmorstein, R., Mondragon, A., and Speicher, D. W. (2010) Crystal structure and functional interpretation of the erythrocyte spectrin tetramerization domain complex. *Blood* **115**, 4843-4852
28. Shammass, S. L., Rogers, J. M., Hill, S. A., and Clarke, J. (2012) Slow, reversible, coupled folding and binding of the spectrin tetramerization domain. *Biophysical journal* **103**, 2203-2214
29. Nicolas, G., Pedroni, S., Fournier, C., Gautero, H., Craescu, C., Dhermy, D., and Lecomte, M. C. (1998) Spectrin self-association site: characterization and study of beta-spectrin mutations associated with hereditary elliptocytosis. *The Biochemical journal* **332 (Pt 1)**, 81-89
30. Henniker, A., and Ralston, G. B. (1994) Reinvestigation of the thermodynamics of spectrin self-association. *Biophysical chemistry* **52**, 251-258
31. Gallagher, P. G., Zhang, Z., Morrow, J. S., and Forget, B. G. (2004) Mutation of a highly conserved isoleucine disrupts hydrophobic interactions in the alpha beta spectrin self-association binding site. *Laboratory investigation; a journal of technical methods and pathology* **84**, 229-234
32. Harper, S. L., Begg, G. E., and Speicher, D. W. (2001) Role of terminal nonhomologous domains in initiation of human red cell spectrin dimerization. *Biochemistry* **40**, 9935-9943
33. Begg, G. E., Harper, S. L., Morris, M. B., and Speicher, D. W. (2000) Initiation of spectrin dimerization involves complementary electrostatic interactions between paired triple-helical bundles. *The Journal of biological chemistry* **275**, 3279-3287
34. Li, D., Tang, H. Y., and Speicher, D. W. (2008) A structural model of the erythrocyte spectrin heterodimer initiation site determined using homology modeling and chemical cross-linking. *The Journal of biological chemistry* **283**, 1553-1562

35. Li, D., Harper, S., and Speicher, D. W. (2007) Initiation and propagation of spectrin heterodimer assembly involves distinct energetic processes. *Biochemistry* **46**, 10585-10594
36. Trave, G., Lacombe, P. J., Pfuhl, M., Saraste, M., and Pastore, A. (1995) Molecular mechanism of the calcium-induced conformational change in the spectrin EF-hands. *The EMBO journal* **14**, 4922-4931
37. Musacchio, A., Noble, M., Pauptit, R., Wierenga, R., and Saraste, M. (1992) Crystal structure of a Src-homology 3 (SH3) domain. *Nature* **359**, 851-855
38. Koch, C. A., Anderson, D., Moran, M. F., Ellis, C., and Pawson, T. (1991) SH2 and SH3 domains: elements that control interactions of cytoplasmic signaling proteins. *Science* **252**, 668-674
39. Ipsaro, J. J., Huang, L., and Mondragon, A. (2009) Structures of the spectrin-ankyrin interaction binding domains. *Blood* **113**, 5385-5393
40. Karinch, A. M., Zimmer, W. E., and Goodman, S. R. (1990) The identification and sequence of the actin-binding domain of human red blood cell beta-spectrin. *The Journal of biological chemistry* **265**, 11833-11840
41. Branton, D., Cohen, C. M., and Tyler, J. (1981) Interaction of cytoskeletal proteins on the human erythrocyte membrane. *Cell* **24**, 24-32
42. Datta, P., Chakrabarty, S., Chakrabarty, A., and Chakrabarti, A. (2007) Spectrin interactions with globin chains in the presence of phosphate metabolites and hydrogen peroxide: implications for thalassaemia. *Journal of biosciences* **32**, 1147-1151
43. Geraci, G., Parkhurst, L. J., and Gibson, Q. H. (1969) Preparation and properties of alpha- and beta-chains from human hemoglobin. *The Journal of biological chemistry* **244**, 4664-4667

44. Bucci, E., and Fronticelli, C. (1965) A New Method for the Preparation of Alpha and Beta Subunits of Human Hemoglobin. *The Journal of biological chemistry* **240**, PC551-552
45. Chakrabarti, A. (1996) Fluorescence of spectrin-bound prodan. *Biochemical and biophysical research communications* **226**, 495-497
46. Kihm, A. J., Kong, Y., Hong, W., Russell, J. E., Rouda, S., Adachi, K., Simon, M. C., Blobel, G. A., and Weiss, M. J. (2002) An abundant erythroid protein that stabilizes free alpha-haemoglobin. *Nature* **417**, 758-763
47. Viguera, A. R., Martinez, J. C., Filimonov, V. V., Mateo, P. L., and Serrano, L. (1994) Thermodynamic and kinetic analysis of the SH3 domain of spectrin shows a two-state folding transition. *Biochemistry* **33**, 2142-2150
48. Pantazatos, D. P., and MacDonald, R. I. (1997) Site-directed mutagenesis of either the highly conserved Trp-22 or the moderately conserved Trp-95 to a large, hydrophobic residue reduces the thermodynamic stability of a spectrin repeating unit. *The Journal of biological chemistry* **272**, 21052-21059
49. Chattopadhyay, A., Rawat, S. S., Kelkar, D. A., Ray, S., and Chakrabarti, A. (2003) Organization and dynamics of tryptophan residues in erythroid spectrin: novel structural features of denatured spectrin revealed by the wavelength-selective fluorescence approach. *Protein science : a publication of the Protein Society* **12**, 2389-2403
50. Grantcharova, V. P., and Baker, D. (1997) Folding dynamics of the src SH3 domain. *Biochemistry* **36**, 15685-15692
51. Ray, S., Bhattacharyya, M., and Chakrabarti, A. (2005) Conformational study of spectrin in presence of submolar concentrations of denaturants. *Journal of fluorescence* **15**, 61-70

52. Kelkar, D. A., Chattopadhyay, A., Chakrabarti, A., and Bhattacharyya, M. (2005) Effect of ionic strength on the organization and dynamics of tryptophan residues in erythroid spectrin: a fluorescence approach. *Biopolymers* **77**, 325-334
53. van Rooijen, B. D., van Leijenhorst-Groener, K. A., Claessens, M. M., and Subramaniam, V. (2009) Tryptophan fluorescence reveals structural features of alpha-synuclein oligomers. *Journal of molecular biology* **394**, 826-833
54. Patra, M., Mukhopadhyay, C., and Chakrabarti, A. (2015) Probing conformational stability and dynamics of erythroid and nonerythroid spectrin: effects of urea and guanidine hydrochloride. *PloS one* **10**, e0116991
55. Hill, S. A., Kwa, L. G., Shammass, S. L., Lee, J. C., and Clarke, J. (2014) Mechanism of assembly of the non-covalent spectrin tetramerization domain from intrinsically disordered partners. *Journal of molecular biology* **426**, 21-35
56. Harper, S. L., Li, D., Maksimova, Y., Gallagher, P. G., and Speicher, D. W. (2010) A fused alpha-beta "mini-spectrin" mimics the intact erythrocyte spectrin head-to-head tetramer. *The Journal of biological chemistry* **285**, 11003-11012
57. Li, D., Harper, S. L., Tang, H. Y., Maksimova, Y., Gallagher, P. G., and Speicher, D. W. (2010) A comprehensive model of the spectrin divalent tetramer binding region deduced using homology modeling and chemical cross-linking of a mini-spectrin. *The Journal of biological chemistry* **285**, 29535-29545
58. Speicher, D. W., DeSilva, T. M., Speicher, K. D., Ursitti, J. A., Hembach, P., and Weglarz, L. (1993) Location of the human red cell spectrin tetramer binding site and detection of a related "closed" hairpin loop dimer using proteolytic footprinting. *The Journal of biological chemistry* **268**, 4227-4235

59. Menhart, N., Mitchell, T., Lusitani, D., Topouzian, N., and Fung, L. W. (1996) Peptides with more than one 106-amino acid sequence motif are needed to mimic the structural stability of spectrin. *The Journal of biological chemistry* **271**, 30410-30416
60. Semisotnov, G. V., Rodionova, N. A., Razgulyaev, O. I., Uversky, V. N., Gripas, A. F., and Gilmanshin, R. I. (1991) Study of the "molten globule" intermediate state in protein folding by a hydrophobic fluorescent probe. *Biopolymers* **31**, 119-128
61. Bolognesi, B., Kumita, J. R., Barros, T. P., Esbjorner, E. K., Luheshi, L. M., Crowther, D. C., Wilson, M. R., Dobson, C. M., Favrin, G., and Yerbury, J. J. (2010) ANS binding reveals common features of cytotoxic amyloid species. *ACS chemical biology* **5**, 735-740
62. Christensen, H., and Pain, R. H. (1991) Molten globule intermediates and protein folding. *European biophysics journal : EBJ* **19**, 221-229
63. Stryer, L. (1965) The interaction of a naphthalene dye with apomyoglobin and apohemoglobin. A fluorescent probe of non-polar binding sites. *Journal of molecular biology* **13**, 482-495
64. Patra, M., Mitra, M., Chakrabarti, A., and Mukhopadhyay, C. (2014) Binding of polarity-sensitive hydrophobic ligands to erythroid and nonerythroid spectrin: fluorescence and molecular modeling studies. *Journal of biomolecular structure & dynamics* **32**, 852-865
65. Reddy, G. B., Kumar, P. A., and Kumar, M. S. (2006) Chaperone-like activity and hydrophobicity of alpha-crystallin. *IUBMB life* **58**, 632-641
66. Xu, W., Yuan, X., Xiang, Z., Mimnaugh, E., Marcu, M., and Neckers, L. (2005) Surface charge and hydrophobicity determine ErbB2 binding to the Hsp90 chaperone complex. *Nature structural & molecular biology* **12**, 120-126

67. Haslbeck, M. (2002) sHsps and their role in the chaperone network. *Cellular and molecular life sciences : CMLS* **59**, 1649-1657
68. Lin, Z., Schwartz, F. P., and Eisenstein, E. (1995) The hydrophobic nature of GroEL-substrate binding. *The Journal of biological chemistry* **270**, 1011-1014
69. Lenne, P. F., Raae, A. J., Altmann, S. M., Saraste, M., and Horber, J. K. (2000) States and transitions during forced unfolding of a single spectrin repeat. *FEBS letters* **476**, 124-128
70. MacDonald, R. I., and Pozharski, E. V. (2001) Free energies of urea and of thermal unfolding show that two tandem repeats of spectrin are thermodynamically more stable than a single repeat. *Biochemistry* **40**, 3974-3984
71. Sedgwick, S. G., and Smerdon, S. J. (1999) The ankyrin repeat: a diversity of interactions on a common structural framework. *Trends in biochemical sciences* **24**, 311-316
72. Grove, T. Z., Cortajarena, A. L., and Regan, L. (2008) Ligand binding by repeat proteins: natural and designed. *Current opinion in structural biology* **18**, 507-515
73. Feng, L., Gell, D. A., Zhou, S., Gu, L., Kong, Y., Li, J., Hu, M., Yan, N., Lee, C., Rich, A. M., Armstrong, R. S., Lay, P. A., Gow, A. J., Weiss, M. J., Mackay, J. P., and Shi, Y. (2004) Molecular mechanism of AHSP-mediated stabilization of alpha-hemoglobin. *Cell* **119**, 629-640
74. Mishra, K., Chakrabarti, A., and Das, P. K. (2017) Protein-Protein Interaction Probed by Label-free Second Harmonic Light Scattering: Hemoglobin Adsorption on Spectrin Surface as a Case Study. *The journal of physical chemistry. B* **121**, 7797-7802
75. Cao, A., and Galanello, R. (2010) Beta-thalassemia. *Genetics in medicine : official journal of the American College of Medical Genetics* **12**, 61-76

76. Weiss, M. J., Zhou, S., Feng, L., Gell, D. A., Mackay, J. P., Shi, Y., and Gow, A. J. (2005) Role of alpha-hemoglobin-stabilizing protein in normal erythropoiesis and beta-thalassemia. *Annals of the New York Academy of Sciences* **1054**, 103-117
77. Bukau, B., and Horwich, A. L. (1998) The Hsp70 and Hsp60 chaperone machines. *Cell* **92**, 351-366
78. Derham, B. K., and Harding, J. J. (1999) Alpha-crystallin as a molecular chaperone. *Prog Retin Eye Res* **18**, 463-509

4.4 Appendix:

Interaction of spectrin fragments with hemoglobin variants

Using the FITC labelling method elaborated in Chapter 5 the K_d values for the association of spectrin fragments to HbA, HbE and HbS were determined. They are tabulated in **Table 4.5**. K_d values are expressed in μM . Error values represent the S.D. of at least three independent experiments.

Table 4.5: K_d values.

Protein name	HbA	HbE	HbS
α-Tetramerization	1.088 \pm 0.09	0.24 \pm 0.1	0.851 \pm 0.07
SH3	0.544 \pm 0.1	0.12 \pm 0.09	0.425 \pm 0.06
Spectrin repeat	0.68 \pm 0.07	0.15 \pm 0.07	0.537 \pm 0.08
α-Dimerization	1.54 \pm 0.08	0.34 \pm 0.08	1.2 \pm 0.08
EF	1.08 \pm 0.11	0.24 \pm 0.1	0.85 \pm 0.07
Actin Binding	2.06 \pm 0.07	0.45 \pm 0.09	1.61 \pm 0.01
β-Dimerization	1.54 \pm 0.07	0.34 \pm 0.08	1.209 \pm 0.08
Ankyrin Binding	1.432 \pm 0.9	0.317 \pm 0.1	1.119 \pm 0.09
β-Tetramerization	1.604 \pm 0.08	0.355 \pm 0.1	1.25 \pm 0.1

While previous data from our lab shows that the apparent dissociation constants are in the low micromolar range a label free method shows the values to be in the nanomolar range (1). This has led to the ‘bead-on-a-string’ model of spectrin hemoglobin interaction. In general 1-2 FITC molecules are labelled onto each spectrin molecule. Considering that using FITC only the hemoglobin binding in the general vicinity of the probe is reflected in measurements while the rest of the binding generates no signal, the higher values of K_d can be explained. A label free method does not suffer from this drawback. It is interesting to note that experiments using spectrin fragments corroborate this hypothesis. Due to the smaller size of the fragments as compared to intact spectrin, smaller K_d values are seen. This is pictorially explained in **Figure 4.15**.

Figure 4.15: K_d determination using FITC.

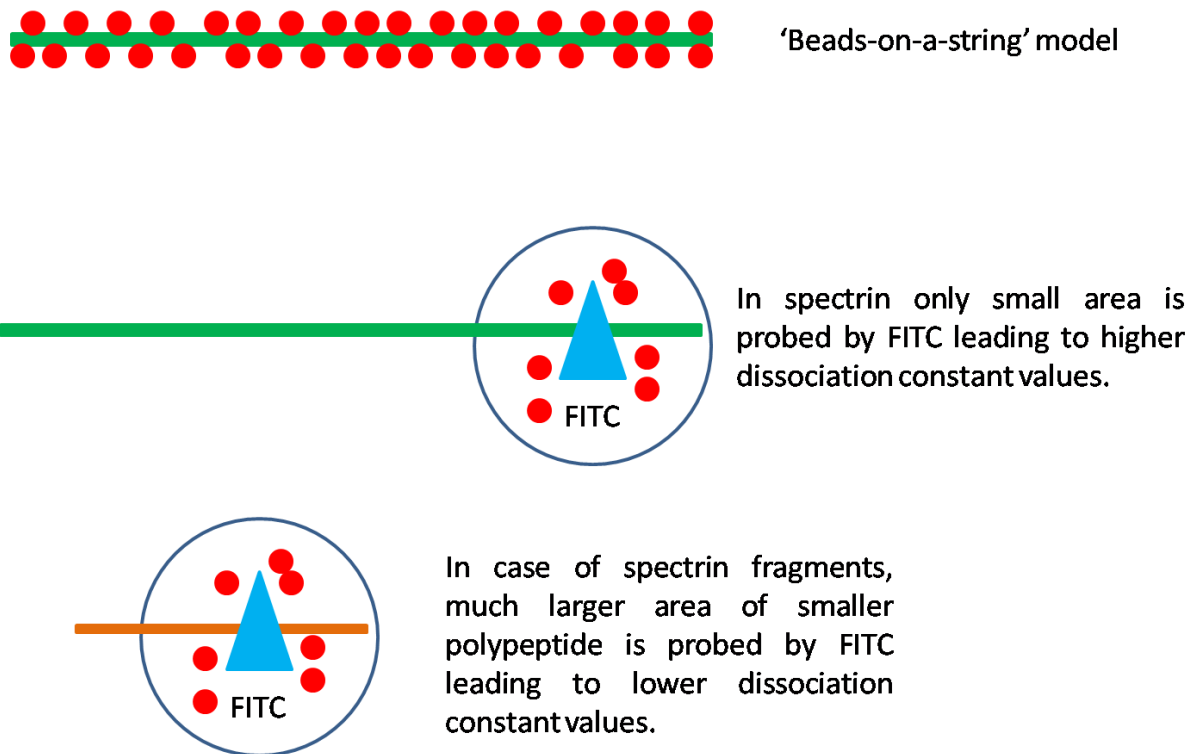


Figure 4.15: Pictorial representation of spectrin labelling by FITC and determination of binding constant of hemoglobin interaction.

1. Mishra, K., Chakrabarti, A., and Das, P. K. (2017) Protein–Protein Interaction Probed by Label-free Second Harmonic Light Scattering: Hemoglobin Adsorption on Spectrin Surface as a Case Study. *The Journal of Physical Chemistry B* **121**, 7797-7802

Chapter 5:

Interactors of spectrin and its biochemical significance

5.1 Introduction

Erythrocytes or red blood cells (RBCs) are the major cellular component of blood and are the primary carriers of oxygen. Hemoglobin the iron containing oxygen transport protein makes up about 90% of the dry weight of RBCs (1). Hemoglobin reversibly binds O₂ at the 6th coordination site of the Fe(II) of its heme prosthetic group (2); however it is well known that auto-oxidation of hemoglobin takes place under *in-vivo* conditions to produce met-hemoglobin [Fe(III)], and peroxides, superoxides and free radicals, collectively known as reactive oxygen species (ROS) are generated as a by-product (3-6). Under normal conditions a certain basal level of hemoglobin oxidation and corresponding level of ROS produced under oxidative stress is always present in RBCs (7). Hemoglobin auto-oxidation also leads to heme degradation and impaired oxygen delivery (8,9).

Under *in-vivo* conditions the RBCs have a well regulated cellular machinery composed of catalases, met-Hb reductases, peroxiredoxins, and glutathione-peroxidases etc. which convert met-Hb to the active form and scavenge ROS (10-13). Since matured, circulating RBCs lack genetic machinery it is important for the cells to preload themselves with anti-oxidant apparatus that should last its lifetime. The most prevalent redox proteins in RBCs include Cu-Zn superoxide dismutase, catalase, peroxiredoxin 2, glutathione peroxidase and met-Hb reductase (14). Together these defence mechanisms keep the usual load of met-Hb less than 1% of total hemoglobin content and effectively fight ROS challenge.

However under certain conditions such as under drug induced stress, hypoxic stress, oxidative stress or by disease states the rate of hemoglobin auto-oxidation and ROS generation is greatly increased (15).

Drugs have been known to increase the rate of hemoglobin auto-oxidation, cause formation of hemichromes and Heinz bodies and generate superoxide and peroxide species. It

is also known that hemoglobin variants that have some structural abnormality are more susceptible to the effects of these drugs (16,17).

The inherited disorders of hemoglobin that cause disease states are of two types, where there is the production of a structurally altered globin chain like in sickle cell disease or where there is a reduced output of one of the two globin genes causing thalasseimas. There is ample evidence that links disease states to increased ROS production, oxidative stress, hemoglobin instability and auto-oxidation.

It is known that hemoglobin dissociation into dimers from tetramers leads to increased ROS generation and oxidative stress (18); this has implications for thalassemic conditions where generation of free globin monomers are expected. Free globin chains are known to generate hemichromes and cause membrane oxidation (19,20).

Abnormal hemoglobin variants are also known to have increased oxidative susceptibility and increased ROS production such as in the case of HbS associated with sickle cell disease (21). This is also the scenario in case of HbE, which is also known to be unstable (22,23). Interestingly it is seen for HbS, a fraction of oxidised hemoglobin remains attached to the RBC membrane where it caused lipid oxidative damage and membrane abnormalities (24).

It is known that under oxidative stress Hb gets attached to the membrane and attached hemoglobin is redox active which in turn causes to membrane damage. Moreover bound hemoglobin is found in complex with other skeletal proteins such as band 4.2, ankyrin and spectrin (25). Similar type of spectrin association as evidenced by decrease in thiol groups of spectrin was noted in model β -thalassemia systems (19).

It is seen that the pathology of hemoglobin diseases is manifested by the membrane attachment of hemeoglobins and free hemes and the resultant lipid peroxidative damage and protein oxidation; for example as seen in sickle cell disease and thalassemia (19,26). These membrane alterations are also visible on storage of blood (27).

Thus it is of prime importance *in-vivo* to mitigate oxidative damage caused by membrane bound heme/hemoglobins. The antioxidant machinery of RBCs is mainly cytosolic and the membrane bound/oxidized hemoglobin and ROS generated thereof is mostly inaccessible to it. Evidence suggests that membrane bound peroxiredoxin-2 is the major neutralizer of such ROS (28).

In this regard it may be hypothesized that in the presence of suitable reducing substrate such as nitrate and ascorbate (29) hemoglobin itself may have a role in neutralizing some of the peroxide generated as it is known to have peroxidase activity and the membrane bound hemoglobins are known to be redox active (25,30). However, this peroxidase activity is what leads to lipid peroxidation in the absence of substrate. Thus some mechanism should also be present to reduce the peroxidase activity of hemoglobin under such conditions.

Keeping in mind the known association of spectrin with membrane localized hemoglobin under oxidative conditions (25) and the known interactions of spectrin-hemoglobins (31,32) we have investigated the role of spectrin in the peroxidase and catalase activity of heme proteins and free heme analogue, hemin.

Spectrin is the major component of the membrane skeleton in RBCs, and it has been shown that spectrin interacts with heme proteins, heme, hemoglobin variants, and globin subunits and has chaperone activity (32-37). While the interactions of spectrin with heme, hemoglobin variants and globin chains have been previously characterized, not much data exists on the biochemical implications of such interactions. Since spectrin is found co-

localized with membrane bound hemoglobin, an important implication of spectrin-hemoglobin interaction would be in the modulation of the peroxidase activity of hemoglobin. Moreover it is known that stress conditions lead to heme loss from hemoglobin which in turn may be accepted by spectrin and may then modulate the enzyme activity of the heme moiety (38). Other heme proteins such as HRP are also known to associate with spectrin and it is also important to figure out if such associations have an effect on their enzyme activity (33).

In the present work we have determined the effect of spectrin interaction on the peroxidase activity of HbA, HbE and HbS as well as their isolated subunits. We have also checked the modulation of catalase activity on spectrin interaction for RBC resident heme protein catalase. Also we have studied modulation of peroxidase activity of non RBC resident cytochrome-c. Moreover to gain added conformational insight we have performed Raman spectroscopy for spectrin bound heme proteins and hemin. Our results show that in general, interaction with spectrin causes an increase in the enzyme activities of all the heme proteins. Raman spectroscopy shows that association to spectrin causes detectable structural change in the heme moiety of the spectrin bound heme proteins.

4.2 Materials and Methods

ABTS, catalase from horse muscle, cytochrome-c from bovine heart, MgCl₂, PMSF, EDTA, p-hydroxymercuribenzoic acid, DTT, thiobarbituric acid(TBA), trichloro-acetic acid (TCA), sodium hydrogen phosphate, hemin chloride, NaOH, acetic acid, Tris, Sephadex G-100, Sepharose CL-4B, DEAE cellulose and CM cellulose were purchased from Sigma. All water used for experiments was purified via a Millipore system.

Stock solutions of cytochrome-c and catalase were made in 100mM phosphate buffer, pH 6.8 and 50mM Tris-HCl, pH 8.0 respectively. Hemin was prepared in 0.01N NaOH. Concentrations for all three were determined spectrophotometrically using molar absorbances

of 106000/M/cm (409nm), 324000/M/cm (405nm) and 58000/M/cm (385 nm) respectively (34,39,40).

5.2.1 Fluorescence binding study of spectrin with heme proteins

The interaction of spectrin with different heme proteins, namely, hemoglobin variants A, E and S, catalase, cytochrome-c and α and β globin subunits from each of the hemoglobin variants were quantified in terms of the apparent dissociation constant (K_d).

Spectrin was covalently labelled with FITC in sodium carbonate-bicarbonate buffer of pH 9.0. 2 mg spectrin dimer was incubated for an hour at 4° C with 50 fold molar excess of FITC, taken in a small volume of N, N-dimethylformamide. The FITC-labelled spectrin (F-spectrin) was separated and purified from the reaction mixture by gel filtration on a Sephadex G-50 column using 10mM Tris-HCl, 20mM KCl, pH 8. The concentration of F-spectrin was determined using Bradford method and that of fluorescein was determined spectrophotometrically from the absorbance at 495 nm using molar extinction coefficient of 76,000. The labelling ratio of fluorescein to spectrin in F-spectrin was determined to be around 2 to 3 fluorescein per spectrin dimer (37,41).

Steady state fluorescence measurements were performed using a Cary Varian fluorescence spectrometer using 1cm path length quartz cuvettes with 5-nm slits for both excitation and emission channels. F-spectrin in the range of 20-50 nM was excited at 495 nm and emission was monitored from 510-600 nm. Sequential additions of different heme proteins from concentrated stock solutions were done and resultant decrease in fluorescence intensity of F-spectrin was monitored at 520 nm.

The extent of fluorescence quenching of F-spectrin as a function of increasing concentrations of different heme protein samples were analyzed using the following

equations (36) to give the apparent dissociation constant (K_d) values of spectrin-heme protein interactions.

$$K_d = \{ [C_0 - (\Delta F / \Delta F_{\max}) \cdot C_0] \cdot [C_L - \Delta F / \Delta F_{\max}] \cdot C_0 \} / \{ (\Delta F / \Delta F_{\max}) \cdot C_0 \} \dots (1)$$

$$C_0 \cdot (\Delta F / \Delta F_{\max})^2 - [(C_0 + C_L + K_d) \cdot (\Delta F / \Delta F_{\max})] + C_L = 0 \dots (2)$$

In equations (1) and (2), ΔF is the change in fluorescence emission intensity at 520 nm for each point on the titration curve and ΔF_{\max} denotes the same when a given heme protein is completely bound to F-spectrin, C_L is the concentration of the ligand (given heme protein) at any given point in the titration curve, and C_0 is the initial concentration of F-spectrin.

The y-axis intercept of the plot of $1/\Delta F$ vs. $1/C_L$ gives the numerical value of $1/\Delta F_{\max}$. In turn the calculated ΔF_{\max} values can be put into equation 1 and the K_d values for each point on the titration curve can be generated, from which the mean K_d value is determined.

All experimental points for binding isotherm were fitted by least-square analysis using the Microcal Origin software package (Version 8.0) from Microcal Software Inc., Northampton, MA. The, K_d values are represented as mean \pm standard error of the mean (SEM) of at least 5 independent experiments.

5.2.2 Peroxidase and catalase activity measurement of heme proteins

The peroxidase activity of, hemoglobin variants, cytochrome-c and globin subunits from each of the hemoglobin variants were determined using the ABTS assay (33,42,43).

The liner range of the peroxidase activity for all the proteins and hemin were determined from a plot of the initial velocity (v_0) of the enzyme activity against the

concentration of the enzyme. In case of the hemoglobin variants, isolated globin chains and cytochrome-c the enzyme activities were measured in the range of 5- 30 nM, in case of catalase it was measured from 0.5-2 nM and in case of hemin it was measured at 50- 200 nM.

Peroxidase activity was measured in 50mM sodium-phosphate-citrate buffer pH 5.0 using 20 mM ABTS and 10 mM H₂O₂ in case of hemoglobin variants, isolated globin chains and cytochrome-c; in case of hemin 4 mM H₂O₂ was used. These concentrations were chosen such that under experimental conditions reproducible measurements could be made with minimum noise. The evolution of coloured product was followed at 405 nm with time using a Cary Eclipse spectrophotometer and the initial linear region was considered for v_0 calculations. The initial velocity of the enzyme reaction was expressed as the rate of disappearance of peroxide with time considering a stoichiometry of 2:1 ABTS coloured product formed to peroxide substrate consumed (43,44).

Similarly the linear range of enzyme activity of catalase was determined from a plot of v_0 versus protein concentration in the range of 0.5- 2 nM catalase (68). Enzyme activity was assayed in 50mM Tris-HCl pH 8.0 buffer using 4 mM H₂O₂. The rate of disappearance of peroxide with time was followed at 240nm with respect to a standard curve of H₂O₂ absorbance (240nm) vs. concentration determined using the permanganate titration method (45). Initial velocity rates were expressed as rate of peroxide consumption with time.

The Michaelis-Menten constants V_{max} and K_m were also determined for each individual heme protein and heme.

5.2.3 Effect of spectrin on enzyme activity of heme proteins

The effect of spectrin on the enzyme activities of the different heme proteins and hemin was determined by measuring the effect spectrin on the initial velocity, K_m and V_{max} values of the enzyme reactions.

To determine the specificity of spectrin induced enzyme activity modulation, the activities of the different heme proteins and hemin were also measured in the presence of BSA as a negative control.

The native peroxidase and catalase activity of spectrin was checked to determine its contribution to measured enzyme activity.

The v_0 , K_m and V_{max} values of enzyme reactions for each of the different heme proteins, hemin and catalase were determined in presence of increasing concentrations of spectrin in the same way as above. In case of hemin the changes were also measured in the presence of 1mM each of the amino acids, histidine, tyrosine, tryptophan and methionine.

To differentiate whether the differences in enzyme parameters, came from the protection of heme proteins and hemin from oxidative damage, or from a modulation of their enzymatic activity, the heme proteins and free heme analogue, hemin, were incubated with a given amount of spectrin in the presence of 4 mM H_2O_2 in the absence of ABTS and the residual enzyme activity was measured with respect to time by addition of ABTS.

Moreover cross-linking of heme proteins to spectrin was checked under these experimental conditions according to previously published protocol (35). Different heme proteins, 0.5 μM - 1 μM each were incubated with 1 μM spectrin in presence of 4 mM peroxide at 37°C for 15 minutes and the resultant mixture was run on a 4% SDS gel and

stained with Coomassie blue and the band b was used for determining relative cross-linking amounts.

5.2.4 Assay of lipid peroxidation by TBA method

Phospholipid vesicles of 100% DOPE composition were prepared using previously elaborated protocol (46). Different combinations of 10 mM total phospholipid concentration of these prepared SUVs were taken and incubated with 10 mM hydrogen peroxide in the presence and absence of 10 nM heme proteins and 40 nM spectrin in combination with 20 mM ABTS. The extent of lipid peroxidation was measured using the TBA method according to previously published protocol (47) using the TBA assay. Briefly, 0.1 ml of sample containing 0.2 μ M total lipid was incubated with 2 ml of the TBA reagent (15% w/v TCA, 0.375 w/v TBA, 0.25 N HCl) in boiling water for 15 minutes and cooled to room temperature. Precipitate was dissolved by addition of 0.2 ml of 1 N NaOH. Lipid peroxidation product malondialdehyde was assayed against a blank at 535 nm. The malondialdehyde concentration was calculated using extinction coefficient of 156000/M/cm.

5.2.5 Raman spectra of heme proteins and hemin in presence and absence of spectrin

Raman spectra were acquired in a Horiba LabRAM HR instrument using a 633nm laser (He-Ne laser, model 25-LHR-151-230, Melles-Griot, U.S.A.) as the excitation source. An epi-illuminated microscope (Nikon 50i, Nikon, Japan) was used both to excite the sample and collect Raman-scattered light in a backscattering geometry. Typically a 60x infinity corrected objective (Nikon Plan Apo, Japan, NA 0.9) was used and 60 second accumulation time was used for a minimum of 2 accumulations. Raman spectra of 300 μ M each of the hemoglobin variants and cytochrome-c were acquired in presence and absence of 3 μ M

spectrin in 1mM Tris-HCl buffer pH 8.0. Similarly the Raman spectra of hemin in powder form, and in solution in presence of spectrin was acquired.

5.3 Results and Discussion

5.3.1 Determination of binding dissociation constants using fluorescein-conjugated spectrin

The heme proteins were found to interact with spectrin with apparent dissociation constants in the low micromolar range. Catalase exhibited auto-fluorescence in the experimentally monitored range and thus dissociation constants in its case could not be determined. It was seen that in general spectrin showed higher affinity for those hemoglobin variants that are known to be more structurally unstable and thus have more perturbed conformations than normal HbA (32). This fact was further strengthened by the observation that spectrin had about the same affinity for the isolated α -globin chains from all the hemoglobin variants, which are known to have identical sequence. On the other hand the β -globin subunits, which carry the actual mutations, from the variant hemoglobins, showed higher affinity for spectrin binding than those from HbA. Spectrin was also found to interact with cytochrome-c with a much higher affinity as compared to hemoglobin interaction. Representative fluorescence quenching curve, double reciprocal plot and binding isotherm of spectrin interaction with cytochrome-c is given in **Figure 5.1**. All binding data is summarized in **Table 5.1**.

Figure 5.1: Spectrin binding to cytochrome-c.

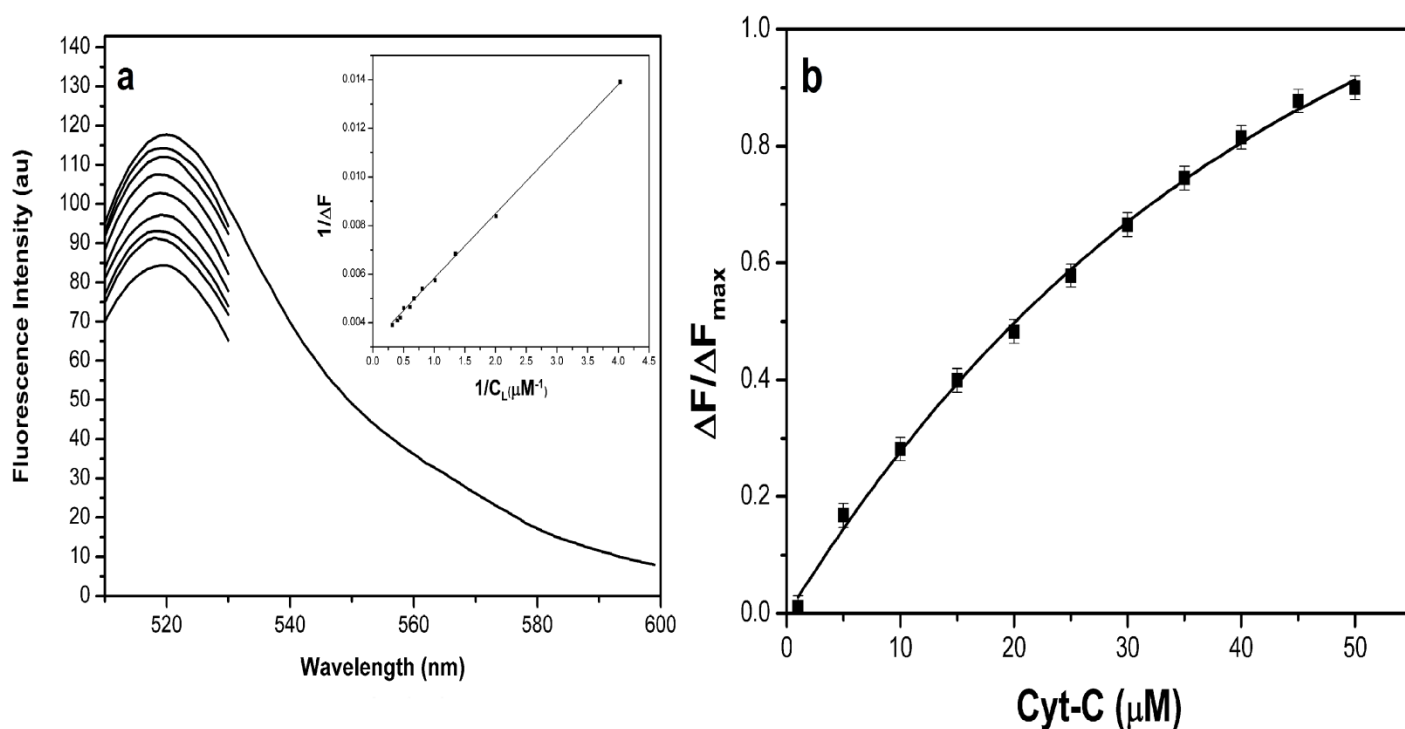


Figure 5. 1: Panel 'a' shows the representative quenching curve of FITC labelled spectrin with cytochrome-c. F-spectrin in the range of 20-50 nM was excited at 495 nm and emission was monitored from 510-600 nm. Sequential addition of cytochrome-c from concentrated stock solution was done and resultant decrease in fluorescence intensity of F-spectrin was monitored at 520 nm. Inset shows the double reciprocal plot of the same from which ΔF_{max} is calculated. Panel 'b' shows the binding isotherm of the same from which K_d value is determined.

Table 5.1: K_d values.

Protein	K_d (μM)
HbA	27.5 ± 1.5
HbA - α	17.5 ± 1.6

HbA - β	25.1 \pm 1.3
HbE	6.1 \pm 1.7
HbE - α	16.3 \pm 1.6
HbE - β	10.2 \pm 1.3
HbS	21.5 \pm 1.1
HbS - α	16.8 \pm 0.9
HbS - β	20.1 \pm 1.4
Cytochrome-c	0.87 \pm 0.5

Table 5.1: The K_d values for the association of different heme proteins and spectrin is tabulated. Error bars represent S.D. of at least three independent experiments.

5.3.2 Determination of liner range of enzyme activity and MM constants

The linear range and the K_m and V_{max} values of the enzyme activities of the heme proteins and hemin were determined and working concentrations were chosen accordingly. Representative plots of the linear range and Michaelis-Menten plots of HbA, HbE and HbS and their globin subunits are given in **Figure 5.2**. And those of catalase, cytochrome-c and hemin are given in **Figure 5.3**. The MM plot of catalase (may not follow MM kinetics) could not be determined due to excessive bubbling under experimental conditions and that of hemin could not be determined due to degradation of hemin at higher peroxide concentrations. The values of the MM constants of the heme proteins and heme is tabulated in **Table 5.2**.

Figure 5.2: Linear range and MM curve of hemoglobins.

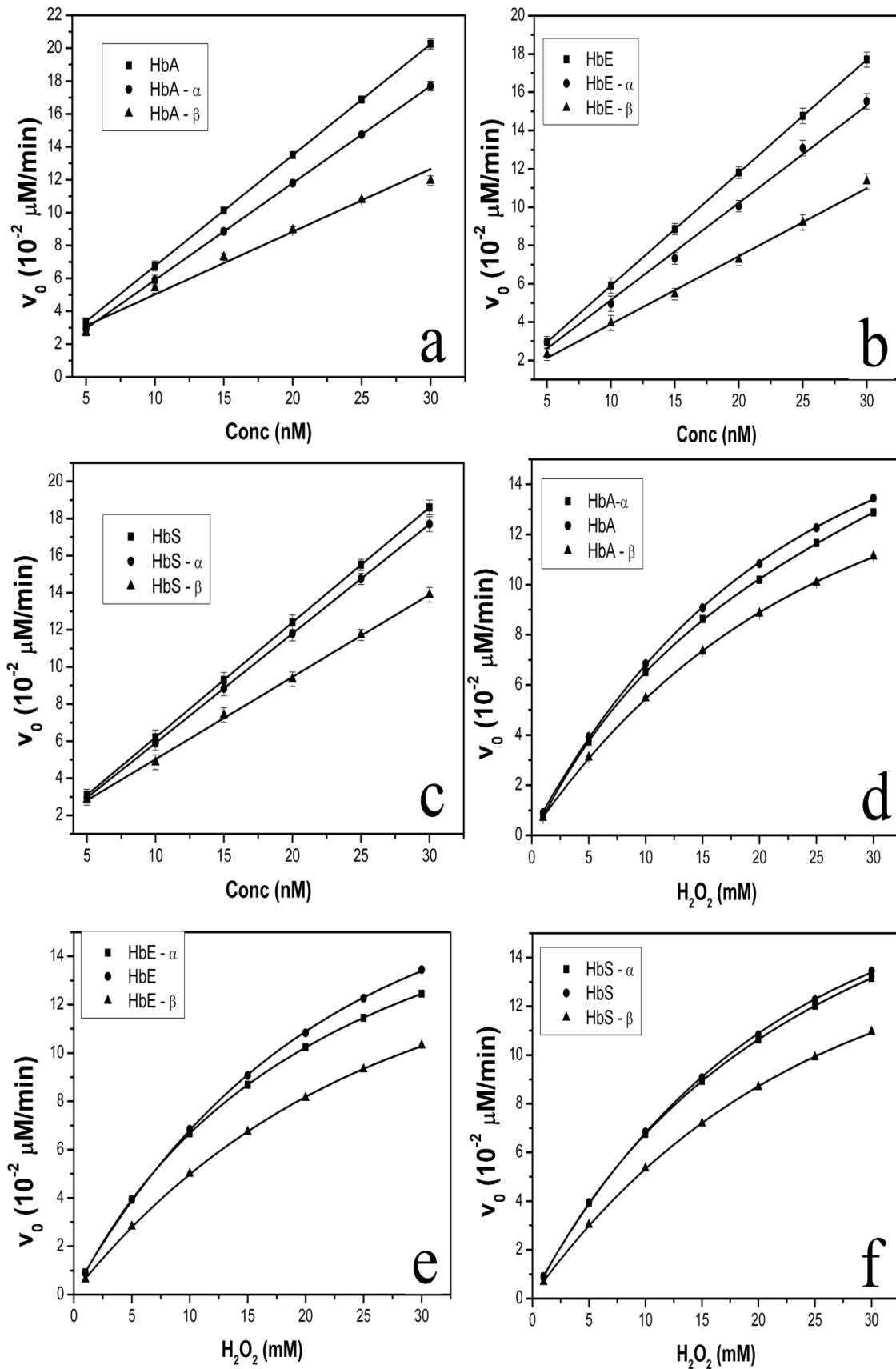


Figure 5.2: *The linear range of hemoglobin variants and their isolated subunits as well as their Michaelis-Menten curves are shown. Peroxidase activity was measured in 50mM sodium-phosphate-citrate buffer pH 5.0 using 20 mM ABTS and 10 mM H₂O₂. The reaction was followed by monitoring the generation of coloured oxidation product of ABTS at 405 nm. The liner range of the peroxidase activity for all hemoglobin variants were determined from a plot of the initial velocity (v₀) of the enzyme activity against the concentration of the enzyme. Panel 'a' shows HbA and its subunits, panel 'b' shows HbE and its subunits and panel 'c' shows HbS and its subunits. Using 20 mM ABTS and 10 nM of each of the respective hemoglobin variants and isolated globin subunits, the MM parameters were determined by plotting the initial velocity against peroxide concentration. Panel 'd' shows HbA and its subunits, panel 'e' shows HbE and its subunits and panel 'f' shows HbS and its subunits.*

Figure 5.3: Linear range of cytochrome-c, catalase, hemin; MM curve of cytochrome-c.

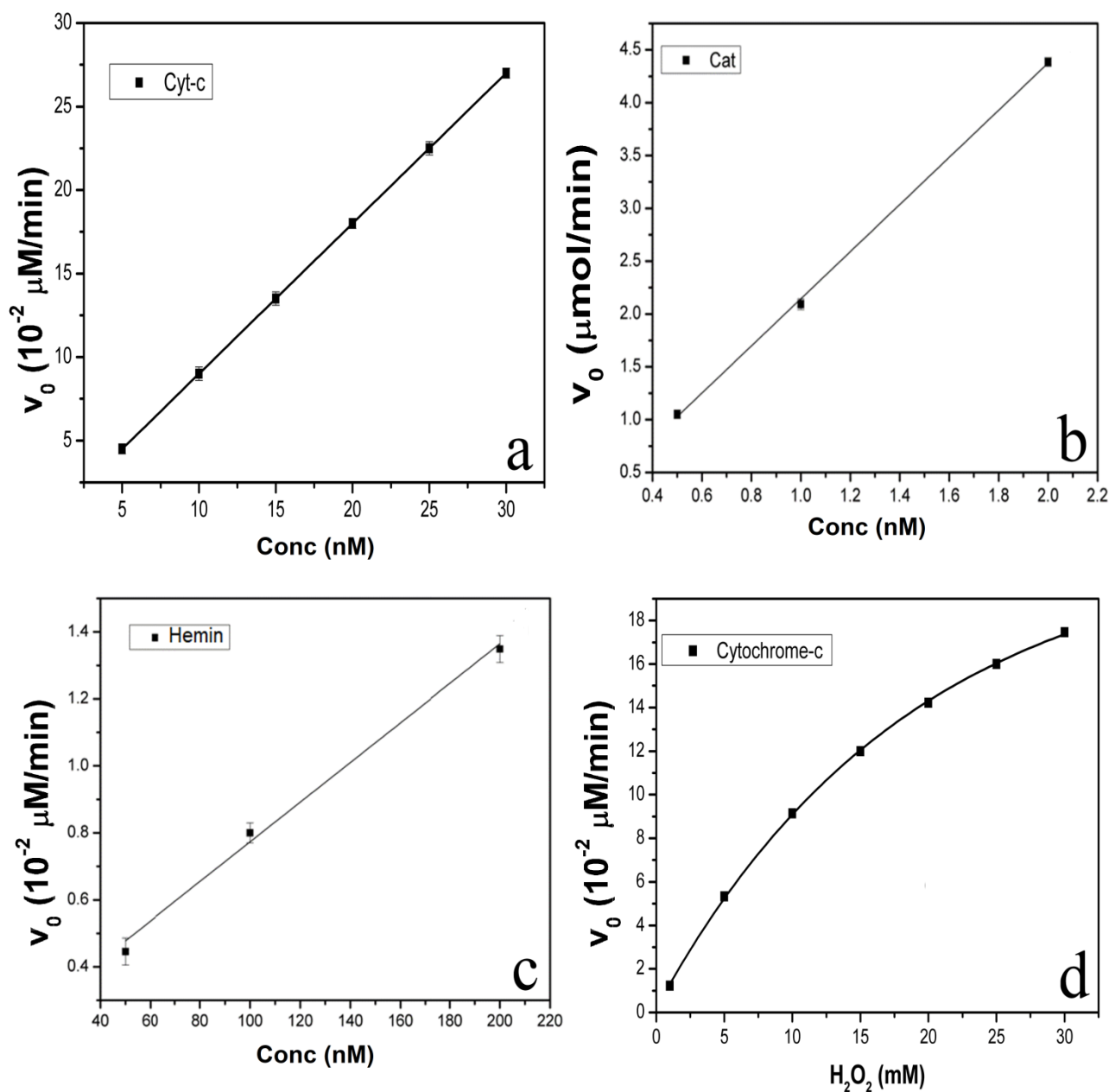


Figure 5.3: The linear range of cytochrome-c, catalase and hemin are shown. The linear range was determined from a plot of the initial velocity (v_0) of the enzyme activity against the concentration of the enzyme. In case of catalase enzyme activity was assayed in 50mM Tris-HCl pH 8.0 buffer using 4 mM H_2O_2 and reaction was followed by monitoring the disappearance of peroxide at 240 nm. In case of cytochrome-c and hemin, 50mM sodium-

phosphate-citrate buffer pH 5.0 and 20 mM ABTS was used with 10 and 4 mM peroxide respectively. The reaction was followed by monitoring the generation of coloured oxidation product of ABTS at 405 nm. Panel 'a' shows linear range of cytochrome-c, panel 'b' shows that of catalase and panel 'c' shows that of hemin. Using 20 mM ABTS and 10 nM cytochrome-c the MM plot was determined and is shown in panel 'd'.

Table 5.2: MM parameters.

Protein	K_m (mM)	V_{max} (10^{-2} $\mu\text{mol}/\text{min}$)
HbA	30 \pm 1 (25 \pm 1)	27 \pm 0.7 (33 \pm 0.5)
HbA - α	28.2 \pm 1 (22 \pm 0.8)	26 \pm 0.9 (32 \pm 0.6)
HbA - β	32 \pm 0.9 (27 \pm 1)	23 \pm 0.6 (28 \pm 0.4)
HbE	23 \pm 0.9 (17 \pm 0.8)	22 \pm 0.7 (29 \pm 0.8)
HbE - α	28.4 \pm 1 (22 \pm 0.9)	26 \pm 0.9 (32 \pm 0.5)
HbE- β	33 \pm 0.7 (29 \pm 1)	23 \pm 0.5 (29 \pm 0.7)
HbS	27 \pm 1 (22 \pm 0.8)	25 \pm 0.7 (31 \pm 0.7)
HbS - α	28.5 \pm 1 (23 \pm 1)	27 \pm 0.9 (32 \pm 0.9)
HbS- β	34 \pm 0.8 (28 \pm 0.9)	22 \pm 0.7 (29 \pm 0.4)
Cytochrome-c	25 \pm 1 (20 \pm 1)	32 \pm 0.5 (37 \pm 0.9)

Table 2: The K_m and V_{max} values of the hemoglobin variants and their isolated subunits and cytochrome-c are listed. Values in parenthesis are those in presence of spectrin. The error bars represent the S.D. of at least three independent experiments.

5.3.3 Effect of spectrin on enzyme activity

Spectrin preparation was found to not possess any catalase or peroxidase activity of its own. Addition of BSA did not alter the enzyme activities of the heme proteins or hemin (data not shown), showing that the modulation of enzyme activities seen on spectrin addition was specific to spectrin. It is seen that in general spectrin addition increased the enzymatic activity of all heme proteins under consideration and hemin in a dose dependent manner. The increase in enzyme activity in the presence of spectrin for hemoglobin variants and isolated globin chains is shown in **Figure 5.4**. The effect of spectrin on the activities of catalase, cytochrome-c, and hemin is given in **Figure 5.5**.

In case of hemin the enzyme activity was monitored in presence of 1mM each of the amino acids His, Tyr, Trp and Met. It is known that in heme proteins the 5th co-ordination site of heme is taken up by amino acids such as His in hemoglobin and Met in cytochrome-c (48-50). This in turn effects the structure of the heme moiety and thereby its activity. Thus the enzyme activity of hemin was checked in the presence of coordinating amino acids to determine if the increase in enzyme activity induced by spectrin was due to co-ordination of amino acids to hemin. It was seen that the presence of the amino acids did not have any effect on the peroxidase activity of hemin (data not shown). The values of the MM constants of the heme proteins and heme in presence of spectrin is tabulated in **Table 5.2**.

Figure 5.4: Effect of spectrin on enzyme activity of hemoglobins.

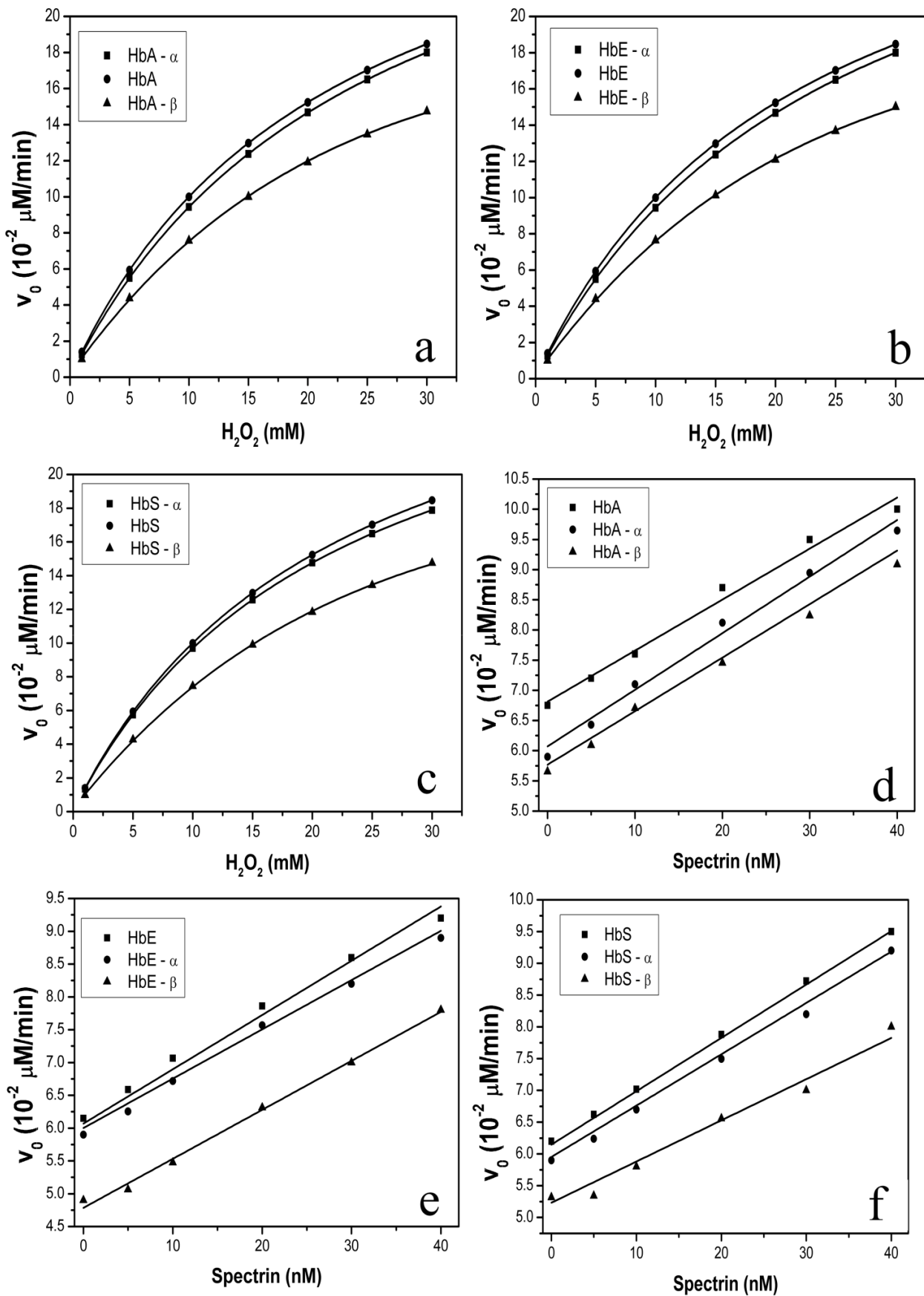


Figure 5.4: Using 10 nM of each hemoglobin variant and isolated globin subunit in presence of 40 nM of spectrin the MM curves of each were determined as above. Panel 'a' shows HbA and its subunits, panel 'b' shows HbE and its subunits and panel 'c' shows HbS and its subunits. The effect of increasing concentrations of spectrin on enzyme activity of hemoglobin was monitored using 10 nM of each hemoglobin variant and their isolated globin subunits. The initial velocity was plotted against spectrin concentration. Panel 'd' shows HbA and its subunits, panel 'e' shows HbE and its subunits and panel 'f' shows HbS and its subunits.

Figure 5.5: Effect of spectrin on enzyme activity of catalase, cytochrome-c & hemin.

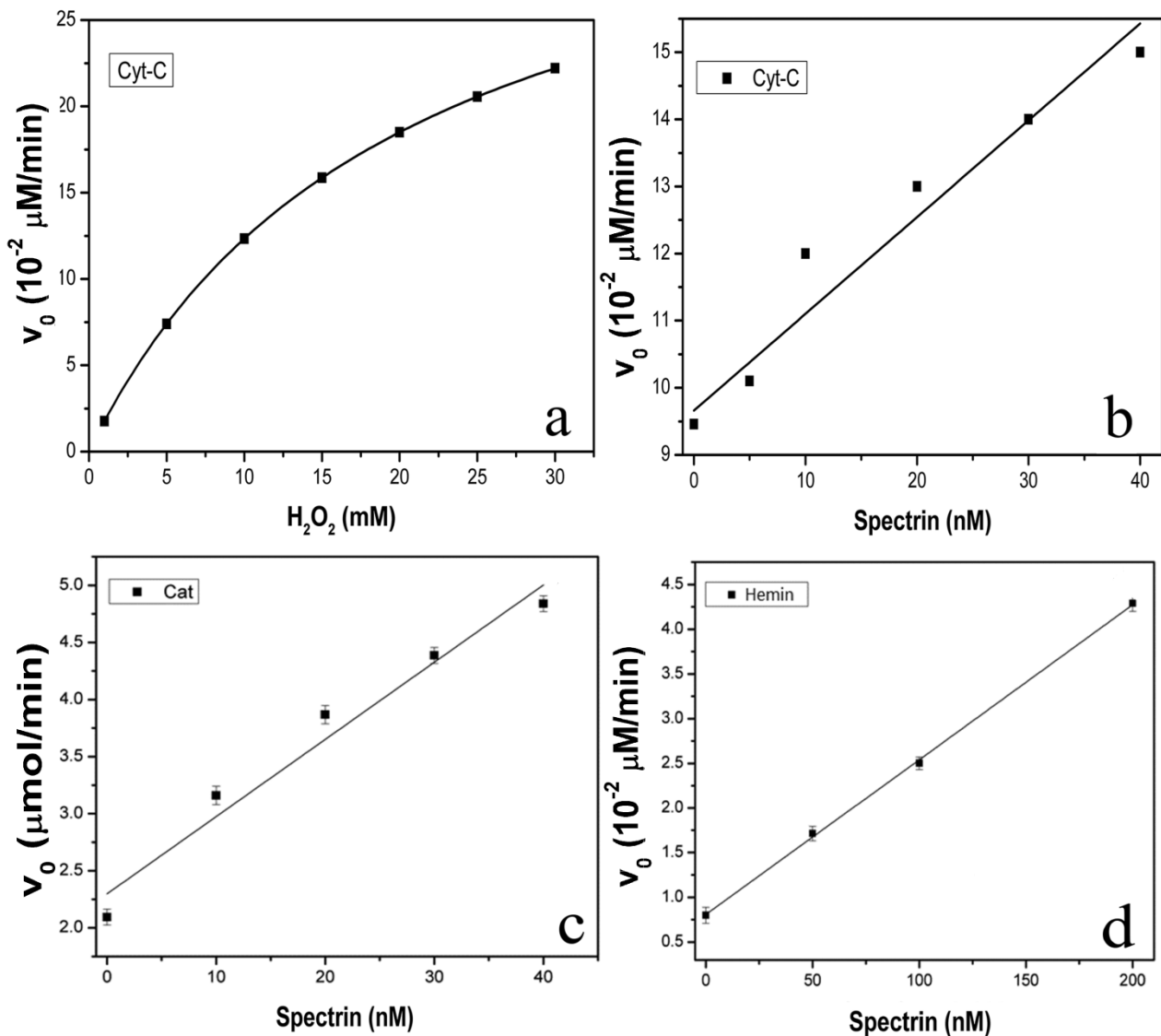


Figure 5.5: Panel 'a' shows the MM curve of 10 nM cytochrome-c in presence of 40 nM spectrin. Panel 'b' shows the initial velocity of 10 nM cytochrome-c in presence of increasing amounts of spectrin. Panel 'c' shows the same for 1 nM catalase and panel 'd' for 100 nM hemin.

It was seen that spectrin offered no protection against loss of enzyme activity in case of the heme proteins. In fact addition of spectrin caused a more rapid loss of activity of heme proteins. However in case of hemin addition of spectrin seemed to delay denaturation by hydrogen peroxide as evidenced by the greater residual activity with time in presence of spectrin versus its absence. It was also seen that under the experimental conditions spectrin formed cross-linked adducts with all the heme proteins except catalase. The extent of cross-linking was analyzed according to the relative densities of band b and it was seen that HbE formed the highest amount of cross-linking followed by HbS and HbA and cytochrome-c. Catalase did not form cross-linked products under experimental conditions.

We have previously shown the oxidative cross-linking of hemoglobin variants with spectrin (35,51). Here we show representative graphs of hydrogen peroxide mediated inactivation of HbA and hemin in presence of spectrin with respect to time, and the cross-linked aggregates of cytochrome-c, HbA, HbE and HbS in **Figure 5.6**.

Figure 5.6: Peroxide mediated deactivation.

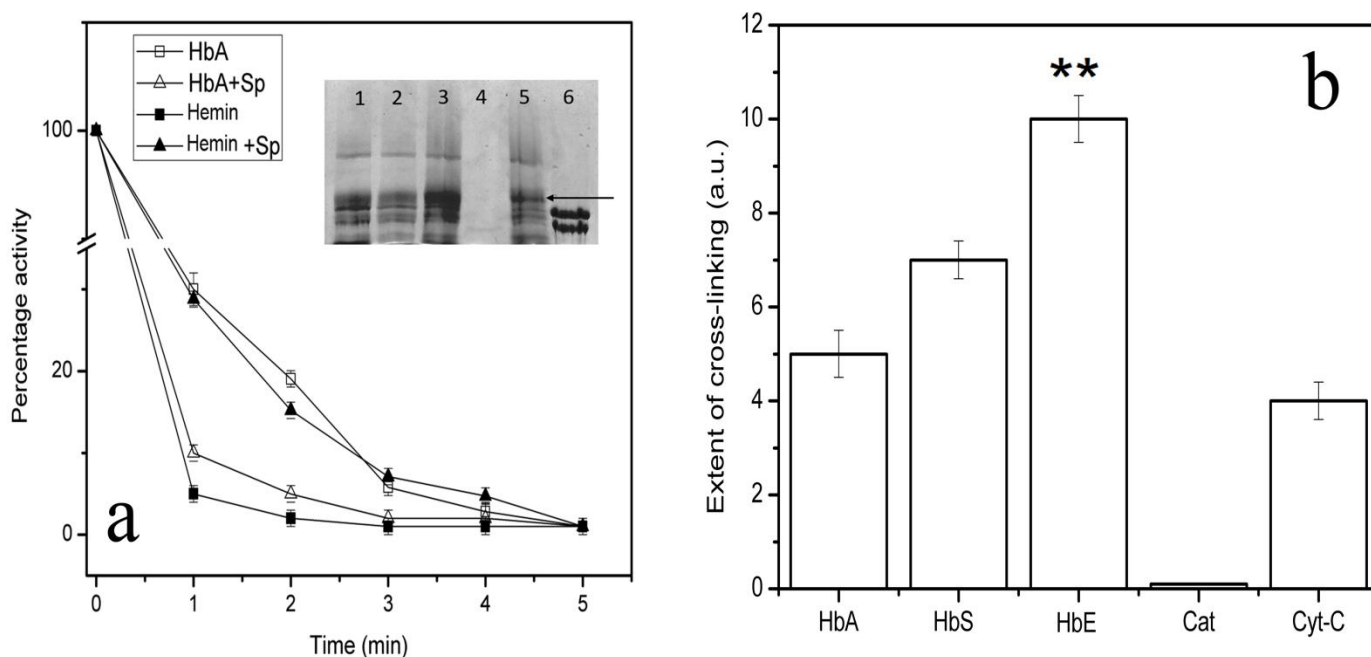


Figure 5.6: Panel 'a' shows the time dependent denaturation of 10 nM HbA and 100 nM hemin in 10 mM peroxide in presence and absence of 40 nM spectrin (Sp). HbA and hemin in presence and absence of spectrin were incubated in peroxide for different times before ABTS was added and initial rate measured. Residual activity was expressed as percentage where native enzyme is considered 100%. Inset shows 4% SDS gel of cross-linked aggregates of 1 μ M each of heme proteins incubated with 1 μ M spectrin in 4 mM peroxide at 37°C for 15 minutes. Lane 1 of inset shows HbS, lane 2 shows HbA, lane 3 shows HbE, lane 4 shows catalase, lane 5 shows cytochrome-c and lane 6 shows purified spectrin. The arrow represents the location of band b. Panel 'b' shows densitometric analysis of band b using ImageJ software. Error bars represent the S.D. of five independent experiments. Spectrin forms significantly greater amount of aggregates with HbE than other hemoglobin variants as tested by t-test with p values < 0.05 .

5.3.4 Assay of lipid peroxidation

Extent of lipid peroxidation was assayed using the TBA method and quantifying the level of malondialdehyde (MDA) produced. It was seen that addition of heme proteins caused a significant increase in the production of MDA over blanks containing only SUVs and peroxide. Addition of ABTS with heme proteins reduced production of MDA and presence of spectrin along with it reduced it the most. Representative graphs for the TBA assay for HbA are given in **Figure 5.7**.

Figure 5.7: Lipid peroxidation.

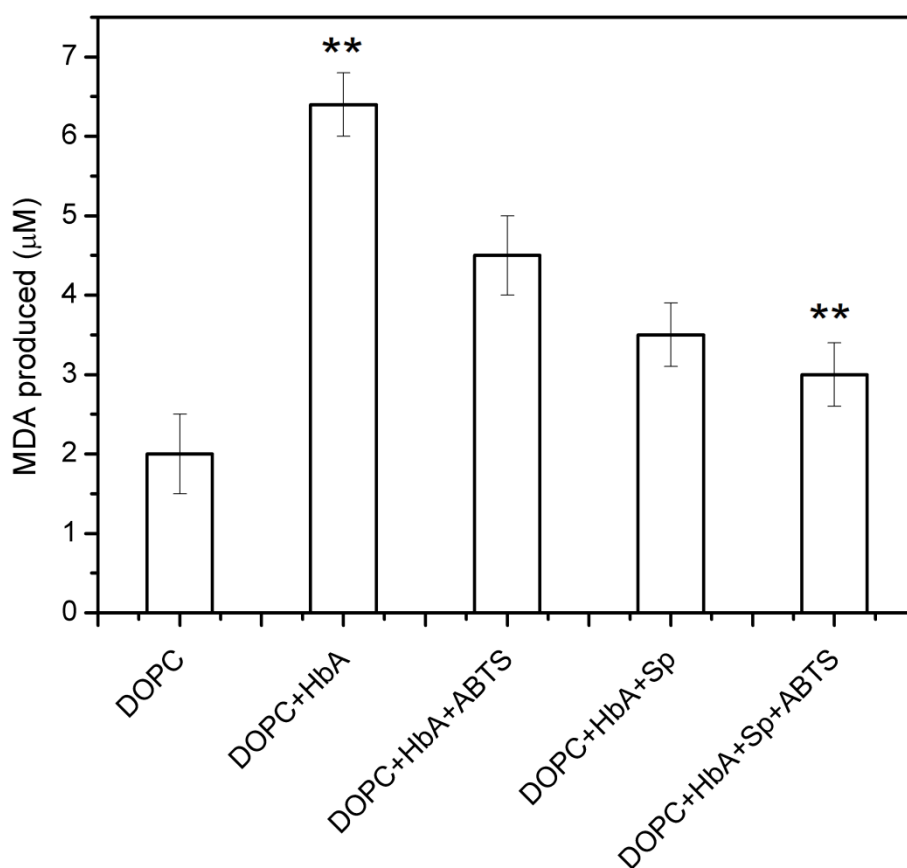


Figure 5.7: 10 mM total phospholipid, of 100% DOPC SUVs were incubated for 15 minutes in 10 mM peroxide with or without 10 nM HbA in presence and absence of 40 nM spectrin (Sp) with or without additional 20 mM ABTS. From these mixtures, 0.2 µM total lipid was

incubated with 2 ml of the TBA reagent in boiling water for 15 minutes and lipid peroxidation product malondialdehyde (MDA) was assayed at 535 nm. Error bars represent the S.D. of five independent experiments. Spectrin significantly reduced MDA formation as tested by t-test with p values < 0.05.

5.3.5 Raman spectra of heme proteins and hemin

The Raman spectra of hemoglobin variants was predominated by the spectra of their prosthetic heme group. Catalase did not show meaningful Raman spectra due to presence of auto-fluorescence. It was found that spectrin binding lead to a change in the spectra of the hemoglobin variants and cytochrome-c in a remarkably similar manner. It was seen that the peaks at positions 977 and 1004 cm^{-1} in all cases in absence of spectrin were overshadowed by a much more intense peak at 981 cm^{-1} in the presence of spectrin. In case of hemin though there was no change seen in the position of the Raman peaks. However, the intensities of the peaks at 1065, 1371 and 1626 cm^{-1} were decreased with respect to peaks besides them in presence of spectrin than in their absence. Representative Raman spectras are shown in **Figure 5.8 & 5.9.**

Figure 5.8: Raman spectra of hemoglobins and cytochrome-c.

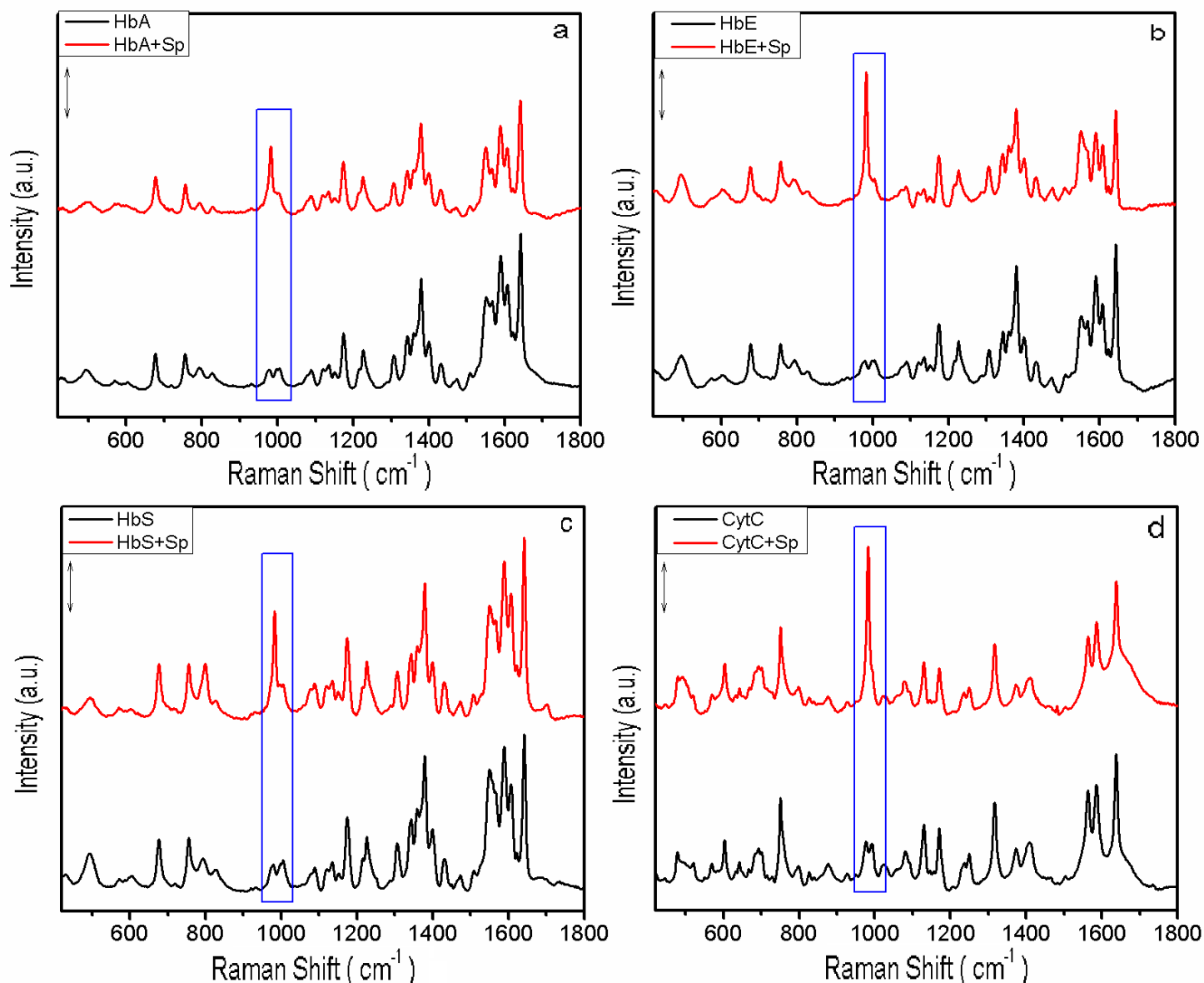


Figure 5.8: Panel 'a' shows the representative Raman spectra of $300\mu\text{M}$ HbA in the presence and absence of $3\mu\text{M}$ spectrin (Sp), panel 'b' shows the same for HbE, panel 'c' for HbS and panel 'd' for cytochrome c (CytC). The bars represent 2000 counts. The peaks where the major change is seen on spectrin binding are boxed.

Figure 5.9: Raman spectra of hemin.

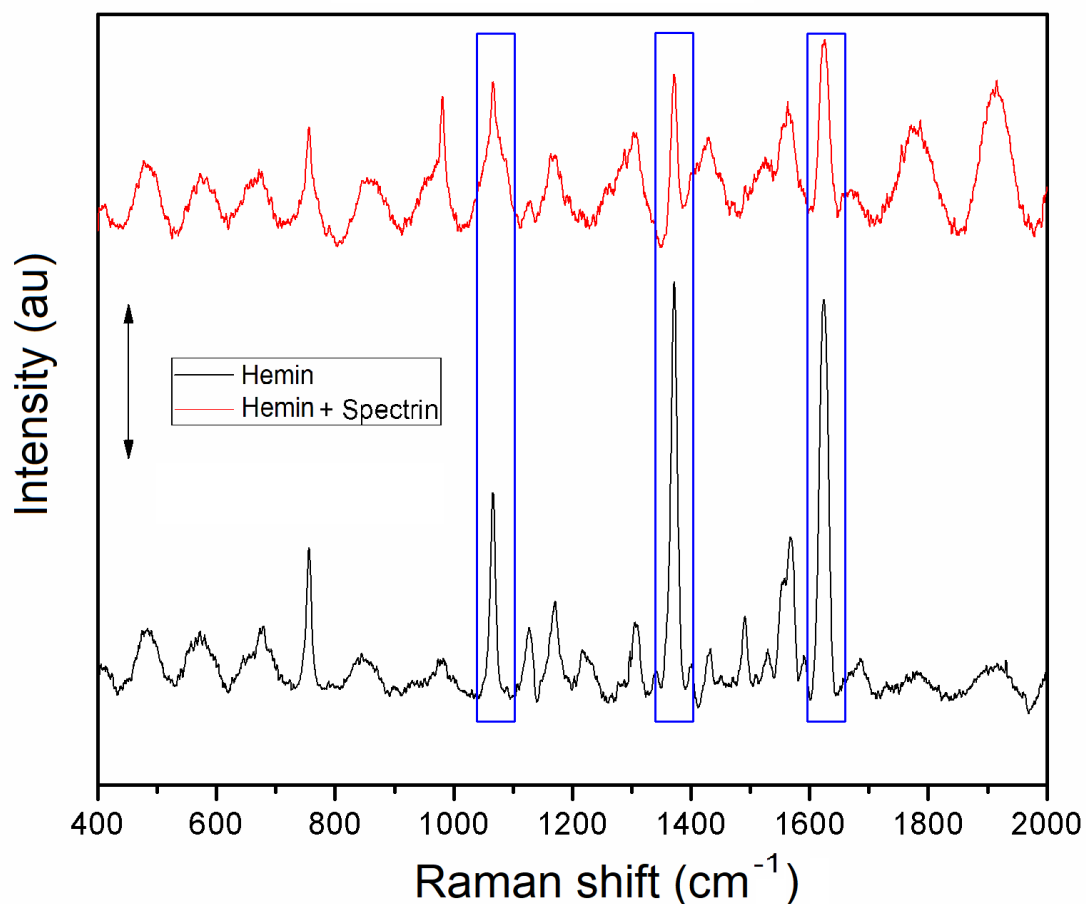


Figure 5.9: The representative Raman spectra of hemin in presence and absence of spectrin is shown. The bar represents 2000 counts. Peaks with the maximum change are boxed.

5.3.6 Discussions

Our data shows that spectrin interacts with the highest affinity to the most unstable/unstructured hemoglobin variant, HbE. This has implications in disease states where the hemoglobin variant associated with it leads to the disease phenotype. The highest affinity is seen for HbE which is also the most unstable among the three variants investigated (23). Previously we have shown the interaction between spectrin and HbA and HbE. This is the

first report for the interaction of spectrin and HbS as well as a comparative study of spectrin with three different hemoglobin variants and their isolated subunits.

It is known that spectrin may act as a chaperone for hemoglobin and heme proteins in general (31), thus an increased affinity of binding would mean more protection of the hemoglobin variant from unfolding and aggregation. It is known that spectrin is a chaperone for α and β globins and it also displays chaperone like property for denatured heme protein HRP (31,33)(31,33).

It is interesting to note that spectrin also interacts with cytochrome-c, a protein which is not found in the RBC but is mitochondria resident, moreover it shows the highest affinity for interaction with spectrin. This points to the fact that spectrin may interact with heme proteins in general; previous reports from our lab have also shown spectrin interaction with a non-RBC heme protein, HRP (33).

Thus far the biological implications of spectrin interacting with heme proteins other than its chaperone function were not known. It was known that spectrin acts like a chaperone for hemoglobin and isolated globin subunits and also for other heme proteins (31). It is interesting to note that spectrin shares structural similarities with a known erythrocyte resident α -globin chaperone, α -hemoglobin stabilizing protein (AHSP); both these proteins share a common three helix bundle motif (52-54). Structural similarity to AHSP taken together with the fact that spectrin shows stronger affinity for structurally perturbed hemoglobin variants and unfolded heme proteins further highlights the chaperone function of spectrin (31,33).

Here we show biochemical significance for spectrin heme protein interaction, namely the enhancement of peroxidase and catalase activity of heme proteins on spectrin binding. It is interesting to note that spectrin is able to cause enzyme activity enhancement of the heme

proteins when both are in the nM range of concentrations while the obtained apparent dissociation constants are in the micro-molar range. This can be due to an artefact generated by our fluorescent label probing method where we effectively probe the interaction of hemoglobin via 1-2 probes per spectrin molecule. However it is known that hemoglobin binds spectrin via a ‘beads on a string’ model (32) and covers its entire surface which suggests a much higher affinity. In fact this is reflected by label free methods of probing spectrin hemoglobin interaction where the dissociation constants are seen to be in the nanomolar range (32).

It is seen that the addition of spectrin increases the enzyme activities of all the heme proteins and hemin. Moreover it is seen that spectrin increases the activity of the isolated α -globin chain more than that of the β -chain. This is in agreement with our observation that spectrin binds relatively unstable heme proteins with higher affinity than stable ones. This trend is also seen in the case of HbA, E and S where maximal increase is seen in case of HbE.

Oxidative stress inside an erythrocyte is a major challenge, especially so in context of the RBC membrane where redox active hemes and hemoglobins give rise to many pathological membrane damages (55,56). The ability of spectrin to enhance peroxidase and catalase activity of heme proteins opens up a potentially novel way to counter this oxidative challenge *in situ*. As we have shown in presence of suitable substrate hemoglobin variants and globin subunits are capable of catalytically removing peroxide. The RBC cytosol has a high concentration of reducing substrates, namely glutathione and NADPH for the existent peroxidase machinery. Hemoglobin may be able to utilize this substrate pool and reduce peroxide.

Similarly it has been shown that spectrin is a heme acceptor and can bind free heme with a dissociation constant of $0.57 \pm 0.06 \mu\text{M}$ (34) and mitigate its toxic effects. Here we

show that spectrin can enhance the peroxidase activity of free heme analogue, hemin, as well, which may in turn help in fighting ROS challenge.

However it is important to note that the major damages to the membrane are actually caused by the redox activity of bound hemes and hemoglobins. Thus spectrin increasing their enzyme activity could be counterproductive and lead to more membrane damage. We have shown in cases where suitable peroxidase substrate is absent, heme proteins form covalently linked aggregates with spectrin and such aggregates are redox inactive. Moreover the extent of cross-linking of spectrin with hemoglobin variants follows expected trends, HbA forms least cross-links, followed by HbS and HbE, which forms the most (35). This inactivation of heme proteins on spectrin linkage must protect the membrane from further oxidative damage. In fact it is seen that on oxidative stress hemoglobins are found attached to spectrin *in vivo* (57).

Our data lends support to this argument. It is seen that spectrin is able to decrease the amount of heme protein mediated lipid peroxidation in the absence of reducing substrates. Also due to its enhancing effect on enzyme activity, it is able to decrease lipid peroxidation to near baseline levels in presence of a reducing substrate.

It is known that haptoglobin, another chaperone binds cell free hemoglobin and the complex was hypothesised to decrease hemoglobin peroxidase activity, however, it was found that the complex retained its activity and consumed ascorbate as reductant (29). This has similarities with our present work, with the difference that hemoglobin redox activity is lost on spectrin cross-linking.

Moreover the ability of spectrin to enhance enzymatic activity extends to other heme proteins, namely catalase, which is a major player in the RBC defence against peroxide, thus spectrin can modulate the pre-existing cellular defence against ROS directly as well.

However, it must be kept in mind that the enhancement in enzyme activity that spectrin causes may come about in one of three ways, that is spectrin may have activity itself, it may give protection against peroxide (a suicide substrate) to the heme proteins and hemin, or it may cause structural alteration upon binding that lead to an enhancement of enzyme activity.

We have already shown that spectrin has no enzyme activity itself. It is known that peroxide is a suicide substrate of peroxidases, thus agents that protect the enzyme from damage are expected to cause a rise in enzyme activity (57,58). Moreover such agents should cause an increase in residual activity; however, it is demonstrated that incubation with peroxide in presence of spectrin actually causes a decrease in residual activity over that in its absence, thereby ruling out this possibility. In the case of hemin though it is seen that residual enzyme activity is increased in the presence of spectrin, which may act by shielding the hemin from peroxide. It has been shown that the increase in enzyme activity of hemin is probably not due to the co-ordination of the 5th site of Fe(III), [Fe(II) in free heme] by amino acids in spectrin as enzyme activity is not increased in presence of even 1mM free amino acids, thus there must be some other mechanism of enzyme activity enhancement.

Using Raman spectroscopy we have shown that conformational alterations take place in hemoglobin variants, cytochrome-c and hemin upon spectrin binding; and these in turn lead to increased enzyme activity. In case of hemoglobin variants and cytochrome-c it is seen that the peak at 977 cm^{-1} due the out of plane deformation mode of the C_a-H bond and the peak at 1004 cm^{-1} due to phenylalanine get replaced by an out of plane deformation mode of the C_a-H bond at 981 cm^{-1} (59-61). This conformational alteration is seen across all the four proteins pointing to the fact that spectrin may interact with heme proteins in the same general way.

In case of hemin though there is no appearance of new peaks, there is a decrease in the relative intensities of the peaks at 1065, 1371 and 1626 cm^{-1} which arise due to in plane deformation of $\text{C}_b\text{-H}_2$ bond, in plane symmetric stretching of pyrrole rings and in plane stretching of $\text{C}_a=\text{C}_b$ bond respectively (62). However it should be noted that this decrease may be due to the changed state (powder and solution) hemin and hemin-spectrin combination are investigated under as it may affect bond polarizability and concurrently peak intensity. However as the relative intensities of these peaks with respect to adjacent peaks have decreased it points to probable conformational alteration.

It can thus be said that the increase in enzyme activity that is seen is an effect of the conformational alterations that spectrin binding causes in RBC resident heme proteins, which are classified as redox regulators, thereby imparting protection under oxidative stress conditions found in disease states.

It can be concluded that spectrin interacts with heme proteins and hemin with apparent dissociation constants in the low micromolar range indicating moderately strong binding. Spectrin binding enhances enzyme activity of heme proteins and hemin which may help mitigate ROS challenge. Contra wise spectrin heme protein cross-linking may abolish redox potential of those proteins which in turn may protect the cell membrane from oxidative damage. It is shown that spectrin binding causes conformational changes in heme proteins and hemin which are detectable by Raman spectroscopy and such changes are thought to give rise to enhancement in enzyme activity.

Abbreviations

ABTS, 2,2'-azino-bis(3-ethylbenzothiazoline-6-sulphonic acid); PMB, para-hydroxymercuribenzoic acid; DTT, di-thiothreitol; RBC, red blood cell; DEAE, diethylaminoethyl; CM, carboxymethyl; HbA, hemoglobin A; HbE, hemoglobin E; HbS, hemoglobin S; MDA, malondialdehyde; TCA, trichloro-acetic acid; TBA, thiobarbituric acid; MM, Michaelis-Menten.

References

1. D'Alessandro, A., Righetti, P. G., and Zolla, L. (2010) The red blood cell proteome and interactome: an update. *Journal of proteome research* **9**, 144-163
2. Yammoto, T., and Palmer, G. (1973) The valence and spin state of iron in oxyhemoglobin as inferred from resonance Raman spectroscopy. *The Journal of biological chemistry* **248**, 5211-5213
3. Johnson, R. M., Goyette, G., Jr., Ravindranath, Y., and Ho, Y. S. (2005) Hemoglobin autoxidation and regulation of endogenous H₂O₂ levels in erythrocytes. *Free radical biology & medicine* **39**, 1407-1417
4. Goldstein, S., Meyerstein, D., and Czapski, G. (1993) The Fenton reagents. *Free radical biology & medicine* **15**, 435-445
5. Tsuruga, M., Matsuoka, A., Hachimori, A., Sugawara, Y., and Shikama, K. (1998) The molecular mechanism of autoxidation for human oxyhemoglobin. Tilting of the distal histidine causes nonequivalent oxidation in the beta chain. *The Journal of biological chemistry* **273**, 8607-8615
6. Wallace, W. J., Houtchens, R. A., Maxwell, J. C., and Caughey, W. S. (1982) Mechanism of autoxidation for hemoglobins and myoglobins. Promotion of

- superoxide production by protons and anions. *The Journal of biological chemistry* **257**, 4966-4977
7. Wallace, W. J., Maxwell, J. C., and Caughey, W. S. (1974) A role for chloride in the autoxidation of hemoglobin under conditions similar to those in erythrocytes. *FEBS letters* **43**, 33-36
 8. Marden, M. C., Griffon, N., and Poyart, C. (1995) Oxygen delivery and autoxidation of hemoglobin. *Transfusion clinique et biologique : journal de la Societe francaise de transfusion sanguine* **2**, 473-480
 9. Nagababu, E., and Rifkind, J. M. (2000) Heme degradation during autoxidation of oxyhemoglobin. *Biochemical and biophysical research communications* **273**, 839-845
 10. Mueller, S., Riedel, H. D., and Stremmel, W. (1997) Direct evidence for catalase as the predominant H₂O₂ -removing enzyme in human erythrocytes. *Blood* **90**, 4973-4978
 11. Cohen, G., and Hochstein, P. (1963) Glutathione Peroxidase: The Primary Agent for the Elimination of Hydrogen Peroxide in Erythrocytes. *Biochemistry* **2**, 1420-1428
 12. Wood, Z. A., Schroder, E., Robin Harris, J., and Poole, L. B. (2003) Structure, mechanism and regulation of peroxiredoxins. *Trends in biochemical sciences* **28**, 32-40
 13. Kinoshita, A., Nakayama, Y., Kitayama, T., and Tomita, M. (2007) Simulation study of methemoglobin reduction in erythrocytes. Differential contributions of two pathways to tolerance to oxidative stress. *The FEBS journal* **274**, 1449-1458
 14. Scott, M. D., Eaton, J. W., Kuypers, F. A., Chiu, D. T., and Lubin, B. H. (1989) Enhancement of erythrocyte superoxide dismutase activity: effects on cellular oxidant defense. *Blood* **74**, 2542-2549

15. Balagopalakrishna, C., Manoharan, P. T., Abugo, O. O., and Rifkind, J. M. (1996) Production of superoxide from hemoglobin-bound oxygen under hypoxic conditions. *Biochemistry* **35**, 6393-6398
16. Wallace, W. J., and Caughey, W. S. (1975) Mechanism for the autoxidation of hemoglobin by phenols, nitrite and "oxidant" drugs. Peroxide formation by one electron donation to bound dioxygen. *Biochemical and biophysical research communications* **62**, 561-567
17. Winterbourn, C. C. (1985) Free-radical production and oxidative reactions of hemoglobin. *Environmental health perspectives* **64**, 321-330
18. Zhang, L., Levy, A., and Rifkind, J. M. (1991) Autoxidation of hemoglobin enhanced by dissociation into dimers. *The Journal of biological chemistry* **266**, 24698-24701
19. Scott, M. D., van den Berg, J. J., Repka, T., Rouyer-Fessard, P., Hebbel, R. P., Beuzard, Y., and Lubin, B. H. (1993) Effect of excess alpha-hemoglobin chains on cellular and membrane oxidation in model beta-thalassemic erythrocytes. *The Journal of clinical investigation* **91**, 1706-1712
20. Brunori, M., Falcioni, G, Fioretti, E., Giardina, B., and Rotilio, G. (1975) Formation of superoxide in the autoxidation of the isolated α and β chains of human hemoglobin and its involvement in hemichrome precipitation. *European journal of biochemistry* **53**, 99-104
21. Hebbel, R. P., Morgan, W. T., Eaton, J. W., and Hedlund, B. E. (1988) Accelerated autoxidation and heme loss due to instability of sickle hemoglobin. *Proceedings of the National Academy of Sciences* **85**, 237-241
22. Strader, M. B., Kassa, T., Meng, F., Wood, F. B., Hirsch, R. E., Friedman, J. M., and Alayash, A. I. (2016) Oxidative instability of hemoglobin E (beta26 Glu-->Lys) is increased in the presence of free alpha subunits and reversed by alpha-hemoglobin

- stabilizing protein (AHSP): Relevance to HbE/beta-thalassemia. *Redox biology* **8**, 363-374
23. Chakrabarti, A., Bhattacharya, D., Deb, S., and Chakraborty, M. (2013) Differential thermal stability and oxidative vulnerability of the hemoglobin variants, HbA2 and HbE. *PloS one* **8**, e81820
24. Hebbel, R. P. (1985) Auto-oxidation and a membrane-associated 'Fenton reagent': a possible explanation for development of membrane lesions in sickle erythrocytes. *Clinics in haematology* **14**, 129-140
25. Welbourn, E. M., Wilson, M. T., Yusof, A., Metodiev, M. V., and Cooper, C. E. (2017) The mechanism of formation, structure and physiological relevance of covalent hemoglobin attachment to the erythrocyte membrane. *Free radical biology & medicine* **103**, 95-106
26. Kuross, S. A., Rank, B. H., and Hebbel, R. P. (1988) Excess heme in sickle erythrocyte inside-out membranes: possible role in thiol oxidation. *Blood* **71**, 876-882
27. Kriebardis, A. G., Antonelou, M. H., Stamoulis, K. E., Economou-Petersen, E., Margaritis, L. H., and Papassideri, I. S. (2007) Progressive oxidation of cytoskeletal proteins and accumulation of denatured hemoglobin in stored red cells. *Journal of cellular and molecular medicine* **11**, 148-155
28. Mohanty, J. G., Nagababu, E., and Rifkind, J. M. (2014) Red blood cell oxidative stress impairs oxygen delivery and induces red blood cell aging. *Frontiers in physiology* **5**, 84
29. Kapralov, A., Vlasova, II, Feng, W., Maeda, A., Walson, K., Tyurin, V. A., Huang, Z., Aneja, R. K., Carcillo, J., Bayir, H., and Kagan, V. E. (2009) Peroxidase activity of hemoglobin-haptoglobin complexes: covalent aggregation and oxidative stress in plasma and macrophages. *The Journal of biological chemistry* **284**, 30395-30407

30. Smith, M. J., and Beck, W. S. (1967) Peroxidase activity of hemoglobin and its subunits: effects thereupon of haptoglobin. *Biochimica et biophysica acta* **147**, 324-333
31. Basu, A., and Chakrabarti, A. (2015) Hemoglobin interacting proteins and implications of spectrin hemoglobin interaction. *Journal of proteomics* **128**, 469-475
32. Mishra, K., Chakrabarti, A., and Das, P. K. (2017) Protein-Protein Interaction Probed by Label-free Second Harmonic Light Scattering: Hemoglobin Adsorption on Spectrin Surface as a Case Study. *The journal of physical chemistry. B* **121**, 7797-7802
33. Chakrabarti, A., Bhattacharya, S., Ray, S., and Bhattacharyya, M. (2001) Binding of a denatured heme protein and ATP to erythroid spectrin. *Biochemical and biophysical research communications* **282**, 1189-1193
34. Das, D., Patra, M., and Chakrabarti, A. (2015) Binding of hemin, hematoporphyrin, and protoporphyrin with erythroid spectrin: fluorescence and molecular docking studies. *European biophysics journal : EBJ* **44**, 171-182
35. Datta, P., Basu, S., Chakravarty, S. B., Chakravarty, A., Banerjee, D., Chandra, S., and Chakrabarti, A. (2006) Enhanced oxidative cross-linking of hemoglobin E with spectrin and loss of erythrocyte membrane asymmetry in hemoglobin E beta-thalassemia. *Blood cells, molecules & diseases* **37**, 77-81
36. Bhattacharyya, M., Ray, S., Bhattacharya, S., and Chakrabarti, A. (2004) Chaperone activity and prodan binding at the self-associating domain of erythroid spectrin. *The Journal of biological chemistry* **279**, 55080-55088
37. Datta, P., Chakrabarty, S., Chakrabarty, A., and Chakrabarti, A. (2007) Spectrin interactions with globin chains in the presence of phosphate metabolites and hydrogen peroxide: implications for thalassaemia. *Journal of biosciences* **32**, 1147-1151

38. Banerjee, M., Pramanik, M., Bhattacharya, D., Lahiry, M., Basu, S., and Chakrabarti, A. (2011) Faster heme loss from hemoglobin E than HbS, in acidic pH: effect of aminophospholipids. *Journal of biosciences* **36**, 809-816
39. Margoliash, E., and Frohwirt, N. (1959) Spectrum of horse-heart cytochrome c. *The Biochemical journal* **71**, 570-572
40. Haber, J., Maslakiewicz, P., Rodakiewicz-Nowak, J., and Walde, P. (1993) Activity and spectroscopic properties of bovine liver catalase in sodium bis(2-ethylhexyl)sulfosuccinate/isooctane reverse micelles. *European journal of biochemistry* **217**, 567-573
41. Chakrabarti, A. (2009) A fluorescence quenching method to study interactions of hemoglobin derivatives with erythroid spectrin. in *Reviews in Fluorescence 2007*, Springer. pp 363-377
42. Haque, E., Debnath, D., Basak, S., and Chakrabarti, A. (1999) Structural changes of horseradish peroxidase in presence of low concentrations of urea. *European journal of biochemistry* **259**, 269-274
43. Chakrabarti, A., and Basak, S. (1996) Structural alterations of horseradish peroxidase in the presence of low concentrations of guanidinium chloride. *European journal of biochemistry* **241**, 462-467
44. Rodriguez-Lopez, J. N., Lowe, D. J., Hernandez-Ruiz, J., Hiner, A. N., Garcia-Canovas, F., and Thorneley, R. N. (2001) Mechanism of reaction of hydrogen peroxide with horseradish peroxidase: identification of intermediates in the catalytic cycle. *Journal of the American Chemical Society* **123**, 11838-11847
45. Maehly, A. C., and Chance, B. (1954) The assay of catalases and peroxidases. *Methods of biochemical analysis* **1**, 357-424

46. Sarkar, S., Bose, D., Giri, R. P., Mukhopadhyay, M. K., and Chakrabarti, A. (2019) Effects of GM1 on brain spectrin-aminophospholipid interactions. *Biochimica et biophysica acta. Biomembranes* **1861**, 298-305
47. Buege, J. A., and Aust, S. D. (1978) Microsomal lipid peroxidation. *Methods in enzymology* **52**, 302-310
48. Droghetti, E., Oellerich, S., Hildebrandt, P., and Smulevich, G. (2006) Heme coordination states of unfolded ferrous cytochrome C. *Biophysical journal* **91**, 3022-3031
49. Arcovito, A., Gianni, S., Brunori, M., Travaglini-Allocatelli, C., and Bellelli, A. (2001) Fast coordination changes in cytochrome c do not necessarily imply folding. *Journal of Biological Chemistry* **276**, 41073-41078
50. Park, S. Y., Yokoyama, T., Shibayama, N., Shiro, Y., and Tame, J. R. (2006) 1.25 Å resolution crystal structures of human haemoglobin in the oxy, deoxy and carbonmonoxy forms. *Journal of molecular biology* **360**, 690-701
51. Chakrabarti, A., Datta, P., Bhattacharya, D., Basu, S., and Saha, S. (2008) Oxidative crosslinking, spectrin and membrane interactions of hemoglobin mixtures in HbEbeta-thalassemia. *Hematology* **13**, 361-368
52. Yu, X., Kong, Y., Dore, L. C., Abdulmalik, O., Katein, A. M., Zhou, S., Choi, J. K., Gell, D., Mackay, J. P., and Gow, A. J. (2007) An erythroid chaperone that facilitates folding of α -globin subunits for hemoglobin synthesis. *The Journal of clinical investigation* **117**, 1856-1865
53. Kihm, A. J., Kong, Y., Hong, W., Russell, J. E., Rouda, S., Adachi, K., Simon, M. C., Blobel, G. A., and Weiss, M. J. (2002) An abundant erythroid protein that stabilizes free α -haemoglobin. *Nature* **417**, 758

54. Yan, Y., Winograd, E., Viel, A., Cronin, T., Harrison, S. C., and Branton, D. (1993) Crystal structure of the repetitive segments of spectrin. *Science* **262**, 2027-2030
55. Chiu, D., and Lubin, B. (1989) Oxidative hemoglobin denaturation and RBC destruction: the effect of heme on red cell membranes. *Seminars in hematology* **26**, 128-135
56. Shinar, E., and Rachmilewitz, E. A. (1990) Oxidative denaturation of red blood cells in thalassemia. *Seminars in hematology* **27**, 70-82
57. Arnao, M. B., Acosta, M., del Rio, J. A., and Garcia-Canovas, F. (1990) Inactivation of peroxidase by hydrogen peroxide and its protection by a reductant agent. *Biochimica et biophysica acta* **1038**, 85-89
58. Moosavi Movahedi, A. A., Nazari, K., and Ghadermarzi, M. (1999) Suicide inactivation of peroxidase by H₂O₂: kinetic equations for peroxidatic oxidation reaction of guaiacol and determination of the kinetic parameters. *The Italian journal of biochemistry* **48**, 9-17
59. Atkins, C. G., Buckley, K., Blades, M. W., and Turner, R. F. B. (2017) Raman Spectroscopy of Blood and Blood Components. *Applied spectroscopy* **71**, 767-793
60. Hu, S., Morris, I. K., Singh, J. P., Smith, K. M., and Spiro, T. G. (1993) Complete assignment of cytochrome c resonance Raman spectra via enzymic reconstitution with isotopically labeled hemes. *Journal of the American Chemical Society* **115**, 12446-12458
61. Wood, B. R., and McNaughton, D. (2002) Micro-Raman characterization of high-and low-spin heme moieties within single living erythrocytes. *Biopolymers: Original Research on Biomolecules* **67**, 259-262

62. Hu, S., Smith, K. M., and Spiro, T. G. (1996) Assignment of protoheme resonance Raman spectrum by heme labeling in myoglobin. *Journal of the American Chemical Society* **118**, 12638-12646

5.4 Appendix:

Interactome of spectrin under normal and HbE-disease conditions: possible role of spectrin in red-ox regulation

The first report of the cytosolic interactome of human erythroid spectrin under normal conditions and in hemoglobin E-disease is presented.

Hemoglobin depleted blood lysate was prepared by the method of Ringrose *et. al.* (1). Human RBC was lysed via incubation against 20 volumes of hypotonic buffer and lysate was cleared via centrifugation. Cytosolic fraction was run on Ni-NTA resin at 200mg protein per 8ml of resin in the same buffer. Hemoglobin depleted fraction was collected, pooled and concentrated.

Human erythrocytic spectrin was prepared as described earlier (2). Purified spectrin was attached to CNBr activated Sepharose resin using the protocol of Kavran *et. al.* (3). Briefly, Human erythroid spectrin was bound covalently to CNBr activated Sepharose beads and it was calculated that 1mg protein was bound per ml of resin. Protein bound resin was equilibrated against 50 mM Na-phosphate buffer pH 7.4, 100 mM NaCl.

100 mg of hemoglobin depleted cytosolic protein fraction was taken in 5 ml of same buffer and incubated with 1 ml of protein bound CNBr agarose overnight. Prey bound resin was washed extensively with 20 column volumes of the same buffer to remove non-specifically bound proteins. Prey proteins were eluted in 20% acetic acid, 1 % SDS. **Figure 5.10** shows representative SDS gel of the different fractions.

Figure 5.10: SDS-PAGE of different fractions.

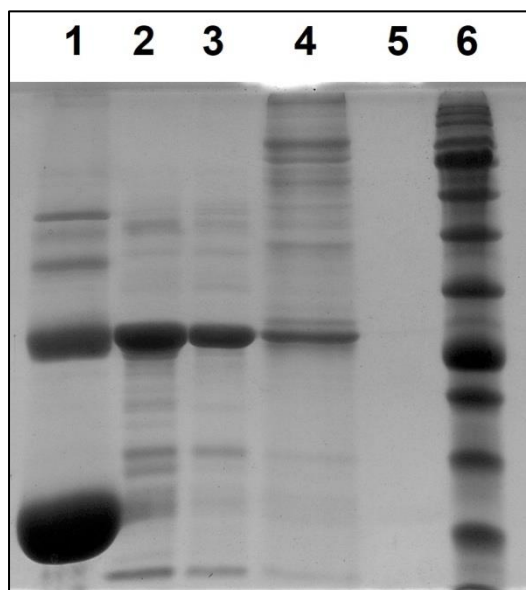


Figure 5.10: Figure shows silver stained 12% SDS gel of the different RBC cytosolic fractions used for interactome analysis. Lane 1 shows crude RBC lysate, bottom most band is for hemoglobin, the next most prominent band is for carbonic anhydrase. Lane 2 shows cytosolic fraction after hemoglobin depletion using Ni-NTA. Lane 3 shows the flow through washings of the prey pool after binding CNBr Sepharose immobilized spectrin. Lane 4 shows the spectrin interacting proteins eluted with 20% acetic acid, 1% SDS. Lane 5 shows the same elution with prey pool incubated with control CNBr quenched with tri-ethanolamine. No detectable proteins were found to bind the resin free of spectrin. Lane 6 shows marker.

For each sample, eluates of three distinct runs were pooled together, concentrated and dialysed against 100 mM Tris-HCL pH 8.0 and 6M GdmHCl and supplied as such to Valerian Chem. Pvt. Ltd., New Delhi, India, who analysed our samples.

25 microlitre samples were taken and reduced with 5 mM TCEP and further alkylated with 50 mM iodoacetamide and then digested with Trypsin (1:50, Trypsin/lysate ratio) for 16 hours at 37 °C. Digests were cleaned using a C18 silica cartridge to remove the salt and dried

using a speed vac. The dried pellet was resuspended in buffer A (5% acetonitrile, 0.1% formic acid).

All the experiment was performed using EASY-nLC 1000 system (Thermo Fisher Scientific) coupled to Thermo Fisher-*QExactive* equipped with nanoelectrospray ion source. 1.0 µg of the peptide mixture was resolved using 25 cm PicoFrit column (360µm outer diameter, 75µm inner diameter, 10µm tip) filled with 1.8 µm of C18-resin (Dr Maesch, Germany). The peptides were loaded with buffer A and eluted with a 0–40% gradient of buffer B (95% acetonitrile, 0.1% formic acid) at a flow rate of 300 nl/min for 100 min.

Figure 5.11 shows representative elution profile.

Figure 5.11: Representative elution profile.

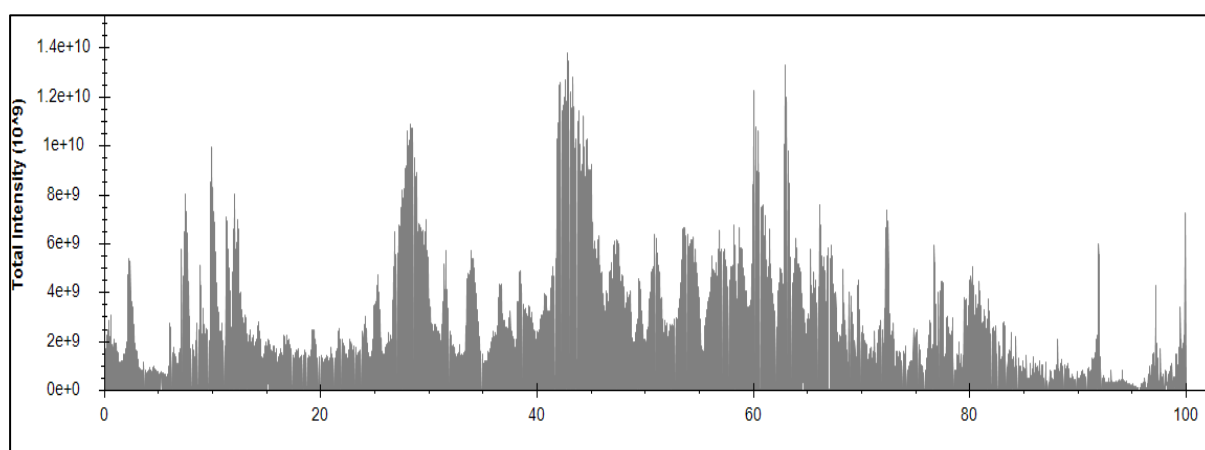


Figure 5.11: Representative elution profile of interacting protein pool is shown.

MS data was acquired using a data-dependent top10 method dynamically choosing the most abundant precursor ions from the survey scan.

All samples were processed and RAW files generated were analyzed with Proteome Discoverer (v2.2) against the Uniprot *Human* reference proteome database. For Sequest search, the precursor and fragment mass tolerances were set at 10 ppm and 0.5 Da, respectively. The protease used to generate peptides, *i.e.* enzyme specificity was set for

trypsin/P (cleavage at the C terminus of “K/R: unless followed by “P”) along with maximum missed cleavages value of two. Carbamidomethyl on cysteine as fixed modification and oxidation of methionine and N-terminal acetylation and phosphorylation on site (S, T, Y) were considered as variable modifications for database search. Both peptide spectrum match and protein false discovery rate were set to 0.01 FDR.

The generated list of spectrin interactors was validated against a quantitative list of complete RBC proteome by Bryk *et. al.* (4) and the top 50% proteins by search engine hit scores were considered. In this way ~312 proteins were identified. List of proteins is given in supplementary **Table ST1 (supporting information)**.

It is important to note that there were no differences in the number or type of proteins interacting with spectrin in both cases; however the relative abundance of the interactors had changed. Spectrin was found to primarily interact with heme-containing red-ox proteins, chaperones, lipid modulating proteins, membrane skeletal proteins, protein quality control maintenance machinery and signaling components. **Figure 5.12** shows a pie chart of the different protein class the interactome of spectrin can be divided into.

Figure 5.12: Different classes of spectrin interactors.

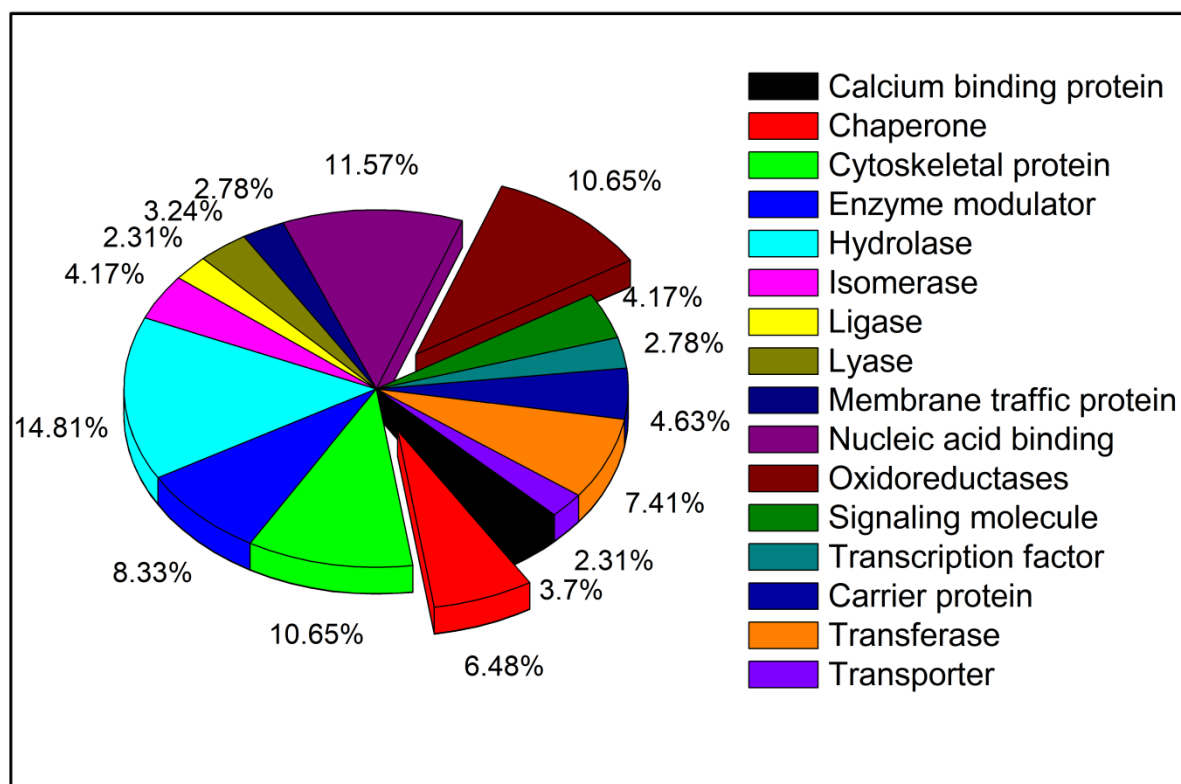


Figure 5.12: Pie chart representing the different classes of proteins that spectrin interacting proteins belong to. Classification of proteins into different classes was done with the help of PANTHER database.

A major class of spectrin interactor is seen to be red-ox active proteins many of which are also heme containing. Interestingly all these proteins are more abundant in hemoglobin E-disease than in normal states. This is in line with our previous observations where we showed E β -thalassemia caused an up-regulation of cytosolic red-ox regulators and chaperones(5). Unstable hemoglobin variants cause oxidative stress leading to accumulation of anti-oxidant machinery (6). Spectrin is known to interact with hemoglobin and heme-containing HRP and act as their chaperone (2)(7). Recently we have shown that spectrin interaction causes enhancement of the peroxidase activity of heme proteins (manuscript under review), this has implications in the clearance of ROS and oxidative stress. The observation that spectrin also

interacts with several other heme-containing proteins and proteins involved in heme management, as well as red-ox regulatory proteins lends support to the idea that spectrin may be involved in oxidative stress management in RBCs. **Table 5.3** tabulates the major spectrin interacting red-ox active proteins and chaperones.

Table 5.3: Major spectrin interacting proteins.

<i>Sl. no</i>	<i>Accession</i>	<i>Description</i>	<i>Abundance Ratio: (D) / (N)</i>	<i>Coverage [%]</i>	<i># Unique Peptides</i>	<i>MW [kDa]</i>	<i>calc. pI</i>	<i>Score Sequest HT:</i>
1	P32119	Peroxiredoxin-2	1.059	96	36	21.9	5.97	9184.46
2	P30043	Flavin reductase	1.059	98	22	22.1	7.65	2905.16
3	P11142	Heat shock cognate 71 kDa protein	1.018	52	38	70.9	5.52	2203.89
4	P00441	Superoxide dismutase	1.113	92	14	15.9	6.13	1989.75
5	P37840	Alpha-synuclein	0.384	66	22	14.5	4.7	1305.62
6	P31948	Stress-induced-phosphoprotein 1	0.553	65	36	62.6	6.8	1145.44
7	P04040	Catalase	1.356	64	33	59.7	7.39	1028.98
8	P68871	Hemoglobin subunit beta	1.204	90	8	16	7.28	984.67
9	P78417	Glutathione S-transferase omega-1	1.17	62	17	27.5	6.6	936.87
10	P50502	Hsc70-interacting protein	1.61	41	20	41.3	5.27	915.7
11	P0DMV9	Heat shock 70 kDa protein 1B	1.447	50	28	70	5.66	880.42

12	P30041	Peroxiredoxin-6	1.488	85	30	25	6.38	781.47
13	P69905	Hemoglobin subunit alpha	1.36	92	14	15.2	8.68	771.87
14	P07451	Carbonic anhydrase 3	0.759	41	13	29.5	7.34	723.7
15	Q06830	Peroxiredoxin-1	1.529	69	18	22.1	8.13	692.47
16	O75347	Tubulin-specific chaperone A	0.725	81	20	12.8	5.29	690.45
17	P02042	Hemoglobin subunit delta	2.463	46	3	16	8.05	638.55
18	P00167	Cytochrome b5	1.305	57	7	15.3	4.96	517.65
19	P62158	Calmodulin	1.249	52	9	16.8	4.22	510.58
20	P07900	Heat shock protein HSP 90-alpha	1.186	40	22	84.6	5.02	490.89
21	P48637	Glutathione synthetase	1.259	43	20	52.4	5.92	437.44
22	P10599	Thioredoxin	1.085	70	8	11.7	4.92	423.1
23	O14618	Copper chaperone for superoxide dismutase	1.015	58	15	29	5.58	419.85
24	P54652	Heat shock-related 70 kDa protein 2	0.93	17	9	70	5.74	405.73
25	P34932	Heat shock 70 kDa protein 4	1.633	47	34	94.3	5.19	396.25
26	P16152	Carbonyl reductase [NADPH] 1	1.001	54	15	30.4	8.32	393.7
27	Q9NZD4	Alpha-hemoglobin- stabilizing protein	3.764	59	10	11.8	5	347.74

28	P35754	Glutaredoxin-1	1.388	80	7	11.8	8.09	299.7
29	P34931	Heat shock 70 kDa protein 1-like	1.031	23	0	70.3	6.02	291.45
30	P17066	Heat shock 70 kDa protein 6	1.011	15	0	71	6.14	250.01
31	P07203	Glutathione peroxidase 1	1.576	69	9	22.1	6.55	199.57
32	P09211	Glutathione S-transferase P	0.73	65	10	23.3	5.64	192.84
33	P48741	Putative heat shock 70 kDa protein 7	0.417	16	4	40.2	7.87	186.93
34	Q9NRV9	Heme-binding protein 1	0.948	72	10	21.1	5.8	185.99
35	O75828	Carbonyl reductase [NADPH] 3	1.03	13	3	30.8	6.18	129.73
36	Q9NZT1	Calmodulin-like protein 5	0.299	42	10	15.9	4.44	126.56
37	P08238	Heat shock protein HSP 90-beta	1.806	15	2	83.2	5.03	118.5
38	Q9BRA2	Thioredoxin domain-containing protein 17	0.744	67	6	13.9	5.52	89.71
39	P04792	Heat shock protein beta-1	1.095	27	3	22.8	6.4	86.99
40	P00387	NADH-cytochrome b5 reductase 3	0.839	14	4	34.2	7.59	84.27
41	P14550	Alcohol dehydrogenase [NADP(+)]	0.784	26	8	36.6	6.79	75.31

42	O43396	Thioredoxin-like protein 1	0.775	26	6	32.2	4.96	66.66
43	Q9UHV9	Prefoldin subunit 2	1.081	38	4	16.6	6.58	61.33
44	O43765	Small glutamine-rich tetratricopeptide repeat-containing protein alpha	0.841	12	3	34	4.87	50.92

Table 5.3: The major red-ox active protein and chaperone protein interacting partners of spectrin are tabulated. Their relative abundances in disease state, hemoglobin E-disease (D) versus their relative abundance in normal state is given as D/N.

1. Ringrose, J. H., van Solinge, W. W., Mohammed, S., O’Flaherty, M. C., van Wijk, R., Heck, A. J., and Slijper, M. (2008) Highly efficient depletion strategy for the two most abundant erythrocyte soluble proteins improves proteome coverage dramatically. *Journal of proteome research* **7**, 3060-3063
2. Basu, A., and Chakrabarti, A. (2015) Hemoglobin interacting proteins and implications of spectrin hemoglobin interaction. *Journal of proteomics* **128**, 469-475
3. Kavran, J. M., and Leahy, D. J. (2014) Coupling antibody to cyanogen bromide-activated sepharose. *Methods in enzymology* **541**, 27
4. Bryk, A. H., and Wiśniewski, J. R. (2017) Quantitative analysis of human red blood cell proteome. *Journal of proteome research* **16**, 2752-2761
5. Chakrabarti, A., Halder, S., and Karmakar, S. (2016) Erythrocyte and platelet proteomics in hematological disorders. *PROTEOMICS–Clinical Applications* **10**, 403-414

6. Basu, A., Saha, S., Karmakar, S., Chakravarty, S., Banerjee, D., Dash, B. P., and Chakrabarti, A. (2013) 2D DIGE based proteomics study of erythrocyte cytosol in sickle cell disease: altered proteostasis and oxidative stress. *Proteomics* **13**, 3233-3242
7. Bhattacharyya, M., Ray, S., Bhattacharya, S., and Chakrabarti, A. (2004) Chaperone activity and prodan binding at the self-associating domain of erythroid spectrin. *The Journal of biological chemistry* **279**, 55080-55088

Chapter 6:

Conclusions

6.1 Conclusions

The major take home messages from this thesis can be summarised as follows –

- **Chapter 1:** Molecular chaperones are one of the key players in protein biology and as such their structure and mechanism of action have been extensively studied. However the substrate specificity of molecular chaperones has not been well investigated. This review aims to summarize what is known about the substrate specificity and substrate recognition motifs of chaperones so as to better understand what substrate specificity means in the context of molecular chaperones. Available literature shows that the majority of chaperones have broad substrate range and recognize non-native conformations of proteins depending on recognition of hydrophobic and/or charged patches. Based on these recognition motifs chaperones can select for early, mid or late folding intermediates. Another major contributor to chaperone specificity are the co-chaperones they interact with as well as the sub-cellular location they are expressed in and the inducibility of their expression. Some chaperones which have only one or a few known substrates are reported. In their case the mode of recognition seems to be specific structural complementarity between chaperone and substrate. It can be concluded that the vast majority of chaperones do not show a high degree of specificity but recognize elements that signal non – native protein conformation and their substrate range is modulated by the context they function in. However a few chaperones are known that display exquisite specificity of their substrate e.g. mammalian Heat Shock Protein 47 (HSP47) collagen interaction. **Figure 1.1** shows an illustration of the chaperone pathways in a generalized cell.
- **Chapter 2:** We investigate the pH induced changes in the structure and stability of erythroid and brain spectrin by spectroscopic methods. We also correlate these

changes with modulations of chaperone potential at different pH. We have followed the pH induced structural changes by circular dichroism spectroscopy and intrinsic tryptophan fluorescence. It is seen that lowering the pH from 9 has little effect on structure of the proteins till about pH 6. At pH 4, there is significant change of the secondary structure of the proteins, along with a 5nm hypsochromic shift of the emission maxima. Below pH 4 the proteins undergo acid denaturation. Probing exposed hydrophobic patches on the proteins using protein-bound 8-anilinonaphthalene-1-sulfonate fluorescence demonstrates that there is higher solvent accessibility of hydrophobic surfaces in both forms of spectrin at around pH 4. Dynamic light scattering and 90° light scattering studies show that the both forms of spectrin forms oligomers at pH ~ 4. Chemical unfolding data shows that these oligomers are less stable than the tetrameric form. Aggregation studies with BSA show that at pH 4, both spectrins exhibit better chaperone activity. This enhancement of chaperone like activity appears to result from an increase in regions of solvent-exposed hydrophobicity and oligomeric state of the spectrins which in turn are induced by moderately acid pH. This may have *in-vivo* implications in cells facing stress conditions where cytoplasmic pH is lowered. **Figure 6.1** shows a diagrammatic representation of the same.

Figure 6.1: pH dependent chaperone activity of spectrin.

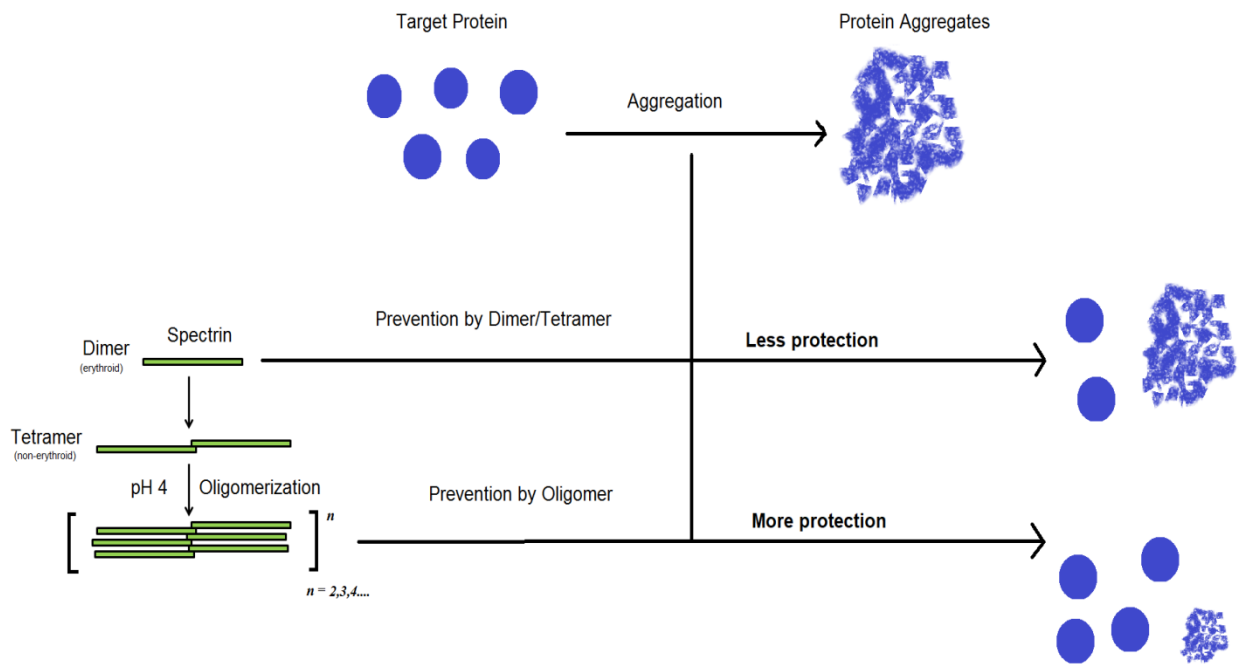


Figure 6.1: diagrammatic representation of the pH dependent chaperone activity of spectrin.

- Chapter 3:** We have probed the chaperone activity of spectrin in presence of hemoglobin and phospholipid SUVs of different compositions to elucidate the effect of phospholipid/hemoglobin binding on chaperone function. It is seen that spectrin displays a preference for hemoglobin over other substrates leading to a decrease in chaperone activity in presence of hemoglobin. A competition is seen to exist between phospholipid binding and chaperone function of spectrin, in a dose dependent manner with the greatest extent of decrease being seen in case of phospholipid vesicles containing aminophospholipids e.g. PS and PE which may have implications in diseases like hereditary spherocytosis where mutation in spectrin is implicated in its detachment from cell membrane. To gain a clearer understanding of the chaperone like activity of spectrin under *in-vivo* like conditions we have investigated the effect of macromolecular crowders as well as phosphorylation and glycation states on

chaperone activity. It is seen that the presence of non-specific, protein and non-protein macromolecular crowders do not appreciably affect chaperone function. Phosphorylation also does not affect the chaperone function unlike glycation which progressively diminishes chaperone activity. We propose a model where chaperone clients adsorb onto spectrin's surface and processes that bind to and occlude these surfaces decrease chaperone activity. **Figure 6.2** shows a diagrammatic representation of the same.

Figure 6.2: Chaperone activity of spectrin in presence of interactors and modifications.

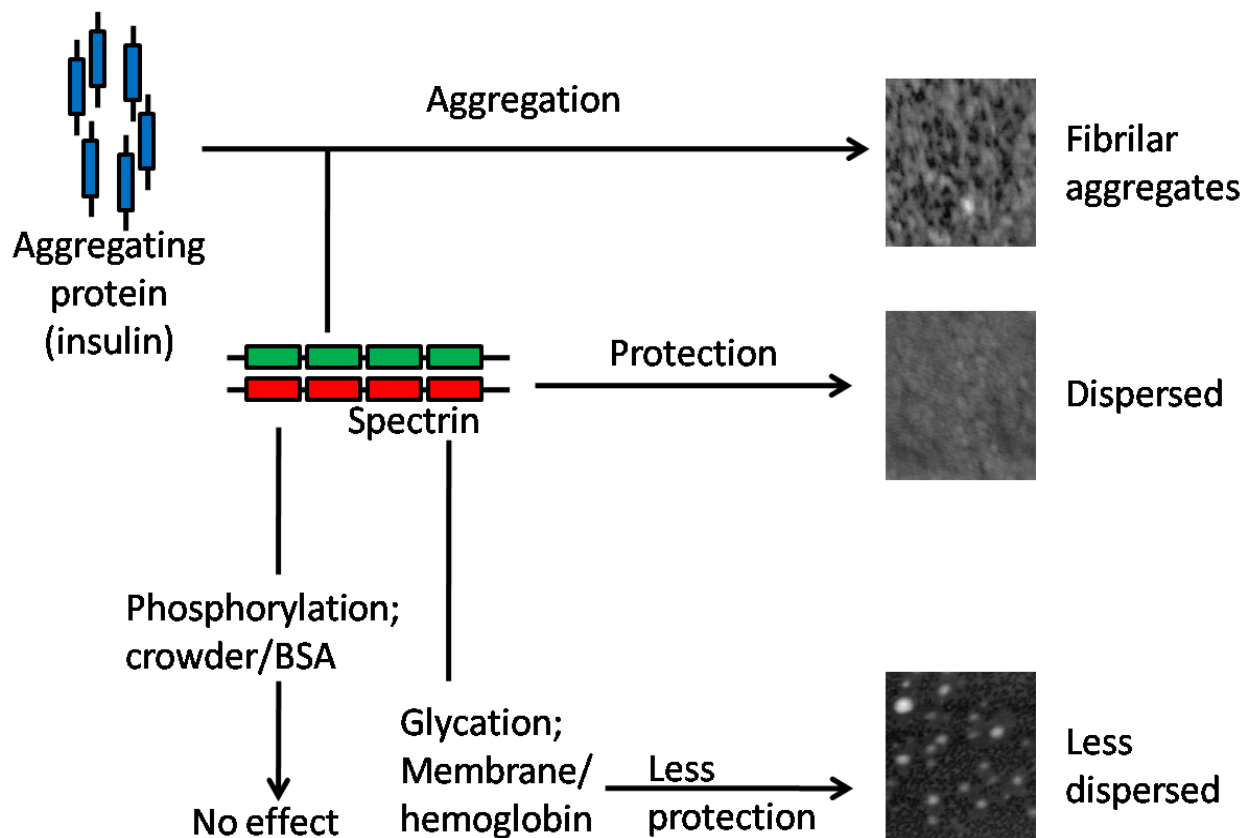


Figure 6.2: Chaperone activity of spectrin in presence of interactors and modifications.

- **Chapter 4:** Here we probe the location and molecular origin of the chaperone activity of multi-domain spectrin using a selection of individual recombinant spectrin domains, which we have characterized using intrinsic tryptophan fluorescence and CD spectroscopy to show their identity to native spectrin. Aggregation assays using insulin, ADH, α - and β - globin as well as enzyme refolding assays using alkaline phosphatase and α -glucosidase show that the chaperone activity is not only localized in the self-association domain but is a generalized property of spectrin domains. This is to our understanding, a unique feature in the case of modular multi-repeat proteins, possibly implicating that the large family of "spectrin-repeat" domain containing proteins may also have chaperone like property. Substrate selectivity of chaperone activity as evidenced by the preferential protection of α - over β -globin chains is seen; which has implications in hemoglobin diseases. Moreover enzyme refolding assays also indicate alternate modes of chaperone action. We propose that the molecular origin of chaperone activity resides in the surface exposed hydrophobic patches of the spectrin domains as shown by ANS (1-anilinonaphthalene-8-sulfonic acid) and prodan (6-propionyl-2[dimethylamino]-naphthalene) binding. We also show that prodan does indeed have a unique binding site on spectrin located at the self-association domain. **Figure 6.3** shows the chaperone activity of the different domains of spectrin.

Figure 6.3: Chaperone activity of spectrin domains.

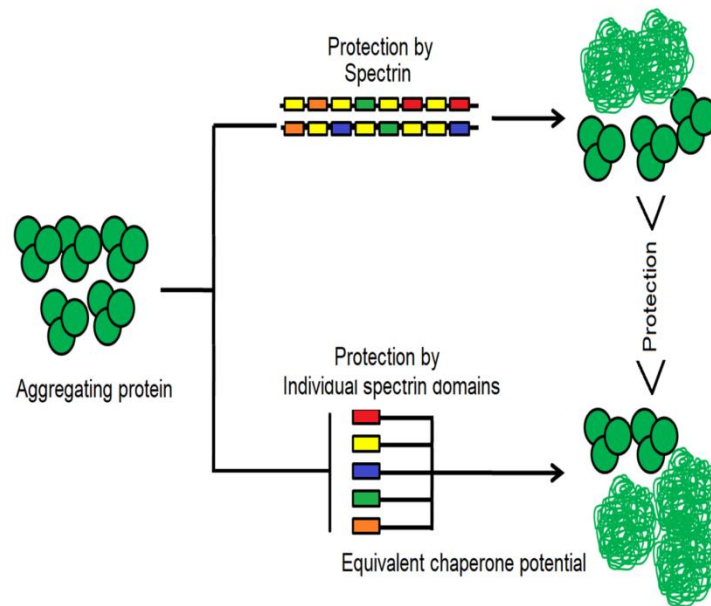


Figure 6.3: Chaperone activity of spectrin domains.

Moreover we also probe the binding of individual spectrin domains to different hemoglobin isoforms and validate the ‘beads-on-a-string’ model of spectrin-hemoglobin binding as shown in **Figure 4.15** and **Table 4.5**.

- **Chapter 5:** Oxidative stress and disease states cause oxidation and membrane attachment of hemoglobin, where its red-ox activity leads to lipid peroxidation and cytoskeletal protein damage. Spectrin which remains attached to hemoglobin is found to increase hemoglobin peroxidase activity in presence of suitable reducing substrate and in this way may help in clearing peroxide generated during hemoglobin oxidation. In the absence of reducing substrate spectrin forms covalently cross-linked aggregates with hemoglobin which display no peroxidase activity, thereby limiting membrane lipid peroxidation. Like its effect on hemoglobin A, spectrin is found to similarly increase peroxidase activity of other hemoglobin variants HbE and HbS and also of isolated globin subunits from all three hemoglobins. This is of importance particularly

in disease states like sickle cell disease and HbE- β -thalassemia where increased oxidative damage and free subunits are present due to defects inherent in hemoglobin variants associated with them. This hypothesis is corroborated by lipid peroxidation experiments. The modulatory role of spectrin also extends to other heme proteins, namely catalase and cytochrome-c. Experiments with free heme and Raman spectroscopy of heme proteins in presence of spectrin show that structural alterations occur in the heme moiety of the heme proteins on spectrin binding which may be the structural basis of increased enzyme activity. This is shown diagrammatically in **Figure 6.4**.

Figure 6.4: Spectrin induced enzyme activity modulation of hemoglobin (Hb).

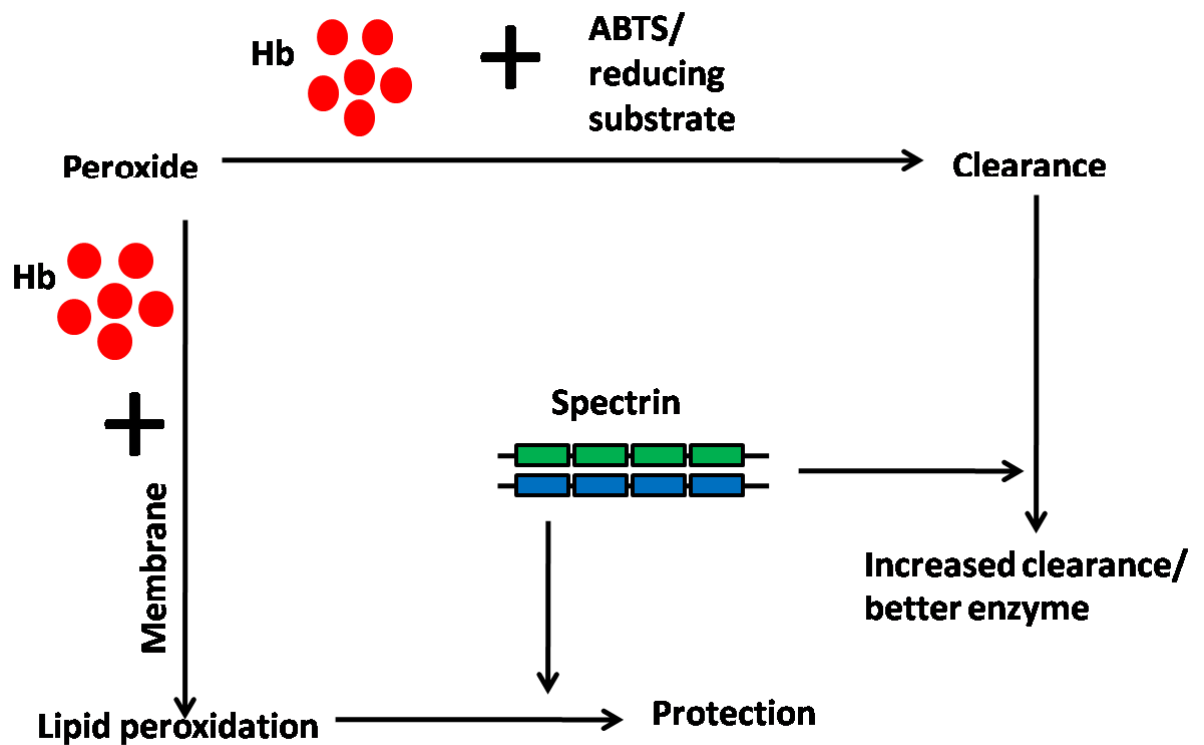


Figure 6.4: Spectrin modulates the enzyme activity of heme proteins like hemoglobin Hb.

We also describe the interactome of spectrin in normal and HbE disease conditions as shown in **Figure 5.12** and **Table 5.3**.

6.2 Future perspectives

Much work still needs to be done to gain a clearer understanding of the chaperone property of spectrin and its interplay with the other functionalities of the protein. Specifically, mutants of spectrin domains need to be generated in order to better elucidate how the hydrophobicity of spectrin interacts with or causes the chaperone activity.

7 Supporting Information:

Table ST1:

Table contains the list of interacting partners of spectrin and their abundance ratios in diseased (D) versus normal (N) conditions.

Accession ID	Description	Abundance Ratio: (D) / (N)	Score Sequest HT:
P00915	Carbonic anhydrase	0.998	12111.65
P32119	Peroxiredoxin-2	1.059	9184.46
P30043	Flavin reductase	1.059	2905.16
P02768	Serum albumin	3.16	2842.62
P07738	Bisphosphoglycerate mutase	1.041	2753.8
Q13228	Selenium-binding protein	1.011	2279.68
P60174	Triosephosphate isomerase	1.199	2251.12
P11142	Heat shock cognate 71 kDa protein	1.018	2203.89
P00558	Phosphoglycerate kinase	0.888	2176.35
P50395	Rab GDP dissociation inhibitor beta	0.864	2058.55
P00441	Superoxide dismutase	1.113	1989.75
P04075	Fructose-bisphosphate aldolase	0.942	1942.05
P62937	Peptidyl-prolyl cis-trans isomerase	0.901	1854.83
P40925	Malate dehydrogenase	1.771	1586.72
P06733	Alpha-enolase	1.389	1484.45

P55072	Transitional endoplasmic reticulum ATPase	0.311	1482.27
P04406	Glyceraldehyde-3-phosphate dehydrogenase	0.511	1475.45
P37840	Alpha-synuclein	0.384	1305.62
P20810	Calpastatin	0.807	1257.94
P04264	Keratin, type II cytoskeletal 1	0.653	1212.18
Q16775	Hydroxyacylglutathione hydrolase, mitochondrial	0.675	1201.93
Q99497	Protein deglycase	1.045	1191.9
P00568	Adenylate kinase	0.409	1191.6
P63261	Actin, cytoplasmic 2	0.385	1174.13
P60709	Actin, cytoplasmic 1	0.385	1174.13
P31948	Stress-induced-phosphoprotein 1	0.553	1145.44
P25786	Proteasome subunit alpha type-1	1.076	1108.92
P35527	Keratin, type I cytoskeletal 9	0.621	1089.07
P04040	Catalase	1.356	1028.98
P18669	Phosphoglycerate mutase	1.041	1014.34
P68871	Hemoglobin subunit beta	1.204	984.67
P62258	14-3-3 protein epsilon	1.344	971.07
P37837	Transaldolase	0.829	959.68
P78417	Glutathione S-transferase omega-1	1.17	936.87
P13798	Acylamino-acid-releasing enzyme	0.931	921.68
P50502	Hsc70-interacting protein	1.61	915.7

P10768	S-formylglutathione hydrolase	0.573	914
P26038	Moesin	1.06	886.17
P0DMV9	Heat shock 70 kDa protein 1B	1.447	880.42
P29401	Transketolase	0.956	841.87
P23528	Cofilin-1	0.532	829.52
P68032	Actin, alpha cardiac muscle 1	0.097	795.32
P68133	Actin, alpha skeletal muscle	0.097	795.32
P30041	Peroxiredoxin-6	1.488	781.47
P30086	Phosphatidylethanolamine-binding protein 1	1.054	776.93
P69905	Hemoglobin subunit alpha	1.36	771.87
P06702	Protein S100-A9	0.237	754.41
Q8NFI4	Putative protein FAM10A5	0.644	727.8
P63104	14-3-3 protein zeta/delta	1.076	726.38
P63267	Actin, gamma-enteric smooth muscle	0.258	725.94
P62736	Actin, aortic smooth muscle	0.258	725.94
P07451	Carbonic anhydrase 3	0.759	723.7
P62979	Ubiquitin-40S ribosomal protein S27a	1.305	720.75
P0CG48	Polyubiquitin-C	1.305	720.75
P62987	Ubiquitin-60S ribosomal protein	1.305	720.75
P0CG47	Polyubiquitin-B	1.305	720.75
P24666	Low molecular weight phosphotyrosine protein phosphatase	0.641	696.66

Q06830	Peroxiredoxin-1	1.529	692.47
P22314	Ubiquitin-like modifier-activating enzyme 1	0.894	691.32
O75347	Tubulin-specific chaperone A	0.725	690.45
P54578	Ubiquitin carboxyl-terminal hydrolase 14	0.64	656.23
P62826	GTP-binding nuclear protein Ran	0.325	641.83
P02042	Hemoglobin subunit delta	2.463	638.55
P06753	Tropomyosin alpha-3 chain	1.351	618.48
P60900	Proteasome subunit alpha type-6	1.052	581.2
O14818	Proteasome subunit alpha type-7	1.21	568.9
P05109	Protein S100-A8	0.336	561.21
P13489	Ribonuclease inhibitor	0.51	554.53
Q9UNZ2	NSFL1 cofactor p47	0.889	551.08
P31939	Bifunctional purine biosynthesis protein PURH	0.568	528.85
P31946	14-3-3 protein beta/alpha	0.853	524.91
P67936	Tropomyosin alpha-4 chain	1.067	521.22
P00167	Cytochrome b5	1.305	517.65
P62158	Calmodulin	1.249	510.58
P17174	Aspartate aminotransferase, cytoplasmic	0.967	509.13
Q04760	Lactoylglutathione lyase	1.097	509.06
P15259	Phosphoglycerate mutase 2	0.948	506.56
P00492	Hypoxanthine-guanine phosphoribosyltransferase	0.847	505.15

P31150	Rab GDP dissociation inhibitor alpha	1.018	503.88
P52565	Rho GDP-dissociation inhibitor	1.213	493.81
P28074	Proteasome subunit beta type-5	1.116	493.52
P07900	Heat shock protein HSP 90-alpha	1.186	490.89
P00352	Retinal dehydrogenase 1	0.53	479.5
P13645	Keratin, type I cytoskeletal 10	0.677	473.84
P52209	6-phosphogluconate dehydrogenase, decarboxylating	0.664	458.06
Q8N0Y7	Probable phosphoglycerate mutase 4	0.991	454.13
P23526	Adenosylhomocysteinase	0.737	453.62
Q9NY33	Dipeptidyl peptidase 3	1.915	445.74
P25325	3-mercaptopyruvate sulfurtransferase	0.771	441.99
P61981	14-3-3 protein gamma	1.236	441.89
P48637	Glutathione synthetase	1.259	437.44
P49247	Ribose-5-phosphate isomerase	0.912	436.97
P10599	Thioredoxin	1.085	423.1
O14618	Copper chaperone for superoxide dismutase	1.015	419.85
Q13630	GDP-L-fucose synthase	0.704	411.11
P54652	Heat shock-related 70 kDa protein 2	0.93	405.73
Q9BS40	Latexin	0.839	399.62
P34932	Heat shock 70 kDa protein 4	1.633	396.25
P16152	Carbonyl reductase [NADPH] 1	1.001	393.7

P28066	Proteasome subunit alpha type-5	1.1	386.17
P02533	Keratin, type I cytoskeletal 14	0.559	375.46
P45974	Ubiquitin carboxyl-terminal hydrolase 5	0.572	370.81
P02788	Lactotransferrin	0.536	366.08
P22061	Protein-L-isoaspartate(D-aspartate) methyltransferase	O-0.428	364.02
P25788	Proteasome subunit alpha type-3	1.171	360.12
P25787	Proteasome subunit alpha type-2	1.053	355.85
P05089	Arginase-1	4.488	349.17
Q9NZD4	Alpha-hemoglobin-stabilizing protein	3.764	347.74
P09972	Fructose-bisphosphate aldolase C	1.522	346.71
P13796	Plastin-2	1.498	343.72
Q9NRX4	14 kDa phosphohistidine phosphatase	1.128	338.35
P09104	Gamma-enolase	1.907	338.02
P58546	Myotrophin	0.671	326.33
P30626	Sorcina	0.676	326.05
Q8TAA3	Proteasome subunit alpha type-7-like	1.245	321.97
P28072	Proteasome subunit beta type-6	1.404	318.91
P02538	Keratin, type II cytoskeletal 6A	0.522	317.25
P07737	Profilin-1	0.736	315.16
P52566	Rho GDP-dissociation inhibitor 2	0.821	310.36
Q9Y281	Cofilin-2	0.549	306.24

P35754	Glutaredoxin-1	1.388	299.7
P07951	Tropomyosin beta chain	1.328	295.51
P43487	Ran-specific GTPase-activating protein	0.771	292.98
Q15819	Ubiquitin-conjugating enzyme E2 variant 2	0.813	291.74
P34931	Heat shock 70 kDa protein 1-like	1.031	291.45
P09493	Tropomyosin alpha-1 chain	2.273	289.95
Q9HC38	Glyoxalase domain-containing protein 4	1.052	281.9
Q96G03	Phosphoglucomutase-2	0.958	275.79
Q5TDH0	Protein DDI1 homolog 2	0.557	275.46
Q7Z4W1	L-xylulose reductase	0.435	275.01
P54725	UV excision repair protein RAD23 homolog A	1.258	272.43
Q8IZP2	Putative protein FAM10A4	0.643	272.06
Q13404	Ubiquitin-conjugating enzyme E2 variant 1	1.048	268.78
O00233	26S proteasome non-ATPase regulatory subunit 9	0.562	268.56
P07205	Phosphoglycerate kinase 2	0.888	267.49
P26447	Protein S100-A4	0.179	266.53
P35908	Keratin, type II cytoskeletal 2 epidermal	0.454	264.73
Q9UL46	Proteasome activator complex subunit 2	0.427	264.6
P08779	Keratin, type I cytoskeletal 16	0.337	251.86
P15374	Ubiquitin carboxyl-terminal hydrolase isozyme L3	0.954	250.86
P17066	Heat shock 70 kDa protein 6	1.011	250.01

P27348	14-3-3 protein theta	0.803	244.4
Q15843	NEDD8	1.732	236.41
P13647	Keratin, type II cytoskeletal 5	0.542	235.67
P28070	Proteasome subunit beta type-4	1.02	233.53
P30740	Leukocyte elastase inhibitor	0.712	229.76
Q9UQ80	Proliferation-associated protein 2G4	0.855	221.04
P53396	ATP-citrate synthase	0.401	219.97
P61088	Ubiquitin-conjugating enzyme E2 N	0.754	217.72
P62942	Peptidyl-prolyl cis-trans isomerase FKBP1A	0.978	215.92
O75368	SH3 domain-binding glutamic acid-rich-like protein	0.676	211.18
P20618	Proteasome subunit beta type-1	1.303	209.77
P51858	Hepatoma-derived growth factor	0.816	208.53
Q04695	Keratin, type I cytoskeletal 17	0.51	204.84
P07203	Glutathione peroxidase 1	1.576	199.57
Q6ICL3	Transport and Golgi organization protein 2 homolog	0.863	198.19
Q01469	Fatty acid-binding protein, epidermal	0.826	194.61
Q16143	Beta-synuclein	0.337	193.55
P09211	Glutathione S-transferase P	0.73	192.84
Q9NTK5	Obg-like ATPase 1	1.005	192.03
P47756	F-actin-capping protein subunit beta	0.38	191.44
P21980	Protein-glutamine gamma-glutamyltransferase	0.181	191.24

Q9H3K6	BolA-like protein 2	0.569	190.57
P63208	S-phase kinase-associated protein 1	0.678	189.76
P48741	Putative heat shock 70 kDa protein 7	0.417	186.93
Q9NRV9	Heme-binding protein 1	0.948	185.99
Q6S8J3	POTE ankyrin domain family member E	0.437	181.35
Q06323	Proteasome activator complex subunit 1	0.522	179.84
P15311	Ezrin	0.642	179.61
O00299	Chloride intracellular channel protein 1	0.429	178.8
P06744	Glucose-6-phosphate isomerase	1.215	178.27
P49773	Histidine triad nucleotide-binding protein 1	0.929	176.69
P35241	Radixin	1.002	175.75
A5A3E0	POTE ankyrin domain family member F	0.42	174.67
Q6XQN6	Nicotinate phosphoribosyltransferase	0.31	173.09
P09417	Dihydropteridine reductase	0.877	170.25
P53004	Biliverdin reductase A	0.38	167.34
Q9Y536	Peptidyl-prolyl cis-trans isomerase A-like 4A	0.928	167.31
Q8IXQ3	Uncharacterized protein C9orf40	1.061	166.17
Q99436	Proteasome subunit beta type-7	1.283	160.34
Q8WUM4	Programmed cell death 6-interacting protein	0.307	159.56
Q9Y4E8	Ubiquitin carboxyl-terminal hydrolase 15	0.349	153.02
P59665	Neutrophil defensin 1	0.266	153
P59666	Neutrophil defensin 3	0.266	153

P30046	D-dopachrome decarboxylase	2.218	152.34
O75223	Gamma-glutamylcyclotransferase	1.043	150.88
Q86VP6	Cullin-associated NEDD8-dissociated protein 1	0.325	150.3
Q9NWX4	UPF0587 protein C1orf123	0.746	146.95
P30085	UMP-CMP kinase	0.351	143.63
P0CG38	POTE ankyrin domain family member I	0.388	141.15
A6NHG4	D-dopachrome decarboxylase-like protein	2.597	140.29
Q3LXA3	Triokinase/FMN cyclase	0.642	139.95
P0CG39	POTE ankyrin domain family member J	0.399	139.27
P68036	Ubiquitin-conjugating enzyme E2 L3	0.761	138.89
O75083	WD repeat-containing protein 1	0.585	138.54
O95336	6-phosphogluconolactonase	0.906	138.53
P04632	Calpain small subunit 1	0.588	136.19
Q9BYX7	Putative beta-actin-like protein 3	0.437	135.39
Q99733	Nucleosome assembly protein 1-like 4	0.951	133.68
Q5JXB2	Putative ubiquitin-conjugating enzyme E2 N-like	0.763	133.64
Q13200	26S proteasome non-ATPase regulatory subunit 2	0.541	132.88
P20073	Annexin A7	0.27	131.41
Q16774	Guanylate kinase	0.79	130.58
O75828	Carbonyl reductase [NADPH] 3	1.03	129.73

Q5VVQ6	Ubiquitin thioesterase OTU1	0.503	128.34
Q9BWD1	Acetyl-CoA acetyltransferase, cytosolic	0.646	128.29
Q9NZT1	Calmodulin-like protein 5	0.299	126.56
Q9BSL1	Ubiquitin-associated domain-containing protein 1	0.285	123.68
P16083	Ribosyldihyronicotinamide dehydrogenase [quinone]	0.132	121.91
P08670	Vimentin	0.778	119.46
P08238	Heat shock protein HSP 90-beta	1.806	118.5
P06703	Protein S100-A6	0.373	118.36
P07195	L-lactate dehydrogenase B chain	1.174	117.47
P49189	4-trimethylaminobutyraldehyde dehydrogenase	0.591	115.88
Q9H479	Fructosamine-3-kinase	0.604	111.33
P49721	Proteasome subunit beta type-2	1.097	107.26
P60953	Cell division control protein 42 homolog	0.446	106.2
P02787	Serotransferrin	3.295	104.49
P43034	Platelet-activating factor acetylhydrolase IB subunit alpha	0.785	103.83
Q9H299	SH3 domain-binding glutamic acid-rich-like protein 3	0.732	103.63
P81605	Dermcidin	0.471	103.49
O43598	2'-deoxynucleoside 5'-phosphate N-hydrolase 1	1.314	100.9
P38606	V-type proton ATPase catalytic subunit A	0.285	99.1

P42330	Aldo-keto reductase family 1 member C3	0.19	97.21
P07384	Calpain-1 catalytic subunit	0.497	96.81
Q9H0R4	Haloacid dehalogenase-like hydrolase domain-containing protein 2	1.111	91.91
P09496	Clathrin light chain A	0.19	91.61
P21333	Filamin-A	0.44	89.81
Q9BRA2	Thioredoxin domain-containing protein 17	0.744	89.71
Q96DG6	Carboxymethylenebutenolidase homolog	0.613	89.37
Q00169	Phosphatidylinositol transfer protein alpha isoform	0.508	87.48
P54920	Alpha-soluble NSF attachment protein	0.219	86.99
P04792	Heat shock protein beta-1	1.095	86.99
Q9Y265	RuvB-like 1	0.398	86.21
P52907	F-actin-capping protein subunit alpha-1	0.367	85.08
P00387	NADH-cytochrome b5 reductase 3	0.839	84.27
Q86YZ3	Hornerin	0.477	82.28
Q14974	Importin subunit beta-1	0.78	81.46
F5H284	Peptidyl-prolyl cis-trans isomerase A-like 4D	1.177	81.38
A0A0B4J2A2	Peptidyl-prolyl cis-trans isomerase A-like 4C	1.177	81.38
P06396	Gelsolin	0.599	80.3
Q15257	Serine/threonine-protein phosphatase 2A activator	0.849	77.85
P55209	Nucleosome assembly protein 1-like 1	0.951	77.64

Q9Y230	RuvB-like 2	0.308	77.37
Q13526	Peptidyl-prolyl cis-trans isomerase NIMA-interacting 1	0.45	77.25
P61978	Heterogeneous nuclear ribonucleoprotein K	0.415	76.34
Q14847	LIM and SH3 domain protein 1	0.313	76.05
Q13867	Bleomycin hydrolase	1.45	76.05
P00491	Purine nucleoside phosphorylase	0.633	75.67
P14550	Alcohol dehydrogenase [NADP(+)]	0.784	75.31
Q7Z3Y7	Keratin, type I cytoskeletal 28	0.678	74.79
O95747	Serine/threonine-protein kinase OSR1	0.879	73.37
Q9BY43	Charged multivesicular body protein 4a	0.757	72.66
Q9UJU6	Drebrin-like protein	0.582	71.5
P30153	Serine/threonine-protein phosphatase 2A 65 kDa regulatory subunit A	0.294	71.18
P31944	Caspase-14	0.593	70.07
P09651	Heterogeneous nuclear ribonucleoprotein A1	1.448	68.96
Q5VW32	BRO1 domain-containing protein BROX	0.836	68.65
O43396	Thioredoxin-like protein 1	0.775	66.66
Q9BV20	Methylthioribose-1-phosphate isomerase	0.667	66.31
P35998	26S protease regulatory subunit 7	0.581	65.47
P14618	Pyruvate kinase PKM	0.142	65.3
Q9H2H8	Peptidyl-prolyl cis-trans isomerase-like 3	0.521	64.14
Q12765	Secernin-1	1.744	64.12

P55786	Puromycin-sensitive aminopeptidase	0.461	64.07
Q15365	Poly(rC)-binding protein 1	0.248	63.96
Q15181	Inorganic pyrophosphatase	0.284	62.8
Q9UDX3	SEC14-like protein 4	0.589	62.73
Q9Y3C6	Peptidyl-prolyl cis-trans isomerase-like 1	0.572	62.69
Q9UBQ7	Glyoxylate reductase/hydroxypyruvate reductase	0.296	62.63
P06132	Uroporphyrinogen decarboxylase	0.775	62.16
P16949	Stathmin	0.869	61.99
O95678	Keratin, type II cytoskeletal 75	0.5	61.87
Q9UHV9	Prefoldin subunit 2	1.081	61.33
P61970	Nuclear transport factor 2	0.908	61.31
P25789	Proteasome subunit alpha type-4	1.048	61.08
Q969T9	WW domain-binding protein 2	0.583	60.73
P13716	Delta-aminolevulinic acid dehydratase	0.553	59.94
P67775	Serine/threonine-protein phosphatase 2A catalytic subunit alpha isoform	0.497	59.86
Q00610	Clathrin heavy chain 1	0.218	56.9
Q96GD0	Pyridoxal phosphate phosphatase	0.713	56.51
P08397	Porphobilinogen deaminase	0.344	56.21
P62714	Serine/threonine-protein phosphatase 2A catalytic subunit beta isoform	0.592	56.14
P12829	Myosin light chain 4	1.739	55.92

P49720	Proteasome subunit beta type-3	0.816	54.75
Q96GG9	DCN1-like protein 1	0.589	54.59
P48739	Phosphatidylinositol transfer protein beta isoform	0.613	54.23
Q96AT9	Ribulose-phosphate 3-epimerase	0.645	54.06
Q5QNW6	Histone H2B type 2-F	1.664	53.26
Q99877	Histone H2B type 1-N	1.664	53.26
P62807	Histone H2B type 1-C/E/F/G/I	1.664	53.26
Q99879	Histone H2B type 1-M	1.664	53.26
Q99880	Histone H2B type 1-L	1.664	53.26
P58876	Histone H2B type 1-D	1.664	53.26
Q93079	Histone H2B type 1-H	1.664	53.26
P54727	UV excision repair protein RAD23 homolog B	0.304	52.86
Q9NR45	Sialic acid synthase	0.545	52.73
O75155	Cullin-associated NEDD8-dissociated protein 2	0.304	52.49
Q56UQ5	TPT1-like protein	0.786	51.3
O43765	Small glutamine-rich tetratricopeptide repeat-containing protein alpha	0.841	50.92
P11766	Alcohol dehydrogenase class-3	0.617	50.48
P23527	Histone H2B type 1-O	1.664	50.19
P33778	Histone H2B type 1-B	1.664	50.19
Q16778	Histone H2B type 2	1.664	50.19

O75832	26S proteasome non-ATPase regulatory subunit 10	0.308	50.01
Q15370	Transcription elongation factor B polypeptide 2	0.849	49.97
P57053	Histone H2B	1.641	49.88
O60814	Histone H2B	1.641	49.88
O60664	Perilipin-3	1.502	49.71
Q8WTU0	Protein DDI1 homolog 1	0.465	49.7
P62805	Histone H4	1.999	49.65